SEQUENCE STRATIGRAPHY AND FACIES DISTRIBUTION IN A MIOCENE CARBONATE PLATFORM; LA RELLANA PLATFORM AREA, SOUTHEASTERN SPAIN

BY

RAFFERTY JEREMIAH SWEENEY

Submitted to the graduate degree program in Geology and the Graduate Faculty of the University of Kansas in partial fulfillment of the requirements for the degree of Master of Science.

_____

Co-chairperson Robert H. Goldstein

_____

Co-chairperson Evan K. Franseen

_____

George Tsoflias

Date Defended: June 13th, 2016

The Thesis Committee for Rafferty Jeremiah Sweeney certifies
that this is the approved version of the following thesis:

Sequence stratigraphy and facies distribution in a Miocene carbonate platform; la Rellana platform area, southeastern Spain

_____

Co-chairperson Robert H. Goldstein

_____

Co-chairperson Evan K. Franseen

Date approved: June 13th, 2016

Abstract

Rafferty Jeremiah Sweeney
Department of Geology, (June 13th, 2016)
The University of Kansas

A 2-dimensional coastal exposure of the Miocene-age Rellana carbonate platform (Cabo de Gata Region, Southeast Spain) provides an opportunity to study the facies and stratigraphy, determine the processes controlling deposition, and reflect on how those processes are expressed in associated basinal deposits. The platform developed on Neogene volcanic substrate that features a drainage divide separating a steep-dipping (~20°) south slope from a shallow-dipping (~5 °) north slope. The north slope steepens distally to 25° (1.3 km N of the drainage divide) before flattening as it eventually reaches the basin floor, defining the margin of the Agua Amarga basin. The Rellana platform formed a rim above the Agua Amarga basin for approximately 8 km and was a major source for carbonate accumulations. The steep southern slope is down dip and laterally equivalent to similar deposits on Ricardillo Peak across the San Pedro Embayment.

Seven depositional sequences (DS1-7) comprising 13 facies are identified on the platform. Earliest carbonate deposition (late Tortonian) is restricted to the lowest elevations on the southern end of the platform (DS1a and b). These topography-filling and volcanic-basement-onlapping deposits contain predominantly heterozoan skeletal facies, suggesting a temperate climate during early platform development. Overlying carbonate strata (DS2) demonstrate continued ramp-dominated deposition on both sides of the drainage divide. These deposits feature an upward-increasing abundance of photozoan skeletal components, culminating in the preservation of detrital *Tarbellastraea* framestone. The third depositional sequence (DS3) contains abundant photozoan reef deposits that suggest a shift to sub-tropical/tropical climate.

Reef development during this sequence is pronounced, and the shallow dip of the northern slope facilitated reef progradation during periods of stillstand and relative sea-level fall. While the steeply dipping southern slope DS3 deposits consist predominantly of fore-reef slope deposits punctuated by periods of reef growth. The uppermost carbonate deposits (DS4-7) consist of oolitic, microbial and local *Porites* reefs that were deposited in normal-to-restricted marine conditions associated with four high-frequency relative fluctuations in sea level. These deposits are interpreted to represent the terminal carbonate complex (TCC) that is well documented throughout the region.

Comparison of the Rellana Platform area stratigraphy with that of Ricardillo Peak, San Pedro Embayment, and La Molata platform within the Rodalquilar Caldera to the southeast, provides a more regional view of the potential controls on carbonate development in the Cabo de Gata area. Results show that the paleoclimatic, paleotopographic and sea level history controls identified in the Rellana Platform area are consistent throughout the Cabo de Gata region, however, paleogeographic effects were also very influential on carbonate development, and responsible for observed variability between the study areas.

Finally, in the third chapter, the Rellana Platform and Agua Amarga Basin are examined with the intention of testing predictive hypothesis regarding platform and basin sedimentary processes. Basinal deposits consist of grainy heterozoan-dominated shallow-water deposits, hemipelagic and pelagic deep-water deposits, carbonate/volcanic sedimentary breccias, as well as high- and low-density turbidites. Analysis of the distribution of the basinal breccias within the Agua Amarga basin demonstrates that the evolution of the Rellana platform had an effect on sediment dispersal into the Agua Amarga basin. During the platform reef phase, the initial reef margin was near the steep basin margin, and sourced coarse breccias into the basin. During a

subsequent sea-level rise, the reef margin stepped backward resulting in backstepping of basinal breccias and an increase in fine-grained basin deposits. Highstand reef progradation towards the basin margin resulted in an increase of coarse-grained, mostly sediment gravity flow deposits in the basin. As sea level fell, reefs continued to prograde and downstep toward the basin, resulting in increasing amounts of coarse-grained basinal deposits, including breccias, that progressively stepped toward the basin center. Our results show that proximity of the reef margin to the basin margin increases the volume of coarse material deposited in the basin. Typical depositional models for resedimented deepwater carbonates fail to reflect the impact of platform topography on sediment redistribution. Our results challenge the highstand shedding model for this setting, suggest an alternative model that reflects observed platform and basinal characteristics, and identify platform paleotopographic controls that influence basinal deposition of coarse debrites in distally steepened ramp systems.

Acknowledgements

I would like to thank the staff at KU for their time and attention throughout my tenure at KU, the support of the faculty and staff makes the University of Kansas's Geology Department a special place. Specifically I would like to thank Dr. Goldstein and Dr. Franseen for the opportunity to participate in the Spain project, and also for their seemingly limitless patience through a prolonged editing process. I would also like to thank my undergraduate advisor Dr. Antun Husinec for his tenacious instruction and support well beyond my time at St. Lawrence University.

I would also like to acknowledge Robert and Elaine Collins, without them none of this would have been possible.

My biggest thank you goes to my wife Erin, who has shown unwavering support and love through the ups and downs of graduate school, early career in a commodity-based business, and life in general. I love you Erin.

Table of contents

APPENDICES

LIST OF FIGURES

LIST OF TABLES

Chapter 1: Project Summary

INTRODUCTION

Miocene carbonate deposits within the volcanic province of Cabo de Gata, southeastern Spain (Fig. 1) are studied herein to test existing assumptions and understanding of carbonate depositional models and systems. The project is focused on Tortonian and Messinian reef complexes, heterozoan carbonate deposits, and paleotopographic features in the area (e.g. Addicott et al. 1978; Esteban, 1979; Esteban and Giner, 1980; Dabrio *et al*., 1981; Dronkert 1985; Muller and Hsü 1987; Braga and Martin 1988; Rouchy 1988; Franseen, 1989; Martin et al. 1989; Braga et al. 1990; Franseen and Mankiewicz, 1991; Franseen *et al.*, 1993; Goldstein and Franseen, 1995; Whitesell, 1995; Esteban, 1996; Esteban *et al*., 1996; Franseen and Goldstein, 1996; Martin *et al*., 1996; Franseen *et al*., 1997a; Franseen *et al*., 1997b; Brachert *et al*., 1998; Franseen *et al*., 1998; Brachert *et al*., 2001; Martin *et al*., 2003; Toomey, 2003; Dillett, 2004; Martin *et al*., 2004; Johnson *et al*., 2005; Dvoretsky, 2009). Field work was completed on a coastal exposure ~4 km northeast of the village of Las Negras, that features Miocene carbonate deposits of the Rellana platform flanking and overlying Neogene volcanic substrate (Franseen and Goldstein, 1996). Through analysis of this exposure, this study seeks to describe the sedimentology and depositional history of the Rellana platform study area and to analyze sea-level, tectonic, paleotopographic, platform morphology and climate controls on carbonate deposition (e.g. Ahr, 1973; Read, 1985; Sarg, 1988; Handford and Loucks, 1993; Mutti *et al.*, 1999; and Schlager, 2005). This study also relates development of the Rellana Platform to neighboring areas; specifically lateral and up-dip equivalent Ricardillo Peak (described by Lipinski, 2010, Toomey, 2003), the time-equivalent La Molata platform within the Rodalquilar

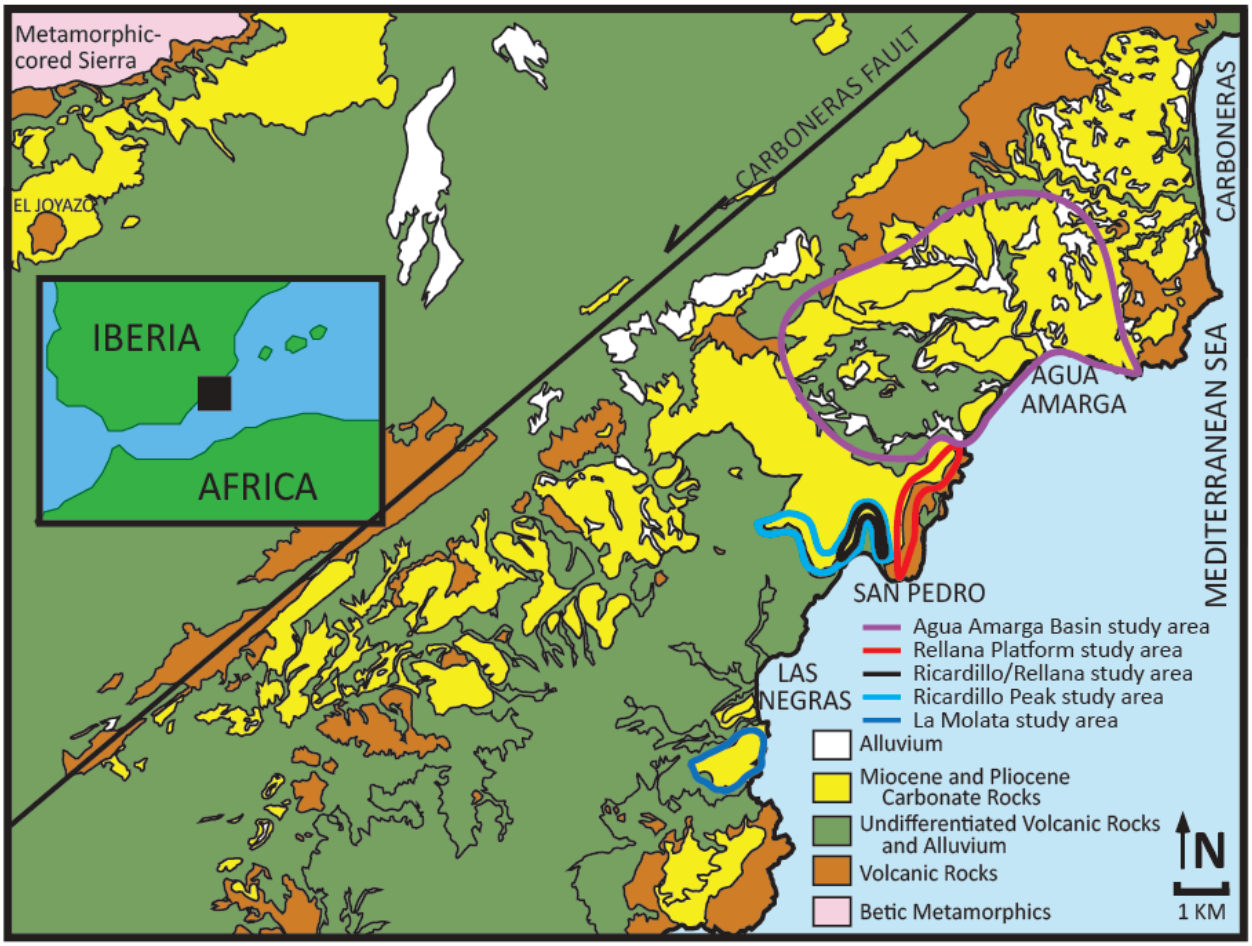

Figure 1: General geologic map of the Cabo de Gata area of southeastern Spain, Inset shows relative location on the Iberian Peninsula. Rellana study area is highlighted within red line. Neighboring, previously described areas are outlined as follows: blue shape indicates the Ricardillo study area (Toomey, 2003), black shape indicates the Ricardillo/Rellana area (Lipinski, 2010), the purple shape indicates the Agua Amarga study area (Dvoretsky, 2009). Modified from: Mapa Geológico de España, 1981; Dvoretsky, 2009; Lipinski, 2010.

caldera to the South (near Las Negras), and downdip basinal deposits of the Agua Amarga Basin (Dvoretsky, 2009) (Fig. 1).

Analysis of the exposed Rellana platform is significant due to the presence of key features that are used to accomplish the following: identify controls on sedimentation, define a platform to basin system, and generate a quantitative relative sea-level curve that enhances local and regional understanding of control of sea level on deposition. This approach is facilitated by the relatively well-preserved paleotopography in the Cabo de Gata region, which requires simple to negligible removal of tectonic tilt. The presence of a drainage divide preserved in the studied coastal exposure demonstrates the impact of paleoslope on platform development. Lateral continuity of the platform deposits into neighboring areas allows for direct comparison between the results from this study and other areas, specifically the development and testing of regional influences.

METHODS

Eleven stratigraphic sections were measured (Appendix 1), and 430 hand samples were collected and described (Appendix 2). From these hand samples, 75 were selected for thin-sections based on facies representation. Thin-sections were prepared at the University of Kansas, impregnated with standard blue epoxy to enhance porosity visibility, polished to 30 microns and described using a binocular microscope (Appendix 3). Measured sections were used in conjunction with outcrop-scale photomosaics to assist tracing of facies contacts, significant surfaces, and genetic units across the platform and into neighboring areas. Surfaces were compiled into line drawings and photomosaic overlays (Appendix 4). Using photomosaics, measured sections and cross sections (Appendix 5), relative sea-level history was constructed using the pinning point method described by Goldstein and Franseen (1995).

This report is divided into two papers: the first paper (Chapter 2) describes the observed facies, their distribution, sequence-stratigraphy, and depositional controls of the Rellana platform and relates those findings to the neighboring Ricardillo Peak and Las Negras areas (La Molata platform). The second paper (Chapter 3) compares the relationship between the Rellana platform deposits described in Chapter 2 to equivalent basinal deposits to test hypotheses of platform control on basin deposition. The controls identified are analyzed to determine their potential application as a predictive tool in developing platform and basin models. Chapters are formatted in the style of Journal of Sedimentary Research.

REFERENCES

Addicott, W. O., Snavely, P. D. Jr., Bukry, D., and Poore, R. Z., 1978, Neogene stratigraphy and paleontology of southern Almeria Province, Spain: an overview. USGS Bulletin, Series 1454, 49 pp.

Ahr, W. M., 1973, The carbonate ramp: an alternative to the shelf model. Transactions of the Gulf Coast Association of Geological Societies, v. 23, p. 2211-225.

Brachert, T. C., Betzler, C., Braga, J. C., and Martin, J. M., 1998, Microtaphofacies of a warm-temperate carbonate ramp (Uppermost Tortonian/Lowermost Messinian (Southeast Spain)). Palaios, v. 13, p. 459-475.

Brachert, T. C., Hultzsch, N., Knoerich, A. C., Krautworst, U. M. R., Stuckrad, O. M., 2001, Climatic signatures in shallow-water carbonates: high-resolution stratigraphic markers in structurally controlled carbonate buildups (Late Miocene, southern Spain). Palaeogeography, Palaeoclimatology, Palaeoecology, v. 175, p. 211-237.

Braga, J. C., and Martin, J. M., 1988, Neogene coralline-algal growth-forms and their paleoenvironments in the Almanzora river valley (Almeria, S.E. Spain). Paleogeography, Paleoclimate, and Paleoecology, v.67, p. 285-303.

Braga, J. C., and Martin, J. M., and Alcala, B., 1990, Coral reefs in coarse terrigenous sedimentary environments (upper Tortonian, Granada Basin, southern Spain). Sedimentary Geology, v. 66, p. 135-150.

Dabrio, C. J., Esteban, M., and Martin, J. M., 1981, The Coral Reef of Nijar, Messinian (Uppermost Miocene), Almeria Province, SE Spain. Journal of Sedimentary Petrology, v. 51, p. 521-439.

Dillett, P. M., 2004, Paleotopographic and sea-level controls on the sequence stratigraphic character of a heterozoan carbonate succession: Pliocene, Carboneras basin, southeast Spain. [Unpublished M.S. thesis]. University of Kansas, Lawrence, KS, 116 pp.

Dronkert, H., 1985, Evaporite models and sedimentology of Messinian and Recent evaporites. GUA Papers of Geology, Series 1, v. 24, 283 pp.

Dvoretsky, R. A., 2009, Stratigraphy and reservoir-analog modeling of upper Miocene shallow-water and deep-water carbonate deposits: Aqua Amarga basin, Southeast Spain. [Unpublished M.S. Thesis]; University of Kansas, Lawrence, KS, 148 pp.

Esteban, M., 1979, Significance of upper Miocene coral reefs of the western Mediterranean: Palaeogeography, Palaeoclimatology, Palaeoecology, v. 29, p. 169–188.

Esteban, M., 1996, An Overview of Miocene Reefs from Mediterranean Areas: General Trends and Facies Models, *in* Franseen, E. K., Esteban, M., Ward, W. C., and Rouchy, J.-M., eds., Models for Carbonate Stratigraphy from Miocene Reef Complexes of the Mediterranean Regions. SEPM Concepts in Sedimentology and Paleontology, Series No. 5, p. 3-54.

Esteban, M., and Giner, J. 1980, Messinian Coral Reefs and Erosion Surfaces in Cabo de Gata (Almeria, southeastern Spain): Acta Geologico Hispanica, v. 15, p. 97-104.

Esteban, M., Braga, J. C., Martin, J., and Santisteban, C., 1996, Western Mediterranean Reef Complexes, *in* Franseen, E. K., Esteban, M., Ward, W. C., and Rouchy, J.-M., eds., Models for Carbonates Stratigraphy from Miocene Reef Complexes of Mediterranean Regions. SEPM Concept in Sedimentology and Paleontology, p. 55-72.

Franseen, E.K., 1989, Depositional sequences and correlation of middle to upper Miocene carbonate complexes, Las Negras area, southeastern Spain [unpublished Ph.D. thesis]:

University of Wisconsin–Madison, 374 p.
Franseen, E.K., and Mankiewicz, C., 1991, Depositional Sequences and Correlation of Middle(?) to Late Miocene Carbonate Complexes, Las Negras and Nijar Areas, Southeastern Spain: Sedimentology, v. 38, p. 871-898.
Franseen, E.K., Goldstein, R.H., and Whitesell, T.E., 1993, Sequence Stratigraphy of Miocene Carbonate Complexes, Las Negras Area, Southeastern Spain: Implications for Quantification of Changes in Relative Sea Level: *in* Loucks, R.G. and Sarg, J.F., eds., Carbonate Sequence Stratigraphy: Recent Developments and Applications, American Association of Petroleum Geologists Memoir 57, p. 409-434.
Franseen, E. K., and Goldstein, R. H., 1996, Paleoslope, Sea-level and Climate Controls on Upper Miocene Platform Evolution, Las Negras Area, Southeastern Spain, *in* Franseen, E. K., Esteban, M., Ward, W. C., and Rouchy, J.-M., eds., Models for Carbonates Stratigraphy from Miocene Reef Complexes of Mediterranean Regions. SEPM Concept in Sedimentology and Paleontology, p. 159-176.
Franseen, E. K., Goldstein, R. H., and Esteban, M., 1997a, Controls on Porosity Types and Distribution in Carbonate Reservoirs: A Guidebook for Miocene Carbonate Complexes of the Cabo de Gata Area, SE Spain. American Association of Petroleum Geologists Education Program, p. 1-150.
Franseen, E. K., Goldstein, R. H., and Farr, M. R., 1997b, Substrate-Slope and Temperature controls on Carbonate Ramps: Revelations from Upper Miocene Outcrops, SE Spain, *in* James, N. P., and Clarke, A. D., eds., Cool-Water Carbonates. SEPM Special Publication, p. 271-290.
Franseen, E. K., Goldstein, R. H., and Farr, M. R., 1998, Quantitative Controls on Location and Architecture of Carbonate Depositional Sequences: Upper Miocene, Cabo de Gata Region, SE Spain. Journal of Sedimentary Research, v. 68, p. 283-298
Goldstein, R. H., and Franseen, E. K., 1995, Pinning points: a method providing quantitative constraints on relative sea-level history. Sedimentary Geology, v. 95, p. 1-10.
Handford, C. R., and Loucks, R. G., 1993, Carbonate depositional sequences and systems tracts-responses of carbonate platforms to relative sea-level changes, *in* Loucks, R.G. and Sarg, J. F., eds., Carbonate Sequence Stratigraphy: Recent Developments and Applications. AAPG Memoir 57, p. 3-42.
Johnson, C. L., Franseen, E. K., and Goldstein, R. H., 2005, The effects of sea level and paleotopography on lithofacies distribution and geometries in heterozoan carbonates, south-eastern Spain. Sedimentology, v. 52, p. 513-536.
Lipinski, C. J., 2010, Stratigraphy of upper Miocene oolite-microbialite-coralgal reef sequences of the terminal carbonate complex: southeast Spain. [Unpublished M.S. thesis] University of Kansas, Lawrence, KS, 116 p.
Mapa Geológico de España, 1981, (1:50,000): Instituto Geológico y Minero de España.
Martin, J. M., Braga, J. C. and Rivas, P., 1989, Coral successions in upper Tortonian reefs in SE Spain. Lethia, v. 22, p. 271-286.
Martin, J. M., Braga, J. C., Betzler, C., and Brachert, T., 1996, Sedimentary model and high frequency cyclicity in a Mediterranean, shallow-shelf, temperate-carbonate environment (uppermost Miocene, Agua Amarga Basin, Southern Spain). Sedimentology, v.43, p. 263-277.

Martin, J. M., Braga, J. C., and Betzler, C., 2003, Late Neogene - Recent uplift of the Cabo de Gata volcanic province, Almeria, SE Spain. Geomorphology, v. 50, p. 27-42.
Martin, J. M., Braga, J. C., and Betzler, C., 2004, Contrasting models of temperate carbonate sedimentation in a small Mediterranean embayment: the Pliocene Carboneras Basin, SE Spain. Journal of the Geological Society, London, v. 161, p. 387-399.
Muller, D. W., and Hsu, K. J., 1987, Event stratigraphy and paleoceanography in the Fortuna Basin (southeastern Spain): a scenario for the Messinian salinity crisis. Paleoceanography, v. 2, p. 679-696.
Mutti, M., Bernoulli, D., Spezzaferri, S., and Stille, P, 1999, Lower and middle Miocene carbonate facies in the central Mediterranean; the impact of paleoceanography on sequence stratigraphy, *in* Harris, P. M., Saller, A. H., and Simo, J. A., eds., Advances in Carbonates Sequence Stratigraphy: application to reservoirs, outcrops, and models. SEPM Special Publication 63, p. 371-387.
Read, J. F., 1985, Carbonate platform facies models. AAPG Bulletin, v. 69, p. 1-21.
Rouchy, J. M., 1988, Relations évaporites-hydrocarbures: l'association laminites-récifs-évaporites dans le Messinien de Méditerranée et ses ensignements, *in* Busson, J., ed., Evaporites et hydrocarbures. Mémoires du Muséum national d'Histoire naturelle (C)., v.55, p. 43-69.
Sarg, J. F., 1988, Carbonate sequence stratigraphy, *in* Wilgus, C. K, Hastings, B. S., Kendall, C, G. St. C, H. W. Posamentier, Ross, C.A., and Van Wagoner, J. C., eds., Sea Level Changes: An Integrated Approach. SEPM Special Publication No. 42, p.155-181.
Schlager, W., 2005, Carbonate sedimentology and sequence stratigraphy. SEPM Concepts in Sedimentology and Paleontology, Series 8, 200 pp.
Toomey, N., 2003, Controls on sequence stratigraphy in upper Miocene carbonates of Cerro de Ricardillo, southeastern Spain. [Unpublished M.S. thesis]: University of Kansas, Lawrence, KS, 114 pp.
Whitesell, T. C., 1995, Diagenetic Features Associated with Sequence Boundaries in Upper Miocene Carbonate Strata, Las Negras, Spain. [Unpublished Master's Thesis]: University of Kansas, 292 pp.

Chapter 2: Stratigraphy and Facies of the Rellana Platform, Regional and Local Controls Related to Paleotopography

Rafferty Sweeney[1], Evan K. Franseen[2] and Robert H. Goldstein[3]

1) Department of Geology, University of Kansas, Lindley Hall, 1475 Jayhawk Blvd., Lawrence, KS, 66044, Ph. # (785) 766-1114, e-mail: rsweeney@ku.edu
2) Department of Geology, University of Kansas, Lindley Hall, 1475 Jayhawk Blvd., Lawrence, KS, 66044, Ph. # (785) 864-2738, e-mail: gold@ku.edu
3) Department of Geology, University of Kansas, Lindley Hall, 1475 Jayhawk Blvd., Lawrence, KS, 66044, Ph. # (785) 864-2723, e-mail: evanf@kgs.ku.edu

CHAPTER SUMMARY

Analysis of marine carbonate deposits on the Rellana Platform, Southeast Spain, facilitates evaluation of paleotopography, relative sea-level history, and paleoclimate controls on facies and stratigraphy on the platform and adjacent areas. Exposure of a drainage divide separating a steep, south-dipping (~20˚) paleoslope from a shallow, north-dipping (~5˚) paleoslope provides the opportunity to describe the impact of paleotopographic variation on contemporaneously deposited carbonate facies. The influence of relative sea level change over this paleotopography is reflected in facies and stratigraphic variations. Climatic influences are known through the late Miocene and are reflected by transition from heterozoan- to photozoan-dominated skeletal assemblages.

Seven depositional sequences (DS1-7) comprising 13 facies are identified. Earliest carbonate deposition (late Tortonian) is restricted to the lowest elevations on the southern end of the platform (DS1a and b). These ramp-like deposits contain predominantly heterozoan skeletal assemblages suggesting a temperate climate during early platform development. Overlying carbonate strata (DS2) demonstrate continued ramp-dominated deposition on both sides of the drainage divide. These deposits feature an upward-increasing abundance of photozoan skeletal components, culminating in the preservation of *Tarbellastraea* framestone. The third depositional sequence (DS3) contains abundant photozoan reef deposits that suggest a sub-tropical/tropical climate. Reef development during this sequence is pronounced and the low accommodation of the shallowly dipping northern slope facilitated reef progradation during periods of still-stand and relative sea-level fall. While the steeply dipping southern slope DS3 deposits consist predominantly of fore-reef slope facies punctuated by periods of reef growth. The uppermost carbonate deposits (DS4-7) consist of oolitic, microbial and local *Porites* reefs

that were deposited in normal to restricted marine conditions associated with four high-frequency, high-amplitude relative fluctuations in sea-level.

Physical tracing of facies, contacts, and genetic units into the neighboring Ricardillo peak area demonstrates lateral continuity of the depositional packages described and enhances the range of the relative sea-level history reconstruction. Comparison of these two areas to the previously studied La Molata area near Las Negras facilitates identification of the role of paleogeographic controls on platform carbonate development. The Rellana platform is generally oriented on strike with the predominant wave direction. Ricardillo Peak is located within a coastal reentrant just leeward of the Rellana Platform. La Molata is located within the Rodalquilar Caldera to the south protected by volcanic highs and the edge of the Caldera just to the north of the platform area. The paleogeographic setting, accompanied with the interaction of relative sea level and substrate paleotopography resulted in variable development of ramp and fringing reef carbonate geometries that demonstrate the importance of paleogeography, paleotopography, paleoclimate and sea level history on the development of carbonate platforms.

INTRODUCTION

Stratigraphic and depositional models are important tools for understanding heterogeneity in carbonate systems. Carbonate platform models (e.g. Ahr, 1973; Read, 1985; Hanford and Loucks, 1993) identify paleoclimate, variations in relative sea level, tectonic influence and substrate topography as influential factors on sequence development. This study analyzes a carbonate platform in the Cabo de Gata region of Southeastern Spain, to analyze the impact of those influences. Upper Miocene carbonate accumulations of the Cabo de Gata region have been the focus of numerous studies (for example; Esteban, 1979; Esteban and Giner, 1980; Dabrio *et al.,* 1981; Franseen, 1989; Franseen and Mankiewicz, 1991; Franseen et al., 1993; Goldstein and Franseen, 1995; Esteban, 1996; Esteban *et al.,* 1996; Franseen and Goldstein, 1996; Mankiewicz, 1996; Franseen *et al.,* 1997b; Franseen *et al.,* 1998, Toomey, 2003; Dillett, 2004; Johnson, 2005; Dvoretsky, 2009; Lipinski, 2010; Hess, 2011 among others). Those studies have led to a detailed understanding of controlling factors important to carbonate system development in the area, including relative sea-level history, climate, and paleotopography. This new study presents data collected from the Rellana carbonate platform, focusing on a 3 km, 2-dimensional coastal exposure that is perpendicular to the platform margin (Fig. 1).

The platform developed on Neogene volcanic substrate and consists of seven depositional sequences (DS1a - DS7) comprising 13 facies (Fig. 2, Table 1). The volcanic substrate features a drainage divide separating a steep-dipping (~20˚) south slope from a shallow-dipping (~5˚) north slope (Fig. 1). The platform formed the rim above the horseshoe shaped Agua Amarga basin for approximately 8 km and was a major source for carbonate accumulations in the basin. Ricardillo Peak (studied by Toomey, 2003) is to the west and features laterally equivalent and updip deposits (Fig. 1). The Rellana platform is ~4.5 km northeast of the well–studied carbonate

complexes of the Las Negras area (Fig. 1). Previous studies have indicated that the Las Negras, Ricardillo and Rellana carbonate complexes experienced the same relative sea-level history and are approximately the same age (Franseen *et al.*, 1998; Toomey, 2003). The carbonate systems developed in the Las Negras area and Ricardillo area are interpreted to have been deposited in an archipelago setting in which carbonates formed fringes around the steep-sided volcanic hills associated with a caldera complex (Franseen, 1996). The Las Negras area was within the Rodalquilar caldera, Ricardillo was on its northern margin, and Rellana was outside of the caldera on one north-facing and one south-facing paleotopographic slope. My study provides the opportunity to compare the role of relative sea-level history and paleotopography where carbonates that developed on shallow and steep substrates were separated by a drainage divide. Comparing deposits near Las Negras, Ricardillo, and the two substrate-slopes of Rellana yields valuable information regarding the role of paleogeography, paleotopography, and relative sea-level history on carbonate platform development.

METHODS

Fieldwork in the Rellana platform area identified seven sequences composed of 13 facies (Table 1, Figures 1, 2, 3). Stratigraphic sections and cross-sections (Appendices 1 and 5), photomosaics (Appendix 4), hand samples (Appendix 2) and thin sections (Appendix 3) were used to characterize facies, trace contacts and significant surfaces, where physical tracing was not possible, and to define genetic units within the platform.

The pinning point method described by Goldstein and Franseen (1995) was used to reconstruct the quantitative relative sea-level history of the platform. Pinning points are

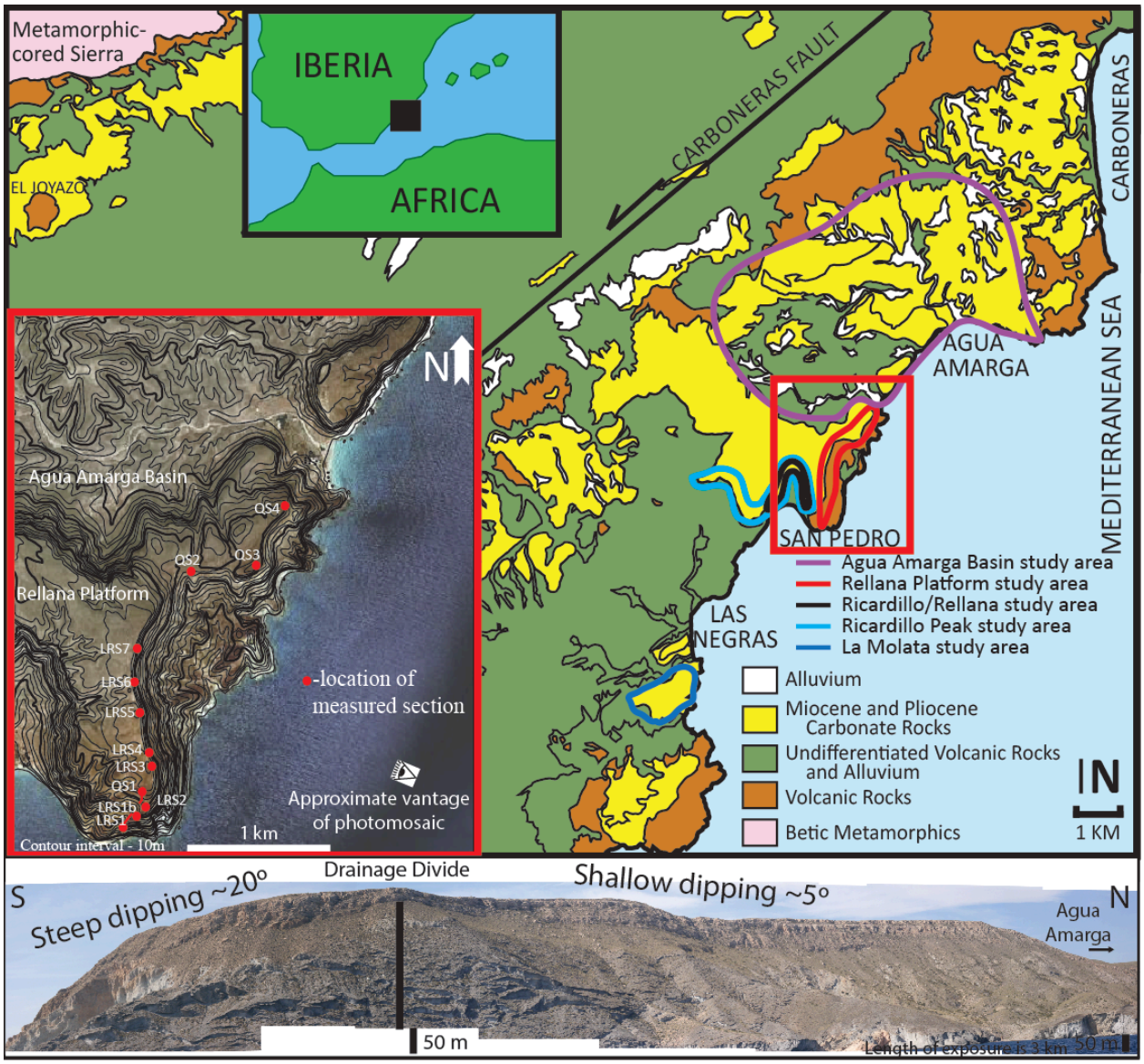

Figure 1: Location and general geological map of the Cabo de Gata region of southeastern Spain, the Rellana study area is indicated by the red highlighted area. Previously described areas immediatly adjacent to the Rellana platform include Ricardillo peak (blue highlighted area; Toomey, 2003), Rellana/Ricardillo area (black highlighted area; Lipinski, 2010) and the Agua Amarga basin (purple highlighted area; Dvoretsky, 2009). Map modified from: Mapa Geológico de España, 1981; Dvoretsky, 2009; Lipinski, 2010. Red rectangle inset and corresponding map shows topographic map (10 m contour interval) overlain on satellite image of Rellana Platform area with location of measured sections.

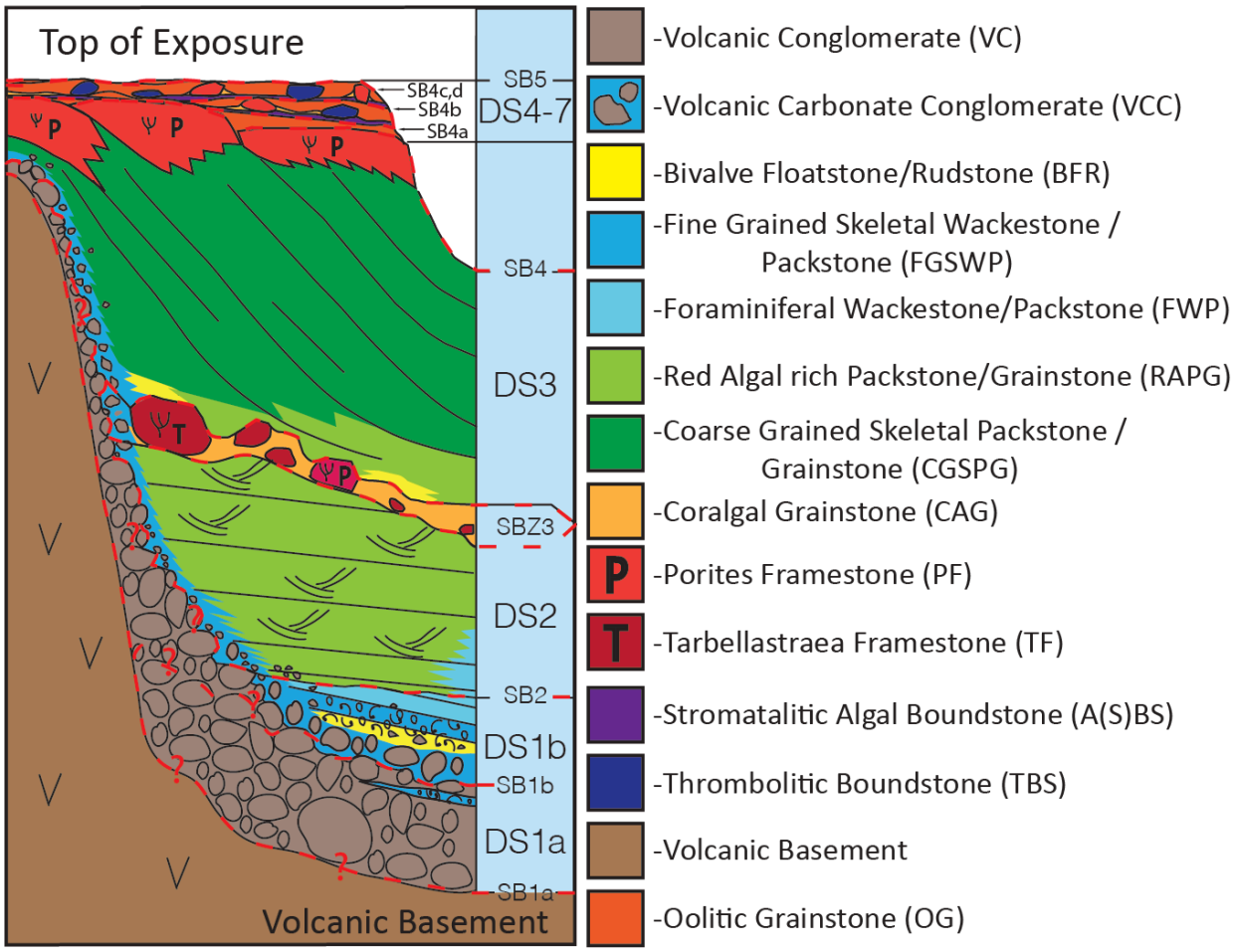

Figure 2: Generalized stratigraphy and facies distribution of the Rellana platform. DS1a, DS1b and the majority of DS2 are confined to the steeply dipping southern margin. DS3 is represented on both sides of the drainage divide, however, *Porites* Framestone (PF) deposits are more abundantly preserved north of the drainage divide, and DS4-7 deposits occur at high elevations (> 248 m above modern sea-level) on both sides of the drainage divide.

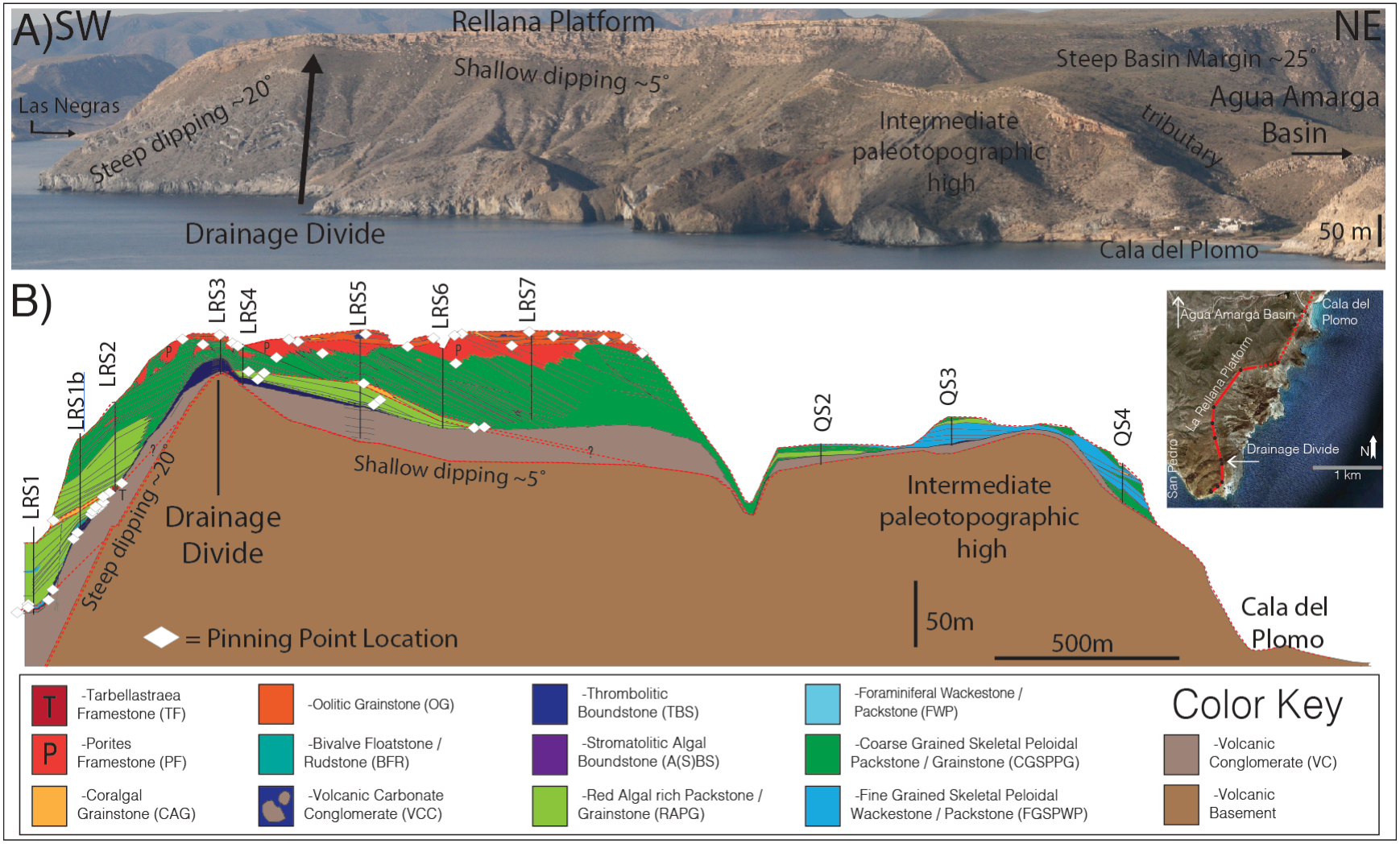
A)SW
Rellana Platform
NE
Las Negras
Steep dipping ~20˚
Shallow dipping ~5˚
Steep Basin Margin ~25˚
Agua Amarga Basin
tributary
Intermediate paleotopographic high
Drainage Divide
50 m
Cala del Plomo
B)
LRS1
LRS1b
LRS2
LRS3
LRS4
LRS5
LRS6
LRS7
QS2
QS3
QS4
Steep dipping ~20˚
Drainage Divide
Shallow dipping ~5˚
Intermediate paleotopographic high
= Pinning Point Location
50m
500m
Cala del Plomo
Agua Amarga Basin
Cala del Plomo
La Rellana Platform
San Pedro
Drainage Divide
N
1 km
Color Key
-Tarbellastraea Framestone (TF)
-Porites Framestone (PF)
-Coralgal Grainstone (CAG)
-Oolitic Grainstone (OG)
-Bivalve Floatstone / Rudstone (BFR)
-Volcanic Carbonate Conglomerate (VCC)
-Thrombolitic Boundstone (TBS)
-Stromatolitic Algal Boundstone (A(S)BS)
-Red Algal rich Packstone / Grainstone (RAPG)
-Foraminiferal Wackestone / Packstone (FWP)
-Coarse Grained Skeletal Peloidal Packstone / Grainstone (CGSPPG)
-Fine Grained Skeletal Peloidal Wackestone / Packstone (FGSPWP)
-Volcanic Conglomerate (VC)
-Volcanic Basement

Figure 3: Paleotopographically corrected schematic cross section of Rellana Platform area and Agua Amarga basin margin. Note steeply dipping southern slope (~15-20 degrees), shallow dipping northern slope (~5 degrees) and distally steepened basin margin (~25 degrees). Well-developed and more extensive progradation occurs in DS3 reef facies north of the drainage divide. DS4-7 overlie an erosional surface on DS3 and consist of microbial coralgal and oolitic facies composing 4 high-frequency sequences. Deposits overlying the intermediate paleotopographic high are likely associated with DS3 and deposits may have been transported from a postulated high to the southwest. White diamonds correspond to pinning points discussed in Depositional Sequences section. Vertical exaggeration of schematic cross section is 3 X.

identified at locations at which ancient sea level can be constrained relative to an arbitrary, geologically relevant datum (modern sea-level in this study) using sedimentologic and diagenetic evidence of sea-level position. Examples of identified pinning points include facies that formed at or near sea level (e.g. *in situ* coral framestone), and subaerial exposure surfaces developed on marine facies. The pinning point method requires that paleotopography either be preserved or reconstructed. Once paleotopography is reconstructed, relative elevations serve as effective proxies for Miocene relative sea-level elevations. In the Rellana study area, paleotopographic reconstruction requires removal of minor post-depositional tilting, as described by Hess (2011) and discussed in detail in the paleotopography section below (Fig. 4). Relative locations of pinning points defined in this study are depicted on the cross section in Figure 3 (a larger version of the cross section in this image is included in Appendix 5). Pinning points and the resulting quantitative relative sea-level curve are in Table 2 and Figure 16. The curve generated using the pinning points can be used as a baseline upon which more interpretive curves can be superimposed (Figs. 21, 22), allowing interpretations based on facies patterns, stacking patterns and stratal geometries to be included in a less quantitative representation of the relative sea-level curve.

Construction and comparison of pinning point curves can be used to correlate physically separate carbonate deposits as well as to identify eustatic, tectonic and autogenic influences. Work in the nearby Las Negras area (Franseen *et al.*, 1993; Goldstein and Franseen 1995; Franseen *et al.*, 1998) has demonstrated a relationship between sequence stratigraphic development and a quantitative sea-level curve. Further work in the Cabo de Gata region (Toomey, 2003; Dvoretsky, 2009; Lipinski, 2010) has been used to bolster understanding of relative sea-level history. Compilation of this data into a quantitative relative sea-level curve,

coupled with age-dating of volcanics interbedded with earliest carbonate deposits yields a regional, quantitative, time-constrained relative sea level curve that can be used as a correlation tool for data presented in this study. The Rellana platform provides access to high-elevation carbonate deposits that have not previously been studied. Inclusion of sea-level history from this platform enhances current understandings of regional relative sea-level history and the impact of this history on the sedimentologic record in the Cabo de Gata region of SE Spain.

GEOLOGIC SETTING

The calc-alkaline volcanic basement of the Cabo de Gata region has been dated at 17 Ma to 6 Ma (Neogene) (Lopez-Ruiz and Rodriguez-Badiola 1980; Serrano 1992) and is separated from metamorphic (Mesozoic and Paleozoic) basement of the Betic Sierras to the northwest by the variably active (Tortonian through Messinian and Pliocene) sinistral strike-slip Carboneras Fault (Rehault *et al.,* 1985, Montenat *et al.* 1987; Platt and Vissers 1989; Montenant and Ott d'Estevou 1990; Fernandez-Soler 2001; Martin *et al.* 2003). Uplift of the Betic mountains and volcanic highs is associated with Eocene to Serravallian (middle Miocene) orogenic compression of the Alpine Orogeny and Neogene volcanic activity associated with transtensional and transpressional stresses between the Iberian and African plates (Rehault *et al.,* 1985, Sanz de Galdeano and Vera, 1992; Montenat and D'Estevou, 1996).

Faulting and erosion of volcanic basement in the Cabo de Gata region resulted in the formation of an archipelago of interconnected basins and volcanic highs upon the flanks of which upper Miocene carbonate deposition occurred (Esteban 1979; Esteban and Giner 1980; Esteban 1996). Regionally it has been demonstrated that carbonate deposits are mostly preserved without much structural deformation (Esteban and Giner, 1980; Franseen and Mankiewicz, 1991; Franseen *et al.*, 1993). Late Messinian (uppermost Miocene) to recent uplift of < .05 mm/yr, and

decreasing through time, has been documented by Brachert *et al* (2001), and minor tilting post-dating Pliocene deposition has been described by Hess (2011; 0.3˚ to the Northeast).

PALEOTOPOGRAPHY

Regionally, paleotopography has been demonstrated to play an integral role in determining depositional trends, facies and morphologies in late Miocene carbonate depositional systems (Franseen *et al.* 1993; Goldstein and Franseen 1995; Franseen and Goldstein 1996; Franseen *et al.* 1997a; Franseen *et al.*, 1998; Dillett 2004; Johnson *et al.*, 2005). Despite the close proximity of the Carboneras fault system, and the documentation of clockwise and counterclockwise rotation of neighboring blocks in southeastern Spain (Calvo *et al.*, 1994) it has been determined that the volcanic province to the south of the Carboneras fault, specifically the area along the coast from Rodalquilar to Carboneras, has not been deformed greatly after Miocene deposition (Franseen and Goldstein 1996; Franseen *et al.,* 1997a; Franseen *et al.,* 1998; Johnson *et al.,* 2005, Dillett 2004, Dabrio *et al.,* 1981; Mankiewicz 1996). As indicated by Hess (2011), the Agua Amarga basin area experienced minor tilting to the northeast; this tilting affected the Rellana study area and was taken into account for paleotopography corrections (see reconstruction section below).

The topography on the volcanic substrate beneath the Rellana platform had a major influence on the development of the platform. Preservation of a drainage divide facilitates analysis of the role of paleotopography on platform development. The drainage divide reaches a maximum height of 220 m above modern sea level and separates a steep south dipping (~12˚-25˚, avg. 20˚) substrate slope, which extends from the drainage divide down to modern sea-level, from a gently north dipping (~3˚-8˚ avg. 5˚) substrate slope that extends 1.35 km from the drainage divide before dropping sharply (~22-30˚ avg. 25˚) into the Agua Amarga basin below

(Figs. 1, 3, Appendix 5). Approximately 500 m north of the Rellana platform exposure is a small outcrop of carbonate deposits that were also described for this study. These deposits overlie an intermediate paleotopographic high that features radially-dipping carbonate deposits dipping ~ 10 - 15°.

Three approximately W-NW- to E-SE-trending normal faults were identified in the field on the southern slope of the Rellana Platform, two of which cut across the entire exposed sedimentary package. The southernmost fault displays < 1 m of offset and extends up through DS2 and the base of deposits associated with SBZ 3, however, no displacement was recognized at the top of SBZ 3 deposits, bedding trends within DS2 show minor dip modification within a few meters of the fault, however, outside of this zone dips are consistent. The middle fault has < 1 m of offset and the northernmost fault displays 5 m of offset.

Two NE-SW-trending faults were identified by Lipinski (2010) on the western exposure of the Rellana platform; there is 8 m of offset on the northern fault and 4 m on the southern. Physical tracing of the faults across the Rellana platform is complicated by vegetation, weathering and terrain. Extrapolation of the faults described by Lipinski (which coincide with a modern drainage feature), yield no faulting where they are expected to crop out to the east (Figs. 3, 4). The relationship between these faults and the post-depositional tilting from Hess (2011) is unknown, and there is no clear connection between faults identified by Lipinski (2010) and those observed in this study.

Reconstruction

The tilt model proposed by Hess (2011) uses fault traces identified by Brachert *et al.* (2002) and tilt on a Pliocene marine planation surface (e.g. Woods, 1980; Hess, 2011) to reconstruct paleotopography in the Agua Amarga basin. Extrapolation and application of this

model to the paleotopographic reconstruction of the Rellana platform and surrounding areas indicates potential for 30 m of post-depositional uplift in the areas furthest from the hinge line (5.23 m of uplift/km). Figure 4 demonstrates extrapolation of this tilt and application to the study areas of interest.

Application of this uplift adjustment to previously described areas necessitates re-evaluation of interpreted relative sea-level histories of Toomey (2003) and Lipinski (2010). Evaluation of regional correlations based on relative sea-level history using this reconstruction is discussed in the discussion section of this chapter. Table 2 lists the pinning points used in this study, the original elevations, and the uplift-adjusted elevations.

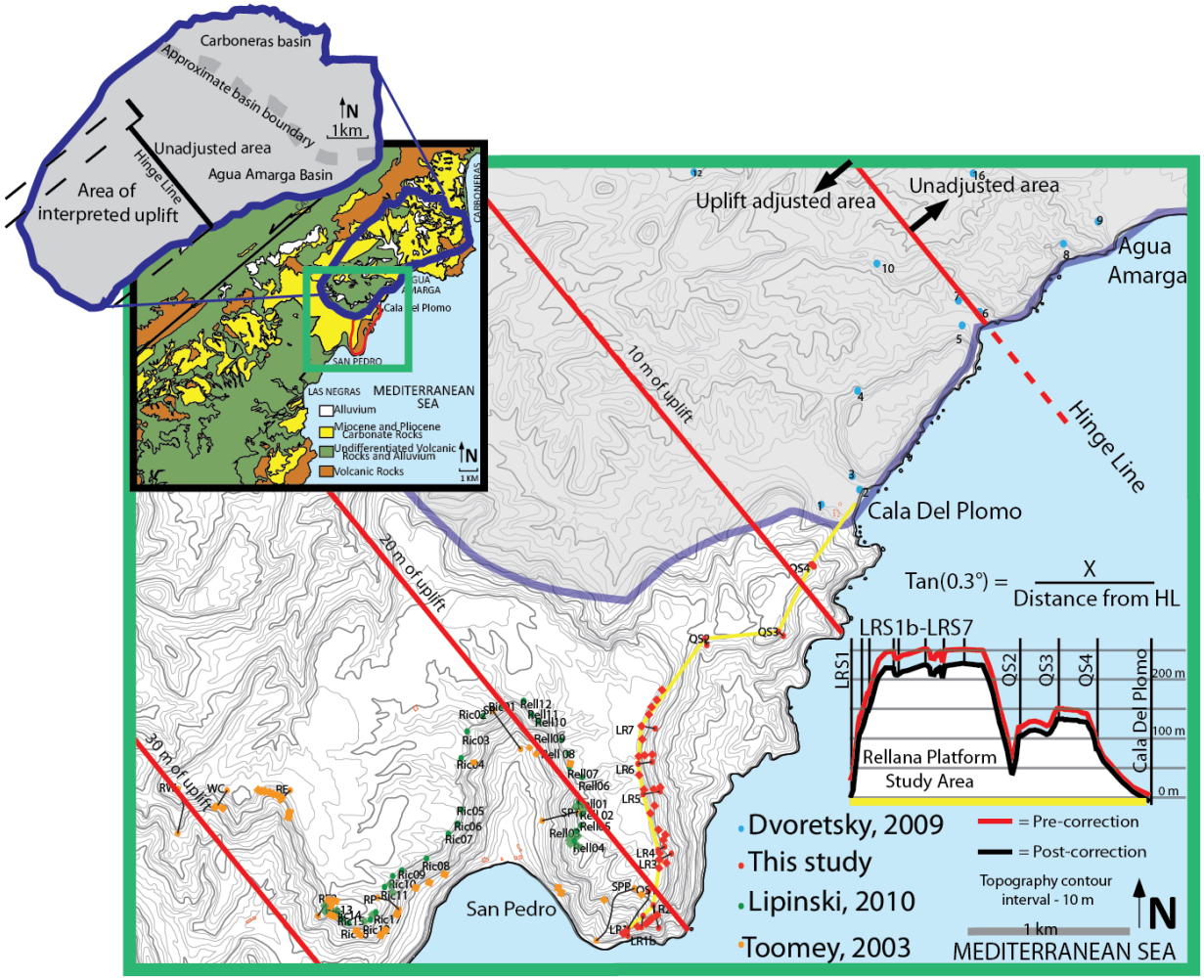

Figure 4: Topographic map of the study area showing application of tilt model from Hess (2011). Blue polygon reflects study area in which Hess (2011) identified and described the Hinge Line feature. Extrapolation of the hinge line to the southwest with 0.3˚ dip is reflected by contoured overlay (red parallel lines). To calculate tilt influence on relative sea-level reconstruction, tilt adjustments are calculated for each pinning point. The location of each stratigraphic section and pinning point are marked on this map, color coordinated to this study and related literature. The schematic model in the lower right shows the variation between unadjusted elevations (red line) versus the adjusted values (black line) along a transect perpendicular to the platform margin (denoted by yellow line).

LITHOFACIES AND DEPOSITIONAL ENVIRONMENTS

Thirteen facies were defined on the platform and distinguished by grain composition, degree of abrasion, sorting and size. Facies for the Rellana platform area were defined using hand sample descriptions (Appendix 2) and refined through thin section analysis (Appendix 3). Characteristics of the facies are summarized in Table 1. Components are listed in decreasing abundance as observed in hand samples and corroborated by thin section analysis. Grain size is described using the Wentworth size classes, and no distinction is made between grains less than 0.0625 mm; grains this size or below are collectively termed 'mud'. Sorting is defined through qualitative analysis of variability of allochem size and distribution. Porosity is determined through visual estimate of pore space in thin-section, emphasized through impregnation with blue epoxy.

The facies identified on the Rellana Platform are grouped into seven depositional sequences the distribution of which is shown in Figure 3. DS1a and DS1b deposits are restricted to the southern end of the Rellana platform, below 66 m. DS2 is present on both the northern and southern slopes, but is thicker (up to 78 m) on the southern end of the platform. DS3 deposits form the bulk of preserved carbonate strata on the Rellana platform and are found on the northern and southern side of the drainage divide. DS4-7 are preserved at the top of the DS3 platform deposits and are on both the northern and southern sides of the drainage divide, ranging in thickness from 0 to 10 m. The following section describes the 13 identified lithofacies and presents interpretations for the environments that resulted in their deposition.

Facies	Components	Grain size / sorting	Sedimentary Structures	Porosity	Depositional Environment
VC Volcanic Conglomerate	Volcanic clasts, bivalves (disarticulated and fragmented), bryozoan fragments, red algal fragments, peloids	Mud to boulder Average (avg.): Cobble Poorly sorted	Centimeter (cm)-scale trough cross bedding, 3 cm scale planar bedding, gradationally fining bedding, meter (m)-scale bedding,	< 5 - 5%- FR, WP	Poorly constrained; Shallow marine, near shore deposition to subaerially exposed
VCC Volcanic Conglomerate with Carbonate Matrix	Volcanic clasts, bivalves (disarticulated, fragmented), foraminifera (and fragments), red algal fragments, intraclasts (CGSPG, FGSWP, FWP, BFR), Coral fragments (P, T), peloids and unknown skeletal components	Mud to boulder Avg.: Cobble Poorly sorted	None visible	< 5% - 15% - MO, BP, BC, WP	Normal marine debris flows - minimum water depth range for deposition is > 10 - 30 m
BFR Bivalve-rich Floatstone- – Rudstone	Bivalves (whole, disarticulated), peloids, gastropods, foraminifera, ostracods, red algae, echinoderm fragments, serpulid worms, coral fragments	Mud to Cobble Avg.: coarse sand Poor to moderate (mod.) sorting	Large bivalve clasts preferentially oriented roughly horizontally, concave orientation variable.	10% - 25%, MO, VUG, FE, WP, BP SH	Isognomon-dominated BFR-Shallow water(<~30m) or deeper Pecten-dominated BFR-20-60 m
FGSWP Fine-Grained Skeletal Wackestone -– Packstone	Peloids, bivalves (disarticulated and fragmented), bryozoans, gastropods, red algal fragments, serpulid fragments, foraminifera, ostracods, echinoderm fragments	Mud to very (v.) coarse sand Avg.: Medium sand Poor to mod. sorting	Massive beds (12 cm - 1.5 m), local thin bedding and laminations (.5 - 3 cm), local thin cross bedding (3 - 5 cm)	5% - 50%, average 10% - MO, BP, WP, FR, FE (rare)	High energy (e) occurrences - 10 -30 m water depth Low e occurrences - 20 - 50 m minimum depth
CGSPG Coarse-Grained Skeletal Packstone- – Grainstone	Bivalves (whole, disarticulated, fragmented), gastropods, serpulid worms, peloids, foraminifera, ostracods, echinoderm fragments, red algal fragments, coral fragments, intraclasts, Bryozoan fragments, coated grains, volcanic clasts	Mud to Pebble Avg.: v. coarse sand Mod. to well sorted	Massive beds (up to 5 m), Planar beds (3 - 5 cm) Laminated to thick (up to 3 m) low angle (<20˚) cross bedding, thin (1 -3 cm) trough cross bedding	10% - 40% average 20 - 25% - MO, BP, WP, VUG, FR, SH	High e occurrences - > 10 - 15 m estimated water depth range. Low e occurrences - forereef slope, 10 - 75+ m interpreted water depth
FWP Foraminiferal Wackestone -– Packstone	Peloids, foraminifera, serpulid worm fragments, bivalves, red algal fragments, gastropods and ostracods	Mud to v. coarse sand Avg.: lower medium/upper fine sand Mod. sorting	Thick (up to 2 m) and dm scale massive beds, thin (1 - 3 cm) planar bedding	< 5% - 40% average 5% - 10% MO, WP, BP, rare VUG	Hemipelagic - pelagic deposition - Deep marine environment, specific depth ranges unknown
RAPG Red Algal Packstone- – Grainstone	Red algae, bivalves, peloids, bryozoan fragments, foraminifera, echinoderm fragments, rare coral fragments, volcanic clasts, gastropods, ostracods	Mud to Cobble Avg.: Coarse to v. coarse sand mod. to poor sorting	Dm scale fining up beds, thick (1 - 4 m) gradationally fining beds, low angle (~10˚ - 20˚) cross beds (.25 - 1.5 m) and thick (1 - 4 m) massive beds.	10% - 40%, average ~20% - MO, BP, SH, FR, rare VUG	Normal marine sedimentation, potential depth range of 30-140 m

Table 1: Descriptive characteristics of the 13 lithofacies identified in this study. Abbreviations used for porosity types are; fracture (FR), intraparticle (WP), moldic (MO), Interparticle (BP), intercrystal (BC), vuggy (VUG), fenestral (FE), shelter (SH) after Choquette and Pray (1970).

Facies	Components	Grain size / sorting	Sedimentary Structures	Porosity	Depositional Environment
CAG Coralgal Grainstone	Coral fragments, serpulid worm fragments, gastropods, bivalves, ostracods, echinoderm fragments, coralline algae, intraclasts, bryozoan fragments, coated grains, volcanic clasts, peloids, foraminifera, unidentifiable skeletal grains	Mud to pebble Avg.: v. coarse sand - gravel Very well to poor sorting	Thick (10 cm to 2 m) massive beds, thin (2 - 5 cm) and thick (5 - 10 cm) trough cross beds.	5% - 50% - MO, BP, BC, WC	High e depositional environment – deposition in <~10 m water depth likely though not definitive
TF *Tarbellastraea* Framestone	Coral (*Tarbellastraea*) molds, bivalves, serpulid worm fragments, peloids, foraminifera, gastropods, ostracods, echinoderm fragments, coralline algal fragments, intraclasts bryozoan fragments, coated grains, volcanic clasts	Mud to cobble/boulder Poor sorting	Massive, topographic relief generating structures	~15%, MO/CH, MO, WP, BP, rare VUG	*In-situ* growth implies water depths between 10 m (head growth forms) - 30 m (branching / stick growth forms)
PF *Porites* Framestone	Coral (*Porites*), bivalves, serpulid worm fragments, peloids, foraminifera, gastropods, ostracods, echinoderm fragments, coralline algal fragments, intraclasts, bryozoan fragments, coated grains, volcanic clasts	Mud to cobble/boulder Poor sorting	Massive, topographic relief generating structures	~15%, MO/CH, MO, WP, BP, rare VUG	*In-situ* implies water depths between 5 - 40 m (branching / stick growth forms) and < 10 m (massive / encrusting growth forms)
ASBS Stromatolitic Boundstone	Peloids, foraminifera, gastropods, ooids (and other coated grains)	Mud to pebble, Clasts avg.: coarse sand, Sample avg.: Mud to v. fine sand Poor sorting	Algal laminations, Laterally linked hemispheroids, stacked hemispheroids	5% - MO, BP, FE, VUG	Normal marine to slightly restricted - low e < 10 m
TBS Thrombolitic Boundstone	Peloids, foraminifera, red algal fragments, gastropods, serpulid worms, coated grains, coral fragments	Mud to Pebble Avg. mud to medium sand Poor to well sorted	Topographic relief building (up to 3 m)	5 - 10% - MO, BP, MO, VUG	High-energy, shallow, near shore deposition likely > 10 - 10 m
OG Oolitic Grainstone	Ooids, coral fragments, bivalves, gastropods, bryozoans, foraminifera, volcanic clasts	Fine sand to pebble Avg.: Upper coarse sand Well - v. well sorted	Thick (5-10 cm) planar cross beds, dm scale trough cross-beds	10% - 40% - average ~20%, MO, BP, WP, FR	High e, shallow marine (< 10 m)

Table 1 continued: Descriptive characteristics of the 13 lithofacies identified in this study. Abbreviations used for porosity types are; fracture (FR), intraparticle (WP), moldic (MO), Interparticle (BP), intercrystal (BC), vuggy (VUG), fenestral (FE), shelter (SH) after Choquette and Pray (1970).

Volcanic Conglomerate – (VC) – present in DS1, 2, 3

Description.--- The Volcanic Conglomerate (VC) facies (Table 1) is composed of volcanic sandstones and conglomerates onlapping volcanic basement. They contain poorly sorted silt- to boulder-sized poly- and monomictic volcanic grains and inter-granular clay particles (Fig. 5A). Skeletal components are generally fragmented and consist of: disarticulated and fragmented bivalves; bryozoans, red algae; encrusting coralline algae; echinoderms; and abundant unidentifiable skeletal components, with the majority of pore space being occluded by silt and/or micrite (Fig. 5B). Clasts range from rounded to angular with minor to moderate abrasion of bioclast ornamentation. Sedimentary structures include: massive beds (Fig. 5C), cm-scale trough-cross bedding, and 3-cm planar bedding. The most distal occurrences are found at the southern end of the Rellana Platform (up to 38 m thick). Deposits thin toward the drainage divide and form a topography-muting wedge on the volcanic substrate. Precise thickness of VC on the northern margin is unknown due to poor exposure. Volcanic clasts > 30 cm within 1 m of the overlying exposure surface typically show concentric cracking and/or autoclastic brecciation. Visual porosity estimates for the VC range from <5% - 5% (Fracture (FR), Intraparticle (WP)).

Interpretation.--- The sedimentary structures, abundant abrasion and cm-scale planar and trough cross-bedding preserved within the VC deposits indicate deposition in a nearshore environment influenced by wave reworking (e.g. Prothero and Schwab, 1996). Concentric cracking and/or autoclastic brecciation of larger volcanic clasts is also seen in basal volcanic conglomerates (immediately overlying volcanic basement) in the Las Negras area, interpreted as evidence for subaerial exposure (Franseen *et al.*, 1993).

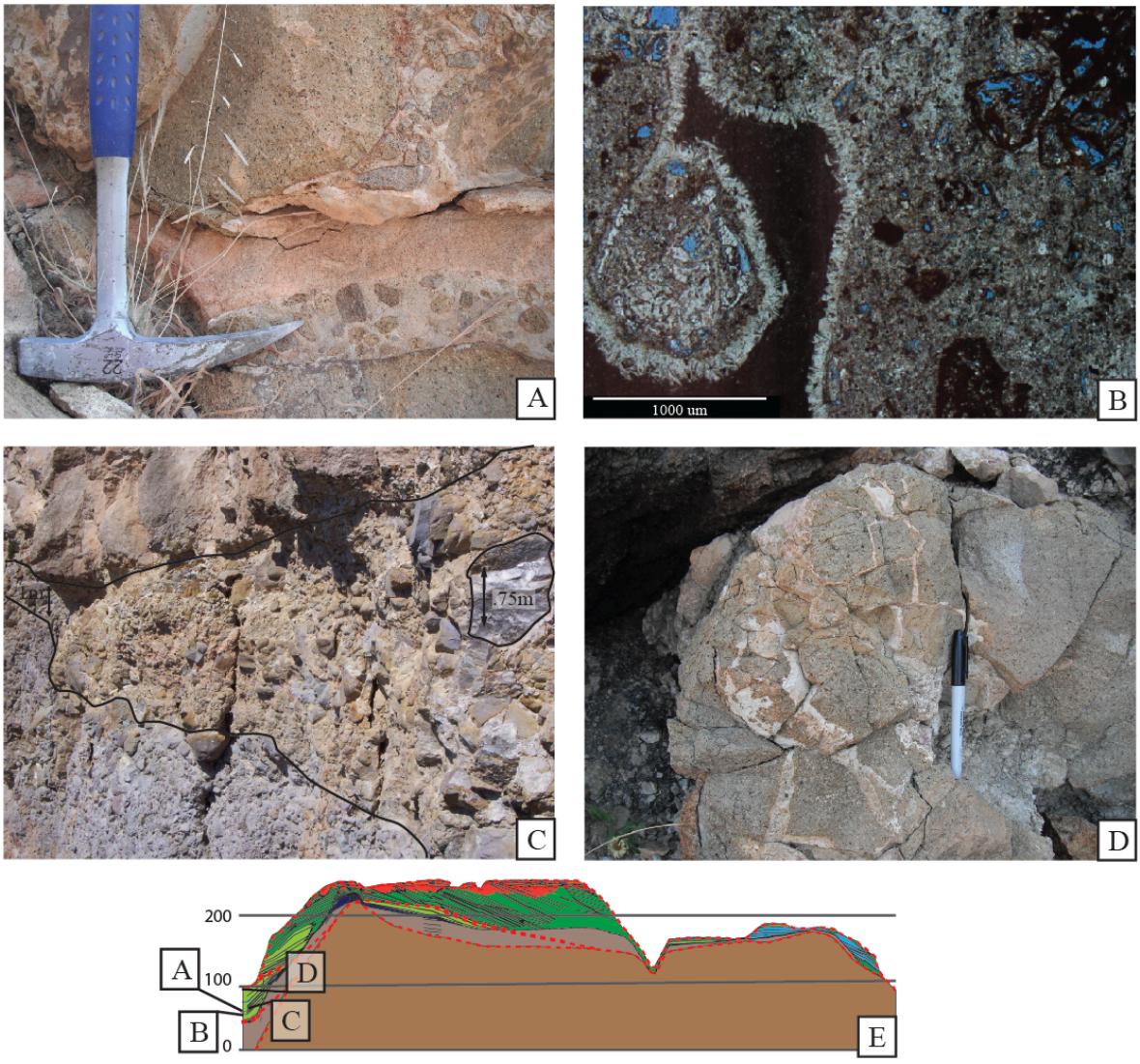

Figure 5: Photographs and photomicrograph of Volcanic Conglomerate (VC) facies with general cross section with respective location of photos and collection points for samples thin sectioned. A) Photograph (near Section LRS1) showing variability of grain-size, rounding and general characteristics of VC facies. Pink colored matrix material is a localized lenticular pocket of well-sorted FGSWP, gray deposits below are volcaniclastic sandstone. Hammer head is 15 cm. B) Photomicrograph of TS34 (cut from sample LRS1-1) showing sub-rounded to rounded volcanic grains with isopachous cement and micritic matrix. 4 X magnification with cross-polarized light, blue epoxy fills pore space. C) Outcrop scale image of southern end of Rellana study area showing transition from VC (basal) to RAPG (upper third) through VCC (middle). Outlined volcanic clast on right of photograph is .75 m thick. D) Photograph showing autobrecciation of volcanic boulder with infilling carbonate cement and volcanic clasts near VC - VCC contact. Pen is 13 cm. E) Generalized cross-section showing the Rellana study area. Elevation is in meters above modern sea-level, red dashed lines represent interpreted sequence boundaries and annotated points correlate to photographs and sampling locations described above.

Volcanic Conglomerate with Carbonate matrix – (VCC) – present in DS1, 2

Description.--- The Volcanic Conglomerate with Carbonate matrix facies (Table 1) contains moderately –to-poorly sorted, rounded to sub-rounded, polymictic volcanic clasts, carbonate intraclasts (BFR, FWP, CGSPG, and FGSWP; see facies descriptions below), and a diverse assemblage of carbonate skeletal components (Fig. 6A, B). Little to no sand-sized or finer siliciclastic material was observed. Abrasion of skeletal components and intraclast rounding varies from minor to abundant, poor sorting is prevalent, and clast size ranges from carbonate mud to volcanic boulder. Skeletal component concentrations are laterally variable and include whole, disarticulated and fragmented bivalves, whole and fragmented foraminifera (primarily benthic), peloids, coralline algal fragments (encrusting, stick form and rare rhodoliths), whole and fragmented gastropods, coral fragments including *Tarbellastraea* and *Porites* and unknown genera (*Siderastraea*?), and unknown skeletal components (generally unidentifiable due to abrasion) (Table 1, Figure 6B). The largest clasts are volcanic boulders (up to .75 m) that locally display concentric cracking (Fig. 6C). The VCC facies lacks internal structure and forms wedge-shaped proximally onlapping and distally draping deposits. This facies directly overlies VC and commonly contains lenticular beds of BFR, FGSWP and/or FWP in the upper 1 - 2 m; the composition of these beds is directly related to the overlying carbonate facies. Rare, isolated pockets of VCC overlying CAG were observed within DS2 (up to 1 m wide, <20 cm thick); all other occurrences are associated with the contact between basal VC and overlying carbonate deposits. VCC deposits, in which volcanic clasts are matrix supported, generally weather recessively and are prone to vegetation, commonly obfuscating contacts (Fig. 6D). Visual porosity estimates range from <5% to 15% (moldic (MO), interparticle (BP), intercrystal (BC), (WP)).

Interpretation.---Significant accumulations of VCC are exposed just south of the drainage divide (Figure 3, 6e), near the LRS2 measured section, Appendices 4 and 5) and are possibly more abundantly preserved, but obscured by vegetation and modern cover. These accumulations (up to 5 m observed) contain matrix-supported clasts (pebble to cobble) that are poorly sorted and generally lack well defined sedimentary structures. The thickest accumulations show poorly defined m-scale fining upward trends (largely defined by gradational reduction of clast size from ~ .75 m at the base to ~ .3m near the top), and are interpreted to be debris flow deposits (e.g. Lowe, 1979). The occurrence of thinner deposits of VCC facies separating basal, shallow-marine/subaerial VC and overlying carbonate deposits across the platform indicates that deposition is related to marine transgression and initial incorporation of volcanic clasts into initial carbonate deposits. The entrainment of volcanic clasts demonstrating spheroidal weathering within marine carbonate material that exhibits no evidence for subaerial exposure indicates that volcanic clasts were locally transported by debris flows from up-dip areas that had been subaerially exposed.

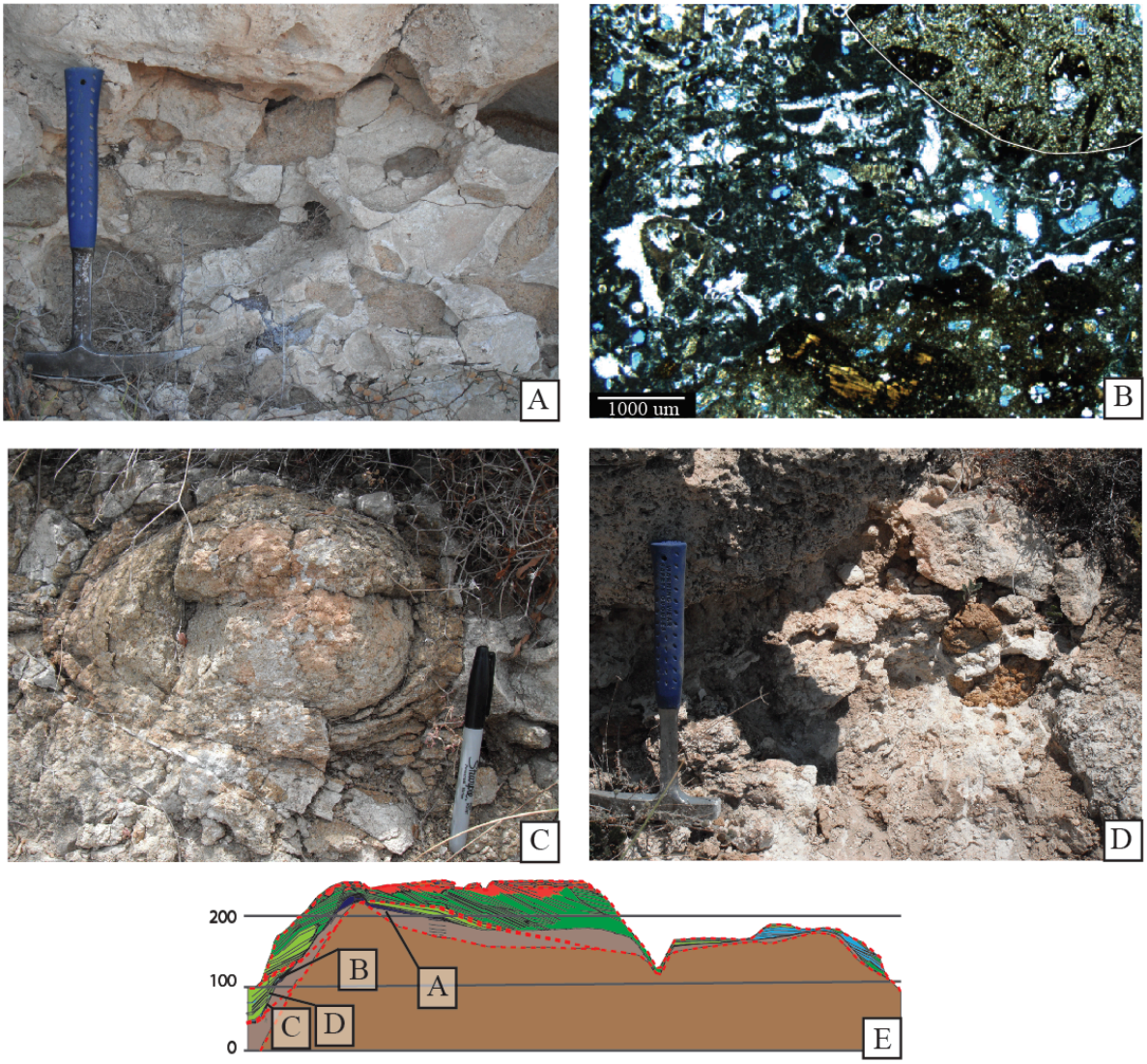

Figure 6: Photographs and photomicrograph of Volcanic Conglomerate with Carbonate matrix (VCC) with general cross section showing respective locations of photos and collection points for samples thin sectioned. A) Outcrop photograph demonstrating sub angular to rounded clasts, clast size range and matrix support framework for VCC deposits. Image from Section LRS3; hammer is 32 cm. B) Photomicrograph of TS60; sample LRS1b-1 showing diverse skeletal assemblage, and abrasion of skeletal material and volcanic grains. Thin white line in upper right accentuates boundary between carbonate sediment and a volcanic clast. 4 X magnification with plain-polarized light, blue epoxy fills pore space. C) Outcrop photograph near section LRS1 showing spheroidal weathering pattern of volcanic clast related to modern exposure, pen is 13 cm. D) Photograph near LRS1b showing sharply gradational upper contact between VCC and overlying RAPG. Note differential weathering between the two units despite similar skeletal assemblages, this is interpreted to be due to a higher micrite content in the VCC deposits. Hammer is 32 cm. E) General cross-section showing Rellana study area. Elevation in meters above modern sea-level, red dashed lines represent interpreted sequence boundaries and annotated points correlate to photographs and sampling locations described above.

Bivalve-rich Floatstone-Rudstone – (BFR) – present in DS1b, DS3

Description.--- The Bivalve-rich Floatstone-Rudstone facies (Table 1) contains carbonate mud to cobble- sized, poorly- to-moderately sorted allochems predominantly consisting of bivalves (whole and disarticulated), peloids, gastropods, and foraminifera, and less commonly: ostracods, red algae, echinoderm fragments, serpulid worms, and rare coral fragments. Whole and fragmented bivalves range in size from 2 cm to 12 cm. The largest whole and disarticulated bivalves were identified as *Isognomon* in the laterally adjacent and upslope equivalent Ricardillo area (Betzler, 2000; Toomey, 2003). They are preferentially oriented horizontally; predominantly concave up, though convex up orientations are not uncommon (Fig. 7A). They display moderately preserved ornamentation. Other allochems are sand sized and show much less preservation of ornamentation (Fig. 7B). Also locally abundant, Pecten bivalves display moderately preserved ornamentation and only minor preference for horizontal orientation, and there is no predominant concave up or down orientation (Figure 7C, D). Occurrences of this facies pinch out up-dip against VC or VCC, and are laterally gradational downdip, interfingering and grading into CGSPG (common in DS3) or RAPG (common in DS1b, less common in DS3). Visual estimates of porosity range from 10-25% and pore types include MO, VUG (vuggy), FE (fenestral), WP, BP, and SH (shelter).

Interpretation.--- Modern *Isognomon* beds are found in shallow-water (< 30 m), temperate to tropical environments (Wilbur, 1983) and at the base of submarine cliffs in shallow, sheltered marine environments (Betzler, 2000; Whorff *et al.,* 1995); however, *Isognomon* shells in the Rellana Platform study area are locally abraded, fragmented and commonly matrix supported, suggesting transport by debris flows and local reworking by currents; There is no correlation between their distribution and occurrence of steep substrates. It is possible that the

bivalves observed in this facies lived higher on the Rellana platform in shallow water and were subsequently reworked and re-deposited down-dip (perhaps by storm events) (Betzler *et al.,* 2000; Fursich and Pandey, 1999; Toomey, 2003). Preservation of whole bivalves and mix of abrasion amount suggests transport distance was not far, although there are no data that constrain transport distance. Similar deposits have been described in the neighboring Ricardillo peak by Toomey (2003) and Betzler (2000) (*Isognomon* rich bed). Other occurrences of pecten rich facies have been described; Betzler (2000) identified pecten rich intervals in the Ricardillo area (considered a sub-unit of the Nodular bryozoan-bivalve facies described with a depth range of 15 – 20 m), and Dillett (2004) identified a Pecten packstone facies with an interpreted water depth between 20 and 60 m based on paleotopographic distribution of Pecten bivalves below a truncated clinoform surface, interpreted to be equivalent to effective wave base (Dillet, 2004). Due to the variability in interpretations regionally, a depth range of 15 – 60 m is assumed for pecten-dominated BFR deposits. Due to the evidence for reworking and transport *Isognomon*-dominated BFR deposits are not used as a water depth control in this study.

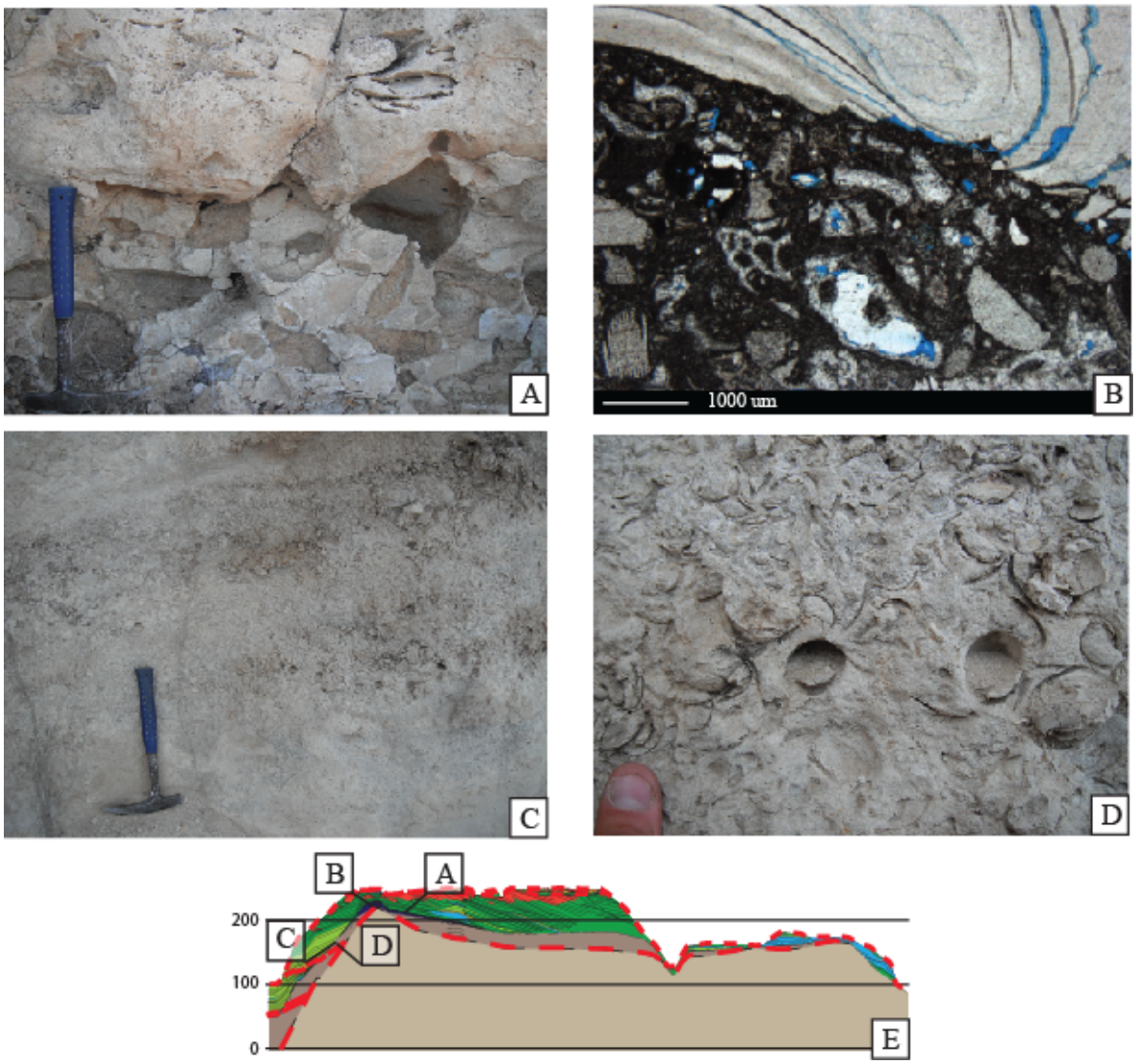

Figure 7: Photographs and photomicrograph of Bivalve Floatstone/Rudstone facies (BFR) with general cross section showing respective locations of photos and collection points for samples thin sectioned. A) Outcrop photograph demonstrating a small group of *Isognomon* bivalve molds overlying VCC deposits, image from Section LRS3, hammer is 32 cm. B) Photomicrograph of TS3; sample LRS3-1 showing diverse skeletal assemblage, and moderate degree of abrasion of skeletal material and grain size variability. 4X magnification with plane-polarized light, blue epoxy fills pore space. C) Outcrop photograph from near section LRS2 showing interfingering and interbedding of BFR with RAPG. Dark shapes observed above and to the right of the hammer are bivalve molds. Hammer is 32 cm. D) Photograph near LRS2 showing close-up of bivalve concentration seen in 5C, note random orientation of molds. Finger is 1 cm across. E) Generalized cross-section showing the Rellana study area. Elevation is in meters above modern sea level, red dashed lines represent interpreted sequence boundaries and annotated points correlate to photographs and sampling locations described above.

Fine-Grained Skeletal Wackestone – Packstone – (FGSWP) – Present in DS1-3

Description.--- The Fine-Grained Skeletal Wackestone - Packstone facies (Table 1) contains moderately- to poorly- sorted carbonate mud to coarse-sand sized (average medium sand) allochems consisting of peloids, bivalves (disarticulated and fragmented), bryozoans, gastropods, red algal fragments and serpulid worm fragments. Minor constituents include ostracods, foraminifera (benthic and pelagic) and echinoderm fragments. Skeletal components display variably preserved ornamentation. Occurrences of this facies within DS1a, Sequence Boundary Zone 3 (SBZ 3) and updip areas in DS3 display more abrasion relative to occurrences in DS1b, DS2 or downdip areas in DS3. Observed sedimentary structures include massive beds (12 cm – 1.5 m thick), local thin bedding or laminations (.5-3 cm), and localized thin low-angle trough cross bedding (3-5 cm). In DS1a, FGSWP deposits occur as highly altered pockets up to 1.25 m long and 12 cm thick (Fig. 8A). These pockets generally have high concentrations of medium sand-sized volcanic grains and abraded skeletal components. The best-preserved lenticular beds show faint low-angle trough cross bedding. In DS1b this facies gradationally overlies VCC and occurs as 12 to 15 cm thick beds gradationally alternating with FWP, with abundantly preserved ornamentation of biotic components and some large (up to 5 cm) skeletal grains. In DS2, FGSWP gradationally overlies RAPG. Skeletal grains are very poorly sorted and exhibit well-preserved ornamentation. No sedimentary structures are visible in FGSWP deposits associated with DS2. SBZ 3 occurrences are well sorted, highly abraded, trough cross-bedded and thinly planar bedded. In DS3, the FGSWP facies is observed interfingering with and gradationally overlying CGSPG deposits, gradationally fining into FWP, as well as in sharp contact with PF and CAG. Where FGSWP interfingers with and gradationally overlies CGSPG (downdip DS3), it tends to be poorly sorted and have better preservation of ornamentation on

grains compared to DS1a and SBZ 3. FGSWP in close proximity to CAG and PF (updip DS3, above 230 m) has poorly preserved ornamentation, moderate sorting, reduced carbonate mud content relative to downdip occurrences, and displays faint trough cross bedding or thin planar beds (2 - 3 cm). Gradational fining upward into FWP is observed at the lowest extent of DS3 on the northern end of the Rellana exposure (near sections QS3 and QS4: Figure 3, Appendix 5). Visual porosity estimates range from 5% to 50% with an average ~10% consisting of MO, BP, WP, and Fracture (FR) pore types.

Interpretation.--- The various occurrences of the FGSWP facies suggest multiple depositional environments. A high-energy marine environment is suggested where this facies is moderately- to well-sorted, ornamentation is not well preserved, faint trough cross bedding or thin planar bedding is present, and gradational transitions into this facies from coarser, less abraded facies below (CGSPG and RAPG) occurs (observed in DS1a, 3, 4 and updip DS3). A modern high-energy bryozoan-rich analog suggests these deposits form in the infralittoral and coastal zone (10 - 30 m deep) (Martin *et al*., 1996; Brachert *et al.,* 1998; Betzler *et al.,* 2000). A maximum relief of 8 m is observed in the Rellana area suggesting a water depth range of 18 - 30 m for occurrences of high-energy FGSWP.

Other occurrences of the FGSWP suggest a lower energy setting where this facies shows preservation of ornamentation, poor sorting, massive bedding and close association with FWP (observed in DS1b or downdip DS3). These downslope equivalents to coarser deposits (CGSPG or RAPG) most likely formed through reworking and downslope transport, and may represent toe-of-slope deposits (after Ahr, 1973; Read, 1985 and others) or deposits associated with debris flows (e.g. Lowe, 1979). A debris flow mechanism is proposed due to the random orientation of clasts, matrix support of rare large clasts, general lack of internal structure or gradational bedding

that would be expected in a turbidite deposit. The possibility for a turbidite origin for these deposits is not ruled out, however, as original sedimentary structures may have been obscured by abundant bioturbation, although no clear bioturbation was observed within FGSWP deposits. Decreased energy could also be related to increase in relative sea level, which is explored in more detail later in this chapter. These occurrences of the FGSWP facies are similar to the Volcaniclastic Foraminiferal Wacke-Packstone (VFWP) facies described in the neighboring Agua Amarga basin by Dvoretsky (2009) and the unbroken mollusk / bryozoan-rich facies described by Esteban (1979) at depths of 30 - 80 m in the modern Mediterranean. Physical tracing of these deposits into the neighboring Ricardillo area indicates they are correlative to downdip extremes of the Coarse Grained Mollusc Bryozoan Packstone (CGMBP) of Toomey (2003). The CGMBP facies of Toomey (2003) has an interpreted water depth range of 30 – 180 m (Table 2). These facies are attributed to deposition by pelagic, hemipelagic sedimentation or low-density turbidity currents (Toomey, 2003). The physical tracing of stratigraphic relationships and relief of FGSWP deposits shows relief as great as 50 m on the northern end of the Rellana platform, suggesting a water depth range similar to that of the modern analog (30 - 80 m) for low energy occurrences of this facies. The extended depth range identified in the Ricardillo area suggests the deeper limit of this range is conservative.

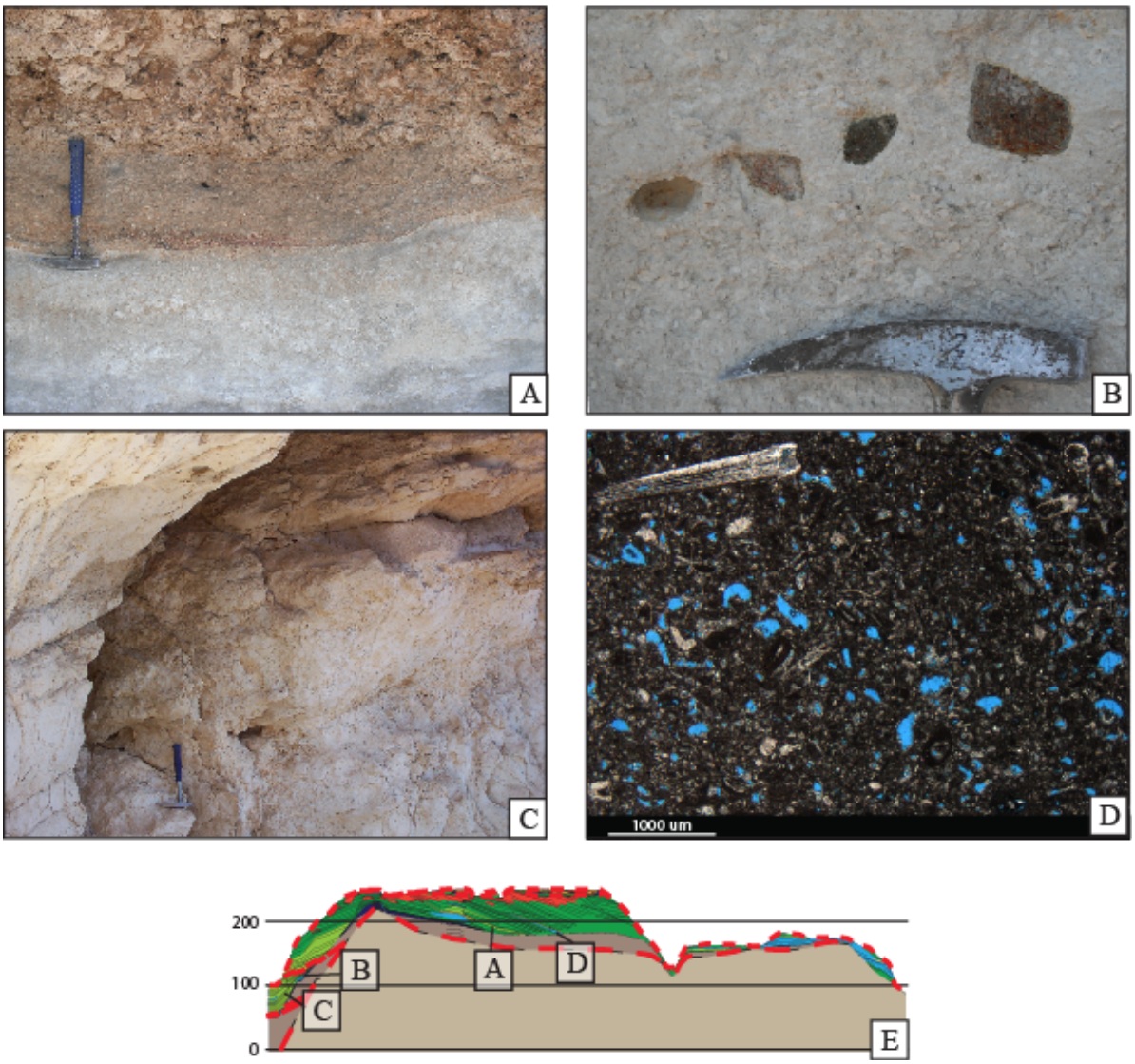

Figure 8: Photographs and photomicrograph of Fine Grained Skeletal Wackestone/Packstone (FGSWP) with general cross section showing respective locations of photos and collection points for samples thin sectioned. A) Outcrop photograph showing contact between well-sorted FGSWP (lower white unit) with poorly sorted FGSWP (lower red unit) and gradationally overlying CGSPG (coarse-grained upper red unit). Hammer is 32 cm. B) Close up of volcanic grains entrained in massive poorly sorted FGSWP of DS2, volcanic clasts aligned with bedding trends. Hammer head is 15 cm and oriented horizontally. C) Outcrop photograph showing sharply gradationally bound well-sorted FGSWP (light red wedge) at the top of a DS2 shoaling upward package. Hammer is 32 cm. D) Photomicrograph of well-sorted FGSWP in DS2 deposits north of the drainage divide displaying prominent moldic porosity. Gastropod shows abnormally high preservation of ornamentation. Scale bar is 1 mm. 4X magnification with plane-polarized light; blue epoxy fills pore space. E) Generalized cross-section showing the Rellana study area. Elevation is in meters above sea level, red dashed lines represent interpreted sequence boundaries, and annotated points correlate to photographs and sampling locations described above.

Coarse Grained Skeletal Packstone-Grainstone – (CGSPG) – Present in DS2-7

Description.--- The Coarse Grained Skeletal Packstone-Grainstone facies (Table 1) contains a wide variety of allochems that encompass the spectrum of observed grain types (excluding abundant pelagic foraminifera and intact *Isognomon* bivalves). Observed allochems include: bivalves, gastropods (including vermetids), serpulid worms, peloids, benthic and pelagic foraminifera, ostracods, echinoderm fragments, red algae (fragments, rhodoliths, branching and 'club' growth forms), coral fragments (*Tarbellastraea*, *Porites* and rare *Siderastrea*), intraclasts of coralgal framestone (PF and TF) and coralgal grainstone (CAG), bryozoans, coated grains, and volcanic grains. Abrasion of these grains is variable and sorting trends range from poor to well; grain size ranges from carbonate mud to very coarse sand. Observed sedimentary structures include massive beds, planar beds (3-5 cm) and laminated to thick (up to 3 m), low-angle (< 20˚) cross bedding, and thin (1 - 3 cm) trough cross bedding. In SBZ 3 all grains show significant abrasion. Bedding geometries consist of trough cross bedding and thin (3-5 cm) planar bedding that onlap detrital boulders of coralgal framestone. Strata are interbedded with and adjacent to CAG. In DS3, abrasion of intraclasts and coral fragments increases significantly downslope in comparison the updip extent of this facies. Echinoderm and red algal fragments generally show moderate to high abrasion and finer grained allochems (e.g. foraminifera, ostracods, and peloids) show minor to moderate abrasion. In DS3 the lowest occurrences of CGSPG onlap paleotopography and grade downdip into and interfinger with RAPG deposits. Above, this facies onlaps and interfingers with CAG and PF in an updip direction, and displays thick low-angle cross beds, thin trough cross beds and massive beds. Locally CGSPG grades up into FGSWP. In DS4-7, planar beds of variable thickness onlap and drape PF and TBS deposits. Beds are thinly laminated or trough cross-bedded. The facies contains highly abraded allochems, with sporadic

angular PF and CAG intraclasts, large coral clasts, and high concentrations of ooids and other coated grains. Visual porosity estimates range from 10% to 40%, with 20 - 25% being average. Types of porosity observed are MO, BP, WP, VUG, FR, and SH.

Interpretation.--- CGSPG is interpreted to be the result of deposition in several marine environments. In SBZ 3, the abundant abrasion of components, close proximity to, and interbedded relationship with CAG, and thin trough cross bedding and planar beds suggest high-energy deposition. This is further supported by the abundant clast-supported detrital (boulder-sized) PF and TF intraclasts and their relatively even distribution throughout the stratigraphic extent of upper DS2 (Figure 1, 3, 9E, Appendix 5). The presence of thick accumulations of moderate- to high-energy deposits (15 m) sharply overlying interpreted deeper-marine facies (FWP) suggests erosion, reworking and re-deposition related to a relative sea-level fall. This is supported by evidence for incorporation of previously subaerially exposed material within stratigraphically equivalent deposits in the Las Negras area to the south (Appendix 5 for basin correlation, Chapter 2 'Regional Stratigraphic Relationships' below for more detail).

In DS3 the stratigraphically lowest occurrence of this facies grades downdip into RAPG and appears contemporaneous with or just preceding initial aggradational reef development (based on bed stacking patterns) (Appendix 5). The inclusion of *Porites* coral clasts in the CGSPG indicates *Porites* reef growth had initiated, however, initial bedding trends do not steepen proximally. Instead, beds drape paleotopography, grade updip into VCC and onlap volcanic basement. These deposits are interpreted to represent the lateral transition from a bypass surface into clinoform development on the steep southern margin. Above this, CGSPG occurs in packages that decrease in dip (25˚ down to ~5˚) downslope from interfingering and interbedded PF and CAG. The variable abrasion of larger grains is interpreted to reflect reworking and

transport of detritus shed from *in situ* reef development updip. The incorporation of reef detritus and the shallowing dip away from *in situ* reef suggests that the DS3 occurrence of CGSPG represent forereef slope deposition in normal marine conditions. A minimum water depth of 75 m is interpreted through physical tracing of clinoform relief. Similar deposits have been described in the neighboring Ricardillo area by Toomey (2003) (Fore Reef Talus facies), which are interpreted to be deposited in water > 40 m deep. In DS4-7 concentrations of coated grains, interbedding and lateral gradation into OG and angular coralgal clasts suggest high-energy deposition in shallow marine conditions. Lipinski (2010) studied the Terminal Carbonate Complex (TCC) on the eastern side of the Rellana platform and described several oolite and skeletal grainstone units that are laterally equivalent to DS4-7 CGSPG deposits (Table 4). Depths attributed to skeletal and oolitic grainstone range from slightly more or less than 10 m (Lipinski, 2010). Based on observations in the Rellana area, CGSPG deposits form in environments with interpreted water depth ranging from < 10 m to 75 m. As a result, this facies is not a useful indicator of sea level position.

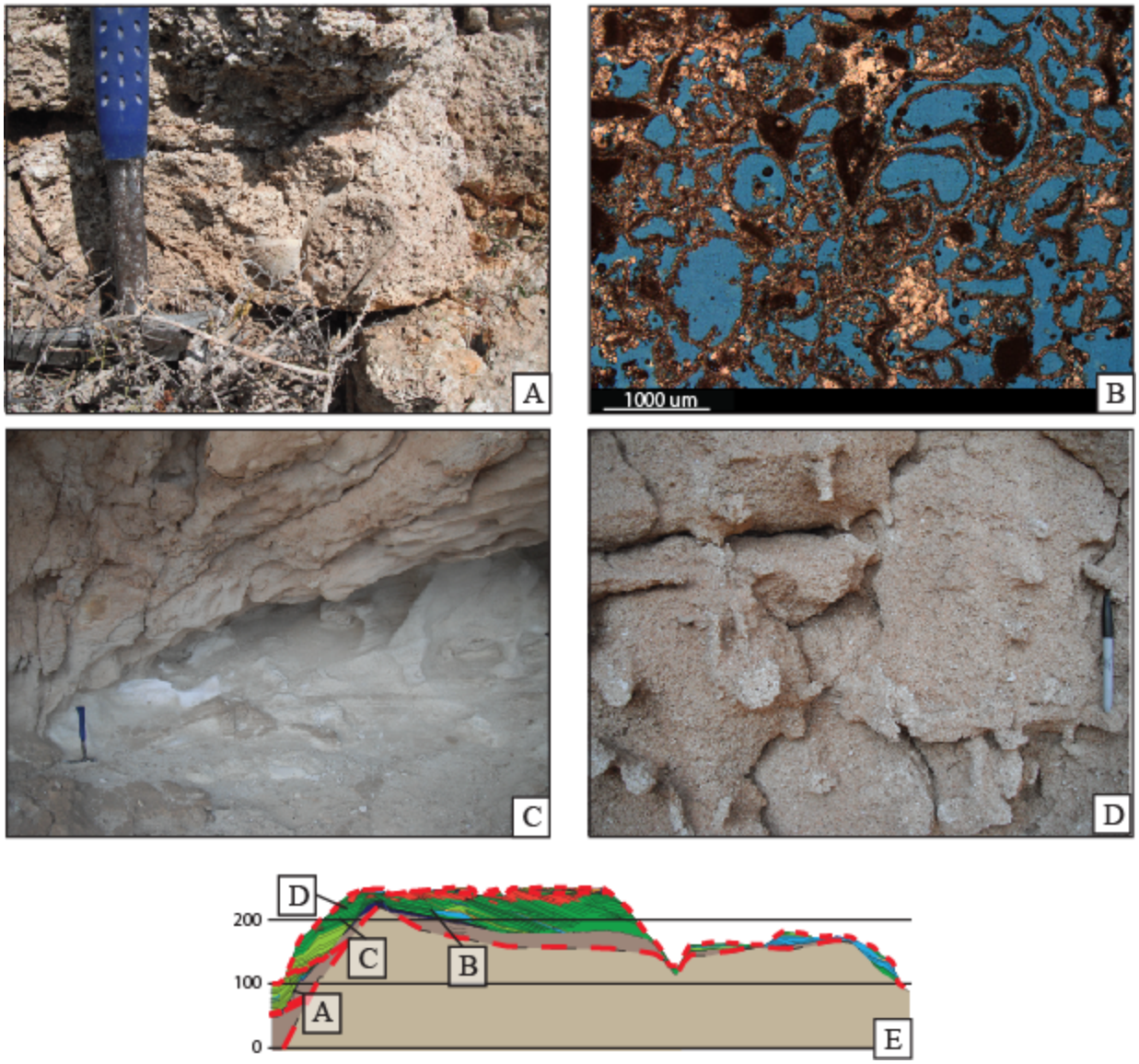

Figure 9: Photographs and photomicrograph of CGSPG with general cross section showing respective locations of photographs and sample collection points. A) Outcrop photo showing diverse skeletal assemblage and poor sorting typical of CGSPG deposits within DS2. Hammer head is 15 cm. B) Photomicrograph of CGSPG deposits north of drainage divide showing diverse, well sorted deposit, large grains are uncharacteristically uncommon (note echinoderm spine, ~1.5 mm) clasts up to 3 cm are common. 4X magnification, plane-polarized light. Blue epoxy fills pore space. Scale bar is 1 mm. C) DS3 CGSPG outcrop photograph shows cross bedding. Hammer is 32 cm. D) Photograph of CGSPG deposits overlying C, featuring abundant bioturbation; ichnofacies unknown. Pen is 13 cm. E) Generalized cross-section showing platform. Elevation in meters above sea level, red dashed lines represent interpreted sequence boundaries, annotated points correlate to photographs and sampling locations described above.

Foraminiferal Wackestone - Packstone – (FWP) – Present in DS1b, 5

Description.--- The Foraminiferal Wackestone - Packstone facies (Table 1) is composed of moderate to poorly sorted, carbonate mud to very-coarse (average grain size of lower medium to upper fine sand) sand-sized allochems, including peloids, foraminifera (planktonic dominant), serpulid worm fragments, bivalves (fragmented, disarticulated uncommon), red algal fragments, gastropods and ostracods. Massive meter, decimeter and thin planar beds drape paleotopography. In DS1b this facies is present in decimeter-scale beds gradationally alternating with FGSWP. In the distal extent of DS3 FWP deposits form massive, thick (up to 2 m) beds with locally visible, faintly preserved thin planar beds. Visual estimates of porosity range from <5-40% and average 5-10%; pore types include MO, WP, BP, rare VUG.

Interpretation.--- Given the high carbonate mud content, the high concentration of planktonic foraminifera, draping bed geometries and lack of distinct sedimentary structures, this facies is interpreted to result from pelagic/hemi-pelagic sedimentation. Bioturbation of these deposits is expected, but is likely masked by the volume of bioturbation or alteration due to exposure coupled with modern diagenesis. This facies is particularly recessive and extremely friable (Fig. 10a).

Foraminiferal Wacke-Packstone facies are described in the Agua Amarga basin (Dvoretsky, 2009) and the Las Negras Area (Franseen *et al.*, 1993) and the Rodalquilar area farther south (Johnson, 2005) as resulting from hemipelagic-pelagic sedimentation. Similar to modern Mediterranean deposits, they are interpreted to be formed at depths greater than 100 m (Carannante *et al.,* 1988). Physical tracing of FWP facies in the Rellana area shows 10 m of relief, indicating a potential water depth range of at least 100 – 110 m.

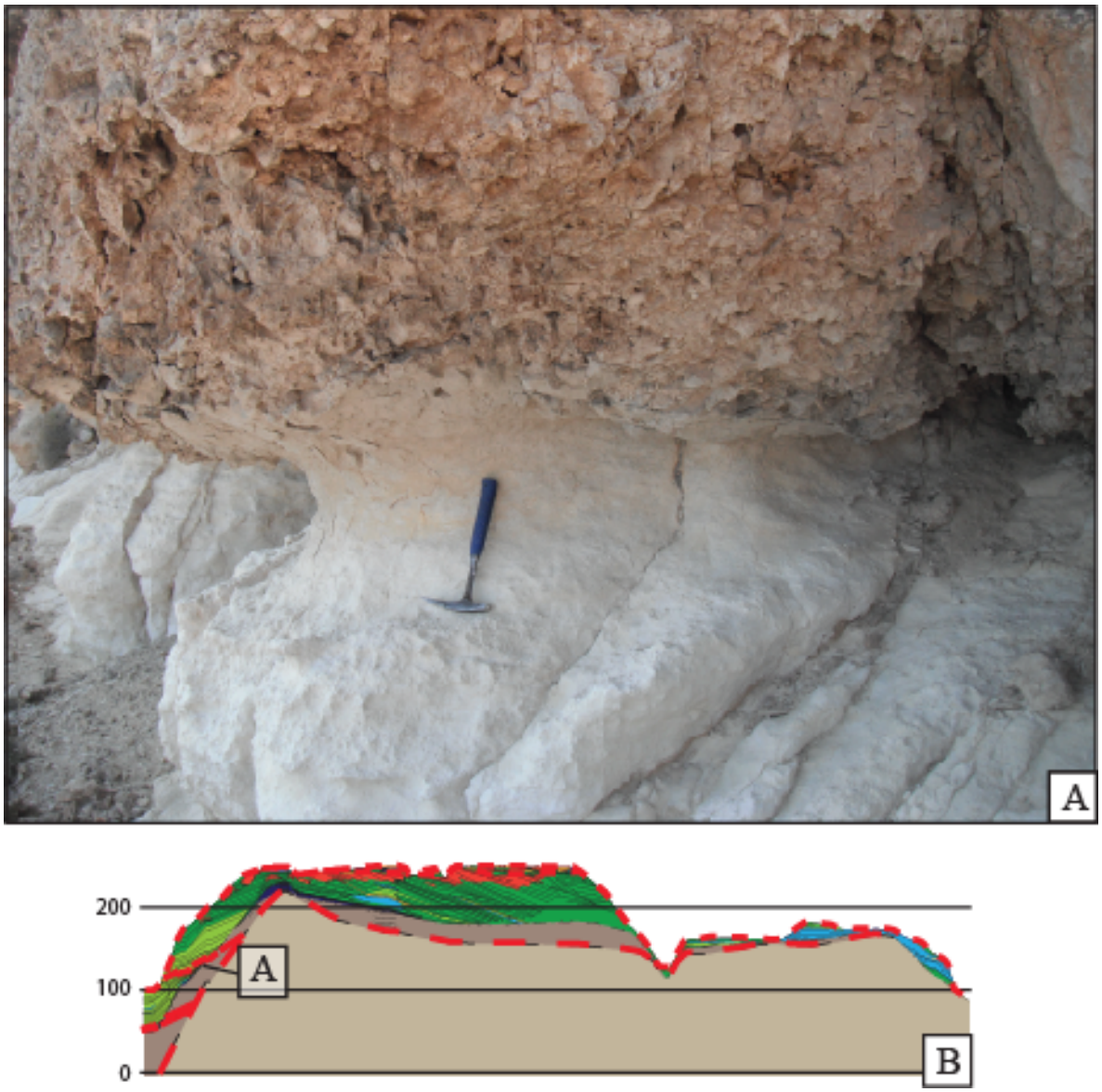

Figure 10: Photograph of Foraminiferal Wackestone – Packstone (FWP) and cross section showing general location. A) Photograph shows erosional truncation of recessive FWP deposits by CAG of SBZ 3. More resistant lower unit is RAPG. These deposits are generally poorly exposed. Hammer is 32 cm. B) Generalized cross-section showing the Rellana study area. Elevation is in meters above sea-level, red dashed lines represent interpreted sequence boundaries and annotated points correlate to photographs and sampling locations described above.

Red Algal Packstone – Grainstone – (RAPG) – Present in DS2, 5

Description.--- The Red Algal Packstone-Grainstone facies (Table 1) contains moderately- to poorly- sorted, carbonate-mud to cobble- sized (average coarse- to very-coarse sand) allochems dominated by the presence of red algae, which occurs as branching, encrusting and rhodolith forms. Also present are whole, disarticulated and fragmented bivalves, peloids, bryozoan fragments, foraminifera (benthic dominant) echinoderm fragments, coral fragments (*Tarbellastraea* and *Porites*), and rare volcanic clasts; other minor constituents include gastropods, and ostracods. All clasts show locally variable abrasion and grain breakage with the range covering the spread from minor to high abrasion. All observed volcanic clasts are sub-round to round. In DS2, RAPG deposits are finer grained (largest grains are 3 - 4 cm volcanic clasts) and locally show faint, poorly preserved (possibly bioturbated) decimeter scale bedding composing well developed, 1 - 4 m thick beds which onlap volcanic basement. Poorly preserved gradational fining is observed both on the individual bed scale and on the well developed bedding scale (1 - 4 m). Locally RAPG gradationally fines up into FGSWP and in DS2 deposits coral content increases near the top of the unit.

In DS3 this facies occurs as basal deposits and as downdip equivalents to CGSPG where it features higher photozoan (e.g. reef-building coral, large benthic foraminifera, increased mud content, abundant peloids) and bryozoan content. Deposits feature coarse (generally > 1 cm) skeletal components (predominantly heterozoan; e.g. rhodoliths and other red algal growth forms including branching and 'club', bivalves, gastropods, echinoderms *sensu* James, 1997) with moderately- to well-preserved ornamentation in finer grained (sand-sized) material composed of abraded, rounded and poorly sorted skeletal components (photozoan and heterozoan components). DS3 RAPG deposits occur as low angle cross-bedded and massive beds that drape

paleotopography, and grade updip into VCC. Stratigraphically higher in the section, beds begin to increase dip proximally where they drape possible clinoform surfaces, grading updip into CGSPG. The facies distinction at this interface is largely determined by photozoan content compared to red algal content; this gradational facies change is driven by coral detritus distribution. Porosity estimates for the RAPG facies range from 10% to 40%, and average around 20% (MO, BP, SH, FR, rare VUG).

Interpretation.--- Facies similar to RAPG were described by Betzler (2000) (Coralline Algal facies) and Toomey (2003) (high coralline algal concentrations in distal Coarse Grained Mollusk Bryozoan facies) in the neighboring Ricardillo peak area. Although they are poorly defined, the decimeter scale fining-up beds within larger fining up packages observed in DS2 seem indicative of turbiditic deposition. Twelve shoaling upward cycles were identified in the neighboring Ricardillo area (Toomey, 2003), cycles are interpreted to be a reflection of increased energy related to repeated relative falls in sea level (more detail in 'Platform Depositional Sequences and Interpretations' section below).

These deposits are laterally equivalent to the coarse grained mollusk bryozoan packstone (CGMBP) described by Toomey (2003) who identified a distal increase in red-algal content, coupled with decreased occurrence of fine grained mollusk bryozoan packstone (FGMBP) (FGSWP equivalent) which is consistent with observations made in the Rellana area. RAPG deposits associated with DS2 are similar to nodular bryozoan-bivalve and the coralline algal facies of Betzler, (2000). Modern analogs for the RAPG, the 'rhodalgal' facies of Carannante *et al*. (1988) suggest deposition in a low energy environment, 40 - 100 m water depth. Further constraints on water depth for equivalent facies were made by Toomey (2003) and based on similarities between components and textures with the modern Mediterranean unbroken

mollusk/bryozoan-rich facies of Esteban (1979) that forms in 30 - 80 m of water. Deposits seen on Rellana are generally finer grained, contain a higher concentration of planktonic foraminifera and carbonate mud, and are interpreted to have formed in a deeper environment, more similar to the 'rhodalgal' facies of Carannante *et al.* (1988). Physical tracing of paleotopographic relief in the Rellana area (45 m) indicates a minimum water depth range of 75 - 125 m for DS2 RAPG deposits.

In DS3 RAPG occurs as the downdip equivalent to CGSPG and reef core (PF, CAG and rare TF) deposits. The preservation of ornamentation of the coarse, predominantly heterozoan skeletal components juxtaposed with the abundant abrasion and rounding of fine-grained material surrounding them indicates that the coarser skeletal components have undergone less transport relative to the fine-grained sediment, and may be at or near original growth position. The fine-grained material is likely sourced from an updip high-energy environment (*sensu* the heterozoan clinoform model of Dillett (2004). The observed transition from paleotopography draping beds observed in the lowest stratigraphic occurrences of RAPG in DS3 up into proximally steepening, RAPG grading updip into CGSPG is interpreted to be due to reef development updip and the transition from bypass sedimentation into clinoform development (more detailed description of this and related features in 'Platform Depositional Sequences and Interpretations' section). The paleotopographic relief of RAPG deposits in DS3 is 40 m, indicating a minimum water depth range of 70 – 120 m.

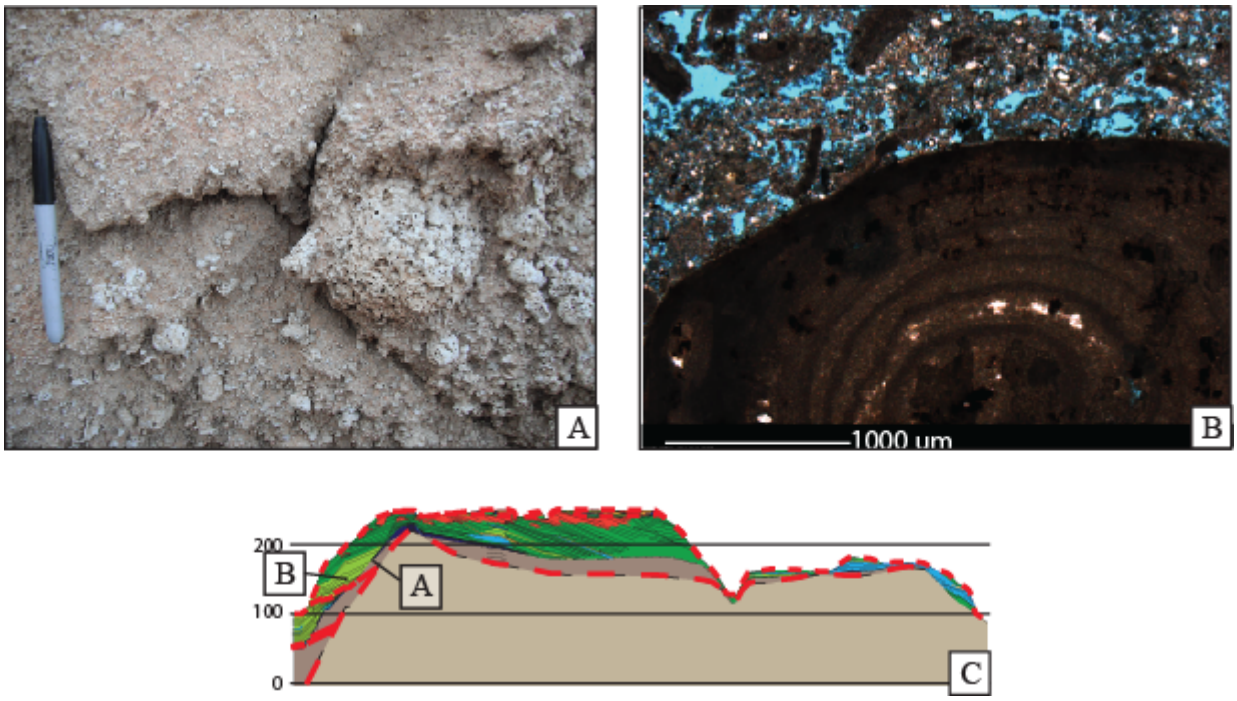

Figure 11: Photograph and Photomicrograph of Red Algal Packstone – Grainstone (RAPG) and general cross section showing respective locations of photos and collection points for samples thin sectioned. A) Photograph of outcrop near section LRS2 showing well developed rhodoliths and poorly developed normal grading. Pen is 13 cm, large rhodolith is 7 cm. B) Photomicrograph of RAPG from DS3 RAPG deposits south of the drainage divide, thin section shows a rhodolith surrounded by finer, abraded skeletal grains with abundant micritization. 10X magnification with plane-polarized light, blue epoxy fills pore space. Scale bar is 1 mm. C) Generalized cross-section showing the Rellana study area. Elevation is in meters above sea level, red dashed lines represent interpreted sequence boundaries and annotated points correlate to photographs and sampling locations described above.

Coralgal grainstone – (CAG) – Present in DS2, 5, 6

Description.--- The Coralgal Grainstone facies (Table 1) contains a diverse assemblage of components that include: coral fragments (*Porites, Tarbellastraea* and *Siderastrea)*, serpulid worms, gastropods, bivalves (disarticulated and fragmented), ostracods (whole and fragmented) echinoderm fragments, red algal fragments, intraclasts, bryozoan fragments, volcanic grains, intraclasts of PF and TF, rare coated grains, peloids, foraminifera and unidentifiable highly abraded grains. These grains show a wide range of roundness, abrasion, and variable sorting. Grain size ranges from carbonate mud to cobble (50 cm); average clast size is 2 - 5 mm (upper v. coarse sand to gravel). Bedding is variable, consisting of thin to thick massive beds (10 cm up to 2 m), thin (2 - 5 cm) and thick (5 - 10 cm) trough cross beds. Generally, this facies is found in close association with coralgal framestones (PF and TF facies) and laps onto both *in-situ* and displaced deposits of the framestone facies. The occurrence of this facies in upper DS2 is widespread and variable. The variability is mostly seen in various concentrations of allochems distributed throughout the stratigraphic extent of the platform unit. Examples of component concentration include stick-morphology coral detritus (*Tarbellastraea* dominant*,* less commonly *Porites*, other coral genera were observed, but due to moldic preservation, not readily identifiable), PF and TF intraclast concentrations, and concentrations of coated grains (observed as lenticular units up to .75 m wide, 10 cm thick), which reach sufficient ooid concentrations to be considered OG facies deposits and are discussed in more detail in the OG facies description below. These concentrations appear to have no clear stratigraphic constraints. In DS3 this facies flanks *in situ* reef core (consisting predominantly of *Porites,* though *Tarbellastraea* and *Siderastrea*) and fills in inter-framework areas. In DS4-7 distribution is similar, although reef development is less pronounced. Additionally, coated grains and ooids are locally abundant, and

CAG deposits interfinger or grade laterally into OG deposits. Visual estimates of porosity range from 5 - 50% and pore types include MO, BP, BC, and WC.

Interpretation.--- The abundant abrasion of skeletal grains, abundant trough cross bedding and general lack of carbonate mud suggests deposition in a high-energy environment. In SBZ 3 CAG deposits onlap and form trough-cross bedded deposits between detrital 'mega-breccia' clasts, and interfinger, interbed and grade into CGSPG and rare OG deposits. Physical tracing of strata over paleotopography suggests a minimum water depth of 30 m, however, this is complicated by a depositional interpretation for SBZ 3 which proposes that these deposits are related to a relative fall in sea-level. This is evidenced by the presence of subaerially altered clasts within marine sediment, facies interpreted as shallow-water deposits spanning a larger paleotopographic range than their depositional environment would suggest (OG), and the subsequent subaerial exposure of SBZ 3 (for more detail, see the 'Platform Depositional Sequences and Interpretations' section in this chapter).

The close proximity to and onlapping of cliff-forming (up to 18 m) *in situ* coralgal framestone facies and high content of coralgal detritus in DS3 CAG deposits suggest deposition associated with reef development (part of the Reef Core facies identified in the Ricardillo area by Toomey (2003). A minimum water depth is more precisely constrained for these deposits by using coral morphology of the *in situ* coralgal framestone facies (5-40 m water depth, Saint-Martin, 1990; Riding *et al.,* 1991; Pomar, 1983; 1991; Esteban, 1996, for details see PF facies description below).

In DS4-7 CAG flanks massive coral heads and branching colonies (up to 3 m) and is interbedded with OG deposits. The massive coral head morphology and abundance of coated grains point toward a shallow, high-energy depositional environment. Massive head coral growth

forms associated with CAG and OG deposits are interpreted to grow in water depths less than 10 m (Massive-coral zone (> 10 m) of Pomar (1983, 1991), the ‘shallow reef wall’ (> 10 m) of Esteban (1996)). The presence of OG deposits also indicates water depths less than 10 m (Ball, 1967; Loreau and Purser, 1973; Hine, 1977; Flugel, 1982; Harris, 1983; Lloyd et al., 1987; Tucker and Wright, 1990; Burchette and Wright, 1992; Major et al., 1996). Paleotopographic relief of CAG deposits in DS4-7 is limited by the lateral discontinuity of the facies in these sequences. The thickest occurrence has a relief of 2 m, suggesting a minimum water depth of 10 – 12 m for CAG deposits in DS4 – 7.

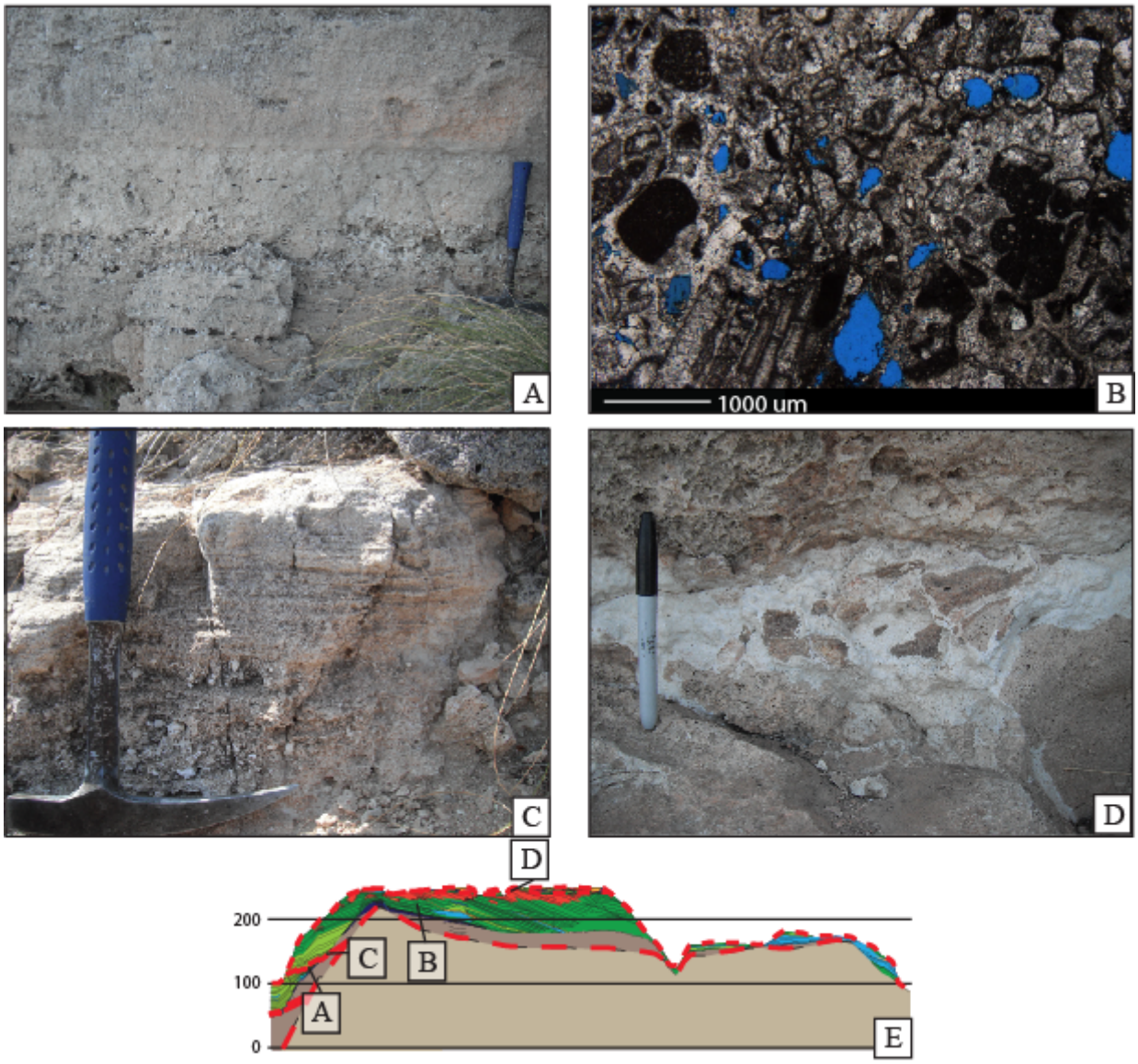

Figure 12: Photographs and photomosaic showing characteristics of the Coralgal Grainstone (CAG) facies and general cross section showing respective location of photos and collection points for thin sectioned samples. A) Photograph of outcrop on SBZ 3 deposits featuring thin (1-2 cm) planar-bedded OG bound by CGSPG below and CAG above, these deposits are nearby potentially *in situ Tarbellastraea* reef growth. Hammer is 32 cm. B) photomicrograph of contact between CAG (lower right) and OG (upper left) featuring rare ooids and abundant coated grains. Sample collected within *in situ Porites* reef deposits of DS3. 4X magnification with plane-polarized light, blue epoxy fills pore space. Scale bar is 1 mm. C) Thin (1-1.5 cm) low angle cross bedded OG deposits in the 3rd sequence of DS 4 - 7. Hammer head is 15 cm. D) Alteration typical of DS 4 - 7 deposits that fills fractures and pore space within DS 4 - 7 OG (lower portion of photo) and other facies (for example, CGSPG and CAG in upper portion of image). Pen is 13 cm. E) Generalized cross-section showing the Rellana study area. Elevation is in meters above sea level, red dashed lines represent interpreted sequence boundaries and annotated points correlate to photographs and sampling locations described above.

Porites Framestone – (PF) – Present in DS2, 5, 6

Description.--- Coral framework in the *Porites* Framestone facies (Table 1) shows up to 5.75 m of vertical development and shows branching/stick growth morphology predominantly, head and encrusting growth morphologies less commonly. Adjacent and inter-framework facies consist of poorly sorted, carbonate mud to very coarse sand sized allochems. Components observed in this facies include *Porites* coral, both *in situ* and detrital, bivalves (fragmented and disarticulated), Vermetid and other gastropods, serpulid worms, peloids, foraminifera, ostracods, echinoderm fragments, coralline algal fragments, intraclasts (CAG, CGSPG), bryozoans, coated grains, rare volcanic grains, and isolated pockets of high carbonate mud content. These grains range from no abrasion/rounding to highly abraded and rounded. Highly abraded and rounded grains appear to be limited to detrital coral fragments, bivalve fragments, intraclasts, and coralline algal fragments. This facies generally lacks sedimentary structures, though rarely framework pore-space infilling sediment displays cm-scale laminations and thin bedding. In upper DS2 this facies occurs only as intraclasts within CAG and CGSPG; these clasts range up to .75 m in size and contain stick morphology *Porites,* preserved as molds. In DS3 this facies is abundant and occurs *in situ* and out of place within the reef core, juxtaposed (*in situ)* and interbedded (out of place) with TF and CAG. Coral morphologies observed in this occurrence include robust branching colonies (up to 5.75 m), massive heads (up to 3 m) and encrusting *Porites* (up to .25 m thick). In DS4-7, PF occurs as massive heads (up to 2 m) and encrusting *Porites* (up to .15 m thick), but it is poorly exposed in outcrop. Visually estimated porosity of the *Porites* Framestone facies averages around 15% and observed pore types include MO/CH, MO, WP, BP and rare VUG.

Interpretation.--- *Porites* is the most commonly observed coral genus in the study region. In upper DS2 it is rare, or difficult to identify confidently. Those that are identified show robust stick morphology indicating an original water depth of 5 - 40 m (the 'upper reef wall' (10 – 40 m) of Saint-Martin (1990), the 'pinnacle zone; (5 – 20 m) of Riding *et al.* (1991), the 'branching-coral zone' (10 - 15 m) of Pomar (1983, 1991) and the 'middle reef wall' (10 - 20 m) of Esteban (1996). The evidence for downslope transport described above indicates some additional water depth for final deposition. In DS3 the facies forms the bulk of the cliff-forming reef core, *in situ* reef showing multiple morphologies of coral growth including branching colonies, massive heads and encrusting growth forms. Branching colonies have been given a depth range of 10 - 15 m by Pomar (1983, 1991). Massive and encrusting coral growth has been attributed to < 10 m depth. Other authors have given a wider, yet roughly equivalent depth range to these coral morphologies (Grasso and Pedley, 1988; Saint-Martin, 1990; Pomar, 1991; Riding *et al.,* 1991; Esteban, 1996). In DS4-7 PF occurs as distinct and clustered massive coral heads, rare robust stick and local encrusting morphologies. Those morphologies indicate a range of water depths comparable to the morphologies observed in the reef core: massive and encrusting morphologies occurring in < 10 m water depth, branching colonies growing in water depths between 10 - 20 m (references as above). In DS4-7 PF and TF deposits are found in close proximity with, and being onlapped by OG deposits. Similar deposits have been described in the neighboring Ricardillo peak area (Toomey, 2003; *Porites*-rich Packstone facies and part of the Reef Core facies, Table 3).

Tarbellastraea Framestone – (TF) – Present in DS2, 3

Description.--- Coral framework in the *Tarbellastraea* Framestone facies (Table 1) has up to 2.5 m of vertical development and shows branching/stick growth morphology

predominantly, and head growth morphology less commonly. Adjacent and inter-framework facies consist of poorly sorted, carbonate mud to very coarse- sand sized allochems including fragmented and detrital *Tarbellastraea* coral, bivalves (fragmented and disarticulated), Vermetid and other gastropods, serpulid worms, peloids, foraminifera, ostracods, echinoderm fragments (rare), coralline algal fragments, intraclasts (CAG, CGSPG) bryozoans, rare coated grains, rare volcanic grains and isolated pockets of carbonate mud. In upper DS2 this facies occurs as highly abraded clasts up to 2 m in size that are not in growth position. Variable coral orientation, tilted and overturned geopetal fabrics, a scoured base, and faint soft sediment deformation below large clasts indicates displacement from original growth orientation. In DS3 *in situ* robust stick (up to 3 m) and massive head (up to ~2.5 m) morphology TF occurs in close proximity to PF and CAG, and is commonly difficult to identify due to alteration (dissolution and secondary cementation). Visual estimates of porosity for this facies are ~15%, consisting of MO/ Channel (CH), MO, WP, and BP pore types. Locally, porosity is enhanced by dissolution of originally aragonitic corals, resulting in a framework of stick-morphology macro-pores.

Interpretation.--- *Tarbellastraea* is the dominant coral genera observed in upper DS2, which is interpreted to have grown in water depths between 10-30 m based on the branching stick morphologies observed (the 'middle reef wall' (10 - 20 m) of Esteban (1996), the 'branching-coral zone' (10 - 15 m) of Pomar (1983, 1991), the 'mid wall' (20 - 30 m) of Grasso and Pedley (1988)) prior to reworking and deposition. Clasts are interpreted to have been eroded and transported during relative sea-level fall associated with Sequence Boundary Zone 3 (SBZ 3); this is discussed further in the 'Platform Depositional Sequences and Interpretations' section. TF shows multiple growth morphologies in DS3, and is one of the facies that makes up the cliff-forming reef core. Observed morphologies include branching and head growth forms. Pomar

(1983, 1991) identified branching growth forms as occurring in 10-15 m water depths; massive corals form in less than 10 m of water depth. Other authors attribute both stick and head growth forms to a broader, but roughly equivalent range of depths (Grasso and Pedley, 1988; Saint-Martin, 1990; Pomar, 1991; Riding *et al.,* 1991; Esteban, 1996). Similar deposits have been described in the neighboring Ricardillo peak area (Toomey, 2003; *Tarbellastraea* Reef facies, Table 3).

Stromatolitic Algal Boundstone – (A(S)BS) – Present in DS4-7

Description.--- The Stromatolitic Algal Boundstone facies contains poorly sorted, carbonate mud to coarse-sand sized allochems that have been incorporated within stromatolitic lamination. Incorporated components include: micrite, abundant peloids, gastropods as well as ooids and other coated grains (common in the 2nd TCC sequence). The average grain size for the facies is mud to very fine sand due to high carbonate mud and peloid content. Observed sedimentary structures include fine wavy to planar laminations defined by alternating fine and coarse grains, stacked hemispheroids and laterally linked hemispheroids (LLH, Logan et al. 1964). Deposits occur along 3 horizons, immediately overlying alteration surfaces forming the basal deposits of the TCC sequences. No stromatolite deposits were observed associated with the 1st sequence. Stromatolite deposits associated with the 2nd sequence are rare and restricted to the southern end of the Rellana platform (below 188 m) where the deposits occur in isolated patches ranging in thickness from 3 - 8 cm, these occurrences contain a high concentration of ooids and coated grains and planar laminations. Deposits associated with the 3rd sequence range in thickness from 5 cm to 20 cm, and are found discontinuously throughout the Rellana area. In the 4th TCC sequence stromatolite development is more laterally continuous and ranges in thickness from 5

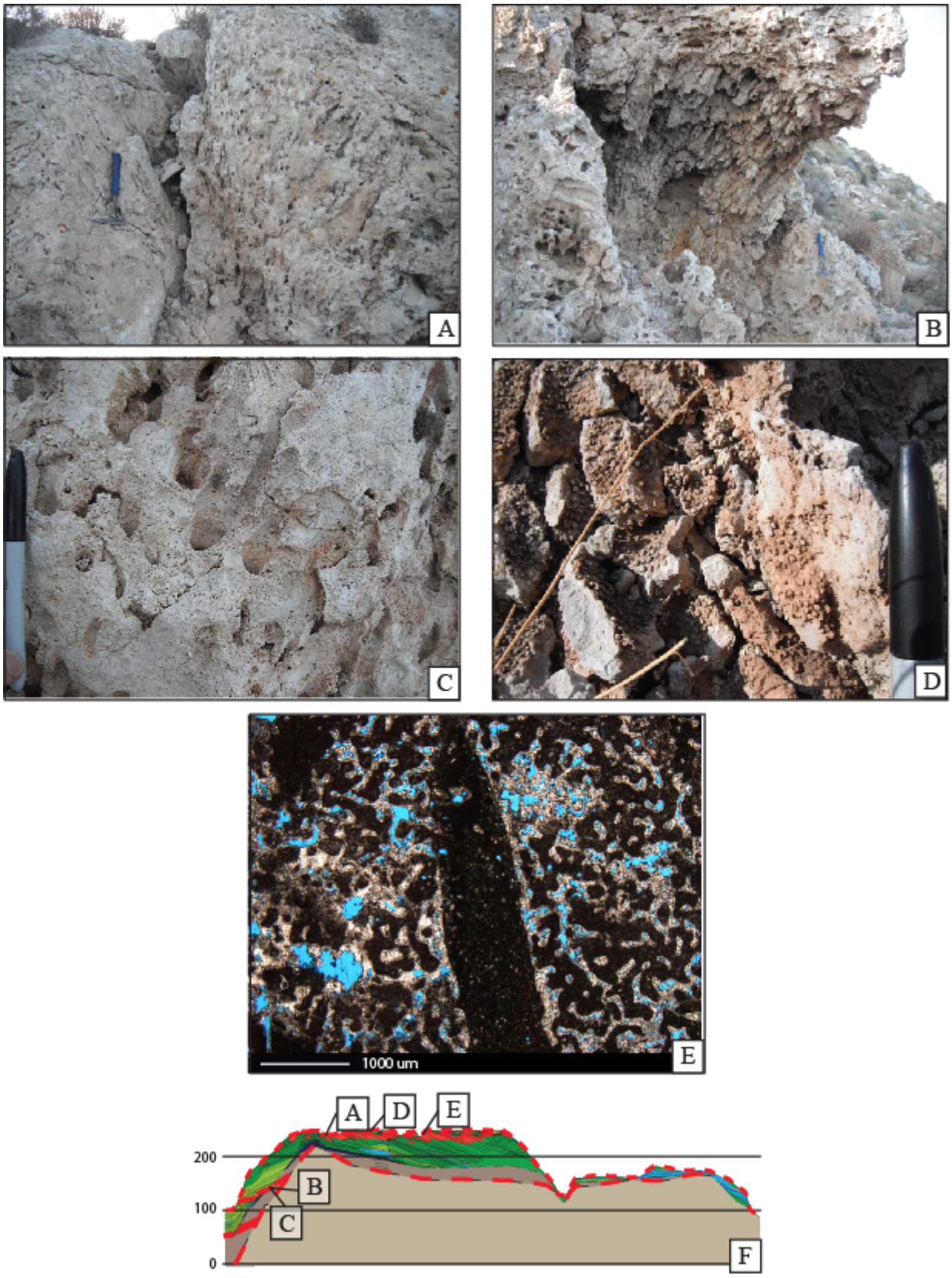
A
B
C
D
1000 um
E
A
D
E
200
B
100
C
0
F

Figure 13: Photographs and photomosaic showing characteristics of the framestone facies and general cross section showing respective location of photos and collection points for thin sectioned samples. A) Photograph of outcrop featuring *in situ Porites* framestone (PF) in DS3 deposits, Coral is identified in the field from preserved molds, visible as vertical tubes in A (hammer is 32 cm) and magnified in image C (pen is 13 cm. B) Photograph of outcrop featuring potentially *in situ Tarbellastraea* framestone (TF) in DS3 deposits, Coral is identified in the field from preserved molds, visible as vertical tubes in B (view is an oblique angle from below, hammer is 32 cm) and magnified in image D (located in flanking CAG deposits nearby), displaying characteristic molds of *Tarbellastraea*. Pen cap is 3 cm. E) Photomicrograph of a boring into *Porites* coral from detrital PF deposits in SBZ 3. 4X magnification with plane-polarized light, blue epoxy fills pore space. Scale bar is 1 mm. F) Generalized cross-section showing the Rellana study area. Elevation is in meters above sea level, red dashed lines represent interpreted sequence boundaries and annotated points correlate to photographs and sampling locations described above.

to 30 cm, the thickest occurrences observed on the northern extreme of the Rellana area. The 3rd and 4th sequence occurrences have wavy laminations and display LLH growth forms (Logan et al. 1964); sequence 4 shows LLH to stacked hemispheroid growth forms. Visual estimates of porosity in this facies average 5% and include MO, BP, FE, and VUG pore types.

Interpretation.--- In TCC deposits from nearby areas, two types of stromatolites were identified; a planar laminated micritic peloidal stromatolite and a planar laminated oolitic stromatolite. The planar laminated micritic peloidal stromatolite is equivalent to the stromatolite deposits identified in the 1st, 3rd and 4th TCC sequences of the Rellana area, and is interpreted to have been deposited in a shallow (< 10 m), low energy marine environment (Hoffman, 1976; Feldman and McKenzie 1997; Toomey, 2003; Lipinski, 2010). The planar laminated oolitic stromatolite is similar to the A(S)BS facies observed in DS5, and is interpreted to have been deposited in shallow water (< 10 m) with moderate to high energy (Ball, 1967; Hoffman, 1976; Lipinski, 2010). The change from wavy to planar laminated stromatolite to stacked hemispheroid stromatolite likely reflects an increase in energy in the depositional environment and a possible increase of water depth (Hoffman, 1976). The limited fauna and abundant preservation of the stromatolite indicates shallow, possible restricted marine conditions. More detailed descriptions of similar stromatolitic facies from the Ricardillo Peak and San Pedro area were made by Lipinski (2009). Stromatolitic deposits were interpreted to have formed in shallow water (< 10 m) with variable energy reflected in stromatolite growth form (digitate growth in low energy and planar growth in higher energy environments, *sensu* Hoffman (1976)). The stromatolites observed on the Rellana platform are interpreted to have formed in an environment similar to that interpreted by Lipinski (2009).

Thrombolitic Boundstone – (TBS) – Present in DS4-7

Description.--- The dominant visible component of the Thrombolitic Boundstone facies (Table 1) is peloids; other allochems observed within thrombolites range from carbonate mud to cobble- sized (average grain size mud- to medium- sand sized) including foraminifera (benthic), red algal fragments (rare), gastropods, serpulid worms, coated grains and coral fragments. Abrasion of these grains is highly variable and ranges from none to highly abraded. TBS deposits show a dark clotted texture visible in hand sample, confirmed as clotted peloidal texture in thin section (Fig. 14D). Deposits of this facies occur in the 2nd, 3rd, and 4th TCC sequences and are onlapped by surrounding facies, indicating that they built topographic relief on the sea floor. In the 2nd sequence, TBS deposits are rare and seen only at the northernmost Rellana exposure, where a single 2 m wide, 0.75 m high thrombolite was observed. It is possible that more occurrences exist in the Rellana area, however, no others were definitively identified in the 2nd sequence. The 3rd sequence deposits are more laterally extensive (up to 6 m) and thicker, (up to 3 m). These deposits occur abundantly north of the drainage divide in the Rellana area. The 4th sequence occurrences are limited to rare, small (less than 1 m thick, 1.5 m wide) deposits throughout the study area. Visual estimates of porosity range from 5-10% and consist of MO, BP, MO, and VUG pore types.

Interpretation.--- The topography-building nature of this facies suggests it was deposited as thrombolitic mounds, which have been documented developing in a wide variety of depositional environments covering a range from >10 m to 200 m water depth. (Braga *et al.*, 1995; Mancini *et al.*, 1998, 2004, 2008; Grotzinger *et al.*, 2000; Mancini and Parcell, 2001; Whalen *et al.*, 2002; Adams *et al.*, 2004, 2005; Batten *et al.*, 2004; Heydari and Baria, 2005; Planavsky and Ginsburg, 2009; Lipinski, 2010; Goldstein *et al*, 2013). In this study area, the

association of a diverse detrital skeletal assemblage, including benthic foraminifera (e.g. miliolids) bivalves, echinoderms, gastropods and coral within the thrombolite suggest more normal marine conditions than A(S)BS deposits (e.g. Goldstein *et al.,* 2013). The presence of coated grains incorporated into algal growth indicates proximity to a shallow, high-energy depositional environment. Lipinski (2009) provided an extensive analysis of thrombolitic facies types in the eastern Ricardillo/western Rellana area, immediately adjacent to the Rellana platform area studied in this report (Table 4). Thrombolites in the Ricardillo/Rellana area were generally more laterally extensive, with significant accumulations occurring in the lowest stratigraphic areas, specifically the western Rellana area. These thick packages of thrombolite were not seen on the eastern side of the Rellana platform, possibly because this was a more open marine setting rather than a lagoonal one. Due to the wide depth constraints associated with thrombolite growth (> 10 - 200 m) the surrounding lithofacies serve as more reliable depth indicators. The TBS deposits are generally closely associated with CAG and OG deposits, indicating a water depth of <10 - 12 m.

Oolitic Grainstone - (OG) - Present in DS2, 6

Description.--- The Oolitic Grainstone facies is dominated by the presence of ooids; additional grains include coral fragments, disarticulated and fragmented bivalves, gastropods, rare bryozoan fragments, rare foraminifera (benthic dominant), and rare volcanic clasts. Grains range from medium sand-sized grains to 1.5 cm skeletal fragments, averaging upper coarse sand size. Grains are generally well sorted and show abundant grain breakage and rounding of non-coated grains, as well as visible coated grain nuclei of (generally unidentifiable skeletal components, rarely volcanic grains). OG occurrences in upper DS2 are restricted to lenticular deposits (up to .75 m wide, 10 cm thick) characterized by diverse skeletal content. These

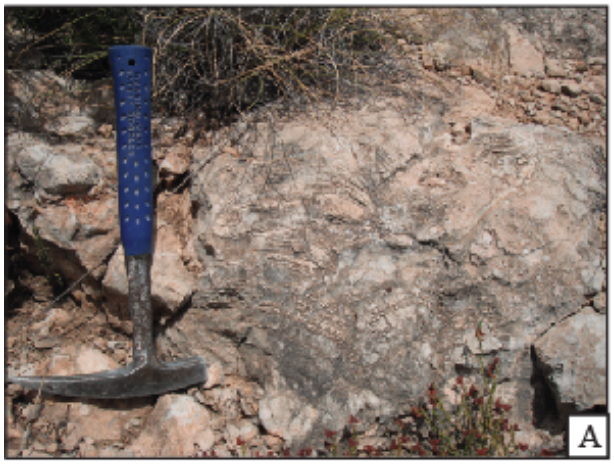
A


B

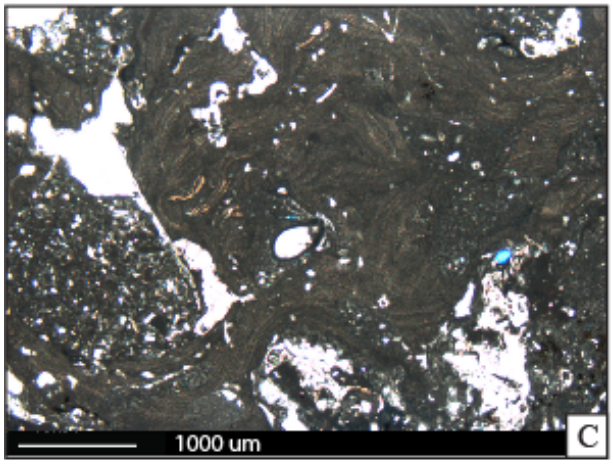
1000 um
C

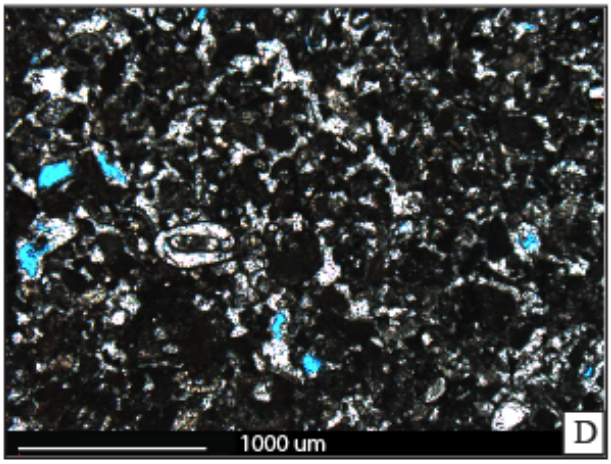
1000 um
D

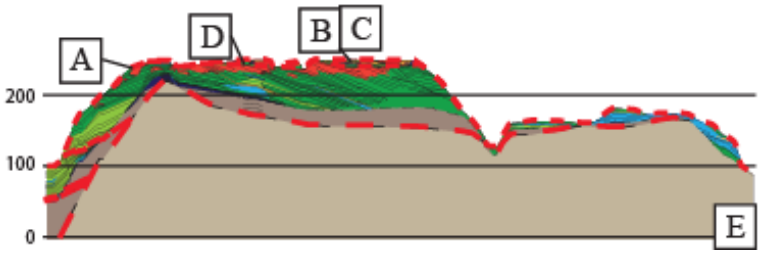
A
D
B
C
200
100
0
E

Figure 14: Photographs and photomosaic showing characteristics of the boundstone facies and general cross section showing respective location of photos and collection points for thin sectioned samples. A) Outcrop photograph of stromatolite facies (A(S)BS) immediately overlying SB4 south of the drainage divide, cut through stromatolitic structure is oblique, but laterally linked hemispheroid growth pattern is visible. Hammer is 32 cm. B) Outcrop photograph of thrombolite facies (TBS) in TCC deposits (black outline). This thrombolite occurs within the second TCC sequence on the north side of the drainage divide (the lowest sequence is amalgamated at this point), red dashed lines indicate position of sequence boundary. Thrombolite is 1.5 m tall. C) Photomicrograph of A(S)BS showing algal structure, 4X magnification with plane-polarized light, sample poorly impregnated with blue epoxy, filling some pore spaces, large pores unfilled and appear white. Scale bar is 1 mm. D) Photomicrograph of a thin section from TBS sample, clotted texture is algal material and peloids. 10X magnification with plane-polarized light. Sample poorly impregnated, blue epoxy fills some pore space. Scale bar is 1 mm. E) Generalized cross-section showing the Rellana study area. Elevation is in meters above sea level, red dashed lines represent interpreted sequence boundaries and annotated points correlate to photographs and sampling locations described above.

deposits display planar and trough cross bedding, and commonly grade laterally into CGSPG. Deposits generally onlap or overlie large (up to 2 m) coral framestone (TF and PF) clasts. Laterally discontinuous OG deposits are found throughout upper DS2, with little or no variation in content or sedimentary structure over the 30 m of paleotopographic relief.

In DS4-7 OG is abundant, forming the majority of the observed sediment. OG deposits are generally trough cross-bedded and beds show a wide variety of dips. A division between deposits north of the drainage divide (which tend to dip to the north) and south of the drainage divide (which dip to the southwest) persists. DS4-7 deposits show a tendency to onlap *in situ* coral framework (PF dominant, and TF rare). Skeletal components observed within OG deposits in DS4-7 are diverse, including gastropods, bivalves, rare red algal fragments, foraminifera (predominantly benthic), bryozoans, and coral fragments. The concentrations of skeletal material, however, are dwarfed by ooid content (up to 90%). Deposits associated with DS6 display rare burrowing. Visual estimates of porosity range from 5-40% and consist of MO, BP, WP, and FR pore types

Interpretation.--- Lipinski (2010) studied TCC deposits in the Ricardillo/Rellana area and described a number of oolitic facies (Table 4). The features observed on the eastern side of the Rellana platform are most consistent with the 'trough cross-bedded ooid grainstone' facies described by Lipinski (2010). The possibility of other oolitic facies is not discounted, but given the trends described for the western Rellana area by Lipinski (2010), it is likely that this is the dominant oolitic facies preserved throughout the Rellana platform. Modern ooids are interpreted to represent high-energy depositional environments in shallow water depths (< 10 m) (Ball, 1967; Loreau and Purser, 1973; Hine, 1977; Flugel, 1982; Harris, 1983; Lloyd et al., 1987; Tucker and Wright, 1990; Burchette and Wright, 1992; Major et al., 1996). A high-energy

depositional setting is supported by the lack of carbonate mud, abundant ooids, highly abraded grains and good sorting. Trough cross-bedding is commonly attributed to sediment-current interaction (Burchette and Wright, 1992, Wright and Burchette, 1996) placing deposits above fair-weather wave base (interpreted in the modern Mediterranean to be ~ 8 m maximum; Fornos and Ahr, 1997). Deposits of DS4 on the western Rellana platform are described as having alternating coarser and finer very thin, gently seaward-dipping beds similar to features that indicate deposition in or near a beach environment (Inden and Moore, 1983; Lipinski, 2010). Additionally, fenestral fabrics have been observed in the study area (Franseen, personal communication). These lines of evidence suggest that the Ooid grainstone facies was deposited in a shoreface environment above fair-weather wave base (< 10 m).

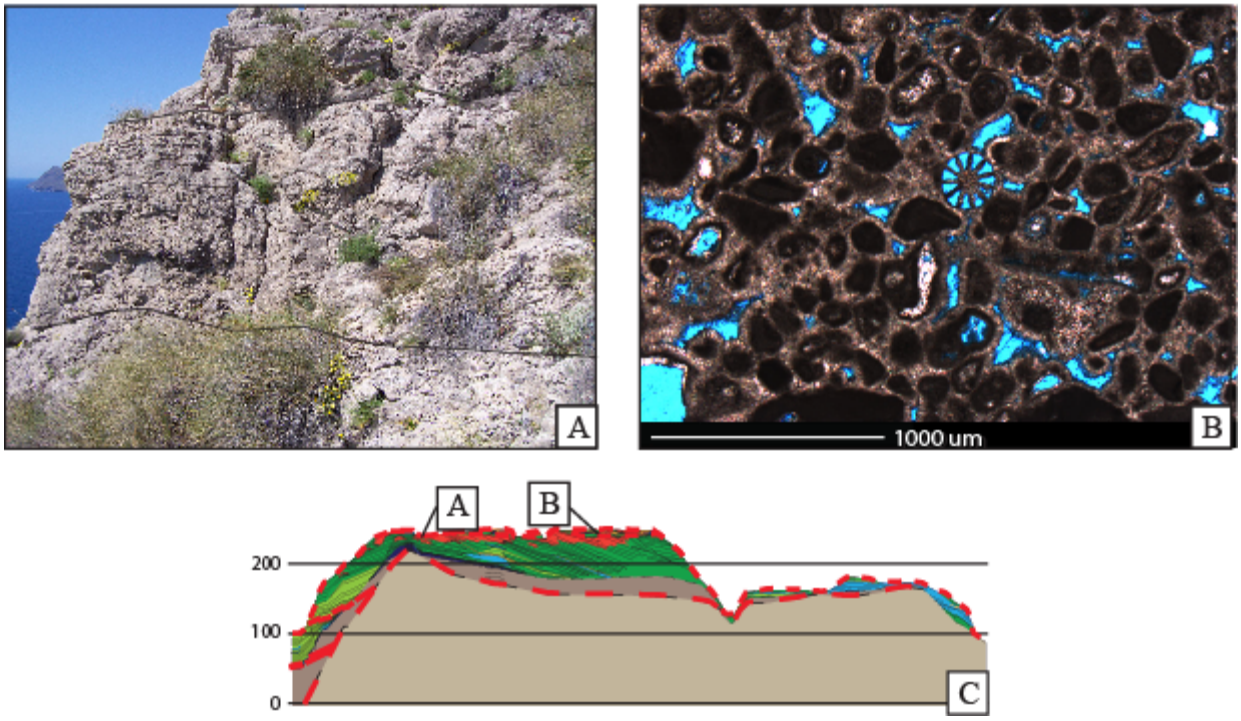

Figure 15: Photograph and photomicrograph of Oolitic grainstone (OG) facies with general cross section showing respective location of photos and collection points for thin sectioned samples. A) Outcrop photograph showing OG facies in TCC deposits just north of the drainage divide. This occurrence of OG shows thin (3 cm) planar to low angle cross bedding. OG facies is outlined by black lines and is 2 m thick. B) Photomicrograph of OG deposit showing a localized concentration of coated grains. In other areas, complete porosity inversion has occurred resulting in oomoldic porosity. 10X magnification with plane-polarized light, blue epoxy fills some pore space. Scale bar is 1 mm. C) Generalized cross-section showing the Rellana study area. Elevation is in meters above sea level, red dashed lines represent interpreted sequence boundaries and annotated points correlate to photographs and sampling locations described above.

PLATFORM DEPOSITIONAL SEQUENCES AND INTERPRETATIONS

Seven depositional sequences (DS1-7) bounded by surfaces with evidence for relative sea-level fall (SB1-5) are recognized in the Rellana study area. They are made up of the 13 facies described above (Table 1) including: volcanic conglomerate (VC), volcanic conglomerate with carbonate matrix (VCC), coarse grained skeletal packstone – grainstone (CGSPG), fine grained skeletal wackestone – packstone (FGSWP), red algal skeletal packstone – grainstone (RAPG), thrombolitic boundstone (TBS), *Porites* framestone (PF), *Tarbellastraea* framestone (TF), coralgal grainstone – breccia (CAG), foraminiferal wackestone – packstone (FWP), bivalve-rich floatstone – rudstone (BFR), Stromatolitic algal boundstone (A(S)BS) and oolitic grainstone (OG). Generalized stratigraphy of the Rellana platform, including general facies distribution within depositional sequences can be seen in figure 2. Detailed lateral distribution and stratigraphic relationships on the platform are depicted in figure 3 and in greater detail in photomosaics, line drawings and cross sections of Appendices 4 and 5.

The facies associated with the seven depositional sequences provide valuable information regarding controls on platform development. Depositional sequences are analyzed and interpreted below, in an attempt to clarify the developmental history of the platform. Elevation references made in the description section refer to the modern elevation of the observed features. Paleotopographic reconstruction of the platform and surrounding areas yields elevations that better represent relative differences in elevation during deposition. These reconstructed elevations (RE) are presented after modern elevations where appropriate (see Paleotopography section above).

Reconstructed paleotopography and facies interpretations are used to develop a quantitative relative sea-level history (Fig. 16) following the "Pinning Point" methodology of Goldstein and Franseen (1995), as described in the methodology section above.

Depositional Sequence 1

Description.--- Depositional sequence 1 (DS1) is the stratigraphically lowest sequence and is observed only on the southern end of the platform (between 48 - 66 m; 26.6 - 45 m RE). It ranges in total thickness from 0 m to over 5 m (full extent unknown, lowest contact covered), and is divided into two genetic packages (DS1a and DS1b) because of the distinctive lithologies and evidence for a potential sequence boundary (SB1b) separating them. DS1a is present between 48 - 56 m (26.6 - 34.6 m RE); DS1b is present between 50 - 66 m (27 - 45 m RE). The characteristics are summarized in the following:

1. SB1 is exposed below an elevation of 48 m and extends laterally ~10 m down to 46 m before being truncated by SB2. SB1 separates facies with marine carbonate components (VC and VCC) from volcaniclastic conglomerates and sandstones and volcanic basement. The contact between basal VC and volcanic basement is difficult to constrain due to cliff forming tendency of the volcanic basement and poor accessibility (Fig. 17B).
2. DS1a deposits consist of VC overlying SB1. VC deposits are up to 2 m thick and onlap SB1. Locally, lenticular beds of well-sorted FGSWP facies occur within 0.5 - 1 m below the SB1b surface.
3. VC grades up into and interfingers downdip with VCC, locally meter-scale lenticular (0.15 – 2.5 m long, 5 - 50 cm high) deposits of poorly sorted FGSWP occur interbedded within VCC.

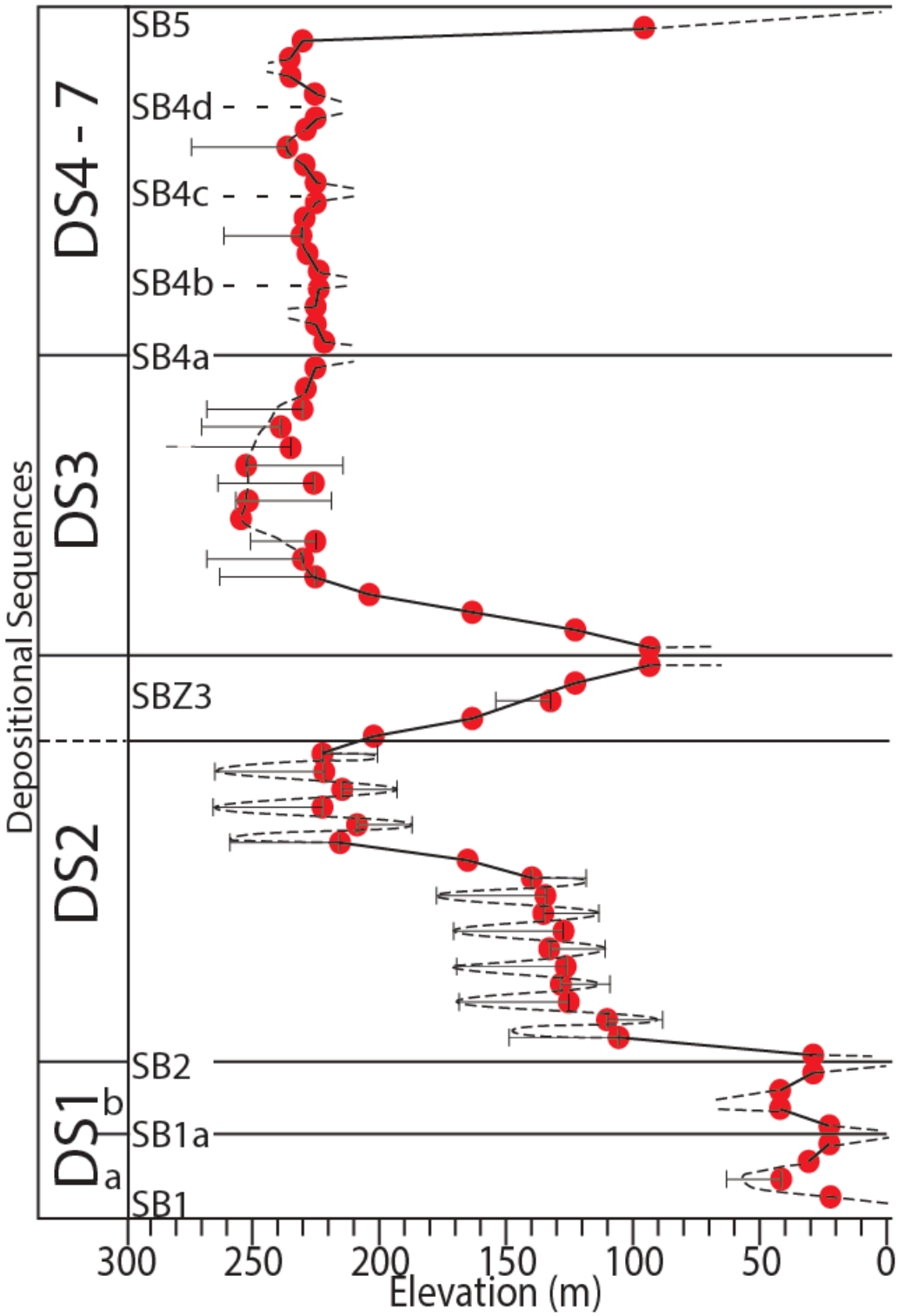

Figure 16: Relative sea-level curve for the Rellana platform study area generated using the pinning point method. Note that DS1 deposits have been subject to deformation during the Miocene, and therefore, any quantitative elevation data are suspect.

Pinning Point (PP) #	Measured Elevation	Corrected Elevation	Relevant Feature
1	48	26.6	lowest exposure of SB1
2	56	44.6	top of PU1 + 10 m FGSWP deposition
3	56	34.6	exposure of top of DS1a
4	50	27	exposure of DS1a
5	50	27	marine sediment overlying lowest exposure of DS1a
6	66	45	top of DS1b deep marine seds
7	66	45	exposure of top of DS1b
8	54	28	lowest extent of SB2
9	54	28	rise past PP8
10	105	104	rise to RAPG max in DS2 package 1
11	101	110	fall results in well sorted FGSWP
12	123	122.2	rise to RAPG max in DS2 package 2
13	119	128.2	fall results in well sorted FGSWP
14	127	126.4	rise to RAPG max in DS2 package 3
15	122	131.4	fall results in well sorted FGSWP
16	129	128.6	rise to RAPG max in DS2 package 4
17	125	134.6	fall results in well sorted FGSWP
18	134	133.8	rise to RAPG max in DS2 package 5
19	131	140.8	fall results in well sorted FGSWP
20	182	164.7	initial DS2 deposits on north slope
21	215	216.5	rise to RAPG max in DS2 package 6
22	198	209.75	fall results in well sorted FGSWP
23	222	223	rise to RAPG max in DS2 package 7
24	203	214.75	fall results in well sorted FGSWP
25	221	222	rise to RAPG max in DS2 package 8
26	212	223.7	fall results in well sorted FGSWP
27	222	203	highest exposure of SBZ3 north end
28	182	164.7	lowest exposure of SBZ3 cap on north slope
29	142	132	TF water depth indicator in SBZ3 deposits
30	142	122	highest occurrence of sub. exp. over south end
31	114	92.7	lowest occurrence of subaerial exposure overlying DS2
32	114	92.7	marine sediment overlying PP29, DS3 deposition begins
33	142	122	continued re-inundation high south end
34	182	164.7	sea level rises past low end exp. on north end
35	222	203	sea level rises past high end exp. on north end
36	241	226.8	aggradational reef growth
37	244	230	secondary aggradational reef growth
38	240	226	potential progradational wedge

Table 2: Pinning point measured and corrected elevations. Corrected elevations account for paleotopographic reconstruction and facies-related water depth indicators.

Pinning Point (PP) #	Measured Elevation	Corrected Elevation	Relevant Feature
39	232	253	highest DS3 deposition
41	235	256.4	height of basal prograding reef after collapse event 2
42	239.5	226.5	elevation of CGSPG deposits associated with prograded reef prior to collapse event 3
43	228	250.4	elevation of basal reef core deposits associated with prograded reef after collapse event 3
44	248	235.5	maximum reef elevation prior to collapse event 4
45	247	239.5	occurrence of massive coral in progradational coral growth following collapse event 4
46	241.5	230	last occurrence of clearly *in situ* DS3 reef core material
47	240	229.8	lowest occurrence of carbonate deposits on top of LR prior to SB4
48	240	224.8	lowest DS5 deposits where SB4 is distinguishable from SB5
49	239.5	221.5	marine sediment overlying PP48
50	243	225	top of preserved DS4
51	243	225	highest exposure of SB4a
52	240	223.1	lowest exposure of SB4a
53	240	223.1	marine sediment overlying PP52
54	248	229.7	measured top of DS5
55	243	230.7	top of DS5 with facies water depth indication
56	248	229.7	highest exposure of SB4b
57	243	225	lowest exposure of SB4b
58	243	225	marine sediment overlying PP57
59	248	229.7	measured top of DS6
60	246	234.3	top of DS6 with facies water depth indication
61	248	229.7	highest occurrence of SB4c
62	243	225	lowest exposure of SB4c
63	245	225.9	marine sediment overlying PP62
64	251	234.1	top of DS7
65	251	234.1	highest exposure of DS7
66	245	230	lowest exposure of DS 7
67	104	94.7	Lowest evidence of exposure SB5

Table 2 continued: Pinning point measured and corrected elevations. Corrected elevations account for paleotopographic reconstruction and facies-related water depth indicators.

4. A potential subaerial exposure surface (SB1b) separates DS1a and DS1b between 50 - 56 m (27 - 34.6 m RE). Below 50 m (27 m RE), SB2 truncates SB1b; above 56 m (34.6 m RE) SB1b is poorly exposed and truncated by SB2.
5. SB1b is overlain by DS1b deposits. At the updip extent of the exposed SB1b surface (56 m; 34.6 m RE) the basal, distally thinning VCC bed grades up into BFR. BFR and VCC are subsequently overlain by and grade up into decimeter-scale alternating beds of poorly sorted FGSWP and FWP.
6. FGSWP and FWP bedding trends grade into VCC and VC up-dip and are truncated by an overlying surface of subaerial exposure (SB2).

Where exposed, SB1 is characterized by autoclastic brecciation and concentric cracking patterns displayed by volcanic clasts at and < 1 m below the surface (Fig. 17D). Lateral tracing of SB1 shows that it forms a distinct break in slope that can be traced on photomosaics between the Rellana and Ricardillo field areas (Appendix 4). Polymictic volcanic conglomerate (VC) overlies SB1, featuring angular to rounded clasts that range in size from medium sand (~350 μm) to 1.5 m boulders with a volcaniclastic matrix (Figure 17E - G). Some volcanic clasts display concentric cracking. Massive beds thicken distally (reaching up to 2 m thick) and onlap the SB1 surface updip. Volcanic clasts within VC are compositionally similar to underlying volcanic basement. Well-cemented lenses of well-sorted FGSWP varying in thickness from 5 - 50 cm and in length from 0.15 - > 2.5 m occur below the SB1b surface. These lenticular beds increase in size, and abundance upwards towards the SB1b surface. This gradational change is accompanied by a decrease in range of clast sizes (reducing to a range of 4 cm - 1 m), an increase in roundness (sub-angular to well rounded), and an increasing occurrence of matrix-supported conglomerate. Observed components within carbonate matrix include disarticulated bivalves, bryozoan

fragments, solitary corals, gastropods and foraminifera (genus unknown due to alteration, miliolid type common, benthic genera appear dominant) as well as abundant volcanic clasts. Observed sedimentary structures within the lenticular units show faint cross-bedding in grainier units and common upward fining.

SB1b is characterized by abundant red staining of carbonate facies underlying the surface as well as concentric cracking and autoclastic brecciation of cobble- to boulder-sized volcanic clasts at and immediately below the surface. Deposits within the altered zone (5-10 cm below the surface) are friable (Fig. 17G). SB1b surface is irregular and amalgamates updip with SB1. The downdip extent is unknown, though photomosaics suggest it is truncated by SB2 at 50 m (27 m RE) (Appendices 4, 5).

A distally thinning bed of VCC (observed thickness ranges from 0.25 m to 1 m) overlies SB1b above 52 m (29 m RE) and grades up (over 5-10 cm) into BFR near the updip maximum of DS1b deposits (~ 58 m; 25 m RE), (Fig. 17E). The BFR and VCC facies are gradationally overlain by steep southwest dipping (~20˚) alternating beds (10 to 30 cm thick) of FWP and poorly sorted FGSWP.

SB2 is irregularly exposed and dips an average 13˚ SW where it truncates carbonate deposits (below 65 m; 44 m RE). Above this elevation the SB2 contact is poorly exposed or amalgamated with SB1 or truncated by SB3. Areas with better preservation show significant red staining and recrystallization. Where the contact overlies VC or VCC directly, the underlying clasts show concentric cracks and autoclastic brecciation.

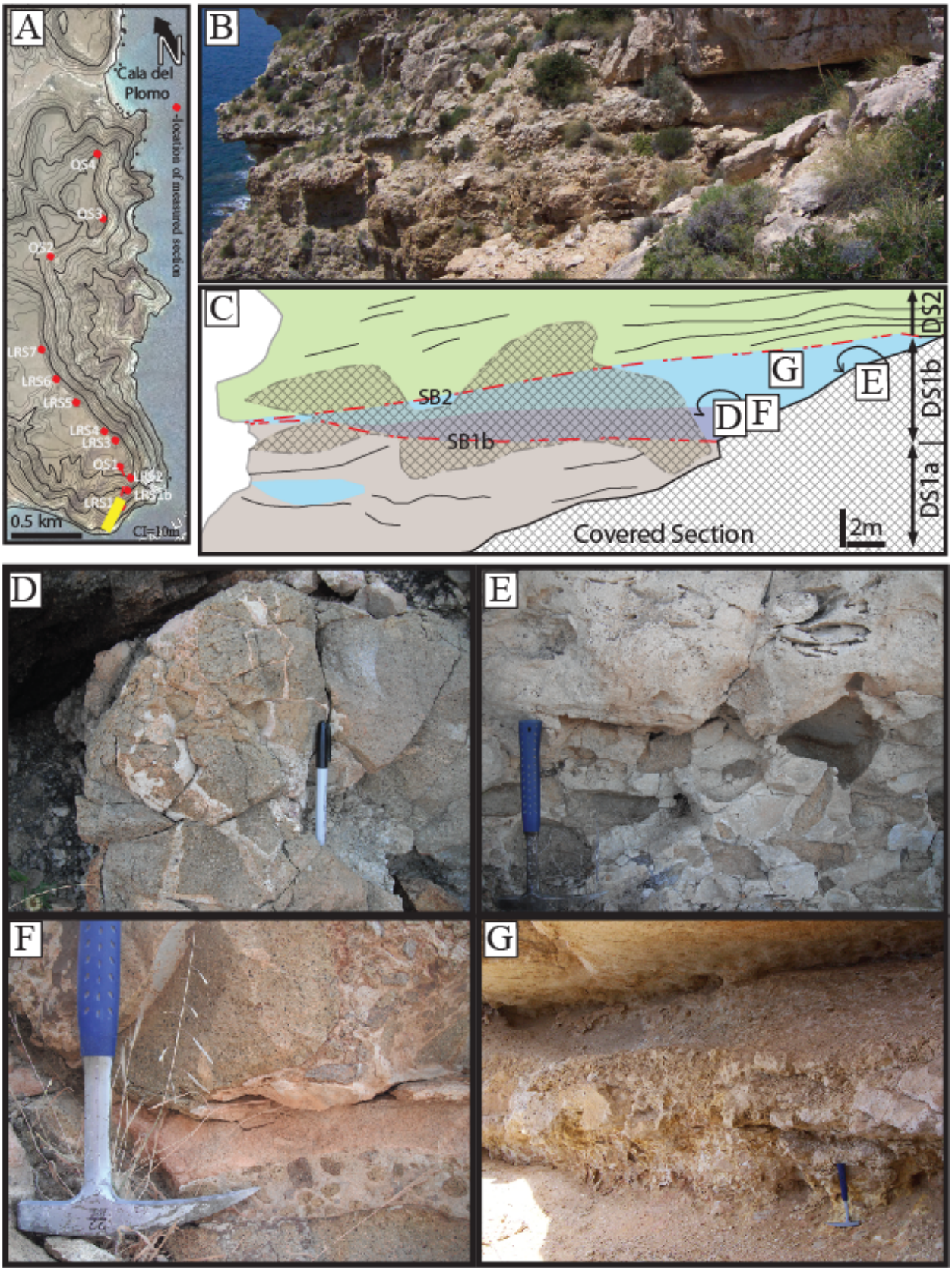
A
N
Cala del Plomo
location of measured section
OS4
OS3
OS2
LRS7
LRS6
LRS5
LRS4
LRS3
OS1
LRS2
LRS1b
LRS1
0.5 km
CI=10m
B
C
DS2
DS1b
DS1a
G
E
D
F
SB2
SB1b
Covered Section
2m
D
E
F
G

Figure 17: Illustrations and photographs depicting characteristics of DS1 deposits. A) General location map with measured sections denoted by red circles. Yellow rectangle identifies location depicted in B. Horizontal scale bar is 0.5 km and contour interval is 10 m. B) Photograph showing the southernmost accessible carbonate deposits on the Rellana Platform consisting of DS1A, DS1b and overlying DS2 associated facies. Photo taken facing south. C) Overlay interpretation of photograph displayed in B distinguishing DS1 and DS2 deposits, as well as identified sequence boundaries, facies, covered areas and location of images D-F. Scale bars in lower right are 2 m, Hashed pattern indicates covered section. The dip trend of SB2 continues down to modern sea level. D) Volcanic cobble (~20 cm) located near DS1 at the southern end of the exposure showing spheroidal weathering resulting from subaerial exposure, Pen is 13 cm. E) Gradational contact between VCC deposits in lower half of picture (large clasts are volcanic cobbles) and BFR deposits above (featuring bivalve molds, 5 - 11 cm). Hammer is 32 cm. F) Photograph showing 3-4 cm thick lens of well-sorted FGSWP within VC deposits. Hammer head is 15 cm G) Exposure of DS1b, distally thinning VCC (lowest bed), gradationally overlain by BFR and finally by less resistant FWP and FGSWP. Most recessive point correlates with SB2, roof material is RAPG. Hammer is 32 cm.

DS1 Interpretation.--- The SB1 contact is recognized as a subaerial exposure surface due to the presence of autoclastic brecciation and concentric cracking of volcanic clasts (interpreted as spheroidal weathering resulting from subaerial exposure) at and immediately underlying the surface as described above (Fig. 17D). In addition, fissuring, erosional sculpting, and similar polymictic volcanic breccia in the adjacent Ricardillo area on the surface separating volcanic basement from marine sediment support the interpretation of subaerial exposure (Toomey, 2003). This contact can be physically traced downdip to 48 m on the southern end of the platform (26.6 m RE, PP1) and may extend down to modern sea-level based on continuation of physically traced features on photomosaics (17B, C), resulting in a conjectured exposure down to -21.4 m RE.

Compositional similarities between the volcanic sediment entrained in deposits overlying SB1 and the adjacent volcanic basement imply DS1 volcanic clasts were sourced from the adjacent high. Lenticular beds of FGSWP indicate marine deposition. Rounding of volcanic clasts and abrasion of skeletal grains, as well as preservation of cross bedding within lenticular beds of well-sorted FGSWP, indicate potential wave reworking. Stratigraphic relief over the interval suggests a minimum relative sea-level rise to a depth of 56 m (34.6 m RE). Lack of evidence for subaerial exposure prior to deposition of overlying VC deposits, and entrainment of spheroidally weathered or autoclastically brecciated volcanic clasts in laterally equivalent VC indicates reworking of previously subaerially exposed volcanic clasts or transport from updip subaerially exposed volcanic basement.

A modern analog with similar skeletal assemblage to the well-sorted FGSWP facies identified in the Mediterranean (Martin *et al*., 1996; Brachert *et al.,* 1998; Betzler *et al.,* 2000) indicates a water depth of 10 -30 m. The abundant abrasion of skeletal fragments and

preservation of cross bedding indicates that the FGSWP deposits preserved in DS1a were likely deposited in a high-energy environment. Based on this evidence, a minimum relative sea level of 66 m (44.6 RE, PP2) is assumed for DS1a deposition.

The SB1b surface separating DS1A and DS1b displays a concentration of spheroidally weathered and autoclastically brecciated volcanic clasts in VC underlying the surface. The potential for downslope transport of subaerially altered volcanic clasts provides a reasonable explanation in contrast to *in situ* subaerial exposure of DS1a deposits. Potential sea level history implications associated with SB1b are speculative (PP3, 4; 56 m (34.6 m RE) and 50 m (27 m RE) respectively, reflecting potential sea level fall down to expose the SB1b surface).

The overlying VCC and localized BFR facies indicate a return to normal marine deposition. *Isognomon* associated with BFR deposits in DS1b are known from modern analogs to be deposited in normal marine water (< 30 m) (Wilbur, 1983; Whorff *et al.,* 1995; Betzler, 2000). Variable abrasion, breakage and random orientation of the BFR *Isognomon* valves imply transport and reworking. BFR deposits observed in DS1b likely reflect deposition in a setting just downslope of *in situ Isognomon* growth. Due to the lack of *in situ* preservation, these deposits cannot be used to confidently constrain depositional water depths beyond the implications of the presence of marine sediments indicating flooding of the Sb1a surface (PP5, 50 m (27 m RE)).

The gradational transition into overlying interbedded FWP and FGSWP indicates continued deepening. These deposits are found up to an elevation of 66 m (45 m RE), indicating flooding to at least this elevation (PP6). Observed FWP facies indicate a deep marine depositional environment suggesting a potential relative sea-level rise up to 166 m (145 m RE). The overlying and truncating alteration surface features abundant red staining and

recrystallization. The surface overlies VC and VCC, increased occurrences of spheroidal weathering, and autoclastic brecciation. It is interpreted as a subaerial exposure surface (SB2). This surface can be physically traced from an updip maximum of 66 m down to 54 m, suggesting sea level fell down past the updip maximum elevation (45 m RE, PP7) to at least 54 m (28 m RE, PP8)

Normal faulting is observed on the southern end of the platform, which offsets (~ 3 m) lower DS2 deposits north of exposed DS1. The extent of displacement of DS1 deposits is unknown due to the lack of an observable offset in the stratigraphy, therefore, interpretations regarding sea-level history are considered speculative for DS1 deposits, with a minimum of 3 m of offset. Due to this uncertainty in reconstruction of paleotopography, magnitudes and positions of sea level fluctuation extracted from DS1 pinning points are considered speculative.

Depositional Sequence 2

Description.--- DS2 is preserved on the steep paleoslope of the platform's southern slope between 54.5 - 142 m (28 - 113.8 m RE), and on the gently dipping northern slope between 182 - 223 m (164.7 - 203 m RE). DS2 deposits range in thickness from 0 - 78 m on the southern slope and 0 - 18 m on the northern slope. DS2 comprises distinctive features, lithofacies and surfaces:

1. A subaerial exposure surface (SB2) overlies DS1 south of the drainage divide between 48 - 66 m (26.6 - 45 m RE). Above 66 m (45 m RE), SB2 overlies volcanic basement. North of the drainage divide SB2 and basal DS2 deposits are not exposed.
2. South of the drainage divide SB2 is overlain by a distally thinning wedge of VC and gradationally overlies VCC, which underlies RAPG and local BFR deposits. North of the drainage divide, basal DS2 deposits are not exposed.

3. Eight massive dm- to dam-scale RAPG-dominated bedsets onlap SB2. Distally, beds fine upward from poorly sorted FGSWP or FWP into RAPG, sharply overlain by well-sorted FGSWP, which is subsequently overlain by a pronounced bedding surface and the basal deposits of the next depositional package. Proximally, sharply bounded distally thinning beds of well-sorted FGSWP onlap VCC and are overlain by RAPG.
4. DS2 is erosionally truncated by a surface characterized by alteration of underlying deposits (within 7-10 cm of the surface), overlain by complexly interbedded CAG, detrital and possibly *in situ* TF, CGSPG, and RAPG (forming upper DS2) capped by a surface of subaerial exposure. This upper package is referred to as Sequence Boundary Zone 3 (SBZ 3).

South of the drainage divide SB2 is overlain by VC above 68 m (47 m RE; covered above 71 m; 50 m RE), and it ranges in thickness from 0 - 35 m. Between 62 - 68 m (41 - 47 m RE), SB2 is overlain by a distally thinning wedge of VCC that onlaps VC deposits and reaches an observed maximum thickness of 3 m near section LRS2 (Figure 3, 18A). Below 62 m (41 m RE), RAPG deposits drape the SB2 surface, and onlap VCC deposits. BFR deposits in DS2 overlie VCC deposits. North of the drainage divide, DS2 BFR deposits do not exceed 1 m thick with the thickest accumulations occurring near the drainage divide (near measured section LRS4, Figure 3, 18A). South of the drainage divide, deposition of BFR is restricted to the updip extent of southern occurrences of DS2 (above 105 m; 84 m RE), where deposits reach a thickness of 7 m (just north of section LRS1B, Figure 3). Laterally BFR interfingers with, and is gradationally overlain by, RAPG (similar in appearance to Figure 17E). Where basal DS2 deposits are exposed north of the drainage divide, they are characterized by 0.2 - 0.3 m of VCC that grades up into RAPG.

The bulk of DS2 consists of sharply bounded bedsets consisting predominantly of RAPG with FWP and FGSWP deposits (Figure 18D, E, F). An idealized stacking consists of basal FWP coarsening up into RAPG through poorly sorted FGSWP. This is overlain by a gradational transition (over 5 cm, Figure 18F) into well-sorted FGSWP, which is sharply overlain by the subsequent bedset.

South of the drainage divide five of these bedsets, each ranging between 0 – 12 m thick, are observed. Distally, bedsets grade from poorly sorted FGSWP and/or FWP into RAPG. Poorly sorted FGSWP has a high mud content, moderately- to well-preserved ornamentation of skeletal fragments and high planktonic foraminifera content, with no observed physical sedimentary structures. RAPG deposits consist of predominantly red-algal fragments, mostly branching, with encrusting forms becoming increasingly more common upwards. Locally, volcanic clasts are incorporated into RAPG deposits (Fig. 18E). Proximally, bedsets are capped by an abrupt gradation into distally thinning wedges of well-sorted FGSWP (up to 1.5 m thick, 5 m long). Occurrences of well-sorted FGSWP within these bedsets have grains that are highly abraded, show massive bedding and poorly defined trough cross-bedding. Bedsets dip away from the drainage divide at an average of 14˚.

North of the drainage divide three bedsets were identified. RAPG deposits onlap VCC between 182 - 222 m (164.7 - 222 m RE). Below 222 m (203 m RE), the lower contact is covered. It is assumed that RAPG deposits onlap, drape and downlap underlying VC. RAPG beds display poorly to well defined dm-scale fining up beds, grouped into 1 - 6 m scale, fining-up units separated by laterally extensive bedding surfaces and a sharp transition into the next overlying bedset (Figs. 18A, B). Bedsets dip to the north with an average dip of 4˚.

DS2 deposits are sharply overlain and truncated by a surface underlain by a red coloration (Fig. 18G). The surface separates previously described bedsets from deposits associated with SBZ3. SBZ3 deposits consist of complexly interbedded CAG, CGSPG, RAPG, OG as well as detrital and possibly *in situ* TF facies, all capped by a surface of significant alteration. CAG is the most abundant facies in SBZ 3 south of the drainage divide, where it contains abundant detrital stick-morphology *Tarbellastraea* coral, intraclasts (TF, CGSPG, CAG, and OG), serpulid worms, gastropods, bivalves (disarticulated and fragmented), ostracods (whole and fragmented), echinoderm fragments, red algal fragments, bryozoan fragments, volcanic grains, coated grains, benthic foraminifera and unidentifiable highly abraded grains. Concentration of grains varies locally; the most notable variations are local increases in coated grain content (predominantly oncoid, locally grading into lenticular beds of OG), intraclast concentrations, and coral concentrations. These concentrations are distributed throughout SBZ3. Detrital clasts (> 0.5 m) become less common downdip. North of the drainage divide, CAG deposits are similar in content, but are less common. Below 206 m CAG interfingers with CGSPG and below 190 m CGSPG deposits grade into RAPG. RAPG deposits extend down to 182 m where they downlap VC deposits. TF boulders occur at or near the base of upper DS2 deposits, are onlapped by surrounding deposits. Some boulders, which occur near the southern slope's updip extent of upper DS2 have geopetal fabrics suggestive of *in situ* preservation (up-oriented). Upper DS2 is capped by an alteration surface with local concentrations of highly weathered volcanic clasts, local caliche cement and formation of upward-widening, sub-vertical fissures up to 0.25 m in length.

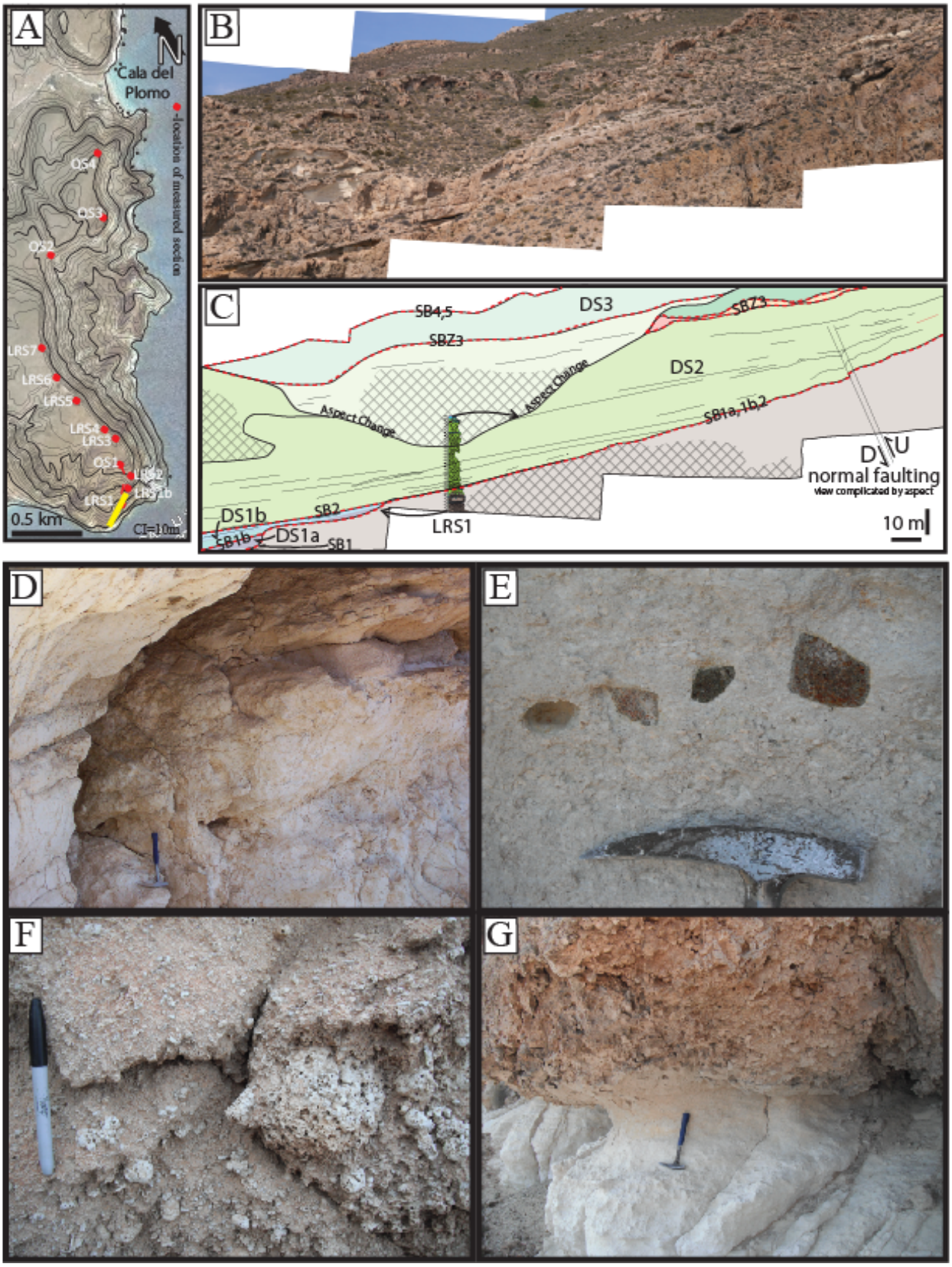
A
N
Cala del Plomo
location of measured section
OS4
OS3
OS2
LRS7
LRS6
LRS5
LRS4
LRS3
OS1
LRS2
LRS1b
LRS1
0.5 km
CI=10m
B
C
SB4,5
DS3
SBZ3
SBZ3
DS2
Aspect Change
Aspect Change
SB1a,1b,2
D
U
normal faulting
view complicated by aspect
DS1b
SB2
SB1b
DS1a
SB1
LRS1
10 m
D
E
F
G

Figure 18: Photographs and illustrations depicting characteristics of DS2 deposits. A) General location map with measured section locations denoted by red dots. Horizontal scale bar is 0.5 km and contour interval is 10 m. Location of photograph in image B is denoted by yellow bar. B) Photomosaic (full version in Appendix 4) showing the distal southern flank of the Rellana platform. Right (NE) end of photomosaic is 0.3 km from drainage divide and consists of DS1-3. Photo taken facing west. Scale visible in C. C) Overlay interpretation of photomosaic displayed in B, illustrating distribution of DS1 (isolated in lower left corner), upper DS2 (concentrated in upper right) and DS2. DS3 spans the photomosaic overlying SBZ3. Note sequence boundaries, facies, location of features depicted in images D-G, measured section LRS1, and the southernmost fault observed on the Rellana platform, partially offsetting carbonate deposits. D) RAPG deposits updip from section LRS1, featuring a bedset boundary marked by a sharply bounded distally thinning wedge of well-sorted FGSWP (black outline). Hammer is 32 cm. E) Poorly sorted FGSWP containing subrounded volcanic gravel; downslope is to the left. Hammer head is 15 cm. F) Proximal RAPG deposits featuring lenticular concentrations of large (up to 7 cm) rhodoliths and red algal fragments. Pen is 13 cm. G) Contact between FWP (recessive sediment behind hammer) and CAG of upper DS2 showing abundant molds of stick-morphology *Tarbellastraea* coral and red staining. This contact locally shows evidence for subaerial exposure, including rare upward widening fissures and spheroidal weathering. Hammer is 32 cm.

DS2 Interpretation.--- The SB2 surface is interpreted to be a sequence boundary indicative of a relative fall in sea level, based on evidence for subaerial exposure as described above. The SB2 surface is traced down to an elevation of 54 m (28 RE, PP8) before becoming untraceable due to lack of exposure. Overlying VC deposition results from reworking of volcanic basement. Overlying and downdip equivalent VCC facies reflect transition into carbonate-dominated deposition resulting from relative sea-level rise past the PP8 elevation (PP9). PP8 and PP9 are designated separately to indicate sea level turn-around occurred at or below 28 m RE.

BFR deposits observed on the Rellana platform locally contain large, disarticulated and whole bivalves identified by Betzler (2000) as *Isognomon.* Modern growth environments for these bivalves suggest shallow (< 30 m), temperate to tropical marine environments, commonly sheltered (Wilbur, 1983; Whorff *et al.,* 1995; Betzler, 2000). Disarticulation and random orientations suggest reworking, though preservation of ornamentation and concentration of bivalve remains indicates little to no abrasion. The more prevalent occurrence of BFR on the southern slope versus the northern slope is likely related to the sheltering effect of the volcanic high, a similar sheltering effect was proposed by Toomey (2003) for the western exposure of Ricardillo Peak indicating a similar predominant wave current direction for the two areas.

The depositional bedsets identified in DS2 cover a maximum paleotopographic relief of 53 m indicating a minimum sea level of 53 m above modern sea level prior to considerations for water depth of the facies. As per the facies interpretations discussed above, the transition from FWP (> 100 m water depth after Carannante *et al.,* 1988) to well-sorted FGSWP (10-30 m water depth) implies a shoaling upward trend. High to moderate abrasion of skeletal grains, and poorly defined trough cross-bedding of the well-sorted FGSWP deposits, as well as the presence of large rhodoliths in RAPG deposits, underlying the well-sorted FGSWP (Fig. 18F), indicates that

these deposits were reworked. Due to the lack of evidence for storm wave interaction (e.g. hummocky cross stratification or oscillatory ripples (Cheel, 1990; Cheel and Leckie, 1992), absence of graded bedding within well-sorted FGSWP beds (expected in deposition via low density sediment gravity flow, (Lowe, 1979)), and presence of trough cross-bedding suggests these features are interpreted to represent reworking by waves or debris flow deposition. If these deposits formed in a carbonate ramp-type environment, abundant bioturbation is expected of the facies below normal wave base.

The bedsets identified in DS2 can be used to quantitatively constrain a relative rise in sea level punctuated by periods of stillstand or relative sea-level fall. The stratigraphically lowest bedsets are concentrated on the southern end of the Rellana platform and can be directly correlated to similar bedsets (cycles) identified by Toomey (2003) in the neighboring Ricardillo area (Bedsets 4 and 5) (Appendix 5). The first fining upward bedset features RAPG deposits up to 105 m, indicating a minimum sea-level rise up to 125 m (104 m RE) to accommodate depositional interpretations (PP10). A relative sea-level fall is interpreted from the presence of gradationally overlying well-sorted FGSWP. The overlying FGSWP extends from 101 m to 117 m indicating that sea level must have continued to rise past and fallen to a minimum depth of 131 m (110 m RE) (PP11).

Continuation of RAPG deposition indicates sea-level rose beyond the PP11 elevation to an elevation sufficient to deposit RAPG up to an elevation of 123 m (102.2 m RE), indicating water depth must have been at least 143 m (122.2 m RE; PP12). Again, the overlying FGSWP deposits indicate a relative fall in sea level. FGSWP ranges from 126 m down to 119 m, therefore sea level must have fallen to at least 152 m (128.2 m RE) (PP13).

The next shoaling upward succession features RAPG deposition up to an elevation of 127 m, indicating sea level rose to a minimum of 147 m (126.4 RE; PP14). As described above, a gradation to overlying FGSWP indicates a relative fall in sea level. FGSWP deposits associated with this shoaling succession are found between 121 m and 128 m, indicating sea level fell to at least 151 m (131.4 m RE) (PP15).

The next shoaling upward succession features RAPG deposition up to an elevation of 129 m, indicating sea level rose to a minimum of 149 m (128.6 m RE; PP16). As described above, gradationally overlying FGSWP indicates a relative fall in sea level. FGSWP deposits associated with this shoaling succession are found between 125 m and 131 m, indicating sea level fell to at least 155 m (134.6 m RE; PP17).

The highest DS2 bedset identified on the southern slope of the Rellana platform features RAPG deposition up to an elevation of 134 m. Lithofacies interpretations allow intepretation of minimum water depth to 154 m. Corrected for uplift RAPG deposits reach up to 133.8 m (PP18). This pinning point represents the maximum elevation reached by rising relative sea level from *in situ* DS2 deposits south of the drainage divide. Overlying FGSWP deposits once again indicate a relative sea-level fall, these deposits range from 131 m to 138 m, indicating a minimum relative fall in sea level to 161 m (140.8 m RE; PP19).

North of the drainage divide, depositional bedsets range in thickness from 1 to 6 m and dip to the north at an average of 4˚. Well-sorted FGSWP deposits gradationally overlie RAPG facies; however they are not concentrated at the updip maximum of the depositional bedset as observed on the southern platform. Rather, they occur above an isolated BFR accumulation. This accumulation is 0.8 m thick and is laterally traceable for 4 m. the depositional bedsets drape this feature. Concentration of well-sorted FGSWP overlying this feature implies that the location of

the BFR was an energy focal point, and increased wave reworking resulted in deposition of the higher energy well-sorted FGSWP facies.

Sea level rise is suggested by the presence of FWP overlying deposits from this shoaling-upward bedset, and can be interpreted from detrital deposits in SBZ3. Further evidence for continued relative rise in sea level is the presence of similar deposits on the north slope of Rellana, which suggest the general trend of punctuated relative sea-level rise continued. The lowest occurrence of DS2 deposits north of the drainage divide is at an elevation of 182 m (164.7 m RE, PP20). Three shoaling upward bedsets are identified north of the drainage divide. The stratigraphically lowest shoaling upward succession on the northern slope of the Rellana platform features RAPG deposition up to an elevation of 215 m, indicating sea level rose to a minimum of 235 m (216.5 m RE; PP21). Following a similar pattern of relative sea-level change to the deposits described on the southern slope of the Rellana platform, gradationally overlying well-sorted FGSWP indicates a relative fall in sea level. FGSWP deposits associated with this shoaling succession are found between 203 m and 198 m, indicating sea level fell to at least 228 m (209.75 m RE; PP22).

The second shoaling upward succession on the northern slope of the Rellana platform features RAPG deposition up to an elevation of 222 m, indicating sea level rose to a minimum of 242 m (223 m RE; PP23). Gradationally overlying well-sorted FGSWP again indicates a relative fall in sea level. FGSWP deposits associated with this shoaling succession are found between 210 m and 203 m, indicating sea level fell to at least 205 m (214.75 m RE; PP24).

The third and final shoaling upward succession preserved on the northern slope of the Rellana platform features RAPG deposition up to an elevation of 221 m, indicating sea level rose to a minimum of 241 m (222 m RE; PP25). Gradationally overlying well-sorted FGSWP again

indicates a relative fall in sea level. FGSWP deposits associated with this shoaling succession are found between 212 m and 213 m, indicating relative sea level rose above and then fell to at least 242 m (223.7 m RE; PP26).

SBZ 3 overlies and truncates previously described bedsets. The red-stained basal surface occurs between 222 m and 182 m. SBZ 3 deposits are characterized by abundant intraclasts of DS2 deposits, boulders of CAG, PF and TF (evidencing disoriented geopetal fabrics), convoluted bedding, and complexly interbedded and interfingering CAG, CGSPG and RAPG, evidencing transport of shallow water facies on top of deep marine facies. North of the drainage divide, deposits associated with SBZ 3 are found between 215 m and 182 m. Above 215 m, the deposits are absent and SBZ 3 is preserved as a surface (SB3). Below 182 m, deposits are covered, and SBZ 3 amalgamates with or truncates SB1 and SB2.

SBZ 3 shows internal evidence of subaerial exposure including spheroidal weathering and autoclastic brecciation of volcanic clasts, localized caliche, and abundant red-staining. Because no diagnostic evidence of subaerial exposure was associated with the red-stained lower boundary, the red staining of that surface is likely related to subaerial exposure after SBZ3 deposits were re-distributed. Despite the lack of evidence for subaerial exposure below the deposits associated with SBZ3, the sequence boundary zone terminology is kept because of the low quality of exposure on the Rellana platform. Documentation of a similar sequence boundary zone from the neighboring La Molata platform (Las Negras) shows that exposure features can be subtle (e.g. on MB2 of Franseen *et al.*, 1993).

The presence of stick-morphology *Tarbellastraea* coral within deposits associated with SBZ3 indicates that water depth at growth position for these corals was 10 - 15 m (Grasso and Pedley, 1988; Pomar, 1994; Esteban, 1996). Given the presence of the TF boulders at the highest

extent of DS2 deposits south of the drainage divide (where they display geopetal fabrics that indicate preserved paleo-up direction and are possibly *in situ*), a minimum water depth of 10 - 15 m can be determined from coral morphologies for deposits found within SBZ 3 south of the drainage divide. This represents a minimum water depth because if the uppermost TF boulders are not *in situ,* they would have been deposited updip, requiring a higher relative sea-level. TF occurrence at the top of DS2, south of the drainage divide, is the first evidence for reef development on the platform. Large detrital coral clasts also occur on the northern slope of the Rellana platform but are far less common. The most prominent coral clast is clearly displaced and is found at an elevation of 142 m, indicating sea level was at an elevation of at least 152 m (132 m RE, PP29) during coral growth.

The upper surface of SBZ 3 can be traced from 222 m (203 m RE, PP27) down to an elevation of 114 m (92.7 m RE, PP31). It shows evidence of subaerial exposure including upward widening fissures and local caliche, indicating sea level fell from above these elevations to below. Pinning points are placed at the lowest extent of the sequence boundary north of the drainage divide (PP28) and the highest extent of SBZ3 south of the drainage divide (PP30) to reflect relative sea level fall past these elevations.

The characteristics of SBZ 3 indicate that it reflects a period of relative sea-level fall. The most likely scenario is that the initial drop in sea level left upslope areas subaerially exposed and aided triggering transport of facies to deeper water environments. Continued relative sea-level fall eventually exposed deposits in the downslope position. Therefore, SBZ 3 represents deposition entirely during falling sea level and is identified as a sequence boundary zone to reflect that the basal surface represents initial fall and potential exposure, and the upper surface is

a discontinuity that represents the continued relative fall in sea level and subsequent subaerial exposure.

Depositional Sequence 3

Description.--- DS3 forms the volumetric majority of preserved carbonate deposits on the platform. It ranges in thickness from 0 m to > 60 m thick (true maximum unknown due to covered section) and consists of skeletal packstone and grainstone that dips away from the drainage divide and can be traced updip into *Porites*-dominated coralgal framestone (PF and less common TF) and grainstone (CAG). DS3 deposits range from 114 to 248 m (92.7 to 230.5 m RE). DS3 is composed of distinctive features, surfaces and lithofacies that are listed from bottom to top:

1) Subaerial exposure surface suggesting relative sea-level fall atop DS2 (SBZ 3)
2) South of the drainage divide, SBZ 3 is overlain by RAPG beds, which interfinger updip with CGSPG. Beds onlap VCC deposits and drape SBZ 3 deposits distally.
3) Overlying RAPG south of the drainage divide and VCC to the north, skeletal packstone (CGSPG) deposits show distally shallowing dips away from updip equivalent *in situ Porites* and *Tarbellastraea* (and *Siderastraea*) PF, TF and CAG.
4) Overlain by a subaerial exposure surface (SB4).

The basal (15 - 20 m) DS3 deposits on the southern end of the Rellana platform are dominated by RAPG facies draping SBZ 3 deposits and onlapping VCC updip. These RAPG deposits feature large (up to 15 cm) rhodoliths, branching and encrusting red algal growth forms, randomly oriented pectinid bivalves with well-preserved ornamentation, and similarly preserved gastropods. These larger grains are surrounded by finer grained (up to v. coarse sand), well sorted, highly abraded sediment. These deposits grade up into CGSPG and develop a proximally

steepening dip. Grain-size, sorting, and abrasion vary, but generally deposits are well sorted, medium- to very coarse-sand sized and moderately-to-highly abraded. Skeletal components seen in the skeletal packstone include: whole, disarticulated and fragmented bivalves, whole and fragmented gastropods, *Porites* and *Tarbellastraea* coral fragments (*Siderastraea* is less commonly present), red algal fragments, bryozoans, foraminifers, echinoderm fragments, green algae and a number of unidentifiable skeletal fragments. CGSPG interfingers updip with a complex stratigraphic framework of *Porites* and less commonly *Tarbellastraea* framestone (PF and TF) and CAG. These facies are cliff-forming and feature prominent coral molds displaying *in-situ* growth and detrital coral clasts. Away from the drainage divide, preserved framestone and downdip equivalent CGSPG is dominated by *Porites*.

Field observations show 135 m of relief observable in DS3 deposits with the highest elevation of 248 m (230.5 m RE) occurring on the northern side of the platform (near LRS6) and the lowest observed deposits (100 m; 91.4 m RE) occurring at the northern extreme of the study area (Fig. 3, Appendix 5). *Porites* is the dominant coral genus observed within DS3 and it has growth forms of branching/stick (up to 5.75 m tall), massive head (up to 3 m tall) and less commonly, encrusting (up to .25 m thick). Other, less common corals are *Tarbellastraea* and *Siderastraea,* which are commonly preserved as molds of stick, and less commonly, head growth forms up to .75 m, localized at the drainage divide. CGSPG facies dip steeply (~20˚ - 25˚) away from framestone and CAG deposits in proximal areas, with dips becoming less steep distally. Deposit thicknesses range from 8 m at the divide to > 60 m (maximum thickness obscured by covered section). The facies change between TF/PF and CAG to CGSPG is characterized by a large amount of TF/PF and CAG detritus, which gradationally fines downdip. This change occurs generally at a break in slope, which separates steeply dipping CAG associated with the

PF, TF and CAG reef from the distally decreasing dips of the CGSPG deposits. Lateral tracing of cliff -forming PF, TF and CAG facies resulted in identification of three basinward-dipping surfaces across which coral growth morphology changed.

DS3 is capped by an erosional surface that truncates bedding trends, features local brecciation, and shows a nearly horizontal erosion surface (dips vary locally, generally ~ 1˚ - 3˚) on the northern end of the exposure that extends 300 m (SB4). There is red staining and localized fissuring near section LRS4. Fissures are upward widening and up to 10 cm deep, infilled with highly altered calcareous sediments. Downdip, this surface shows evidence for subaerial exposure or is erosionally truncated along SB5.

DS3 Interpretation.--- SBZ 3 is interpreted to represent deposits associated with a relative fall in sea level and subaerial exposure, as described previously. The overlying deposits (RAPG and CGSPG) indicate a return to marine deposition. Deposits at the extreme northern extent of the study area (overlying the intermediate paleotopographic high) are likely related to DS3 deposition due to the elevations of occurrence of the deposits (105 m to 182 m; 98 - 175 m RE), although no physical correlation could be confidently traced in the field (Appendix 4, 5). The presence of *Porites* clasts in FWP and poorly sorted FGSWP support the strata being deeper water DS3 deposits. Isolated occurrences of CAG and boulder sized (up to .5 m) PF intraclasts indicate potential reef development (as near measured section QS4), but no *in situ* reef material was observed.

The lowest DS3 deposits preserved on the Rellana platform are exposed on the southern end of the platform (at 114 m, 92.7 m RE; PP32). Marine sediments overlie the SBZ3 surface up to an elevation of 222 m, 203 m RE (PP35), indicating flooding of the highest extent of subaerial exposure south of the drainage divide (142 m, 122 m RE, PP33), and flooding of the subaerial

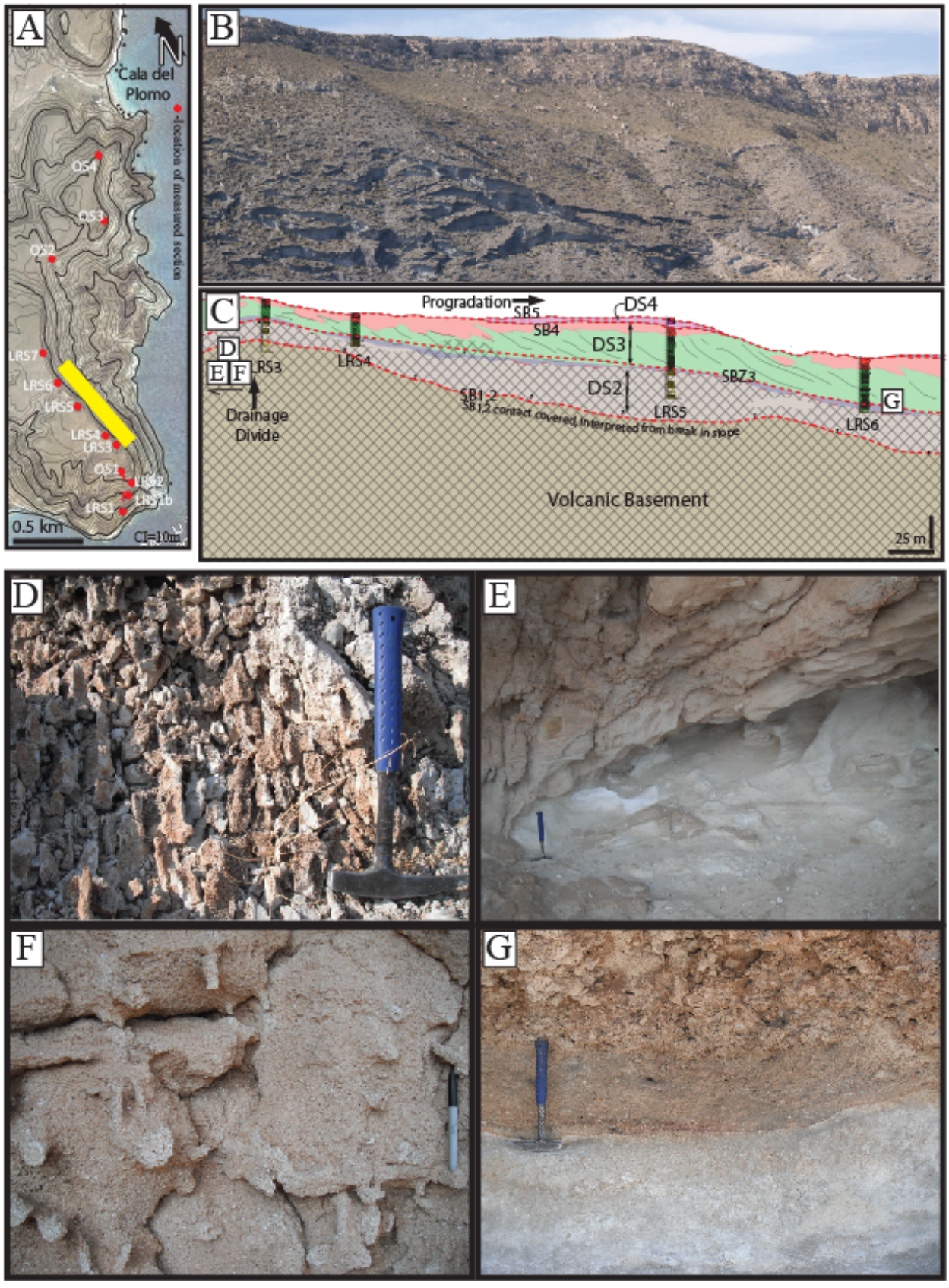
A
N
Cala del Plomo
location of measured section
DS4
DS3
DS2
LRS7
LRS6
LRS5
LRS4
LRS3
DS1
LRS2
LRS1b
LRS1
0.5 km
CI=10m
B
C
Progradation
SB5
SB4
DS4
DS3
DS2
SBZ3
D
E F
LRS3
LRS4
LRS5
LRS6
G
Drainage Divide
SB1-2
SB1,2 contact covered, interpreted from break in slope
Volcanic Basement
25 m
D
E
F
G

Figure 19: Photographs and illustrations depicting characteristics of DS3 deposits. A) General location map with measured section locations denoted by red dots. Location of photograph in B is marked with yellow rectangle. Horizontal scale is 0.5 km; contour interval is 10 m. B) Photograph showing outcrop exposure of typical DS3 deposits. Deposits pictured are located just north of the drainage divide located at left (south) end of image. DS3 deposits comprise the majority of visible cliff-forming deposits near the top of the exposure. Photo taken facing SW. C) Overlay interpretation of photograph B, illustrating general distribution of depositional sequences, sequence boundaries, facies, measured sections, location of features depicted in D-G below as well as notes on interpreted reef development. Red overlay polygon represents *in situ* PF (dominant) and TF (less common) with surrounding CAG and CGSPG deposits that are largely indistinguishable at this scale. The green overlay polygon indicates downslope deposits from *in situ* reef development and commonly displays proximally steepening dip patterns. DS2 deposits in this image are largely covered; the lower amalgamated sequence boundaries are interpreted to coincide with a significant break in slope. Images D-F below are located south of the drainage divide Their precise location can be seen in Appendix 5. D) Photograph of CAG deposits on the flank of *in situ* coral growth (not depicted). The surface is covered with molds of stick growth morphology *Tarbellastraea* coral showing a preferential orientation with the longest axis pointing downslope (towards photographer). Hammer is 32 cm. E) Cross bedding developed in downdip equivalent deposits to PF and TF. Cross bedding of CGSPG (and RAPG basally) is concentrated south of the drainage divide and is potentially related to increased sediment transport associated with abundant bypass down the steeper paleoslope. F) Bioturbation located in CGSPG deposits within the highest deposits on the south side of the drainage divide, ichnogenera are unknown. Pen is 13 cm. G) Surface showing contact between finer-grained CGSPG (medium - coarse sand) with a low coralgal content with coarser-grained CGSPG (very coarse to gravel) with a high coralgal content. This contact is traced updip (to the left/South) into a truncation surface overlying *in situ* reef deposits (annotated in C). Hammer is 32 cm.

exposure surface SB3 north of the drainage divide (lowest exposure at 182 m, 164.7 m RE, PP34). Basal DS3 deposits consist of RAPG draping the shallow-dipping paleotopography created by SBZ 3 deposits; they onlap VCC updip. These beds are overlain by RAPG deposits that interfinger updip and grade up into CGSPG, with proximally steepening bedding. The large (up to 15 cm) rhodoliths appear to be at or near growth position, and are surrounded by highly abraded, finer grained deposits. The juxtaposition of the highly abraded, fine-grained material with well-ornamented, seemingly minimally transported heterozoan components indicates that the abraded, fine-grained sediment likely originated from upslope. Dillett (2004) presented a model to describe similar deposits in a heterozoan clinoform, in which an autochthonous coarse fraction of the sediment (in this case the rhodolith and other red algal growth forms in addition to minimally abraded bivalves and gastropods) grows on the clinoform slope. Fine grained sediment (the allochthonous fine fraction) is transported downdip from a high energy environment. In the Dillett model, transportation was interpreted to be from a wave truncation surface. Transportation possibly was caused by storm events, or similar triggers. The sediments were then heavily bioturbated, obfuscating bedding and other sedimentary structures (Dillett, 2004).

The shift from RAPG to CGSPG coincides with the development of proximally steepening dips. Proximally increasing coral content in CGSPG deposits suggests reef re-initiation had occurred, and the proximally steepening dips are interpreted to be the base of developing clinoforms. No bedding surfaces are directly traceable from these early clinoforms into *in situ* coral growth. Rather, coral material present in the lowest CGSPG deposits is interpreted to have bypassed from upslope coral growth due to the steep paleotopography of the volcanic basement (up to 45˚ locally). The lack of preserved *in situ* coral associated with

deposition of the lowest CGSPG deposits is likely due to this bypass tendency, or Miocene erosion.

The exposure of DS3 on the Rellana platform is approximately perpendicular to the strike of the platform margin, facilitating identification of geometries within the reef-core complex. Earliest *in situ* reef development is seen at an elevation of 234 m (215 m RE), extends laterally for ~5.5 m and features 2-5 m thick coral growths (predominantly *Porites*, with rare *Tarbellastraea*, and *Siderastraea*) and associated facies (CGSPG, CAG) that pinchout rapidly away from the highest point. Aggradation results in reef growth up to at least 241 m (RE 222 m; PP 36). These deposits are interpreted to represent aggradational, patch reef-like growth. Aggradational reef deposits are dominated by branching coral growth morphology, however, heads and rare encrusting corals were also encountered, suggesting deposition occurred in > 10 m to slightly <10 m water depths. A second aggradational coral growth example 60 m to the north has similar coral diversity and morphologies, and shows aggradational growth up to 244 m (230 m RE, PP37). These two coral growth examples are situated on either side of the drainage divide at similar elevations and possibly developed contemporaneously (Appendix 5). A clinoform-like Porites-dominated reef 'wedge' overlies the northern aggradational growth. This wedge extends to the north, interfingering downslope with CGSPG interpreted to be forereef deposits. The juxtaposition of the aggradational growth to a laterally continuous (22 m) 'wedge' potentially represents a transition in reef development from aggradational to progradational geometry, likely related to relative sea-level changes shifting from rising to highstand stages (*sensu* Schlager, 2005 and references within).

The location of *in situ* coral deposits in DS3 demonstrate multiple truncation surfaces that are analyzed to determine if they are associated with downstepping events and subsequent

progradation, or are reflective of a collapse event independent of relative seal level changes. These features are visible on the northern side of the drainage divide, where low substrate slope enhances reef progradation. Truncation surfaces are evidenced by a pronounced erosion surface overlying proximal beds, without a quantifiable decrease in relative sea level (as indicated by coral morphologies *sensu* Pomar, 1991). Downstepping events are identified where a pronounced erosion surface is accompanied by a > 5 m interpreted relative fall in sea-level, implied by reef morphologies and distribution distally relative to truncated proximal reef development (*sensu* Pomar, 1991). Locations of the truncation surfaces identified as downstepping events can be used to enhance relative sea level history.

Progradational coral growth extends down from 240 m (221 m RE) to an elevation of 232 m. Facies interpretations (5 – 40 m depth range for stick morphology PF) indicate a minimum sea level position of 245 m (226 m RE; PP 38) for initial progradational reef development. Planar bedded, well-sorted CGSPG deposits overlie the progradational *in situ* reef development described above. The abundance of detrital PF and CAG deposits within this CGSPG coupled with thin planar bedding, and good sorting indicates deposition in a high-energy environment. The surface separating the planar-bedded CGSPG from overlying reef core deposits is considered truncation surface 1. It shows no evidence for subaerial exposure, and overlying reef material occurs down to 232 m (213 m RE) at its updip maximum, with facies suggesting a maximum sea level elevation at 253 m RE (PP39). The interruption in reef core development does not reflect a drop in relative sea level, so it is likely this scour surface is related to a reef calving event and not downstepping.

The second truncation surface occurs 125 m north of LRS4 (Fig. 3, Appendix 5). The truncation surface is traceable laterally for 180 m before amalgamating with forereef bedding

surfaces, becoming indistinguishable from normal bedding. Below the truncation surface, stick-morphology PF deposits indicate a minimum relative sea level of 245 m (231.3 m RE, PP40). *In situ* coral material is found overlying the truncation surface down to an elevation of 235 m, suggesting a maximum sea level of 265 m (256.4 m RE, PP41). The range of depths known for the observed coral growth morphologies overlap across the truncation surface, so no downstepping can be definitively identified at this location, and the truncation surface could be related to slope failure.

Continued progradation extends 255 m across the northern slope of the Rellana platform at which point continuous *in situ* reef deposition is interrupted. This progradation reaches an elevation of 239.5 m and the facies suggest sea level elevation was at least at 244.5 m (226.5 m RE; PP42). CGSPG, interpreted as forereef slope deposits, extend 15 - 20 m farther north, displaying dips (~ 20˚), truncated by modern erosion, similar to those below that are physically traceable updip into *in situ* reef core deposits. These CGSPG deposits are interpreted to be equivalent with maximum progradation of reef core prior to the third truncation surface. Resumed *in situ* progradation of reef core follows the third interpreted truncation surface and is found down to an elevation of 228 m. The presence of stick coral growth morphology in the reef indicates a relative sea level maximum of 268 m (250.4 m RE, PP43). Minimum water depth is indicated by the shallowest *in situ* reef deposits, immediately overlying the truncation surface (242.5 m; 224.5 m RE). This range of elevations reflects the potential window of water depths before and after collapse, indicating this surface could have formed without a change in relative sea level.

Just 40 m north of LRS6 is the highest exposure of the fourth potential downstepping event. This surface is marked by a change in coral growth morphology. Deposits below the

truncation surface display stick growth morphology (5 - 40 m depth range; *sensu* Pomar, 1983; Saint-Martin, 1990; Riding *et al.*, 1991; Pomar, 1991; Esteban, 1996), indicating a minimum relative sea level of 253 m (235.5 m RE, PP44). Reef material is found below this surface down to an elevation of 233 (215 m RE) where branching coral morphologies are observed, indicating sea level elevation of at most 273 m (255 m RE); PP33 is placed in the depth range reflected by these indicators (235.5 to 255 m RE). These deposits are separated from elevation equivalent massive and encrusting coral growth morphologies (up to 1 m thick) by a traceable (330 m laterally) surface. This surface is overlain by *in situ* reef core deposits down to an elevation of 228 m (212 m RE). The massive head and encrusting reef growth morphologies are indicative of water depth in < 10 m water depth (Grasso and Pedley, 1988; Saint-Martin, 1990; Pomar, 1991; Riding *et al.,* 1991; Esteban, 1996). Relative sea-level fall is interpreted to have been below 257 m (239.5 m RE; PP45). The change from stick to massive and head coral morphologies implies a shift to shallower water depths, however the overlapping of associated depth ranges indicates that this truncation surface and subsequent coral growth could have developed without invoking a change in relative sea level.

Continued progradation 155 m over the northern slope of the Rellana platform represents the last definitively *in situ* reef core deposits, occurring at 241.5 m (230 m RE, PP46), and expressed as massive growth morphology PF. CGSPG deposits associated with these *in situ* reef core deposits show increasing dips near the most distal coral deposits (reaching up to 28˚ downdip from the most distal *in situ* reef core deposits). Additional CGSPG beds occur more distally, up to 20 m, and reach a maximum dip of ~30˚. These steeply dipping deposits downlap on older forereef deposits and are interpreted to be equivalent to subsequently eroded reef core deposits. The increasing dips are interpreted to indicate over-steepening of the reef margin. This

is likely in response to the increase in accommodation as the reef margin approached the distally steepened basin margin. PP47 is placed at the most distal of these bedding trends, and is interpreted to represent relative sea level during the final deposition of preserved *in situ* DS3 reef material on the platform. The CGSPG deposits occur at an elevation of 240 m. Interpreted sea level elevation from CGSPG facies interpretations is 245 m (229.8 m RE).

Additional CGSPG deposits occur north of the most distal reef core deposits, onlapping the potentially oversteepened surface associated with the final truncation surface. No updip gradation is observed associated with these deposits. They are compositionally similar to forereef slope deposits and are tentatively interpreted to represent reworking and re-deposition of oversteepened reef margin prior to exposure of the platform associated with continued relative sea-level fall (forming SB4). These deposits occur at an elevation of 240 m and are truncated by SB4. The similarities these CGSPG deposits share with those interpreted as forereef deposits leads to a similar water depth interpretation, indicating sea level elevation was at least 245 m during their deposition (229.8 m RE), prior to subaerial exposure (SB4). PP48 is located 80 m west of LRS5 and marks the lowest elevation that SB4 and SB5 are distinguishable on the Rellana platform (240 m; 224.8 m RE); below this elevation SB4 is truncated by SB5.

Features visible on the Rellana platform indicating that SB4 is a subaerial exposure surface are not definitive. The presence of upward-widening fissures, erosional scouring (possibly up to tens of meters) and possible caliche cement development are the only characteristics observed in the field area. Caliche cement development observed is currently exposed to modern weathering, thus its exposure during SB4 is questionable and it may be Pliocene in age or later. The basal surface for DS4 it is a regionally recognizable surface that has well-documented evidence for subaerial exposure including; chalkification, micritization,

rhizoliths, autoclastic brecciation, caliche, possible soil development, laminated crusts, vertical fissures, circum-granular cracks, meniscus cements, and fenestrae (Esteban and Giner, 1980; Dabrio et al. 1981; Franseen and Mankiewicz, 1991; Whitesell, 1995; Franseen et al., 1996). Given the high elevation of SB4 on the Rellana platform relative to neighboring areas with documented subaerial exposure features, subaerial exposure is assumed.

Depositional Sequences 4-7

Description.--- DS4-7 are found capping exposures 248 m above modern sea-level (229.7 m RE). In total, outcrop of these four sequences have a thickness of 0 m to 12 m thick. Strata dip gently to the southwest (dips vary from ~0˚ to 5˚). DS4-7 are bounded above and below by subaerial exposure surfaces. These sequences are discussed together due to genetic similarities. DS 4-7, as a composite unit, is laterally and vertically heterogeneous and contains distinctive lithofacies and geometries. A general vertical succession through DS 4-7 deposits on the Rellana platform is described below.

1) Subaerial exposure surface SB4, as described above.
2) Sequence 4: trough cross-bedded OG locally overlies alteration surface; within the OG deposits, there are branching *Porites* (up to 1.5 m tall) coral colonies; flanking CAG and CGSPG occur locally.
3) Subaerial exposure surface (SB4a).
4) Sequence 5: stromatolitic boundstone at the base; overlain by trough cross-bedded and massive OG with rare TBS growths up to 2.5 m
5) Subaerial exposure surface (SB4b)

6) Sequence 6: heterogeneous package containing thrombolitic boundstone (TBS); coralgal framestones (TF, PF); flanking oolitic grainstone (OG); coralgal grainstone (CAG).
7) Subaerial exposure surface (SB4c)
8) Sequence 7: stromatolitic boundstone and localized pockets of skeletal peloidal grainstone; stromatolitic and thrombolitic boundstones
9) Capped by subaerial exposure surface identified as SB5

The lowest sequence (DS4) is preserved throughout the study area and generally consists of trough cross-bedded OG deposits with rare occurrences of small (up to 1.5 m) *in situ Porites* branching colonies, flanked by onlapping CAG deposits. Sequence 4 thickness ranges from 10 cm to 2 m, is amalgamated with SB4 south of the drainage divide. It is visible north of the drainage divide up to 243 m (226.3 m RE), and is laterally discontinuous but traceable over 80 m before being truncated by SB4b. The overlying subaerial exposure surface (SB4b) is the boundary between the DS4 and DS5. DS5 is visible north of the drainage divide between a maximum elevation of 248 m (229.7 m RE) and 243 m (225 m RE). DS5 deposits consist of trough cross bedded OG and TBS growths up to 1.5 m. These growths are concentrated in the deposits to the north of the drainage divide, where sequence 5 is thicker (up to 5 m). Stromatolitic boundstone is prevalent overlying the alteration surface capping sequence 5, and is visible throughout DS 4-7 deposits on the Rellana platform. Sequence 6 is found between 248 m (229.7 m RE) and 243.2 m (225.2 m RE) and consists of abundant trough cross-bedded OG deposits, common thrombolite growths (up to 3 m tall, 6 m wide) and *in situ Porites* reef colonies (stick morphology dominant, rare head and encrusting morphologies) and ranges in thickness from 1 m to 5 m. At the position of the drainage divide and to its north, sequence 7 is

poorly preserved and can be found between 251 m (234.1 m RE) and 245 m (225.9 m RE). Locally DS7 has A(S)BS overlying the basal alteration surface, and locally consists of thin (up to .5 m) deposits of trough cross-bedded OG. DS7 is laterally discontinuous and ranges in thickness from 0 to .75 m. DS4-7 sediments tend to be highly recrystallized and further sedimentological characteristics are difficult to identify. DS 4-7 deposits are capped by subaerial exposure surface 5 (SB5), which spans the platform down to modern sea level.

The four microbial, oolitic and coralgal sequences associated with DS 4-7 are described in the neighboring Ricardillo area (Fig. 1) by Lipinski (2010) and Goldstein *et al.* (2013). To expand upon work done in those studies, those data were included in the sea-level history reconstruction for DS4-7, presented below.

DS 4-7 Interpretation.--- The 4 microbial, oolitic and coralgal sequences associated with DS 4-7 are regionally recognized and attributed to high-amplitude cyclic glacioeustacy and evaporitic drawdown of the Mediterranean (Franseen et al., 1993; Goldstein and Franseen, 1995; Franseen et. al., 1996; Franseen et al., 1998), representing the culmination of Miocene carbonate deposition in the Mediterranean region (Terminal Carbonate Complex (TCC) of Esteban (1979)). Initial descriptions of TCC deposits in Ricardillo/Rellana study area (Fig. 1) by Toomey (2003) were expanded upon by Lipinski (2010) and Goldstein *et al.* (2013). Physical tracing between the Ricardillo/Rellana TCC deposits and those observed on the eastern side of the Rellana platform (this study) is complicated by covered section and the laterally variable nature of the TCC deposits; however, the alteration surface separating DS5 and 6 was correlated through a drainage on top of the Rellana Platform. Comparison of TCC-equivalent deposits on the relatively unstudied eastern exposure of the Rellana platform with those described on the western margin by Lipinski (2010) provides increased potential for 3-dimensional analysis of TCC deposit

distribution, and increased constraints on highstand maximums within TCC deposits (after application of adjustments for uplift (*sensu* Hess, 2011). These data can be seen in figure 21.

In the Ricardillo/Rellana area, DS4 overlies SB4 between 181 m (160 m RE) and 239 m (212.5 m RE), indicating a relative rise in sea level (Fig. 21, point 1r). These deposits are described as bioturbated ooid grainstone facies (> 10 m water depth) that are gradationally bounded updip and overlain by trough cross-bedded ooid grainstone facies (< 10m water depth). Further gradation updip (and overlying) includes planar-bedded ooid grainstone facies (< 2m water depth). Locally, upward gradation continues into volcaniclastic-rich planar bedded ooid grainstone facies (<3m water depth); with a local cap of fenestral ooid grainstone facies (subaerial exposure; Lipinski, 2010; Goldstein *et al*, 2013; for facies descriptions see Table 4) indicating sea level rise up to a minimum of 243 m (212.5 m RE) (Fig. 21).

DS4 deposits on the Rellana platform are limited to the areas of relatively flat paleotopography of the northern-most end of the exposure between 239.5 m (221.5 m RE, PP49) up to 243 m (225 m RE (PP50), indicating flooding up to that elevation. These deposits are generally poorly preserved due to abundant vegetation, and recessive tendencies. Where deposits are positively identifiable they consist of low angle trough cross-bedded to planar bedded ooid grainstone (OG facies, Table 1) that reach a maximum observed thickness of 2.5 m. The stratal package described in the Ricardillo/Rellana area for DS4 indicates shoaling upward deposition culminating in subaerial exposure (evidenced by fenestral ooid grainstone facies at 243m). Deposits preserved in the Rellana study area reflect continued sea-level rise sufficient to deposit trough cross-bedded to planar bedded ooid grainstones (Table 4), suggesting water depths < 10 to < 3 m during deposition, indicating a minimum rise in relative sea-level up to 246 m (228 m RE) prior to the subaerial exposure described in the Ricardillo/Rellana area. It is possible that the

fenestral fabric identified by Lipinski (2010) was not observed in the northern Rellana platform due to poor quality exposure (no cohesive samples could be obtained), and these deposits represent deposition in the immediate foreshore or possibly backshore environment (Ball, 1967; Inden and Moore, 1983), similar to the fenestral ooid grainstone facies of Lipinski (2010), up to the maximum reconstructed elevation (225 m, PP 50/51). Exposure of these deposits indicates a relative sea level fall down to at least 240 m (223.1 m RE, PP52) as evidenced in the Rellana study area and down to 184.6 m (166.6 m RE, PP4r) in Ricardillo.

DS5 is found throughout the Ricardillo/Rellana study area and the Rellana platform. In the Ricardillo/Rellana area, DS5 is divided into low-elevation and high-elevation stacking patterns (Lipinski, 2010). At low elevations, isolated trough cross-bedded ooid bivalve facies are overlain by laterally extensive thrombolite boundstone interbedded with trough cross-bedded ooid grainstone deposits 184.6 - 221 m (164.1 - 202.5 m RE). Locally these deposits shoal upward into volcaniclastic-rich planar bedded ooid grainstone and local caps of fenestral ooid grainstone. At high elevations (221 - 257m; 202.5 - 228.25 m RE) deposits are dominated by trough cross-bedded ooid bivalve grainstone interbedded with thrombolite boundstone facies. These deposits are sharply overlain (with local gradational contacts) by cross-bedded ooid grainstone, which follows a shoaling up trend through volcaniclastic-rich planar bedded ooid grainstone into fenestral ooid grainstone. At the highest elevations (242 - 257 m; 213.5 m - 228.5 m RE) only trough cross-bedded ooid bivalve grainstone and thrombolite boundstone facies are observed. These deposits reflect a sea level rise up to 22.5 m (RE), (PP5-8r).

DS5 deposits on the eastern side of the Rellana platform are more limited in their elevation range than those described by Lipinski (2010), ranging from 240 - 243 m (223.1 - 229.7 m RE, PP53 and 54 respectively, reflecting inundation). Isolated and rare occurrence of

Porites framestone (PF facies; Table 1) within the northernmost DS5 deposits on the Rellana platform and immediately overlying the drainage divide of the Rellana platform (up to 243 m, 230.7 m RE; PP55) indicate earlier reef development than identified in the Ricardillo/Rellana area (not seen until DS6). Evidence for subaerial exposure of DS5 deposits ranges from 248 m down to 243 m on Rellana (229.7 m to 22m RE, PP 56, 57 respectively). Subaerial exposure in the Ricardillo/Rellana area indicates relative sea level fell to at least 186.1 m (166.1 m RE, PP10r)

Lipinski (2010) described DS6 deposits as featuring locally laterally extensive stromatolites overlain by massive ooid grainstone that grade up into trough cross-bedded ooid grainstone with interbedded *Porites* boundstone (PF facies equivalent). The *Porites* boundstone is thick (up to 6 m) and laterally extensive at low elevations (181 -217 m; 159.75 - 196 m RE). Above 200 m (179 m RE), *Porites* boundstone occurs as isolated patches (< 2 m wide and < 3 m thick). High elevations (217 - 240 m; 196 m - 212 m RE) feature laterally extensive stromatolites overlain by trough cross-bedded ooid grainstone interbedded with isolated *Porites* boundstone (Lipinski, 2010).

DS6 deposits on the eastern margin of the Rellana platform show a slightly higher range of elevations, with occurrences observed between 243 - 248 m (225 - 229.7 m RE, PP58, 59 respectively). PF deposits occur up to 246 m implying minimum relative sea level rise to 246 m (234.3 m RE, PP60). PF deposits within DS6 on the eastern margin are abundant and range in width from 1 to 63 m, with average width in the 20 - 30 m range. Thicknesses of PF deposits range from 1 to 6 m. The extensive PF deposits observed in DS6 could potentially be fringing reef growths on shallow substrate. No lagoonal deposits, or deposits with high carbonate mud concentrations or other evidence for low energy during deposition were observed in the study

area, excluding microbialites, which have been shown to be deposited in a wide range of water depths and energy levels (Braga et al., 1995; Mancini et al., 1998; Grotzinger et al., 2000; Mancini and Parcell, 2001; Whalen et al. 2002; Adams et al., 2004; Batten et al., 2004; Mancini et al., 2004; Adams et al., 2005; Heydari and Baria, 2005; Mancini et al., 2008; Planavsky and Ginsburg, 2009; Lipinski, 2010). So reef development was apparently not extensive enough to result in lagoon development. SB4c ranges from 248 m down to 243 m on the Rellana platform (229.7 m and 225 m, PP 61, 62 respectively). Subaerial exposure in the Ricardillo/Rellana area indicates relative sea level fell to at least 186.1 m (166.1 m RE, PP14r).

The final depositional sequence (DS7) is truncated by modern erosion. Deposits in the Ricardillo/Rellana field area occur < 211.5 m (197 - 211.5 m; 176 - 191.5 m RE) and consist of paleotopography-draping stromatolites and overlying thrombolitic boundstone (rarely overlain by trough cross-bedded ooid grainstone) (Lipinski, 2010). On Rellana DS7 deposits are observed between 245 - 251 m (225.9 - 234.1 m RE, PP63 and 64) and range in thickness from 0 to 2 m. No thrombolitic material was observed on the northern slope of the platform, one displaced PF deposit showing encrusting and massive head growth morphology was found near section LRS7, indicative of <10 m of water depth during deposition (Grasso and Pedley, 1988; Saint-Martin, 1990; Pomar, 1983; Pomar, 1991; Riding *et al.,* 1991; Esteban, 1996). DS7 is overlain by SB5, which extends down to modern sea level. Sea level would have reached and fell below the highest elevation of DS7 (251 m, 234.1 m RE, PP63, 64), down past lowest exposed DS7 deposits (at 245m, 230 m RE, PP66) to the lowest elevation SB5 is discernable on the Rellana Platform (104 m, 94.7 m RE, PP67). Presumably relative sea level continued to fall to near or below modern sea level. SB5 is characterized by abundant caliche, rhizoliths, and vertical

fissures and cannot be distinguished from the modern exposure surface. This sequence boundary marks the end of marine deposition on the Rellana platform.

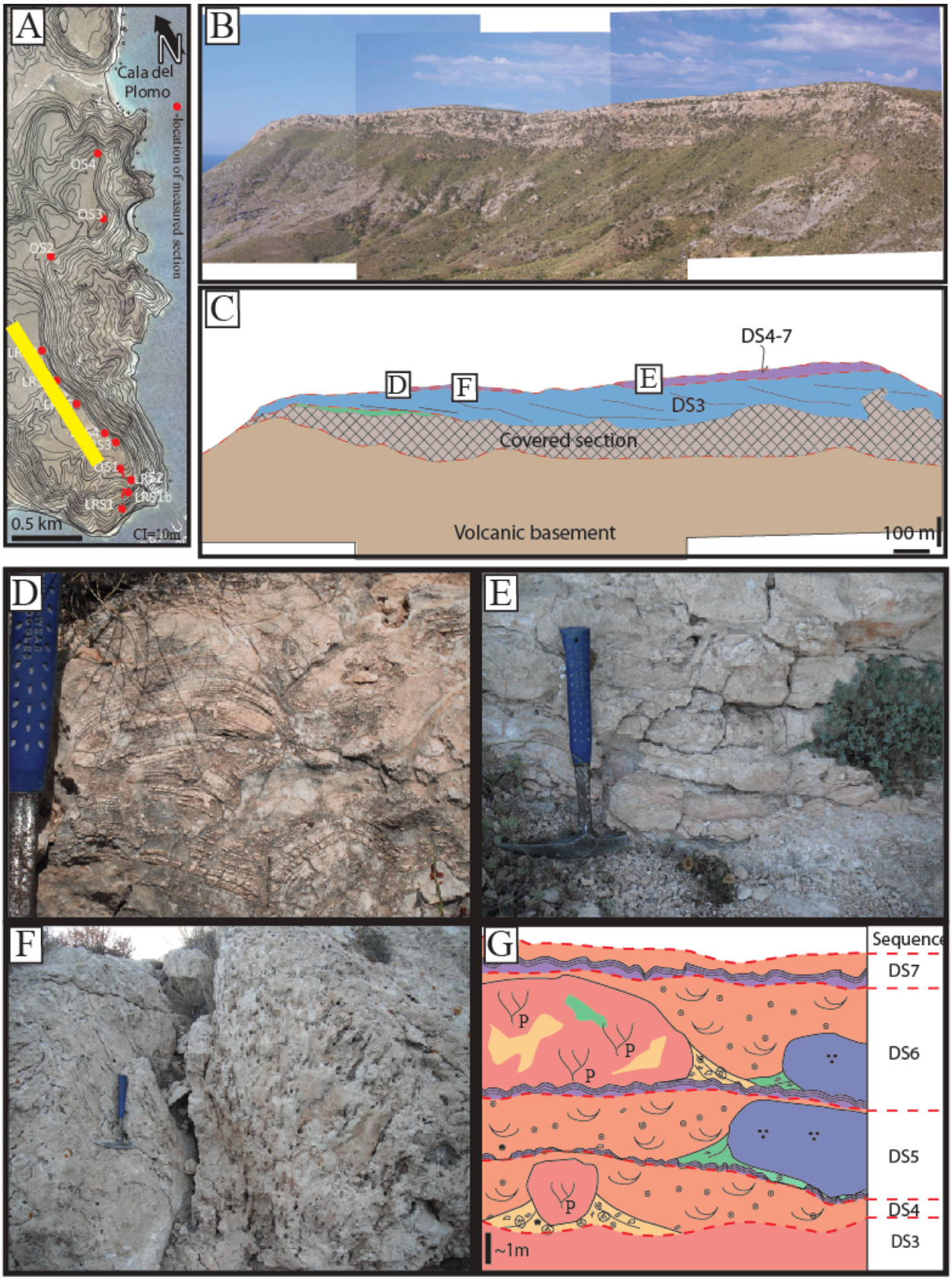
A
N
Cala del Plomo
location of measured section
QS4
QS3
QS2
QS1
LRS2
LRS1
0.5 km
CI=10m
B
C
DS4-7
D
F
E
DS3
Covered section
Volcanic basement
100 m
D
E
F
G
Sequence
DS7
DS6
DS5
DS4
DS3
P
~1m

Figure 20: Photographs and illustrations demonstrating characteristics and features of DS 4-7 deposits on the Rellana platform. A) General location map with measured section locations denoted by red dots. Location of photograph in image B is denoted by yellow box. Horizontal scale bar is 0.5 km and contour interval is 10 m. B) Photomosaic showing the extent of the Rellana platform north of the drainage divide. Photo taken looking SW (scale in image C shows vertical scale at drainage divide.). C) Overlay interpretation of photomosaic B illustrating distribution of depositional sequences north of the drainage divide. Note the limitation of DS 4-7 deposits to the highest elevations with relatively smooth paleotopography. Scale in lower right corner based on thickness at drainage divide. Interpretations not carried through covered section for simplicity. D) Photograph of A(S)BS showing laterally linked hemispheroid growth morphology, Hammer handle is 3 cm wide. E) Photograph showing DS 6-7 sequence contact (near head of hammer) with overlying A(S)BS, CGSPG and overlying trough cross-bedded OG deposits. Hammer is 32 cm. F) *In situ Porites* stick morphology coral colonies, flanked by CGSPG and CAG deposits. Hammer is 32 cm. G) Generalized stratigraphy of DS 4-7 deposits on the Rellana platform. OG deposits are present in all sequences. A(S)BS is present basally in sequences 6-7. PF (and rare TF) is rarely present in sequence 4 and very common in sequence 5, where patch reef facies reach up to 3 m tall and 6 m wide. TBS is common in sequence 5 and 6. Sequence 7 is highly recrystallized, associated with exposure by SB5.

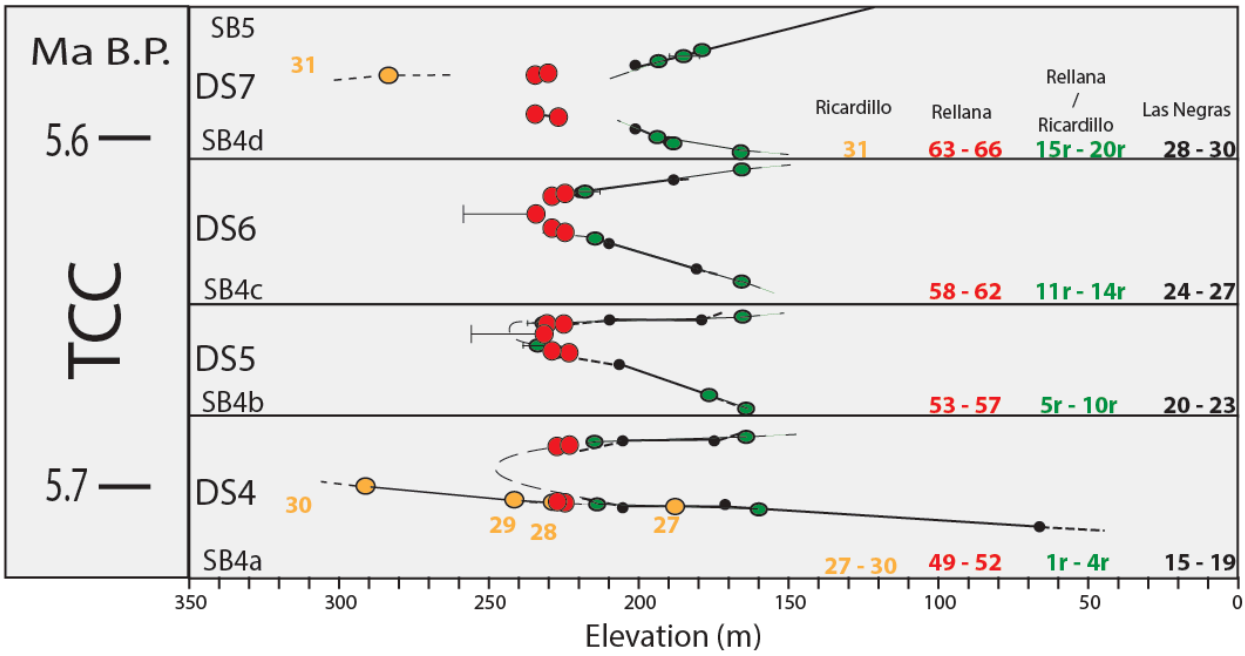

Figure 21: Cumulative relative sea-level curve focusing on TCC (DS4) combining uplift-adjusted data from Ricardillo Peak (orange dots; Toomey, 2003), Rellana Platform (red dots; this study), Ricardillo/Rellana TCC (green dots; Lipinski, 2010) and Las Negras relative sea-level history (black dots; Franseen *et al.*, 1998). Age constraints are specific to Las Negras curve; other data points were placed on the curve using correlation and comparison of sequences within the TCC. Therefore, for all data points other than those identified by Franseen *et al.* (1998), age is relative, and assumed from position on a smoothed curve.

Lithofacies Classification	Key features	Characteristic grain types	Prominent structures, bedding, and thickness	Depositional environment
Trough cross-bedded ooid grainstone	Trough cross-beds	80-99% ooids (0.4-0.8 mm), gastropods (20-90% in interbeds), bivalves (5-15% in interbeds), serpulid worms (35- 95% in interbeds)	Troughs generally oriented N-S or S-N; S1 interbeds 1-3 cm thick; unit thickness 0.66-11.1 m	High energy, < 10 m water depth, shoreface beach envir.
Bioturbated ooid grainstone	Discontinuous laminations and burrows	80-99% ooids (0.15-0.75 mm), gastropods (20-60% interbeds), bivalves (10-20 % interbeds), serpulid worms (10-95% interbeds)	Common discontinuous laminae; interbeds commonly 1-4 cm; common burrows; unit thickness 0.2-1.4 m	Low- moderate energy, offshore envir. > 10 m
Planar bedded ooid grainstone	Planar beds; <5% volcaniclastic grains	81-99% ooids (.2-1.2 mm), gastropods (1-10% interbeds), bivalves (5-15% interbeds), serpulid worms (45-95% interbeds), 0-5% volc. Grains	Decimeter-scale planar beds shallowly dip 1-11 degrees; alternating coarser/finer very thin beds; unit thickness 0.28-0.93 m; fenestrae	Moderate-high energy, < 2 m water depth, foreshore beach envir.
Massive ooid grainstone	Lack of bedding	79-99% ooids (0.15-2 mm, pisoids up to 3mm), bivalves, gastropods, serpulid worms	Common burrows; larger grain sizes; poorer sorting; unit thickness 0.83-2.11 m	Low-moderate energy, > 10 m depth
Volcaniclastic- rich planar bedded ooid grainstone	Planar beds; >5% volcaniclastic grains	75-95% ooids (0.16-1.2 mm), 5-16% volc. grains (0.4-12 mm)	Decimeter-scale planar beds shallowly dip 2-7 degrees, fenestrae high in section, unit thickness 0.24-	Moderate- high energy, < 3 m depth, foreshore beach envir.
Fenestral ooid grainstone	Dominant fenestral fabric	75-99% ooids (0.2-1.1 mm), volc. Grains	Fenestrae; rhizoliths; meniscus cements; unit thickness 0.1-0.4 m	Subaerial exposure
Cross-bedded oolitic gastropod grainstone	Abundant gastropods; cross- stratification	Ooids, 17-72% (commonly 30- 60%) gastropods, peloids	Tabular cross-beds; possible microbial influence, unit thickness 0.47-1.3 m	Moderate- high energy, shallow, near-shore envir.
Trough cross-bedded ooid bivalve grainstone	Abundant bivalves; trough cross-beds	50-75% ooids (0.15-0.65 mm), 15-30% (up to 90 locally at base) bivalves, 4-12% volc. Grains	Trough cross-beds; interbedded with thrombolite boundstone; unit thickness 0.71-5.2 m	High energy, < 10 m water depth, near- shore envir.
Thrombolite boundstone	Dark clotted texture	Commonly 15-60% peloids, gastropods, bivalves, ooids, calc. red algae, serpulid worms	Clotted texture made of peloids; unit thickness 0.27-5 m	High energy, shallow, near-shore envir.
Stromatolite	Fine planar laminae; rare digitate (S4);	Up to 60% peloids, ooids, 5-15% volc. Grains	Finely laminated; clotted texture; alternating coarser/finer laminae; unit thickness 0.05-0.7 m	Low-high energy; shallow near- shore envir.
Porites boundstone	Abundant Porites; micrite	*Porites*, gastropods, bivalves, serpulid worms, ooids, calc. red algae, clionid sponges, peloids	Massive coral heads 1-3 m wide and 2-3 m thick; unit thickness 0.64-6.2 m	High energy, <10 m water depth

Table 3: Summary chart of TCC facies identified by Lipinski, 2010. Grain types are listed in order of abundance. Sx= Sequence X; volc. = volcaniclastic; calc. = calcareous; envir. = environment (Lipinski, 2010).

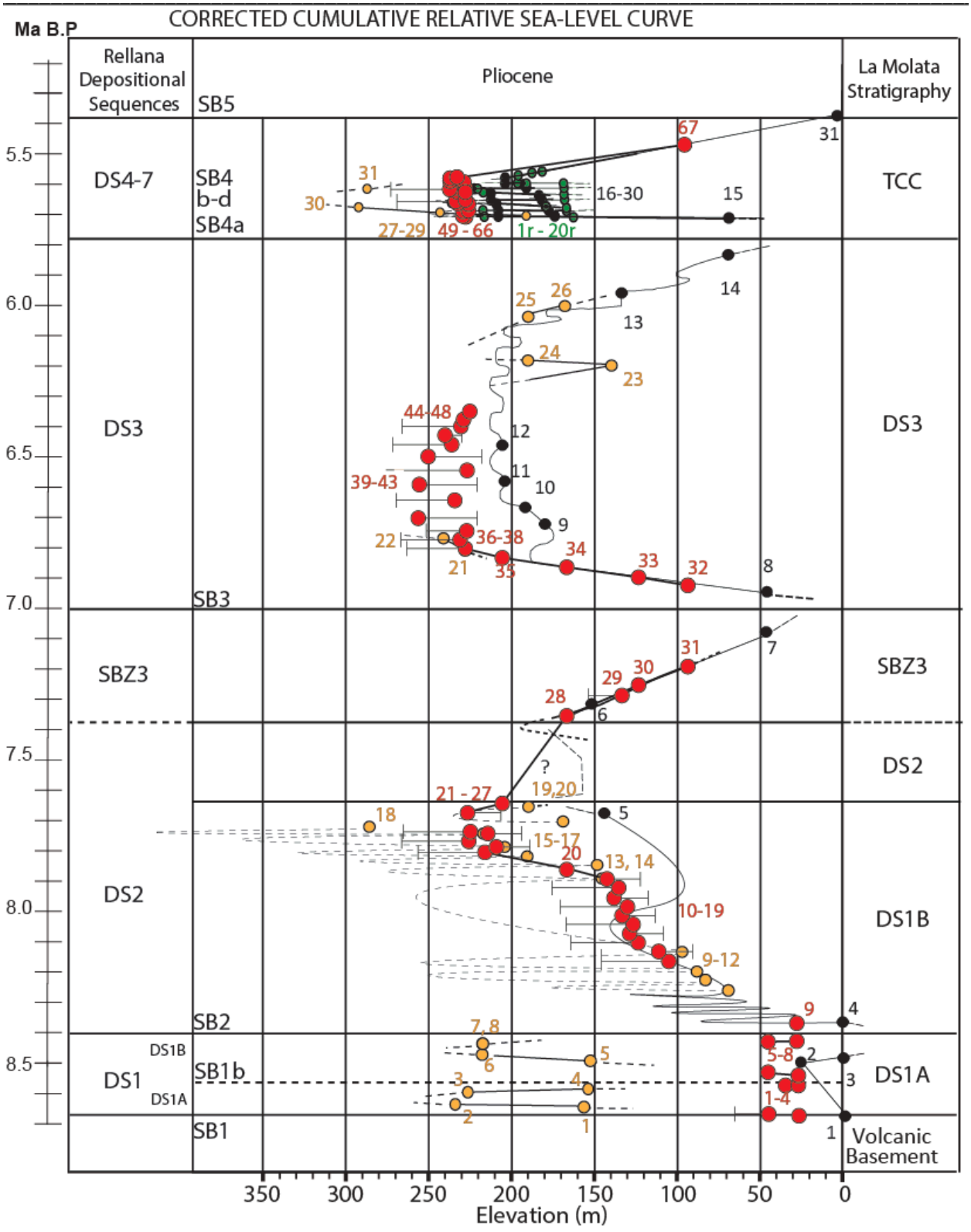
CORRECTED CUMULATIVE RELATIVE SEA-LEVEL CURVE
Ma B.P
Rellana Depositional Sequences
Pliocene
La Molata Stratigraphy
SB5
DS4-7
SB4 b-d
SB4a
TCC
DS3
SB3
SBZ3
DS2
DS1B
DS1
SB1b
DS1A
SB2
SB1
Volcanic Basement
5.5
6.0
6.5
7.0
7.5
8.0
8.5
350
300
250
200
150
100
50
0
Elevation (m)
16-30
27-29
49 - 66
1r - 20r
44-48
39-43
36-38
21 - 27
19,20
15-17
13, 14
10-19
9-12
7, 8
5-8
1-4

Figure 22: Cumulative relative sea level curve combining uplift-adjusted data from Ricardillo Peak (RiP) (orange dots; Toomey, 2003), Rellana Platform (ReP) (red dots; this study), Ricardillo/Rellana TCC (RR) (green dots; Lipinski, 2010) and Las Negras (LN) (black dots; Franseen *et al.*, 1998). Age constraints are specific to Las Negras curve. Other data points were placed on the curve based on correlations and comparison of depositional sequence interpretations made in this study and those studies related to the aforementioned field areas. Therefore, for all data points other than those identified by Franseen *et al.* (1998) (black dots), age is approximate and assumed based on the most simple sea level history. The compressed TCC section is presented in more detail in Figure 21.

DISCUSSION

Regional Stratigraphic Relationships

Correlation of the north and south slopes of the Rellana platform with neighboring, previously studied areas yields additional information regarding relative sea level history and controls on carbonate deposition. Specifically the roles of paleogeography, paleotopography and relative sea level can be examined in each area to assist in identification of predictable controls on carbonate deposition. Nearby carbonate platform deposits compared to the Rellana platform include Ricardillo Peak (Toomey, 2003; Lipinski, 2010), and the La Molata area within the Rodalquilar caldera (Franseen *et al.,* 1993; Fig. 1, 23).

Ricardillo peak is located 2.5 west of the Rellana platform exposure. The Ricardillo Peak area (Studied by Toomey, 2003) spans the San Pedro embayment between Ricardillo Peak and the southern end of the Rellana platform through 6.75 km of generally continuous outcrop (Figs. 1, 23). Ricardillo peak is a basement high (309 m) which marks a separation between the Rodalquilar caldera deposits to the south from the Agua Amarga basin to the north. Correlation of Ricardillo Peak deposits to Agua Amarga basin deposits via the Rellana platform facilitates inter-basin correlation between the Rodalquilar caldera and Agua Amarga basin.


Agua Amarga Basin
330 m
352 m
391 m
267 m
252 m
Fernan Perez
315 m
341 m
309 m
242 m
San Pedro
328 m
269 m
370 m
313 m
307 m
191 m
Ricardillo Peak
Rellana Platform
330 m
319 m
274 m
170 m
172 m
316 m
332 m
268 m
Las Negras
360 m
250 m
134 m
Dominant Swell Direction
Hortichuelas
324 m
Rodalquilar Caldera
356 m
234 m
La Molata Field Area
320 m
Rodalquilar
365 m
445 m
265 m
218 m
488 m
310 m
Mediterranean Sea
Key
Elevations (m)
Sea level
0-100
100-200
200-300
300-400
400-500
Caldera outline
Volcanic highs outline
1 km

Figure 23: Location map showing location of Rellana Platform, Ricardillo Peak, Las Negras and the La Molata field area relative to the modern coast and predominant swell direction. Note the Las Negras area (specifically the La Molata field area of Lipinski, 2010) is located within the Rodalquilar Caldera, whereas Ricardillo Peak and Rellana platform areas are not. Modified from Lipinski, 2010; Rodalquilar Caldera location after Arribas, *et al*., (1995); dominant swell direction based on modern Mediterranean (Lionello and Sanna, 2005).

Deposits described by Toomey (2003) consist of 14 lithofacies (Table 5), which comprise 5 depositional sequences (DS1A, DS1B, DS2, DS3 and TCC). DS1A and DS1B consist of coarse-grained carbonates and volcanic detritus; DS2 consists of fining-upward carbonate cycles; DS3 is dominated by reef and forereef units; and the TCC (Terminal Carbonate Complex) consists of ooid grainstone and stromatolitic boundstone (Toomey, 2003). General stratigraphy of the Ricardillo Peak study area and correlative depositional packages can be seen in Figure 24 (regional cross section available in Appendix 5). Toomey (2003) drafted a relative sea-level curve for Ricardillo Peak. This curve was used in this study after application of an uplift adjustment (*sensu* Hess, 2011) (Fig. 4). The TCC of Ricardillo Peak was further studied by Lipinski (2010). Lipinski (2010) described 11 lithofacies comprising 4 high-frequency, high-amplitude sequences (DS 4-7). These facies show variability in content and distribution; however their general composition consists of oolitic grainstones, algal boundstones and coralgal framestones and boundstones. Described facies are summarized in Table 3.

La Molata is a southeast-facing platform on the northern interior of the Rodalquilar caldera (Rytuba *et al.,* 1990) and is south of the Rellana platform. Deposits on the Molata platform have been the focus of numerous studies (Franseen *et al.*, 1993; Goldstein and Franseen, 1995; Franseen and Goldstein, 1996; Franseen *et al.*, 1997a; Franseen *et al.*, 1997b; Franseen *et al*., 1998). Its stratigraphy consists of five depositional sequences (DS1A, DS1B, DS2, DS3, TCC) composed of nine facies (Franseen *et al.*, 1993) (Table 5). These deposits are generally similar to those observed on the Rellana platform in composition, character and stratal packaging (Fig. 25).

FACIES	GEOMETRY	COMPONENTS	SED. STRUCTURES	DEP. ENV.
Volcanic Conglomerate (VC)	Massive	Volcanic clasts Volcanic matrix	None	Shallow water to exposed
Carbonate Matrix Conglomerate (CMC)	Bedded, up to 2m, thick	Volcanic clasts (up to 40cm) Carbonate matrix	Lacks sorting or grading	Normal marine debris flows in water 30-35m
Fine grained mollusk bryozoan packstone – (FGMBP)	Bedded, up to 1.5m thick with small to medium-scale cross-beds and planar beds	Abraded mollusk and bryozoan fragments forams, echinoid fragments, brachiopods, red algal fragments	Cross-beds and planar beds, burrows (*Thallasanoides*?)	Normal marine, 10-30m, increased energy
Coarse grained mollusk bryozoan packstone (CGMBP)	Massive to planar bedded, up to 2.5m thick	Mollusk and bryozoan fragments bryozoans are un-abraded and mainly stick morphology. Forams, echinoid fragments, volcanic clasts, red algae, brachiopods, solitary corals, and volcanic clasts	Planar beds, generally fine upwards	Normal marine, 30-180m, low energy
Bryozoan-rich packstone (BRP)	Bedded, .5-2.5m thick	Mollusk and bryozoan fragments, forams, echinoid fragments, volcanic clasts, red algae, brachiopods, solitary corals.	Planar bed, cross-beds	Normal marine, >20m
Halemida Bryozoan packstone (HPB)	Massive, 1.5m thick	Halimeda molds, bryozoan and mollusk fragments, echinoids, forams	None	Normal marine, 30+m
Stromatolitic boundstone (BS)	Planar, 1.5m thick	Ooids, stromatolites, mollusks	LLH stromatolites and large 3m heads in ooid grainstone or wackestone matrix	Shallow intertidal, <10m
Reef Core (RC)	Massive, 2.5-4m thick	*Porites* (stick and encrusting morphology), *Tarbellastraea* and *Siderastrea* heads, Halimeda, mollusks, bryozoans, echinoids, forams	None	Reef crest to reef wall, 10-40m, high energy
Fore reef talus (FRT)	Dipping clinoforms mimic underlying topography	*Porites*, mollusks, bryozoans, forams, large stromatolites, OG intraclasts	Clinoforms are truncated at upper boundary	Fore-reef slope, 40+m
Tarbellastraea reef (TR)	Massive, 2-3m thick	*Tarbellastraea* molds (sticks), mollusks, bryozoans, forams	None	Normal marine, 20-30m
Ooid grainstone (OG)	Bedded, sometimes cross-bedded in upper portions.	Ooids, mollusks, bryozoans, forams, large stromatolites, OG intraclasts	Small and large scale cross-beds, planar beds	High energy, 5-20m, intertidal channel deposits
Fenestral ooid grainstone (FOG)	Bedded, .5-1m thick beds	Ooids, mollusks, rare volcanic clasts	Shallow dipping beds, alternating coarse/fine laminations	Beach
Porites- rich packstone (PRP)	Massive, grades into CGMBP	*Porites* fragments, mollusks, bryozoans, mud	Mound shaped	62-98m of water
Vermetid framestone (VF)	On-laps volcanic basement, grades into cyclic DS2 units	*Vermetid* gastropods, serpulids, mollusk fragments, peloids	none	Hard, steep substrates in 30-35m of water

Table 4: Ricardillo area facies, From Toomey, 2003

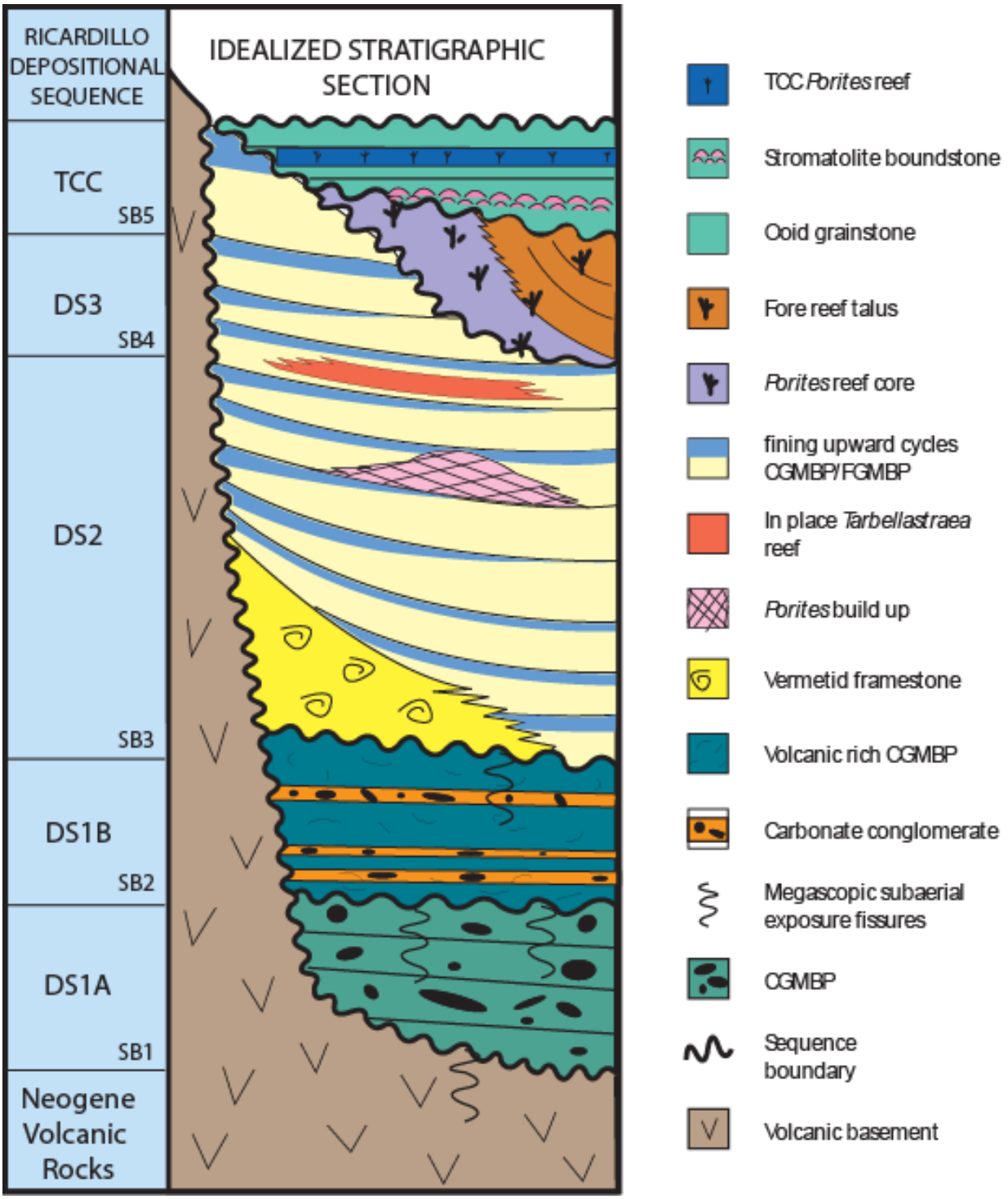

Figure 24: Generalized stratigraphy of the Ricardillo Peak study area showing relative position of depositional sequences, sequence boundaries and facies observed by Toomey (2003).

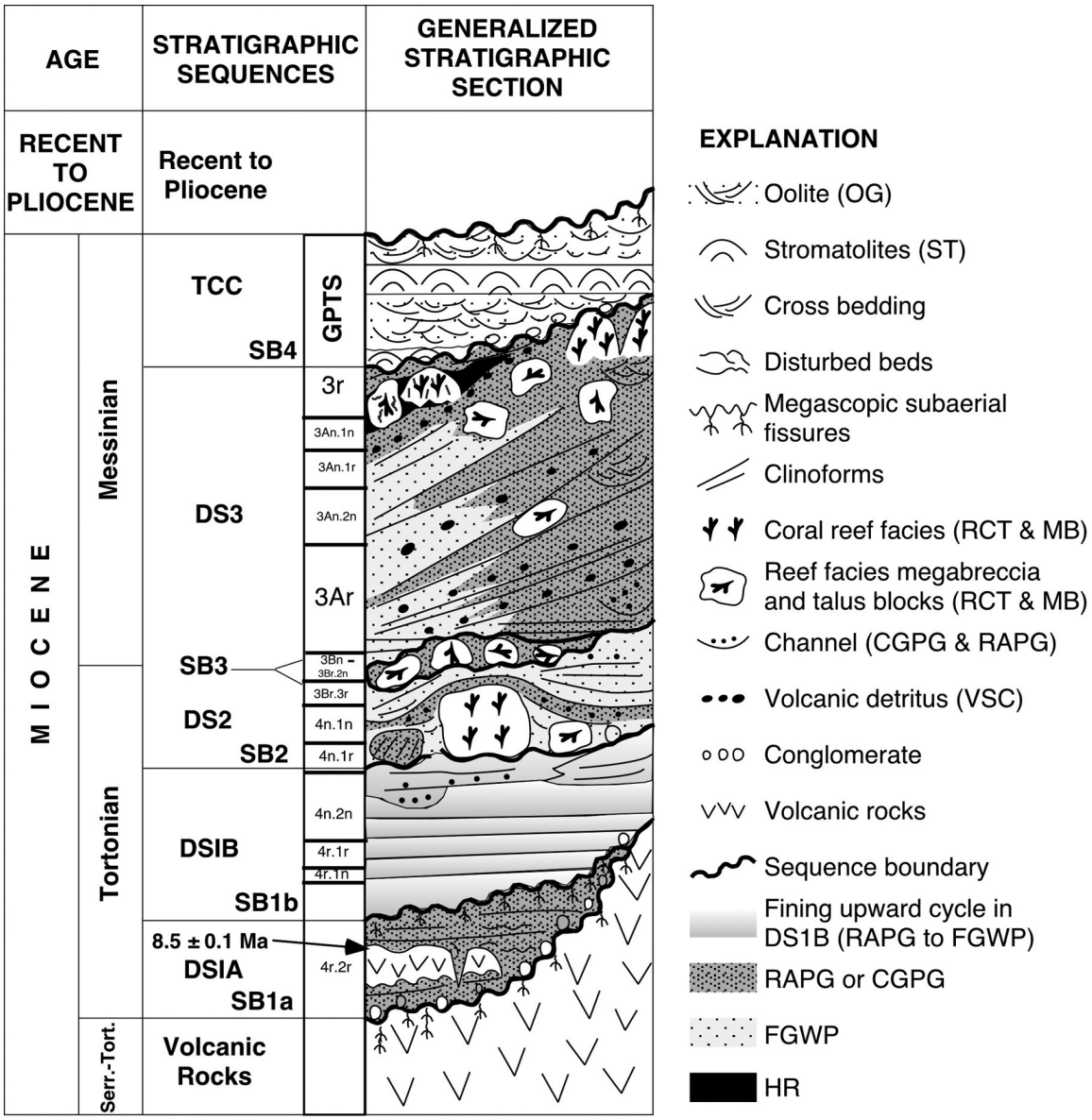

Fig. 25: Generalized stratigraphy of the La Molata area. Ages shown are determined from paleomagnetic and a radiometrically dated volcanic unit within DS1A. GPTS chrons (Cande and Kent, 1995) are based on correlations made by Franseen *et al.* (1998). Facies, abbreviations and stratigraphic sequence names from Franseen *et al.* (1993).

Facies	**Bedding** (dips)	**Skeletal & Non-Skeletal Components**	**Dominant Grain Sizes**	**Porosity** (Visual Estimates)	**Cements**	**Other**
Reef Core or Talus (RCT)	Massive; locally tabular (0-30 degrees)	Porites dominant framework, locally serpulids; encrusting, fragmented and branching red algae, foraminifera, bryozoans, bivalves, gastropods, echinoderms, peloids, coated grains, intraclasts, volcaniclasts	Mud to Boulder	Less than 5 – 25%; Avg. less than 10% MO, BP, GF, VUG, FR	Dolomite-equant or spherulitic/polyhedral crystals, micritic and fibrous to bladed calcite, coarse (poikilitic) calcite	Coral framework is minor compared to matrix, local vadose fabrics
Halimeda-Rich Beds (HR)	Massive; very thinly to thickly bedded (0-30 degrees)	Halimeda; coralline algae (fragments, rhodoliths, crusts_. serpulids, bivalves, Porites bryozoans, gastropods, volcaniclastics	Coarse sand to pebble	5-50%; Avg. 15-25% MO, BP, VUG	Dolomite, fibrous to bladed isopachous calcite, equant calcite, poikilitic calcite	Occurs in reef core to distal foreslope positions
Coarse-Grained Packstone/Grainstone (CGPG)	Well bedded, thinly to very thickly bedded, local cross bedding and cross lamination (< 10-30 degrees)	Bivalves, coralline algae (fragments, rhodoliths, crusts, branching), echinoderms, bryozoans, gastropods, serpulids, Porites fragments, foraminifera, ostracods, peloids, coated grains, volcaniclastics, intraclasts	Medium sand to pebble	5-40%; Avg. 10-15% MO, BP, VUG	Equant dolomite, fibrous to bladed, isopachous calcite, equant calcite	Normally graded units locally; common as channel-fill deposits
Volcaniclastic / Carbonate Conglomerate (VCC)	Massive	Volcanic clasts, coralline algae (fragments), bryozoans, bivalves, solitary corals, gastropods, serpulids, benthic and planktonic foraminifera, echinoderms	Mud to boulder	5-45%; Avg. 15-20% MO, BP, WP, VUG	Equant dolomite, equant calcite	Mostly matrix-support texture
Volcaniclastic Sandstone / Conglomerate (VSC)	Thinly to thickly bedded (0-30 degrees)	Volcanic clasts, coral, serpulids, coralline algae (fragments), bivalves, gastropods, bryozoans, peloids	Mud to cobble	10-35%; Avg. 20% MO, BP, WP, VUG	Rare: locally equant dolomite	Common as channel-fill or wedge-shaped deposits
Fine Grained Wackestone / Packstone (FGWP)	Massive; locally thinly to thickly bedded, locally laminated and cross laminated (< 10 degrees)	Planktonic foraminifera, coralline algae (fragments), bivalves, echinoderms, gastropods, peloids, volcaniclastics	Mud to fine sand; locally pebble	5-40%; Avg. 10-15% MO, BP, VUG	Rare equant dolomite, equant calcite locally	Extensive bioturbation characteristic
Red Algal-rich Packstone / Grainstone (RAPG)	Massive, thinly to thickly bedded, (< 10 degrees)	Coralline algae (fragments, rhodoliths), bryozoans, bivalves, gastropods, benthic and planktonic foraminifera, solitary corals, echinoderms, serpulids, peloids, intraclasts, volcaniclastics	Silt to granule	5-45%; Avg. 15-20% MO, BP, VUG	Equant dolomite, equant calcite	Common as channel-fill deposits or wedge-shaped deposits
Megabreccia 1 (MB1)	Massive, isolated blocks; encased in strata dipping < 10 degrees	Tarbellastraea, Porites, coralline algae (crusts, fragments), bryozoans, peloids, planktonic and benthic foraminifera, serpulids, bivalves, echinoderms, gastropods	Mud to boulder	0-25%; Avg. 5-15% MO, BP, GF, VUG	Fibrous to bladed isopachous calcite; equant calcite cement; bladed-equant dolomite	Clast matrix is more abundant than coral framework
Megabreccia 2 (MB2)	Layers 1-3 m thick; some isolated blocks encased in strata dipping 0-10 degrees	Porites, coralline algae (crusts, fragments), serpulids, bryozoans, foraminifera, gastropods, bivalves, echinoderms, peloids, intraclasts, composite grains, volcaniclastics	Coarse sand to boulder	5-40%; Avg. 10-20% MO, BP, GF, VUG	Fibrous to bladed isopachous calcite; equant calcite, equant dolomite	Matrix in clasts is more abundant than coral framework

Table 5: Characteristics of facies identified by Franseen *et al.* (1993) in the La Molata area. Abbreviations used for porosity types are; fracture (FR), intraparticle (WP), moldic (MO), Interparticle (BP), intercrystal (BC), vuggy (VUG), fenestral (FE), shelter (SH), growth framework (GF) after Choquette and Pray (1970)

DS1.--- DS1 deposits are the earliest carbonate deposits preserved on the Rellana platform and are problematic to correlate. Evidence for faulting of DS1 strata prior to DS2 deposition in the Rellana platform and Agua Amarga basin (Franseen *et al*., 1997b; Dvoretsky, 2009) areas makes localized tectonic displacement difficult to quantify (minimum of 5 m of offset observed on the Rellana Platform). The DS1a (after Franseen, 1993) deposits of La Molata are roughly correlative to DS1 of Ricardillo and Rellana, insofar as they demonstrate similar concentrations of volcanic conglomerates and sandstones, and represent the earliest preserved carbonate strata in the area. Differential tectonic uplift is suggested in the region because DS1 material on Ricardillo peak is at an elevation of ~230m (Toomey, 2003) and DS1a in the Rodalquilar caldera is at 0-30m (Franseen et al, 1993). Due to Miocene tectonic displacement of these deposits, precise correlations remain unknown.

DS2.--- DS2 deposits of the Rellana platform consist of stacked fining-upward cycles, capped by interbedded coarse-grained debrites and pelagic/hemipelagic material. Toomey (2003) identified 12 similar cycles in the Ricardillo area which onlap volcanic basement from 60 m up to 302 m on Ricardillo peak. Cycles as defined by Toomey (2003) consist of CGMBP gradationally capped by fine-grained molluscan bivalve packstone (FGMBP, Table 4; considered locally equivalent to well-sorted FGSWP on the Rellana platform). Physical tracing between Ricardillo Peak and the Rellana platform demonstrates that the lowest cycle observed on the southern slope of Rellana is the fourth cycle identified by Toomey (2003). Deposits below this on Rellana do not contain distinguishable cycles, and any abraded fine-grained material associated with shoaling deposition is likely present in the matrix of VCC deposits and is indistinguishable as a cycle. No definitive correlation could be made between DS2 deposits on

Rellana north of the drainage divide with the southern slope of the Rellana platform or the Ricardillo Peak area.

A similar depositional sequence dominated by fining-upward, cyclic, red-algal packstones and planktonic foraminifera wackestones-packstones was described in the Rodalquilar caldera on La Molata, Cerro El Romeral, and Cerro del Cuervo (DS1b of Franseen *et al.*, 1993, Johnson *et al.,* 2005). These deposits are found from present-day sea level up to an elevation of 150 m truncated by sequence boundary 2 and the erosional base of MB1 (Franseen *et al.*, 1993). The close similarities in biota between the red-algal packstones and facies on Rellana/Ricardillo, and similar onlapping geometries, suggest these units are correlative. The overlying SBZ3 of Rellana is considered to be equivalent to MB1, DS2 and MB2 of La Molata. The presence of *Tarbellastraea* framestones within latest DS2 deposits further supports correlation of these units, as in all locations this represents the earliest development of *Porites* and *Tarbellastraea* framestones.

DS3.--- DS3 deposits on Rellana generally consist of *in situ* reef core development updip and coarse-grained, skeletal packstone grainstone that fines downdip, forming fore-reef slope deposits with distally decreasing dips (maximum observed range on Rellana platform is 27˚ - ~5˚). These deposits were physically traced into the neighboring Ricardillo area on the southern end of the Rellana platform

DS3 deposition in the Ricardillo area features *in situ* reef development similar to that seen in DS3 on the Rellana platform. Proximally, mixed encrusting, stick and head coral growth morphologies are described (Toomey, 2003), indicative of a lower reef crest environment (5 -10 m, *sensu* Esteban, 1996). The majority of DS3 deposits within the Ricardillo peak area DS3

deposits are interpreted to be upper reef wall (5 – 40 m, after Saint-Martin, 1990; Riding *et al.*, 1991; Esteban, 1996). These deposits reportedly lack internal structure and cover over 100 m of relief with little to no variability in reef growth morphology, indicating they are not time-equivalent and likely represents a series of prograding and downstepping reefs (Toomey, 2003).

A similarly volumetrically significant, coral reef dominated depositional sequence has been described on La Molata. The DS3 of Franseen *et al.*, (1993) is dominated by *Porites* framestones and forereef-slope strata. The similar biota, facies and geometries suggest these units are correlative.

DS4-7.--- DS4-7 deposits consist of 4 microbial, oolitic and coralgal sequences that are regionally recognized and widely considered to represent the culmination of Miocene carbonate deposition in the Mediterranean region (Terminal Carbonate Complex (TCC) of Esteban (1979)). Physical tracing between the TCC deposits described by Lipinski (2010) and those observed on the eastern side of the Rellana platform is complicated by covered section and the laterally variable nature of the TCC deposits; however the alteration surface (SB4b) separating the 2nd and 3rd TCC sequences (DS5, DS6) was correlated through a drainage on top of the Rellana Platform. Comparison of TCC equivalent deposits on the relatively unstudied eastern exposure of the Rellana platform with those described on the western margin by Lipinski (2010) provides increased potential for 3-dimensional analysis of TCC deposits, and increased constraints on highstand maximums within TCC deposits.

Lipinski (2009) correlated four depositional sequences in the TCC deposits from La Molata, Rellana, and into Ricardillo. Regionally, these sequences appear to correlate throughout the western Mediterranean (Esteban *et al.,* 1979; Goldstein et al. 2014).

Relative Sea Level History

Comparison of the relative sea-level curves for the Rellana platform, Ricardillo Peak and La Molata demonstrate similar relative sea level history across all three areas with some notable exceptions (Fig. 21, 22).

- The wide range demonstrated by data points in DS1 is attributed to known tectonic displacement of the earliest carbonate deposits in all the study areas (Franseen *et al*., 1997b; Toomey, 2003; Dvoretsky, 2009).
- Correlation of individual fluctuations of relative sea level during DS2 (DS1b in La Molata) is conjecture, however, there is a greater number of cyclic bedsets in the Ricardillo and Rellana areas than in the Rodalquilar caldera area. This indicates that cyclic deposition continued to be externally forced through DS2 time. Additionally, no evidence was seen on the Rellana platform for the two events of megabreccia deposition seen in the Rodalquilar caldera (La Molata). Thus the MB1, DS2 and MB2, as described on La Molata, are lumped into the regression associated with the end of DS2 and formation of SBZ3.
- Downstepping events have been described in late DS3 on Molata (Franseen, 1993), with reef framework preserved down to an elevation of 135 m. No reefs are preserved on the Rellana platform below 225 m in the youngest DS3 deposits.
- Relative sea level history of the TCC deposits on the Rellana platform is very limited, with only thin TCC deposits preserved on the platform. Despite this there is good similarity between the relative sea level history curves generated for La Molata, Ricardillo Peak (Lipinski, 2010) and this study. Notable additions provided by this data

set is an increase in depth range for the DS4 and DS7, and quantification of the turn around elevations in DS5 and 6 as evidenced by the coral growth morphologies observed at the highest elevations.

Generally, the data from Ricardillo Peak and Rellana platform plot at consistently higher elevations than the data from La Molata, despite applying the Hess (2011) correction for tilting. The consistency between the Ricardillo and Rellana data suggests these areas are consistent between one another, however, the reconstruction results in comparable highstand pinning points associated with DS3 reef development on La Molata appearing ~35 meters lower in comparison with Ricardillo and Rellana. The consistency of TCC indicates that locally the simple tilt model used for paleotopographic reconstruction is likely close to truth. However, inconsistencies regionally illustrate that either: the tilt correction is inadequate and that the structural model is overly simple for precise reconstruction of paleotopography, or the highstands observed on Rellena/Ricardillo are not time equivalent to those observed on La Molata.

Paleogeography and Substrate Paleoslope

Placing the previously described deposits into a regional paleogeographic context facilitates comparison of the areas to determine the impact wave, wind energy or other paleogeographic effects had on platform development. The relative location of the Rellana, Ricardillo and La Molata study areas are depicted in Figure 23. The North slope of the Rellana platform was a continuous platform margin facing northeast toward the open sea. The South slope was a narrow south-facing promontory separating the San Pedro Embayment from the open sea. The San Pedro Embayment was a 1.5? km long N-S embayment, opening to the south, steeper on its east side than on its west side. Ricardillo peak is located on the west side of that

embayment, and it hosts an east-southeast-facing carbonate platform. La Molata is located on the north side of the Rodalquilar caldera, a horseshoe-shaped basin that would have been somewhat open to the east (Arribas, *et al.*, 1995). It houses an east-southeast facing carbonate platform.

Assuming that the predominant wave direction during the Miocene was similar to the modern Mediterranean, waves would have originated from the Northeast and East (Lionello and Sanna, 2005). The Rellana platform's Northern slope would have been fully exposed to these waves. The steep south-facing slope of the Rellana platform would have been protected from this wave energy by being partially in the lee of the paleohigh defined by the drainage divide. Deposits of the Ricardillo area within the N-S oriented San Pedro embayment would have been somewhat protected from direct impact of wave energy because of the platform's location within the embayment. The Rellana side (East side) of the embayment would have been even more protected from wave energy, because of its location in the lee of incoming waves within the embayment. The east-southeast-facing La Molata platform, located within the Rodalquilar Caldera, would likely have been protected from direct impact of the highest wave energy and may have been in a more restricted setting relative to the northern slope of Rellana. The influence of paleogeographic setting is discussed below for each depositional sequence

DS1.--- At Rellana, DS1 deposits are preserved solely on the steep southern margin, and are absent from the northern margin. Because of this, no comparison can be drawn between time-equivalent deposits developing on variable paleoslope. The absence of DS1 equivalent material in the Rellana study area is due to the distally steepening nature of the north slope. DS1 equivalents to the north likely correspond to Basin Units 1 and 2 of Dvoretsky (2009) in the

Agua Amarga Basin. The paleotopography of the Agua Amarga Basin to the north is discussed in more detail in Chapter 3 of this study.

Due to tectonic displacement of DS1 deposits, most attempts to isolate controls on deposition are conjecture. The steep slope on the southern slope of the Rellana platform likely encouraged bypass of upslope sediments resulting in the deposition of VC and VCC layers. Preservation of DS1 deposits in topographic depressions high on Ricardillo peak, at the base of the steep slope of the southern Rellana platform and in the base of the paleovalley associated with the Aqua Amarga basin indicate that it may be preferentially preserved in areas where the deposits were sheltered from currents. On La Molata, DS1 equivalent deposits feature ramp geometries and show evidence for alternating current energies (mud-rich and mud-poor packstones, units with abraded skeletal grains and rounded volcaniclasts juxtaposed with units containing preserved, large, unabraded mollusks (Franseen *et al.*, 1993).

DS2.--- On the southern slope of Rellana, DS2 deposits transition from the steep paleoslope of the volcanic basement downdip onto the reduced slope of the SB2 surface. This transition is reflected in a shift from interfingering with VCC and onlap onto basement, to draping bedding trends.

DS2 deposits north of the drainage divide are less volumetrically significant, and are laterally constrained on top of the platform.-The preferential preservation of the FGSWP on the northern DS2 bedsets could be related to the gentle paleotopographic slope upon which these bedsets developed. The shallow slope resulted in a wider swath of material in normal wave base, resulting in a more laterally continuous FGSWP facies belt than on the southern slope, where the

steep dip would have limited the potential width of a sediment-wave interaction zone (e.g. Franseen *et al.*, 1998).

DS2-equivalent deposits on La Molata (DS1b of Franseen *et al.*, 1993) display features similar to the packages described by Toomey (2003) on the eastern flank of Ricardillo Peak and the southern bedsets on the Rellana platform. The northern slope of the Rellana platform features higher concentrations of well-sorted FGSWP indicating some wave interaction likely influenced DS2 deposition. It was insufficient to winnow mud completely from these facies however, so deposition must have occurred below normal wave base, if not below storm wave base. In late DS2, the wave energy associated with being exposed to the predominant swell direction likely encouraged early reef development, resulting in preservation of *Tarbellastraea* and *Siderastrea* corals. The lack of definitively *in situ Tarbellastraea* reef development on the Rellana platform limits the confidence in interpretations regarding the position of initial reef growth. The presence of *in situ* reef on the southern slope of the Rellana platform at an elevation consistent with the break in slope of the distally steepening northern slope (~150 m) provides an explanation for why these reefs were not preserved north of the Drainage divide. It is possible they developed on the steeply dipping Agua Amarga Basin margin and were redistributed downslope (BU4 of Dvoretsky, 2009). The relative timing and basinal characteristics associated with this process are discussed in more detail in Chapter 3.

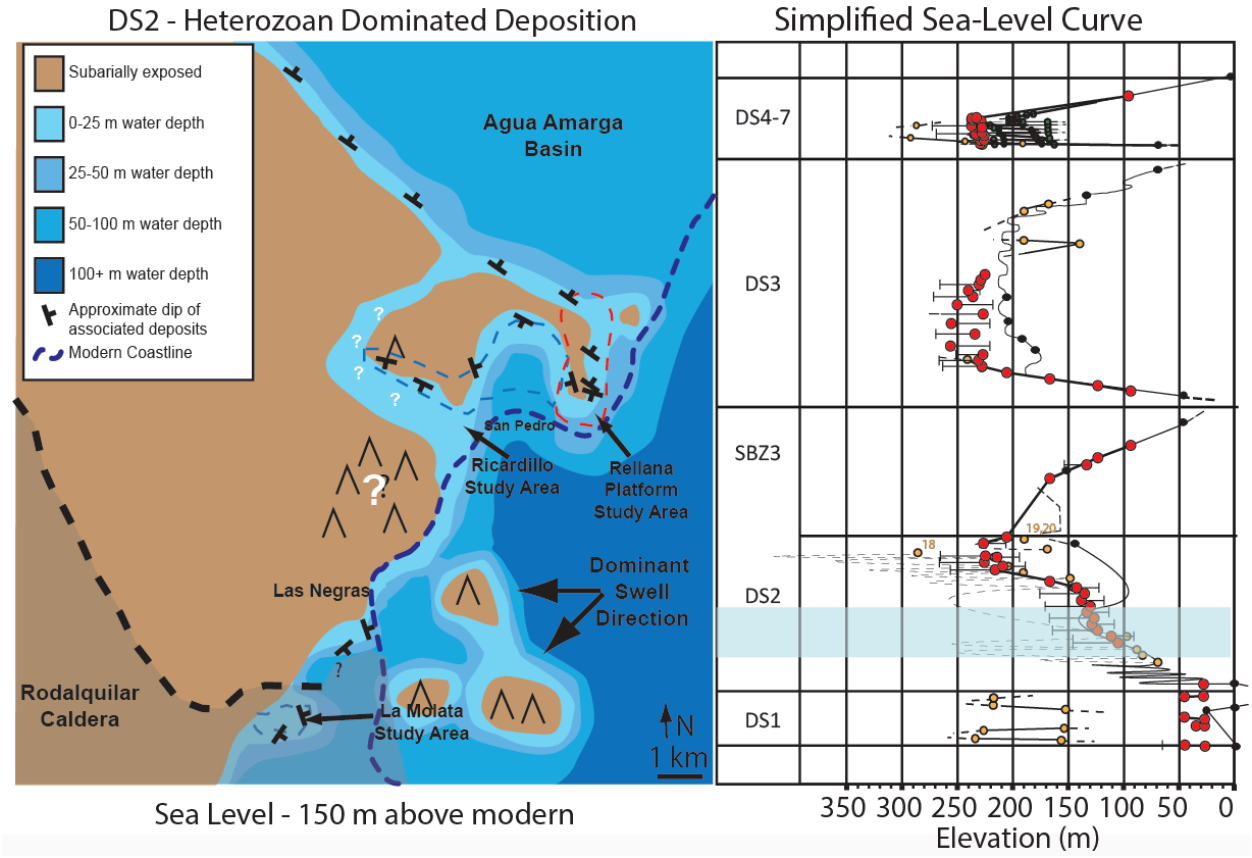

Figure 26: Left) Paleogeographic map of the Rellana Platform, Ricardillo Peak and La Molata field areas for DS 2 time. Note the La Molata field area of Lipinski, 2010 is located within the Rodalquilar Caldera, whereas Ricardillo Peak and Rellana platform areas are not. Modified from Lipinski, 2010; Rodalquilar Caldera location after Arribas, *et al*., (1995); dominant swell direction based on modern Mediterranean (Lionello and Sanna, 2005). Right) simplified version of the relative sea-level curve from Figure 22 with a blue rectangle highlighting the approximate time interval associated with the paleotopographic map. During DS2, carbonate deposition consisted of heterozoan ramp deposits onlapping the volcanic highs.

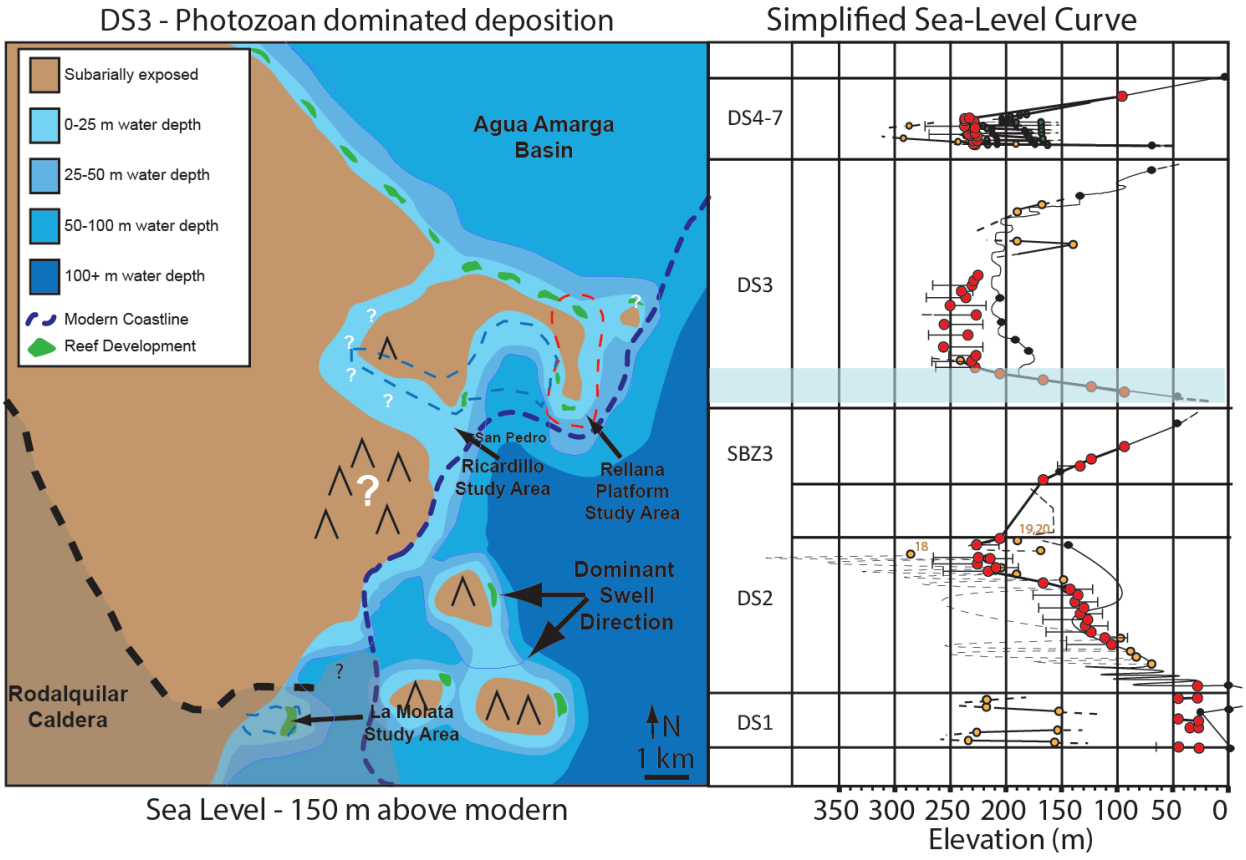

Figure 27: Left) Paleogeographic map of the Rellana Platform, Ricardillo Peak and La Molata field areas for early in DS3 time. Note the La Molata field area of Lipinski, 2010 is located within the Rodalquilar Caldera, whereas Ricardillo Peak and Rellana platform areas are not. Modified from Lipinski, 2010; Rodalquilar Caldera location after Arribas, *et al*., (1995); dominant swell direction based on modern Mediterranean (Lionello and Sanna, 2005). Right) simplified version of the relative sea-level curve from Figure 22 with a blue rectangle highlighting the approximate time interval associated with the paleotopographic map. During DS3 carbonate deposition consisted of photozoan reef deposits initially aggrading and subsequently prograding downdip from the volcanic highs.

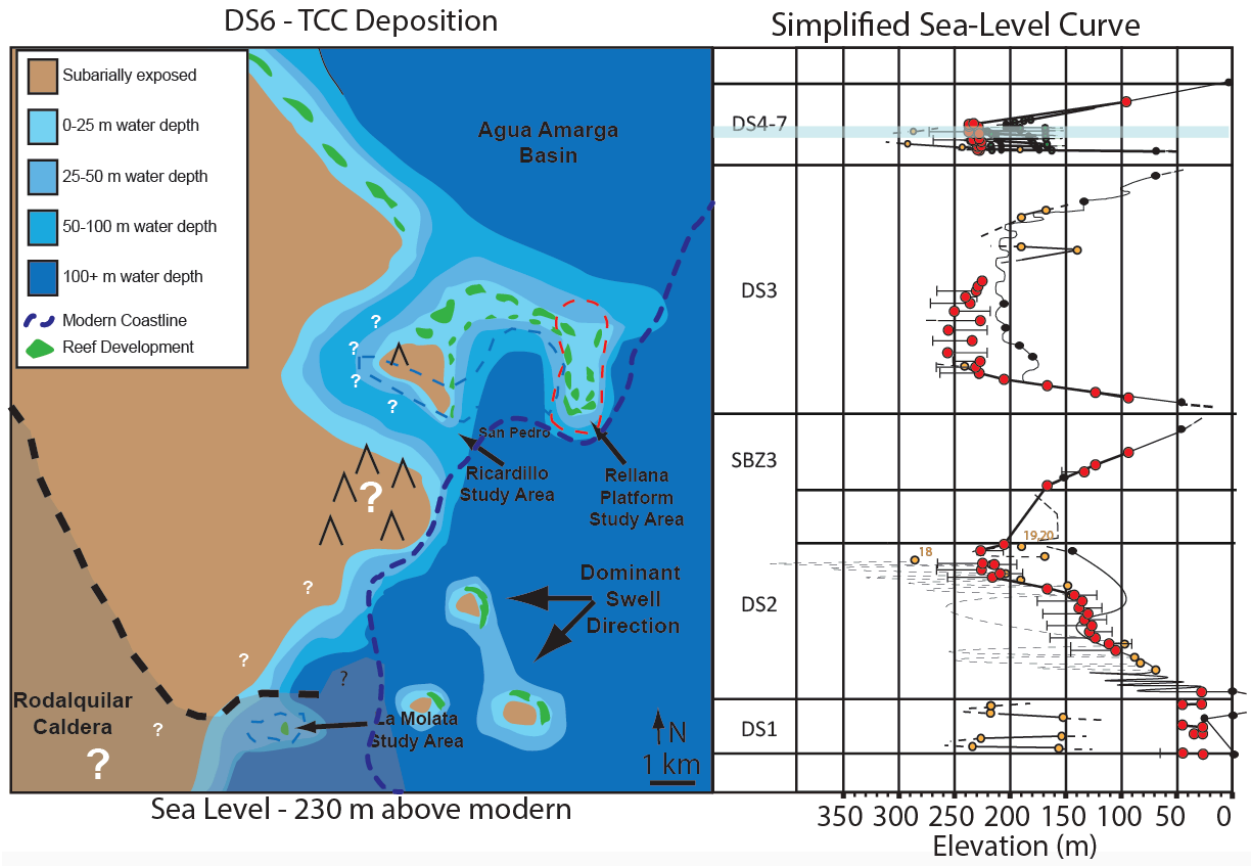

Figure 28: Left) Paleogeographic map of the Rellana Platform, Ricardillo Peak and La Molata field areas for highstands of DS4-7 in the TCC. Note the La Molata field area of Lipinski, 2010 is located within the Rodalquilar Caldera, whereas Ricardillo Peak and Rellana platform areas are not. Modified from Lipinski, 2010; Rodalquilar Caldera location after Arribas, *et al*., (1995); dominant swell direction based on modern Mediterranean (Lionello and Sanna, 2005). During DS4-7 carbonate deposition consisted of cyclic stromatolitic, thrombolitic, oolitic and coralgal deposition. Additionally, The map shows locations where *insitu* reefs were identified in the field (DS6). The large number of reefs preserved in the Rellana and Ricardillo areas relative to the Molata indicates that the influence of paleogeographic controls may have influenced reef development during the TCC. Right) simplified version of the relative sea-level curve from Figure 22 with a blue rectangle highlighting the approximate time interval associated with the paleotopographic map.

DS3.--- The influence of paleotopography is most visible in DS3 deposits due to the relation of reef development in response to relative sea-level changes, specifically during periods of progradation. North of the drainage divide, progradational and downstepping truncated clinoforms advance out over the shallow substrate. On the southern side of the drainage divide, large amounts of CGSPG are deposited on the flanks of the steep paleoslope, and do not develop sigmoidal geometries to the same extent as those developed on the north side of the platform. The northern slope features over 800 m of progradation including some possible downstepping events. The southern slope features *in situ* reef deposits with only ~80 m of progradation and detritus of coralgal framestones likely related to downstepping events.

Thus, the influence of paleoslope on the type and distribution of deposits observed on the Rellana platform is most clearly visible when comparing DS3 development north and south of the drainage divide. The low accommodation over the shallow-dipping northern slope resulted in progradation whereas the southern slope is characterized by poor preservation of reef core material and abundant fore-reef slope deposition. This variation is interpreted to be a result of less accommodation over the shallow paleoslope north of the drainage divide, encouraging progradational development (*sensu* Schlager, 2005), but it could be also due to the fact that the southern slope was too steep to preserve *in situ* reefs and that it was protected from wave energy. Ricardillo peak, on the west side of the San Pedro embayment, shows reefs mostly prograding over a gentle substrate (Toomey, 2003), similar to the northern slope of Rellana. The over 1.5 km of reef progradation of Ricardillo is attributed to DS3 reef deposits on the eastern flank of Ricardillo Peak. Little to no preservation of reefs is described on the steeper, leeward western flank of Ricardillo Peak (Toomey, 2003), which also would have been in the lee of wave energy.

On La Molata, DS3 reefs prograded 935 m laterally; calculated progradation rates demonstrate a decrease in progradation rate as clinoform height increases (Franseen *et al.,* 1998). This relationship ma help explain the stark contrast in progradation reach between the north and south slope of the Rellana platform. Reefs on the north slope were able to prograde more easily given the < 50 m accommodation, whereas the southern slope had steeper slopes and much more accommodation and required a much larger volume of forereef sediment filling in accommodation for reefs to prograde.

DS4.--- In the Ricardillo/Rellana areas DS4 overlies SB4 between 181 m (160 m RE) and 239 m (212.5 m RE). Further rise in sea level beyond this is indicated in the Rellana area and are found at 239.5 m (226.5 m RE) and up to 243 m (225 m RE). These deposits are described by Lipinski (2010) as bioturbated ooid grainstone facies (Table 4) that are gradationally bounded updip and overlain by trough cross-bedded ooid grainstone facies (Table 4). The trough cross-bedded ooid grainstone facies grades updip into planar-bedded ooid grainstone facies (Table 4). These deposits continue grading up into volcaniclastic-rich planar-bedded ooid grainstone facies (Table 4), with a local cap of fenestral ooid grainstone facies (Table 4).

DS4 Deposits on the Rellana platform are limited to the areas of relatively flat paleotopography on the northern-most end of the exposure and are generally poorly preserved due to abundant vegetation and recessive tendencies. Where deposits are positively identifiable, they consist of low angle trough cross-bedded to planar-bedded ooid grainstone (OG facies, Table 1), which reached a maximum observed thickness of 2.5 m. No gradational transitions were observed, however, the poor quality of DS4 preservation on the Rellana platform made detailed description difficult. A potential topography-building reef or thrombolite growth was

observed at the extreme north end of the outcrop. Its close inspection was thwarted by unstable terrain. The stratal package described by Lipinski for DS4 indicates shoaling upward deposition culminating in subaerial exposure (evidenced by fenestral ooid grainstone facies). Deposits preserved in the Rellana study area reflect sea-level rise sufficient to deposit trough cross-bedded to planar-bedded ooid grainstone. These deposits are similar to the volcaniclastic planar-bedded facies and trough cross-bedded facies described by Lipinski (2010) (Table 4), suggesting water depths < 10 to < 3 m during deposition, indicating a minimum rise in relative sea level up to 246 m (228 m RE) prior to the subaerial exposure of the DS4 deposits identified by Lipinski (2010).

DS4 deposits on La Molata are only preserved on the eastern margin of the Molata platform. It features laterally extensive basal stromatolites and laterally extensive thrombolites interbedded with and overlain by trough cross-bedded ooid grainstone (Lipinski, 2010). The sequence ranges in thickness from 1.35 to 8.5 m, considerably thicker than preserved DS4 deposits on the Rellana platform. This restriction to the eastern side is interpreted to be controlled by relative sea-level interacting with the east-dipping SB4-equivalent surface (Lipinski, 2010).

DS5.--- DS5 is found throughout the Ricardillo/Rellana study area and the TCC deposits of the Rellana platform. Lipinski describes DS5 as being divided into low-elevation and high-elevation stacking patterns. Laterally extensive thrombolite boundstone interbedded with trough cross-bedded ooid grainstone deposits are dominant at low elevations; below 184.6 - 221 m (164.1 - 202.5 m RE) with local shoaling upwards gradation into volcaniclastic-rich planar bedded ooid grainstone and local caps of fenestral ooid grainstone. These deposits overlie isolated, trough cross bedded ooid bivalve facies. At high elevations (221 - 257m; 202.5 - 228.25

m RE), deposits are dominated by trough cross-bedded ooid bivalve grainstone interbedded with thrombolite boundstone facies. These deposits are sharply overlain by cross-bedded ooid grainstone, and then volcaniclastic-rich planar bedded ooid grainstone and fenestral ooid grainstone. At the highest elevations (242 - 257 m; 213.5 m - 228.5 m RE) only trough cross-bedded ooid bivalve grainstone and thrombolite boundstone facies are observed.

DS5 deposits in the Rellana platform area are more limited in their elevation range than those described by Lipinski (2010), ranging from 240 - 243 m (223.1 - 229.7 m RE), Subtle variations between DS5 deposits on the eastern side of the San Pedro embayment and the deposits in the Rellana platform area (this study) are noted; however, this is likely related to descriptive approach and level of detail of description. Of particular note is the isolated and rare occurrence of *Porites* framestone (PF facies; Table 1) within the northernmost DS5 deposits on the Rellana platform and immediately overlying the interpreted drainage divide of the Rellana platform. No reef development is described in the Ricardillo or Molata areas during DS5. This isolated reef development may be related to better exposure to wave and wind energy on the windward (northern) side of the Rellana platform, with Rellana and La Molata lying in more protected settings.

DS6.--- Lipinski (2010) described DS6 deposits in both the Ricardillo peak and La Molata areas as featuring locally laterally extensive stromatolites overlain by massive ooid grainstone that grade up into trough cross-bedded ooid grainstone with interbedded *Porites* boundstone (PF facies equivalent). The *Porites* boundstone is thick (up to 6 m) and laterally extensive at low elevations (181 -217 m; 159.75 - 196 m RE). Above 200 m (179 m RE) *Porites* boundstone occur as isolated patches (< 2 m wide and < 3 m thick). High elevations (217 - 240

m; 196 m - 212 m RE) feature laterally extensive stromatolites overlain by trough cross-bedded ooid grainstone interbedded with isolated *Porites* boundstone (Lipinski, 2010).

DS6 deposits in the Rellana platform area show a slightly higher range of deposition, with occurrences observed between 243 - 248 m (225 - 229.7 m RE). PF deposits occur up to 246 m implying minimum relative sea level of 251 m (234.3 m RE) to accommodate observed stick growth morphology coral (5 – 40 m water depth; *sensu* Riding *et al.,* 1991). PF deposits within DS6 in the Rellana Platform area are abundant and ranging in width from 1 - 63 m, with average width in the 20 - 30 m range. Thicknesses of PF deposits range from 1 to 6 m. The vast extent of PF deposits observed in DS6 could potentially be fringing reef growths on shallow substrate, however, the continued presence of oolitic grainstones and reef development on time-equivalent surfaces down dip also suggests high energy, rather than protected lagoonal deposits as would be expected behind a barrier reef. No lagoonal deposits, or deposits with high carbonate mud concentrations or other evidence for low energy during deposition were observed in the study area, excluding microbialites, which have been shown to be deposited in a wide range of water depths and energy levels (overlying isolated, basal trough cross bedded ooid bivalve facies (Braga et al., 1995; Mancini et al., 1998; Grotzinger et al., 2000; Mancini and Parcell, 2001; Whalen et al. 2002; Adams et al., 2004; Batten et al., 2004; Mancini et al., 2004; Adams et al., 2005; Heydari and Baria, 2005; Mancini et al., 2008; Planavsky and Ginsburg, 2009; Lipinski, 2010).

The widespread distribution of Porites during deposition of this interval may be related to decreasing aridity, or may be due to sea level reaching an elevation above 251 m, drowning many of the topographic elements that may have led to restriction in other areas. Note that

Porites reefs are found throughout the Ricardillo embayment, and this indicates that sea level was high enough to inundate the north-south promontory and drainage divide on its east side.

DS7.--- The final depositional sequence within the TCC (DS7) is truncated by modern erosion. Deposits are preserved as an erosional remnant on La Molata and feature basal stromatolites overlain by thrombolitic boundstones interbedded with cross-bedded oolitic gastropod grainstone and overlain by trough cross-bedded ooid grainstone. In the Ricardillo Peak field area, DS7 deposits occur below 211.5 m (197 - 211.5 m; 176 - 191.5 m RE) and consist of paleotopography-draping stromatolites and overlying thrombolitic boundstone (rarely overlain by trough cross-bedded ooid grainstone) (Lipinski, 2010). In the Rellana platform area, DS7 deposits are observed between 245 - 251 m (225.9 - 234.1 m RE) and range in thickness from 0 to 2 m. No thrombolitic material was observed on the Rellana platform, however one displaced PF deposit showing encrusting and massive head growth morphology was found, near section LRS7, indicative of <10 m water depth during deposition (Grasso and Pedley, 1988; Saint-Martin, 1990; Pomar, 1983; Pomar, 1991; Riding *et al.,* 1991; Esteban, 1996). DS7 is overlain by SB5, which extends down into the Agua Amarga basin, suggesting relative sea-level fall to near or below modern sea-level.

Summary.--- Due to the interpreted exposure to the predominant swell direction of the Rellana platform, it was hypothesized that the patch-reef development observed in the Ricardillo and Las Negras areas was related to reef development in a lagoonal environment behind a reef margin of some type. The Rellana platform was examined to determine if such a margin could be identified. Given the sporadic occurrence and limited lateral continuity of the observed coral

growth in the TCC of the Rellana platform, it seems unlikely that such a reefal margin developed on the Rellana platform.

Paleoclimate Discussion

DS1.--- DS1 is dominated by deposits that contain biota similar to that defined as 'molechfor' lithofacies of Carannante *et al.* (1988), the 'bryomol' and 'foramol' lithofacies of Lees and Buller (1972), and the Heterozoan Association of James (1997). These lithofacies are known to be associated with cold-temperate to subtropical conditions. An increasing red algal content in DS1b suggests warming (transition into the 'rhodalgal' facies of Carannante *et al.* (1988)) into more temperate conditions.

Other influences other than cool temperatures are known to lead to heterozoan deposition. Nutrient excess from runoff, increased water depth and upwelling can all have an effect. Excessive nutrients in runoff can lead to decline or demise of reef populations, explaining the lack of chlorozoan constituents. It is worth noting that significant reef development on the Rellana platform lacked significant time-equivalent volcaniclastic debris, likely due to the inundation of most of the volcanic source areas. Heterozoan deposits, equivalent to DS1, are described throughout SE Spain (Addicott *et al.,* 1978; Esteban and Giner, 1980; Dabrio *et al.,* 1981; Braga and Martin, 1988; Esteban, 1996; Franseen and Goldstein, 1996; Franseen *et al.,* 1997; Toomey, 2003; Dillett, 2004) and into the greater Mediterranean (Esteban, 1996), indicating that a localized process like excessive nutrient-laden runoff is not a major control.

The regional nature of these heterozoan deposits also indicates that localized upwelling of cool, nutrient-rich water is likely not solely responsible for the occurrence of heterozoan deposits

on the Rellana platform. It is possible that a temperate climate coupled with upwelling could lead to heterozoan development (Rouchy, 1982, 1988; Franseen *et al.,* 1997).

Alternatively, a deepwater setting could be invoked to explain the heterozoan dominance, regardless of climatic conditions. If reef development was occurring during DS1, chlorozoan skeletal fragments would be expected to bypass the steep paleoslope. These components are largely absent, however, indicating that there was likely no reef development updip.

DS2.--- The RAPG deposits that dominate DS2 are similar to the 'rhodalgal' lithofacies of Carannante *et al.* (1988) and the 'foramol' lithofacies of Lees and Buller (1972) typical of a temperate or subtropical climate. The majority of the deposits of DS2 are dominated by heterozoan association deposits (after James, 1997). The presence of volcanic conglomerates (VC and VCC) indicate nutrient-rich runoff was likely entering the system, however regionally correlative heterozoan deposits indicate the observed heterozoan association is not related to excessively nutrient-rich runoff. Physical tracing of DS2 beds into updip Vermetid framestones indicates water depth could have been significant (as much as 280 m according to Toomey (2003)), however the presence of high energy occurrences of FGSWP interbedded with RAPG indicates deposition at this water depth was not continuous, therefore depth was not the major control on heterozoan development. Although towards the top of DS2, occurrence of FWP indicates deep hemipelagic conditions, the regional relationships indicate a temperate climate coupled with upwelling are still the most likely explanations for the occurrence of heterozoans (Rouchy, 1982, 1988; Franseen *et al.,* 1997b).

The deposits associated with SBZ 3 feature the first evidence for the photozoan association (James, 1997; and also similar to the 'chlorozoan' facies of Lees and Buller (1972))

on the Rellana platform. These deposits contain abundant detrital *Tarbellastraea* and less commonly *Porites* coral, predominantly showing robust branching and stick growth morphologies. The presence of these components indicates a warming trend into warm subtropical to tropical climate conditions.

DS3.--- The basal deposits of DS3 south of the drainage divide are characterized by deposits similar to the 'rhodalgal' facies of Carannante *et al.* (1988) and the 'heterozoan association' of James (1997) These deposits grade up into skeletal packstone and local grainstone (CGSPG) that interfinger updip with abundant PF, TF and CAG facies. These coral rich facies are similar to the photozoan association and associated reefal facies (James, 1997 and references within), which are interpreted to represent warm, tropical conditions. This transition between a heterozoan-dominated system to a photozoan-dominated is likely a continuation of the warming trend identified in DS2.

DS4 – 7.--- The facies observed within DS 4 - 7 on the Rellana platform contain variable biotic concentrations. The facies in DS4 tend to display a lower, less diverse skeletal content than deposits of higher sequences. Lipinski (2010) has also described a diversifying biota in subsequent sequences, and this diversification is attributed to a transition to more normal marine conditions caused by decreasing aridity. Despite this initial lack of diversity, the preserved biota and facies indicate a subtropical to tropical climate during DS 4 - 7 deposition. The cyclicity of the DS 4 - 7 deposits has been attributed to high-frequency, sea level fluctuations associated with glacial eustasy (Franseen and Goldstein, 2004).

CONCLUSIONS

1) The Miocene (Tortonian-Messinian) Rellana platform is composed of seven depositional sequences (DS1, DS2, DS3 and DS 4 – 7, the Terminal Carbonate Complex) composed of 13 lithofacies and separated by surfaces of subaerial exposure or correlative conformity. Volcanic detritus and lenticular carbonate units grading into alternating coarse-grained and fine-grained carbonates compose DS1; DS2 is composed of RAPG deposits showing fining upward cycles; abundant reef and forereef units make up DS3; and DS 4 - 7 consist of oolitic grainstone, coralgal framestone and microbial boundstone.
2) Analysis of DS 4 - 7 deposits show they are equivalent to TCC deposits as described throughout the region; the hypothesis that these deposits formed in a lagoonal environment behind a prominent marginal reef complex was examined and found not to be supported by the distribution of reef, oolitic and thrombolitic facies on the platform and in the surrounding region. Reef material is more common in field areas located outside of the Rodalquilar caldera, however reef development is limited to patch reef growths. No prominent marginal reef complex was found preserved.
3) A drainage divide is exposed on the Rellana platform, separating a steeply dipping (~20˚) southern slope from a gently dipping (~5˚) northern slope. DS1 and DS2 were restricted to the base of the steeply dipping southern slope, which dramatically influenced the nature of the deposits by facilitating debris flows and similar processes, which with sea level change, yielded the decameter scale, shoaling-upward RAPG bedsets characteristic of DS2. On the northern slope, abundant reef progradation and downstepping events are clearly visible in DS3, whereas on the southern slope, abundant coralgal and coarse-grained skeletal material

is preserved with significantly less development of *in situ* reef deposits. On the southern slope, it is possible that reef production was decreased due to less-than-optimal orientation to the predominant wave direction, or that sediment was bypassed downslope below modern sea level.

4) The paleogeographic distribution and orientation of the Rellana Platform, Ricardillo Peak and La Molata platform impacted the nature of the carbonates that developed. The north slope of the Rellana platform was exposed to the highest wave energy and as a result, saw increased reef progradation during DS3 and earlier reef development during the TCC than other areas studied.
5) Construction of an interpretive relative sea-level curve for the platform allows the relative sea-level history of each depositional sequence to be interpreted. DS1 deposits were deposited during a relative rise in sea level, with a relative fall in sea level at SB1a. SB2 represents a relative fall in sea level, with a subsequent rise in sea level resulting in the deposition of DS2. Another relative fall in sea level caused deposition and later exposure of SBZ 3. Another rise leads to the aggradational stage of DS3, followed by progradational and downstepping geometries suggesting a rise, stillstand, and fall in sea level, eventually exposing the top of the Rellana platform (SB4). DS 4 - 7 deposits (TCC) were deposited during high-frequency, high-amplitude sea-level fluctuations with a general deepening trend; these deposits are capped by SB5 which exposed the entire platform and marked the end of marine carbonate deposition on the platform.
6) Climatic indicators such as heterozoan assemblages and then reef development indicate a warming trend throughout the development of the platform. DS1 is dominated by cool to

temperate heterozoan assemblages. DS2 shows initial introductions of photozoan components to carbonate deposition (TF reef development). DS3 shows a transition from a heterozoan association into a prominent photozoan reef system. DS 4 - 7 (TCC) deposits demonstrate continuation of the subtropical to tropical conditions.

REFERENCES

Addicott, W. O., Snavely, P. D. Jr., Bukry, D., and Poore, R. Z., 1978, Neogene stratigraphy and paleontology of southern Almeria Province, Spain: an overview. USGS Bulletin, Series 1454, p. 49.

Ahr, W. M., 1973, The carbonate ramp: an alternative to the shelf model. Transactions of the Gulf Coast Association of Geological Societies, v. 23, p. 2211-225.

Ball, M.M., 1967, Carbonate Sand Bodies of Florida and the Bahamas: Journal of Sedimentary Petrology, v. 37, p. 556-571.

Betzler, C., Martin, J. M., Braga, J.C., 2000, Non-tropical carbonates related to rocky submarine cliffs (Miocene, Almeria, southern Spain). Sedimentary Geology, v. 131, p. 51-65.

Brachert, T. C., Betzler, C., Braga, J. C., and Martin, J. M., 1998, Microtaphofacies of a warm-temperate carbonate ramp (Uppermost Tortonian/Lowermost Messinian (Southeast Spain)). Palaios, v. 13, p. 459-475.

Brachert, T.C., Hultzsch, N., Knoerich, A.C., Krautworst, U.M.R., Stuckrad, O.M., 2001, Climatic signatures in shallow-water carbonates: high-resolution stratigraphic markers in structurally controlled carbonate buildups (Late Miocene, southern Spain). Palaeogeography, Palaeoclimatology, Palaeoecology, v. 175, p. 211-237.

Braga, J. C., and Martin, J. M., 1988, Neogene coralline-algal growth-forms and their paleoenvironments in the Almanzora river valley (Almeria, S.E. Spain). Paleogeography, Paleoclimate, and Paleoecology, v. 67, p. 285-303.

Burchette, T.P., and Wright, V.P., 1992, Carbonate ramp depositional systems: Sedimentary Geology, v. 79, p. 87-115.

Calvet, F., Zamarreno, I., and Valles, D., 1996, Late Miocene Reefs of the Alicante-Elche Basin, Southeast Spain, *in* Franseen, E.K., Esteban, M., Ward, W.C., and Rouchy, J.-M., eds., Models for Carbonate Stratigraphy from Miocene Reef Complexes of the Mediterranean Regions, SEPM Concepts in Sedimentology and Paleontology Series No. 5, p. 177-190.

Calvo, M., Osete, M.L., and Vegas, R., 1994, Paleomagnetic rotations in opposite senses in southeastern Spain. Geophysical Research Letters, v. 21, no. 9, p. 761-764.

Carannante, G., Esteban, M., Milliman, J.D., and Simone, L., 1988, Carbonate Lithofacies as paleolatitude indicators: problems and limitations. Sedimentary Geology, v. 60, p. 333-346.

Cheel, R.J., 1990, Grain fabric in hummocky cross-stratificated storm beds: genetic implications. Journal of Sedimentary Petrology, v. 6, no. 1, p. 102-110.

Cheel, R.J., and Leckie, D.A., 1992, Coarse-grained storm beds of the Upper Cretaceous Chungo Member (Wapiabi Formation), Southern Alberta, Canada. Journal of Sedimentary Petrology, v. 62, no. 6, p. 933-945.

Cunningham, K.J., 1995, An upper Miocene sedimentary succession, Melilla basin, northeastern Morocco [Unpublished PhD thesis]: University of Kansas, Lawrence, KS, p. 371.

Dabrio, C. J., Esteban, M., and Martin, J. M., 1981, The Coral Reef of Nijar, Messinian (Uppermost Miocene), Almeria Province, SE Spain. Journal of Sedimentary Petrology, v. 51, p. 521-439.

Dillett, P. M., 2004, Paleotopographic and sea-level controls on the sequence stratigraphic character of a heterozoan carbonate succession: Pliocene, Carboneras basin, southeast Spain. [Unpublished M.S. Thesis]. University of Kansas, Lawrence, KS, p. 116.

Dvoretsky, R. A., 2009, Stratigraphy and reservoir-analog modeling of upper Miocene shallow-water and deep-water carbonate deposits: Agua Amarga basin, Southeast Spain. [Unpublished M.S. Thesis]; University of Kansas, Lawrence, KS, p. 148.

Esteban, M., 1979, Significance of the upper Miocene coral reefs of the western Mediterranean. Paleogeography, Paleoclimatology, Paleoecology, v. 29, p. 169-188.

Esteban, M., and Giner, J. 1980, Messinian Coral Reefs and Erosion Surfaces in Cabo de Gata (Almeria, southeastern Spain): Acta Geologico Hispanica, v. 15, p. 97-104.

Esteban, M., 1996, An Overview of Miocene Reefs from Mediterranean Areas: General Trends and Facies Models, *in* Franseen, E. K., Esteban, M., Ward, W. C., and Rouchy, J.-M., eds., Models for Carbonate Stratigraphy from Miocene Reef Complexes of the Mediterranean Regions. SEPM Concepts in Sedimentology and Paleontology, Series No. 5, p. 3-54.

Esteban, M., Braga, J. C., Martin, J., and Santisteban, C., 1996, Western Mediterranean Reef Complexes, *in* Franseen, E. K., Esteban, M., Ward, W. C., and Rouchy, J.-M., eds., Models for Carbonates Stratigraphy from Miocene Reef Complexes of Mediterranean Regions. SEPM Concept in Sedimentology and Paleontology, p. 55-72.

Esteban, M., and Giner, J., 1980, Messinian coral reefs and erosion surfaces in Cabo de Gata (Almeria, southeastern Spain). Acta Geologica Hispanica, v. 15, p. 97-104.

Feldman, M., and McKenzie, J.A., 1997, Messinian stromatolite-thrombolite associations, Santo Pola, SE Spain: an analog for the Paleozoic? Sedimentology, v. 44, p. 893-914.

Fernandez-Soler, J.M., 1996, El volcanismo calco-alcalindo de Cabo de Gata (Almeria), estudio volcanologico y petrologico. Sociedad Almeriense de Historia Natural, Almeria, p. 295.

Flugel, E., 1982, Microfacies Analysis of Limestones: New York, Springer-Verlag, p. 106-129.

Franseen, E.K., 1989, Depositional sequences and correlation of middle to upper Miocene carbonate complexes, Las Negras area, southeastern Spain [unpublished Ph.D. thesis]: University of Wisconsin–Madison, 374 p.

Franseen, E.K., Goldstein, R.H., and Whitesell, T.E., 1993, Sequence stratigraphy of Miocene carbonate complexes, Las Negras area, southeastern Spain: Implications for quantification of changes in relative sea level, in Loucks, R.G. and Sarg, J.F., eds., Carbonate Sequence Stratigraphy: Recent Developments and Applications, AAPG Memoir 57, p. 409-434.

Franseen, E. K., and Goldstein, R. H., 1996, Paleoslope, Sea-level and Climate Controls on Upper Miocene Platform Evolution, Las Negras Area, Southeastern Spain, *in* Franseen, E. K., Esteban, M., Ward, W. C., and Rouchy, J.-M., eds., Models for Carbonates Stratigraphy from Miocene Reef Complexes of Mediterranean Regions. SEPM Concept in Sedimentology and Paleontology, p. 159-176.

Franseen, E. K., Goldstein, R. H., and Esteban, M., 1997a, Controls on Porosity Types and Distribution in Carbonate Reservoirs: A Guidebook for Miocene Carbonate Complexes of the Cabo de Gata Area, SE Spain. American Association of Petroleum Geologists Education Program, p. 1-150.

Franseen, E. K., Goldstein, R. H., and Farr, M. R., 1997b, Substrate-Slope and Temperature controls on Carbonate Ramps: Revelations from Upper Miocene Outcrops, SE Spain, *in* James, N. P., and Clarke, A. D., eds., Cool-Water Carbonates. SEPM Special Publication, p. 271-290.

Franseen, E. K., Goldstein, R. H., and Farr, M. R., 1998, Quantitative Controls on Location and Architecture of Carbonate Depositional Sequences: Upper Miocene, Cabo de Gata Region, SE Spain. Journal of Sedimentary Research, v. 68, p. 283-298.

Franseen, E.K., and Goldstein, R.H., 2004, Build-and-Fill: A Stratigraphic Pattern Induced in Cyclic Sequences by Sea Level and Paleotopography: Geological Society of America Abstracts with Programs, v. 36, p. 377.

Franseen, E.K., and Mankiewicz, C., 1991, Depositional sequences and correlation of middle(?) to late Miocene carbonate complexes, Las Negras and Nijar areas, southeastern Spain: Sedimentology, v. 38, p. 871-898.

Grasso, M. and Pedley, H.M., 1988, The sedimentology and development of Terravecchia Formations carbonates (upper Miocene) of north central Sicily: possible eustatic influence on facies development. Sedimentary Geology, v. 57, p. 131-149.

Goldstein, R. H., and Franseen, E. K., 1995, Pinning points: a method providing quantitative constraints on relative sea-level history. Sedimentary Geology, v. 95, p. 1-10.

Harris, P.H., 1977, The Joulters ooid shoal, Great Bahama Bank, *in* Peryt, T.M., ed., Coated grains: New York, Springer-Verlag, p. 132-141.

Hess, A. V, 2011, Heterozoan Carbonate Lithofacies and Sequence Stratigraphy: A Study of Pliocene Strata of the Agua Amarga Basin, Southeastern Spain. [Unpublished M.S. thesis] University of Kansas, Lawrence, KS, p. 256.

Hine, A. C., 1977, Lily Bank, Bahamas; history of an active oolite shoal: Journal of Sedimentary Petrology, v. 47, p. 1554-1581.

Hine, A. C., and Neumann, A. C., 1977, Shallow Carbonate-Bank-Margin Growth and Structure, Little Bahama Bank, Bahamas: AAPG Bulletin, v. 61, p. 376-406.

Hoffman, P., 1967, Algal Stromatolites: Use in Stratigraphic Correlation and Paleocurrent Determination: Science, v. 157, p. 1043-1045.

James, N.P., 1997, The Cool-Water Carbonate Depositional Realm, *in* James, N.P., and Clarke, J., eds., Cool-Water Carbonates, SEPM Special Publications, p. 1-20.

Johnson, C. L., Franseen, E. K., and Goldstein, R. H., 2005, The effects of sea level and paleotopography on lithofacies distribution and geometries in heterozoan carbonates, south-eastern Spain. Sedimentology, v. 52, p. 513-536.

Lees, A. and Buller, A.T., 1972, Modern temperate-water and warm-water shelf carbonate sediments contrasted. Marine Geology, v. 13, p. M67-M73.

Lionello, P., and Sanna, A., 2005, Mediterranean wave climate variability and its links with NAO and Indian Monsoon: Climate Dynamics, v. 25, p. 611-623.

Lipinski, C. J., 2010, Stratigraphy of upper Miocene oolite-microbialite-coralgal reef sequences of the terminal carbonate complex: southeast Spain. [Unpublished M.S. thesis] University of Kansas, Lawrence, KS, p. 116.

Lloyd, R.M., Perkins, R.D., and Kerr, S.D., 1987, Beach and shoreface ooid deposition on shallow interior banks, Turks and Caicos Islands, British West Indies: Journal of Sedimentary Petrology, v. 57, p. 976-982.

Lopez-Ruiz, and Rodriguez-Badiola, E., 1980, La Region Volcanica Neogena del Sureste de Espana. Estudios Geologicos, v. 36, p. 5-63.
Loreau, J.P., and Purser, B.H., 1973, Distribution and ultrastructure of Holocene ooids in the Persian Gulf, *in* Purser, B.H., ed., The Persian Gulf, Holocene Carbonate Sedimentation in a Shallow Epicontinental Sea: New York, Springer-Verlag, p. 279-328.
Lowe, D.R., 1979, Sediment gravity flows: their classification and some problems of application to natural flows and deposits. SEPM Special Publication, no. 27, p. 75-82.
Major, R.P., Bebout, D.G., and Harris, P.M., 1996, Recent evolution of a Bahamian ooid shoal; effects of Hurricane Andrew: GSA Bulletin, v. 108, p. 168-180.
Mapa Geológico de España, 1981, (1:50,000): Instituto Geológico y Minero de España.
Mankiewicz, C., 1996, The Middle to Upper Miocene carbonate complex of Nijar, Almeria Province, southeastern Spain, *in* Franseen, E.K., Esteban, M., Ward, W.C., and Rouchy, J.-M., eds., Models for Carbonates Stratigraphy from Miocene Reef Complexes of Mediterranean Regions, SEPM Concept in Sedimentology and Paleontology Series No. 5, p. 141-158.
Martin, J. M., Braga, J. C., Betzler, C., and Brachert, T., 1996, Sedimentary model and high frequency cyclicity in a Mediterranean, shallow-shelf, temperate-carbonate environment (uppermost Miocene, Agua Amarga Basin, Southern Spain). Sedimentology, v. 43, p. 263-277.
Martin, J. M., Braga, J. C., and Betzler, C., 2003, Late Neogene - Recent uplift of the Cabo de Gata volcanic province, Almeria, SE Spain. Geomorphology, v. 50, p. 27-42.
Montenat, C., Ott, D'Estevou, P., and Mase, P., 1987, Tectonic-sedimentary characters of the Betic Neogene basins evolving in a crustal transcurrent shear zone (SE Spain). Bulletin Centres Rech. Explor.-Prod., Elf-Aquitaine, v. 11, p. 1-22.
Montenat, C., and Ott D'Estevou, P., 1990, Le basin de Nijar-Carboneras et le couloir de Bas-Andarax, *in* Montenant, C., ed., Les Bassins Neogenes Du Domaine Betique Oriental (Espagne): Institut Geologique Albert-de-Lapparent, Paris, Documents et Travaux Institut Geologique Albert-de-Lapparent, p. 129-164.
Montenat, CH. and Ott D'Estevou, P**.**, 1996, Late Neogene basins evolving in the Eastern Betic transcurrent fault zone: an illustrated review, *in* Friend, P. F. and Dabrio, C. J., eds., Tertiary basins of Spain: the stratigraphic record of crustal kinematics. p. 323-329. Cambridge University Press, Cambridge.
Pomar, L., Obrador, A., Fornos, J., Rodriguez-Perea, A., eds., 1983, El Terciario de las Baleares (Mallorca-Menorca), Guia de las Excursiones del X Congreso Nacional De Sedimentologia. Institut D'Estudis Balearics and Universitat de Palma de Mallorca, 233 pp.
Pomar, L.., 1991, Reef geometries, erosion surfaces and high-frequency sea-level changes, Upper Miocene reef Complex, Mallorca, Spain: Sedimentology, v. 38, p. 243-269.
Platt, J.P., and Vissers, R.L.M., 1989, Extensional collapse of thickened continental lithosphere: a working hypothesis for the Alboran sea and Gibraltar arc: Geology, v. 17, p. 540-543.
Read, J. F., 1985, Carbonate platform facies models. AAPG Bulletin, v. 69, p. 1-21.
Rehault, J. P., Boillot, G. and Mauffret, A., 1985, The western Mediterranean basin, in Stanley, D.J. and Wezel, F.C., eds., Geologic Evolution of the Mediterranean Basin. Springer-Verlag, New York, p. 101-130.

Riding, R., Martin, J. M., and Braga, J. C., 1991, Coral-stromatolite reef framework, Upper Miocene, Almeria, Spain: Sedimentology, v. 38, p. 799-818.
Rouchy, J. M., 1982, La crise èvaporitique Messininenne de Méditerranée: nouvelles propositions pour une interpretation genetique: Paris, Bulletin du Museum National d'Histoire Naturelle, v. 50, p. 267.
Rouchy, J. M., 1988, Relations évaporites-hydrocarbures: l'association laminites-récifs-évaporites dans le Messinien de Méditerranée et ses ensignements, *in* Busson, J., ed., Èvaporites et hydrocarbures. Mémoires du Muséum national d' Histoire naturelle (C), v. 55, p. 43-69.
Rytuba, J. J., Arribas, A. Jr., Cunningham, C. G., Mckee, E. H., Podwysocki, M. H., Smith, J. G., Kelly, W. C., and Arribas, A., 1990, Mineralized and unmineralized calderas in Spain; Part II, evolution of the Rodalquilar caldera complex and associated gold-alunite deposits: Mineralium Deposita, v. 25 (Suppl), p. S29-S35.
Sanz De Galdeano, C. and Vera, J.A., 1992, Stratigraphic record and palaeogeographical context of the Neogene basins in the Betic Cordilleran, Spain: Basins Research, v. 4, p. 21-36.
Serrano, F., 1992, Biostratigraphic control of Neogene volcanism in Sierra De Gata (southeast Spain): Geologie en Mijnbouw, v. 71, p. 3-14.
Shackleton, N.J., Hall, M.A., and Pate, D., 1995, Pliocene stable isotope stratigraphy of site 846: Proceedings of the Ocean Drilling Program, Scientific Results, v. 138, p. 337-355.
Toomey, N., 2003, Controls on sequence stratigraphy in upper Miocene carbonates of Cerro de Ricardillo, southeastern Spain. [Unpublished M.S. Thesis]: University of Kansas, Lawrence, KS, p. 114.
Tucker, M.E., and Wright, V.P., 1990, Carbonate Sedimentology: Oxford, Blackwell Scientific Publications, p. 482.
Valles Roca, D., 1986, Carbonate facies and depositional cycles in the upper Miocene of Santa Pola (Alicante, SE Spain): Revista d'Investigacions Geologiques, v. 42/43, p. 45-66.
Walker, R. G., 1975, Generalized facies models for resedimented conglomerates of turbidite association: Geological Society of America, Bulletin, v. 86, p. 737–748.
Whitesell, T. C., 1995, Diagenetic Features Associated with Sequence Boundaries in Upper Miocene Carbonate Strata, Las Negras, Spain. [Unpublished Master's Thesis]: University of Kansas, p. 292.
Whorff, J.S., Whorff, L.L., Sweet, M.H., 1995, Spatial variations in an algal turf community with respect to substratum slope and wave height. Journal of Marine Biology Association, U.K., v. 75, p. 429-444.
Wilbur, K.M., 1983, The Mollusca. Ecology, v. 6, p. 695.
Woods, A.J., 1980, Geomorphology, deformation, and chronology of marine terraces along the Pacific coast of Central Baja California, Mexico: Quaternary Research, v. 13, p. 346-364.

CHAPTER 3:

Examining the relationship of development of the Rellana Platform to deposits in the Agua Amarga Basin: Cabo De Gata Region, Southeastern Spain

Rafferty Sweeney, Evan K. Franseen and Robert H. Goldstein

1) Department of Geology, University of Kansas, Lindley Hall, 1475 Jayhawk Blvd., Lawrence, KS, 66044, Ph. # (785) 766-1114, e-mail: rsweeney@ku.edu
2) Department of Geology, University of Kansas, Lindley Hall, 1475 Jayhawk Blvd., Lawrence, KS, 66044, Ph. # (785) 864-2738, e-mail: gold@ku.edu
3) Department of Geology, University of Kansas, Lindley Hall, 1475 Jayhawk Blvd., Lawrence, KS, 66044, Ph. # (785) 864-2723, e-mail: evanf@kgs.ku.edu

CHAPTER SUMMARY

Typical depositional models for resedimented deepwater carbonates fail to reflect the potential impact of platform topography on sediment distribution. This study focuses on a 2-dimensional coastal exposure approximately perpendicular to the margin of the Rellana platform, and builds upon work done in the Agua Amarga basin (Cabo de Gata region, Southeast Spain) to demonstrate the effects of paleotopography and fluctuation of relative sea level on sediment redistribution into the basin. The results for the study area indicate that the position of the reefal margin in relation to a low-angle, basinward sloping substrate versus a distally steepened substrate slope (basin margin) controls the nature of sediment transport into the basin. Furthermore, stratal packaging, relative sea-level history and faunal variations indicate that a highstand shedding model does not accurately reflect the timing of coarse material redistribution into the basin.

The Rellana platform developed on Neogene volcanic substrate that features a drainage divide separating a steep-dipping (~20˚) south slope from a shallow-dipping (~5˚) north slope. The shallow-dipping north substrate slope steepens to ~25˚ distally (1.3 km N of the drainage divide) and flattens when traced into the adjacent basin. This steep surface is herein referred to as the 'basin margin' and defines the southwestern margin of the Agua Amarga basin. The Rellana platform rims the Agua Amarga basin for approximately 8 km and was a major source for carbonate sediment in the basin. Seven sequences on the platform document evolution from a heterozoan ramp, to photozoan reef, with variable coralgal content, to a shallow marine microbial/oolitic system. Basinal deposits consist of grainy heterozoan-dominated shallow-water

deposits, hemi-pelagic and pelagic deep-water deposits, carbonate/volcanic debrites, and high- and low-density turbidites.

During the reefal platform phase, initial diverse reef margin development was near or on the steep basin margin, and coarse debrite breccias accumulated in the basin. The debrite breccias show a backstepping geometry related to the initial stages of a subsequent sea-level rise. As the rise continued, the reef margin retrograded 1.3 km, back to the platform drainage divide, and basin deposits transitioned to fine-grained materials. Highstand *Porites*-rich reef progradation towards the basin margin resulted in an increase in coarse-grained, mostly sediment gravity flow deposits in the basin. This increase was most pronounced once the reefal margin prograded to within 400 m of the basin margin. As sea level fell, reefs continued to prograde and downstep toward the basin resulting in increasing amounts of coarse-grained basinal deposits, including debrite breccias, that progressively stepped toward the basin center. The results of this study show that increasing proximity of the reef margin to the basin margin increases the volume of coarse material deposited in the basin. Additionally, the traditional highstand shedding model associated with rimmed platforms does not explain the lowstand or early transgressive, and falling stage redistribution of sediment into the basin. The results of this study indicating an alternative timing for deposition of coarse-grained basinal sediments may apply to other carbonate systems that are characterized by antecedent topography that shows a transition from low-angle basinward substrate slope to distal steepening of the slope.

INTRODUCTION

Studies of Miocene carbonates of the Cabo de Gata region in southeastern Spain have been useful in furthering understanding of the influence of paleotopography, paleoclimate and relative sea-level history on the development of carbonate platforms and neighboring basins (e.g. Esteban, 1979; Esteban and Giner, 1980; Dabrio *et al.,* 1981; Braga and Martin, 1988; Franseen, 1989; Franseen and Mankiewicz, 1991; Franseen et al., 1993; Goldstein and Franseen, 1995; Esteban, 1996; Esteban *et al.,* 1996; Franseen and Goldstein, 1996; Mankiewicz, 1996; Betzler *et al.,* 1997; Franseen *et al.,* 1997b; Franseen *et al.,* 1998, Betzler *et al.*, 2000; Toomey, 2003; Dillett, 2004; Johnson *et al.*, 2005; Dvoretsky, 2009; Lipinski, 2010; Goldstein *et al.,* 2012). This study presents data collected from the Rellana carbonate platform, which forms the southwestern margin of the Agua Amarga basin (Figure 1). Located ~4 km northeast of the town of Las Negras, the Rellana platform is laterally equivalent to and downdip of the Ricardillo Peak area to the west (Fig. 1). Miocene deposits in the Ricardillo peak area were described by Toomey (2003) and Lipinski (2010); these deposits are discussed in Chapter 2.

The focus of this study is a 3 km coastal transect roughly perpendicular to the platform margin. The Rellana platform developed on a Neogene volcanic substrate and consists of 7 depositional sequences (DS1-7) composed of 13 facies (Fig. 2, Table 1). The surface on top of the volcanic substrate features a drainage divide separating a steep-dipping (~20˚) south slope from a shallow-dipping (~5˚) north slope (Fig. 1, 3). The shallow-dipping north slope steepens distally to a steep (25˚) basin margin (1.3 km N of the drainage divide). It eventually flattens as it reaches the basin floor. The Rellana platform is one of the most extensively developed platforms in the Cabo de Gata area. It formed the rim above the Agua Amarga basin for approximately 8

km and was a major source for carbonate accumulations in the adjacent Agua Amarga basin (Goldstein and Franseen, 2002; Dvoretsky *et al.,* 2008; Dvoretsky, 2009; Dvoretsky *et al.,* 2009; Goldstein *et al.,* 2012; Dvoretsky *et al*., 2014).

An excellent summary of carbonate slopes and platform margins by Playton *et al.,* 2011 illustrates that the controlling drivers behind generalized variations in carbonate-slope-deposit types and related architectures are unclear and poorly understood within the platform to basin system. Identification of the intrinsic (e.g. temporal faunal variations, ramp to rim evolution, lithified margin sediment type and platform morphology) and extrinsic (accommodation change, relative timing of collapse events, growth escarpment development, bypassed toe-of-slope accumulations, oceanographic effects, slope height, tectonic activity and external sediment input) controls on carbonate slope development illustrate the complexity of these systems and the large potential for variability. This study seeks to identify the importance of these controls in development of a platform-to-basin system.

Typical depositional models for resedimented deepwater carbonates involve highstand shedding of material to form line-sourced wedges and debris aprons (Cook and Enos, 1977; Cook and Mullins, 1983; Schlager and Chermack, 1979; Mullins and Cook, 1986; Coniglio and Dix, 1992; Playton *et al.*, 2011 and references within). A study of Agua Amarga basinal facies (Goldstein *et al.,* 2012) demonstrated that the antecedent topography of the Agua Amarga basin strongly influenced the distribution of basinal sediment, resulting in a depositional model that contrasts with traditional carbonate slope and toe-of-slope models by demonstrating the influence of a funneling mechanism. This study builds upon that the work in the Agua Amarga basin (e.g. Martin *et al.*, 1996; Franseen *et al.*, 1997a; Dvoretsky *et al.*, 2009; Goldstein *et al.*,

2012; Dvoretsky *et al*., 2014). It has been hypothesized that the characteristics of strata in the basin are the result of platform processes related to the interplay among relative sea-level, paleotopography, and the reef margin location relative to the basin margin (Goldstein *et al.*, 2012). In particular, hypotheses included:

1. Initially, a large relative rise in sea level (>100m) results in deposition of photozoan reefs at high elevations, corresponding to hemipelagic-pelagic deposits, low-density turbidites and uncommon high-density turbidites in the basin. Due to the relatively flat (~5°) surface separating the reef margin from the steep basin margin, little coarse sediment made it into the basin.

2. Subsequent relative sea-level fall resulted in reefal platform production shifting closer to the steep basin margin and eventually resulted in subaerial exposure of the platform, resulting in an erosion surface within the basinal deposits.

3. An increase in coarse debris delivered to the basin is driven by subaerial exposure of the platform and resulting erosion, or by close proximity of the reef margin to the steep basin margin.

4. Later, backstepping basinal breccias capped by turbidite successions that fine up into hemipelagic-pelagic sediments in the basin have been attributed to a relative sea-level rise. These basinal features are predicted to correspond to the reef margin shifting away from the steep basin margin. Based on reef development in nearby areas (e.g. Las Negras), the period following this relative rise in sea level represents late transgression and early highstand, with minor aggradation predating progradation on the platform. The dominant basin deposits at this time are fine-grained, resulting from the separation of the reef and basin margins.

5. Progradational and onlapping breccias and coarse turbidites cap the basinal succession. These deposits are predicted to reflect progradation and downstepping of the reef margin and forereef deposits during sea-level stillstand and fall. Increasing proximity of the reef margin to the steep basin margin leads to increasingly coarse material being deposited into the basin.

To test these hypotheses and identify controls on the platform and basin system it is necessary to reconstruct the development of the platform and basin with emphasis on the relationship between platform processes and related deposits in the Agua Amarga basin. I hypothesize that the paleotopography would result in an alternative model to the traditional highstand shedding model. During highstand shedding, the majority of slope and toe-of-slope deposition occurs as a result of increased platform production after inundation; there is less sediment transport into the basin when the platform is subaerially exposed and carbonate production on the platform shuts down (*sensu* Coniglio and Dix, 1992, Schlager *et al.,* 1994, Playton *et al.,* 2011). Results from my study indicate that distally steepened antecedent topography below a platform produces an alternative to highstand shedding, where coarse materials are transported into the basin when sea level is low and closely associated with a steeply dipping basin margin, or during late highstand and falling sea level (forced regression).

Additionally, because this study documents the location of the reefal margin in relation to time-equivalent basinal deposits, the results can be used to test the hypothesis that distance between the reefal margin and basin margin acts as a primary control on the ability of coarse sediment gravity flow deposits to reach the basin. When the reefal margin has backstepped onto a gently sloping surface, far from the basin margin, one would hypothesize that high density sediment gravity flows generated from the reefal margin and forereef slope would be deposited

immediately downslope on the gently dipping surface. Essentially, coarse sediments would be stored on that surface as sediment gravity flows lose energy, and would not reach the basin or steep basin margin. Where the reefal margin is close to the steep basin margin, coarse sediment gravity flows would be able to reach the steep basin margin, where they would gain energy and reach the basin. There is likely a critical distance between the reefal margin and steep basin margin that would allow coarse sediment gravity flows to continue across the gently dipping surface and down the steep basin margin and into the basin. Similarly, one can evaluate a simple hypothesis that the lateral extent of coarse sediment gravity flow deposits is controlled by lateral position of the reefal margin. The closer the reefal margin is to the basin, the farther one might expect coarse sediment gravity flow deposits would extend into the basin. Another hypothesis that can be tested from the data available, is that sediment gravity flows gain more energy, and thus protrude into the basin farther, where they have a greater distance to flow down a steep slope. Simply comparing the elevation of the reefal margin on a steep slope to the distance coarse

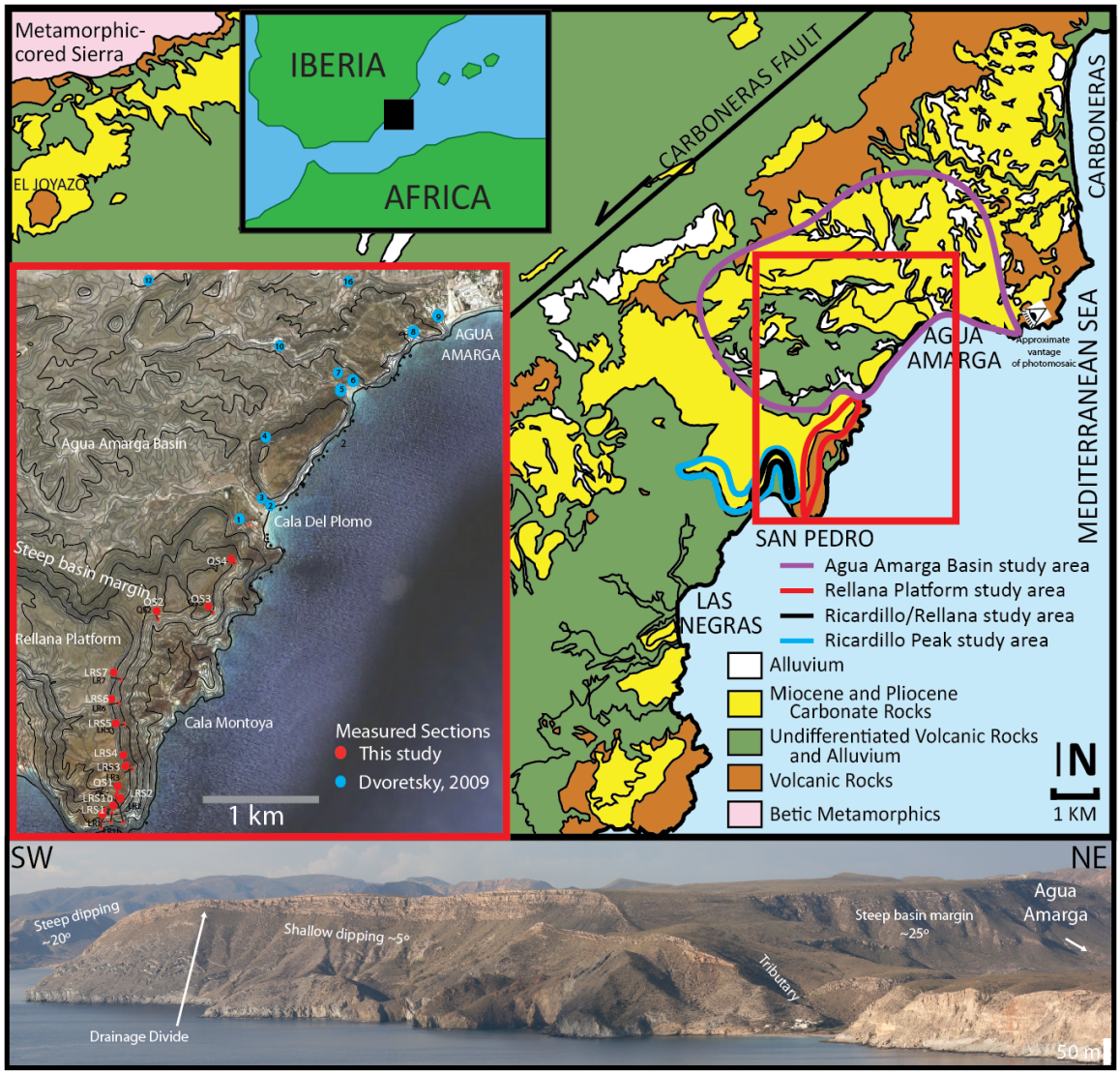

Figure 1: Location and general geological map of the Cabo de Gata region of southeastern Spain, the Rellana study area is indicated by the red highlighted area. Previously described areas immedately adjacent to the Rellana platform include Ricardillo peak (blue highlighted area; Toomey, 2003), Rellana/Ricardillo area (black highlighted area; Lipinski, 2010) and the Agua Amarga basin (purple highlighted area; Dvoretsky, 2009). Map modified from: Mapa Geológico de España, 1981; Dvoretsky, 2009; Lipinski, 2010. Red rectangle inset and corresponding map shows topographic map (10 m contour interval) overlain on satellite image of Rellana Platform area with location of measured sections. Photomosaic below shows the general morphology of the Rellana platform.

GEOLOGIC SETTING

The Agua Amarga basin is located 35 km northeast of Almeria, Spain within the Cabo de Gata Natural Park (Figure 1, 2). Calc-alkaline volcanic basement of the Cabo de Gata region is dated at 17 Ma to 6 Ma (Neogene) (Lopez-Ruiz and Rodriguez-Badiola, 1980; Serrano, 1992) and is separated from metamorphic (Mesozoic and Paleozoic) basement of the Betic Sierras to the northwest by the variably active (Tortonian through Messinian and Pliocene) sinistral strike-slip Carboneras Fault (Rehault *et al.,* 1985; Montenat *et al.,* 1987; Platt and Vissers, 1989; Montenat and Ott D'Estevou, 1990; Fernandez-Soler, 2001; Martin *et al.,* 2003). Uplift of the Betic mountains and volcanic highs is associated with Eocene to Serravallian (middle Miocene) orogenic compression of the Alpine Orogeny and Neogene volcanic activity associated with transtensional and transpressional stresses between the Iberian and African plates (Rehault *et al.,* 1985, Sanz de Galdeano and Vera, 1992; Montenat and Ott D'Estevou, 1996).

Faulting and erosion of the volcanic basement of the Cabo de Gata region resulted in formation of an archipelago of interconnected basins and volcanic highs forming the substrate for upper Miocene carbonate deposition (Esteban, 1979; Esteban and Giner, 1980; Esteban, 1996). Locally, carbonate deposits are considered mostly preserved without much structural deformation (Esteban and Giner, 1980; Franseen and Mankiewicz, 1991; Franseen *et al.*, 1993). Late Messinian (uppermost Miocene) to recent uplift of < .05 mm/yr slowed through time (Brachert *et al.,* 2001). The hypothesis for regional differential uplift of the entire Cabo de Gata volcanic province, with maximum uplift in the western areas since the late Miocene (Martin *et al*., 2003) is generally accepted. In the Agua Amarga basin area and southwest, localized tilting has been described by Hess (2011; 0.3˚ to the northeast). Removal of this tilt from the Agua

Amarga basin and Rellana and Ricardillo areas to the southwest allows for local reconstruction of paleotopography (Figure 2).

METHODOLOGY

The Rellana platform was described using measured stratigraphic sections, 430 hand samples and 75 thin sections to describe facies, identify their distribution and to develop a quantitative relative sea-level history for the platform. Physical tracing into equivalent deposits in the Ricardillo area (Toomey, 2003) and the Terminal Carbonate Complex (TCC) deposits of the Rellana/Ricardillo area (Lipinski, 2010) provided more data to further constrain relative sea-level history and clarify development of the platform. Where physical lateral tracing was not possible, photomosaics were used to assist. Descriptions of the Agua Amarga basinal deposits are used in this study as the primary source for stratigraphic and lithologic data from the Agua Amarga basin (Dvoretsky *et al.,* 2008; Dvoretsky *et al.,* 2009; Goldstein *et al.,* 2012; Dvoretsky *et al.,* 2013).

Where physical tracing was impossible because of local pinchout, post depositional erosion, or poor exposure; units were correlated using relative sea-level curves generated for each area, including the quantitative curve developed for the neighboring Las Negras area (Franseen *et al.,* 1993; Goldstein and Franseen, 1995; Franseen *et al.,* 1998; Fig. 4). Each relative sea-level curve was constrained with *pinning points*, points of quantitative constraint on position of sea level relative to a geologically relevant datum (Goldstein and Franseen, 1995). Modern sea level was used as the datum in this study. Examples of identified pinning points include facies that formed at or near sea level (e.g. *in situ* coral framestone), and subaerial exposure surfaces

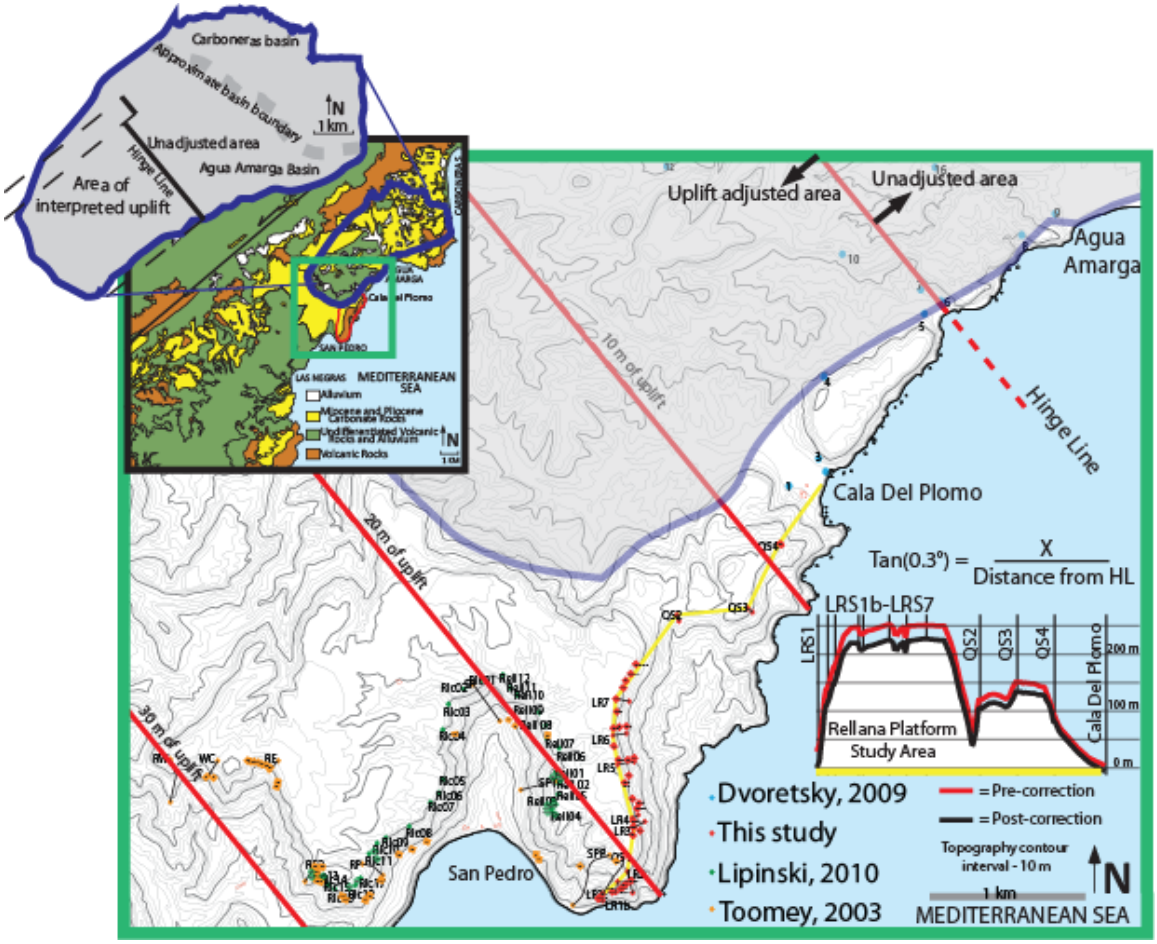

Figure 2: Topographic map of the study area showing application of tilt model from Hess (2011). Blue polygon reflects study area in which Hess (2011) identified and described the hinge line feature. Extrapolation of the hinge line to the southeast and 0.3˚ tilting trend to the southwest is reflected by contoured overlay (red parallel lines). Even uplift parallel to the hinge line is assumed. To calculate tilt influence on relative sea-level reconstruction, tilt adjustments are calculated for each pinning point (data point that provides constraint on relative sea level through time). The location of each stratigraphic section and pinning point are marked on this map, color-coded to related literature. The schematic model in the lower right shows the variation between unadjusted elevations for stratigraphic section tops (red line) versus the adjusted values (black line) along a transect perpendicular to the platform margin (denoted by yellow line).

developed on marine facies. The pinning point method requires that paleotopography either be preserved or reconstructed. Back-calculation of original elevations following the tilt model proposed of Hess (2011) results in uplift reductions as much as 29.8 m in the Ricardillo Peak area (Fig. 2). This model assumes linear extrapolation of the hinge line defined by Hess (2011).

Once paleotopography is reconstructed, elevations serve as effective proxies for Miocene relative elevations. Pinning point locations on the Rellana Platform are identified in Figure 3, the resulting curve in Figure 4. Detailed description of pinning points on the Rellana Platform can be found in Chapter 2. The pinning points prepared for the study areas were compared with the quantitative pinning point curve that has been developed for the neighboring Las Negras area. By comparing these curves it is possible to construct a pinning point curve that represents minimal sea-level fluctuations necessary to generate the stratigraphic character that is observed in these deposits.

Paleotopography

The Rellana platform features a drainage divide that separates a steeply south-dipping (~20°) slope from a shallow north-dipping (~5°) slope that extends for 1.3 km before distally steepening into a steep dipping (~25°) slope that extends from 150 m down to modern sea level. At Cala del Plomo, the basin margin measures 23° forming a steep-sided paleovalley that extends 3,900 m inland along the toe-of-slope of the Rellana platform. This paleovalley is 850 m wide and dips approximately 1.2° to the east-northeast; it acted as a funneling mechanism for material sourced from the Rellana platform. A more in-depth discussion of the paleotopography of the Agua Amarga basin and its influence on basin sediment distribution can be found in Goldstein *et al.,* (2012). The intermediate paleotopographic high separating the Rellana platform

from the Agua Amarga basinal deposits along the coastal exposure reaches a maximum elevation of 150 m, roughly equivalent to the elevation of the basin margin. Carbonate deposits capping this feature show dipping trends that radiate from the peak, indicating it was a separate paleo-high from the Rellana platform, the extent of which is unknown due to the limit of modern exposures.

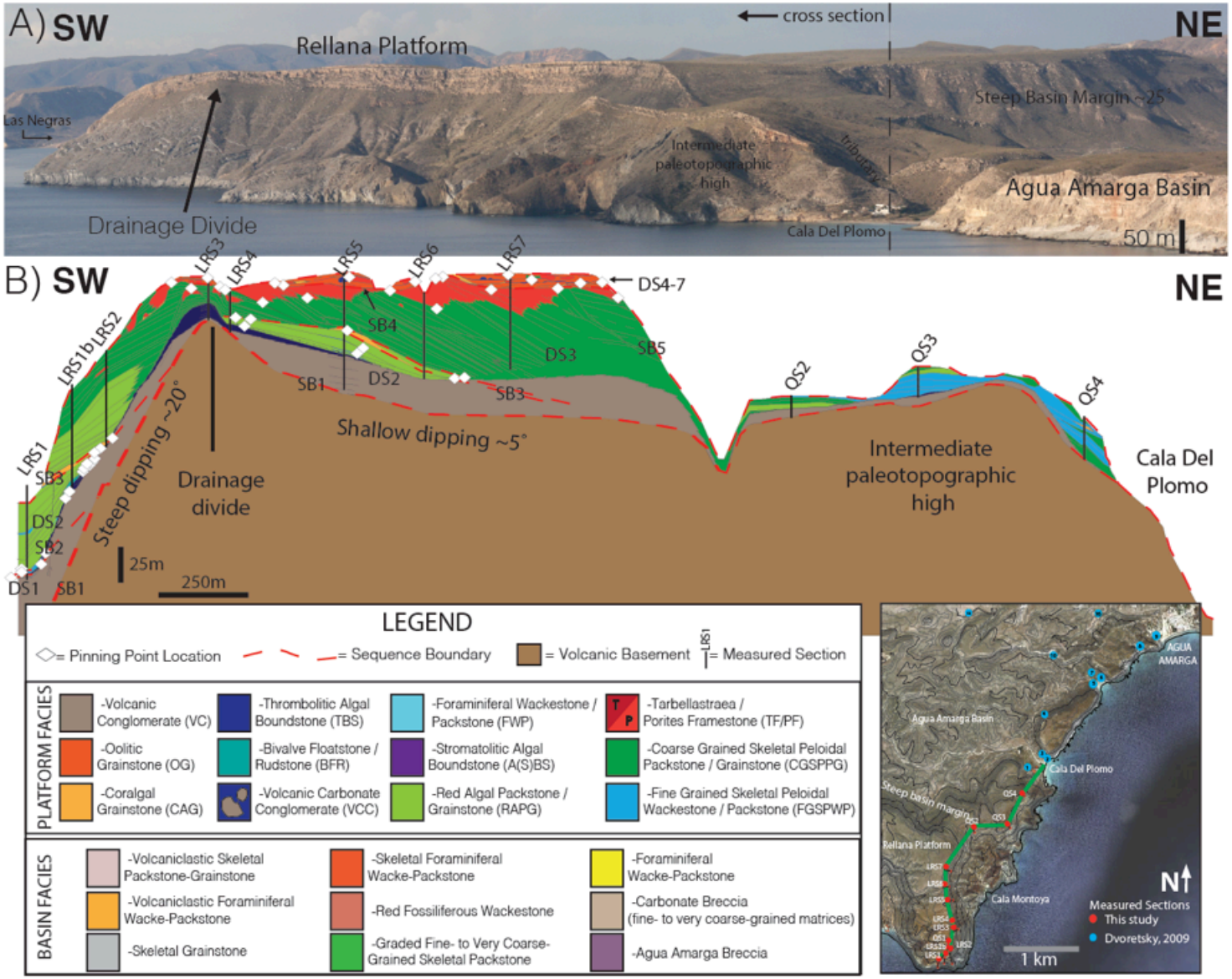
A) SW
NE
cross section
Rellana Platform
Las Negras
Steep Basin Margin ~25
Intermediate paleotopographic high
Tributary
Agua Amarga Basin
Drainage Divide
Cala Del Plomo
50 m
B) SW
NE
LRS1
LRS1b
LRS2
LRS3
LRS4
LRS5
LRS6
LRS7
DS4-7
SB1
SB2
SB3
SB4
SB5
DS1
DS2
DS3
Steep dipping ~20°
Shallow dipping ~5°
Drainage divide
25m
250m
QS2
QS3
QS4
Intermediate paleotopographic high
Cala Del Plomo
LEGEND
= Pinning Point Location
= Sequence Boundary
= Volcanic Basement
= Measured Section
PLATFORM FACIES
-Volcanic Conglomerate (VC)
-Thrombolitic Algal Boundstone (TBS)
-Foraminiferal Wackestone / Packstone (FWP)
-Tarbellastraea / Porites Framestone (TF/PF)
-Oolitic Grainstone (OG)
-Bivalve Floatstone / Rudstone (BFR)
-Stromatolitic Algal Boundstone (A(S)BS)
-Coarse Grained Skeletal Peloidal Packstone / Grainstone (CGSPPG)
-Coralgal Grainstone (CAG)
-Volcanic Carbonate Conglomerate (VCC)
-Red Algal Packstone / Grainstone (RAPG)
-Fine Grained Skeletal Peloidal Wackestone / Packstone (FGSPWP)
BASIN FACIES
-Volcaniclastic Skeletal Packstone-Grainstone
-Skeletal Foraminiferal Wacke-Packstone
-Foraminiferal Wacke-Packstone
-Volcaniclastic Foraminiferal Wacke-Packstone
-Red Fossiliferous Wackestone
-Carbonate Breccia (fine- to very coarse-grained matrices)
-Skeletal Grainstone
-Graded Fine- to Very Coarse-Grained Skeletal Packstone
-Agua Amarga Breccia
AGUA AMARGA
Agua Amarga Basin
Cala Del Plomo
Steep basin margin
Rellana Platform
Cala Montoya
N
Measured Sections
This study
Dvoretsky, 2009
1 km

Figure 3: Exposure of the Rellana platform and toe-of-slope basin deposits in Agua Amarga (Fig. 3 continued). A) Photomosaic of the east facing exposure of the Rellana Platform. Carbonate reef-rich deposits generally form resistant deposits on the top of the volcanic deposits. B) Cross section through the Rellana platform showing relative location of measured sections (LRS1-QS4 and AA 2, 5, 6, 8, 9 (Dvoretsky, 2009), Depositional Sequences (DS1-DS7), Basin unit designations (Dvoretsky, 2009) Sequence Boundaries (SB1-5) and lithofacies (color coded) (Table 1, 2). Due to abundant cover, SB1a and amalgamated sequence boundaries updip are picked at a significant break in slope. Vertical exaggeration of cross section is 4 X. Inset satellite image shows relative location of cross section (green line) and measured sections from this study (red dots, platform) and Dvoretsky (2009, basin, blue dots).

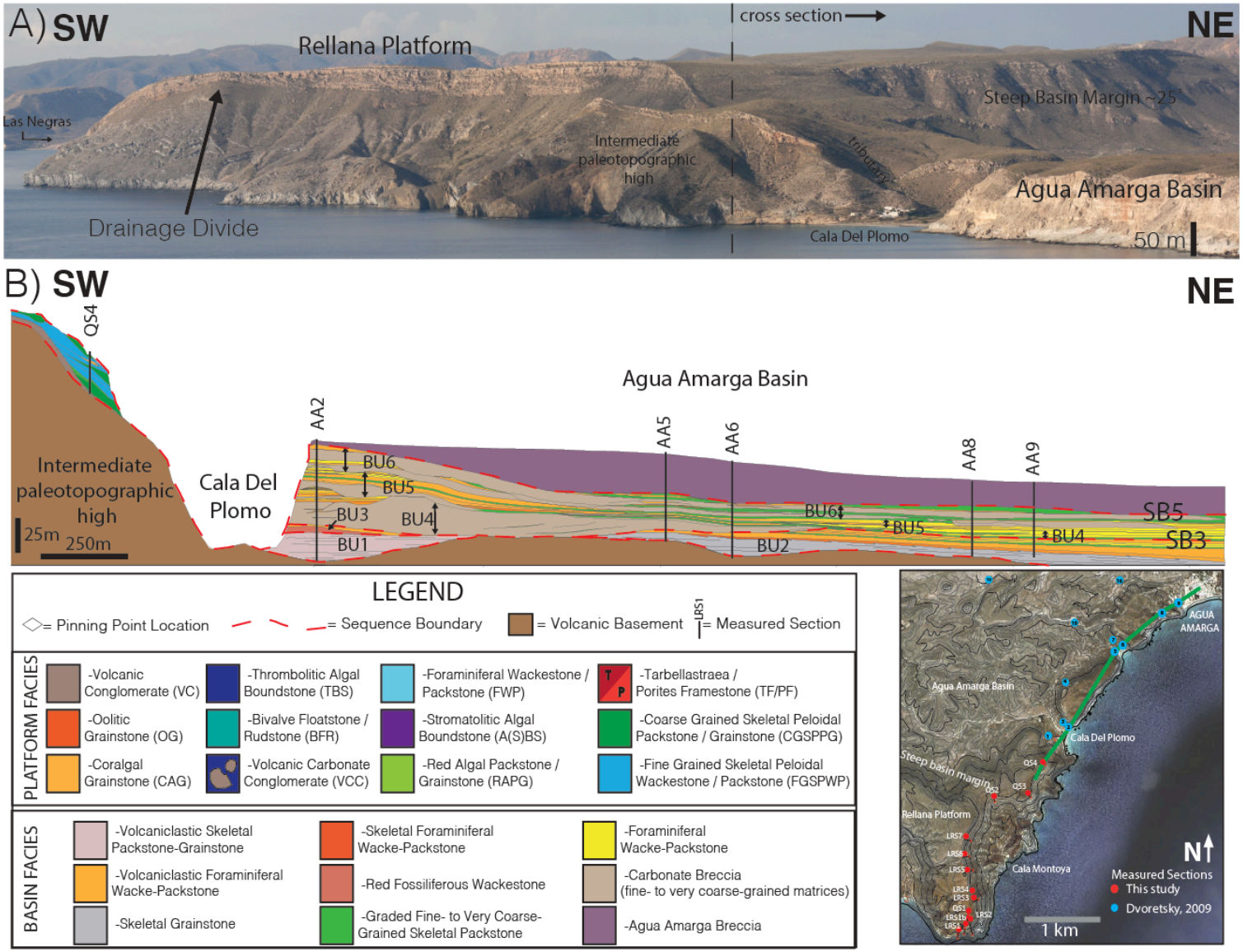
A) SW
NE
Rellana Platform
cross section
Las Negras
Steep Basin Margin ~25
Intermediate paleotopographic high
tributary
Drainage Divide
Agua Amarga Basin
Cala Del Plomo
50 m
B) SW
NE
QS4
Agua Amarga Basin
AA2
AA5
AA6
AA8
AA9
Intermediate paleotopographic high
Cala Del Plomo
BU6
BU5
BU3
BU4
BU1
BU2
SB5
SB3
25m
250m
LEGEND
= Pinning Point Location
= Sequence Boundary
= Volcanic Basement
LRS1 = Measured Section
PLATFORM FACIES
-Volcanic Conglomerate (VC)
-Thrombolitic Algal Boundstone (TBS)
-Foraminiferal Wackestone / Packstone (FWP)
-Tarbellastraea / Porites Framestone (TF/PF)
-Oolitic Grainstone (OG)
-Bivalve Floatstone / Rudstone (BFR)
-Stromatolitic Algal Boundstone (A(S)BS)
-Coarse Grained Skeletal Peloidal Packstone / Grainstone (CGSPPG)
-Coralgal Grainstone (CAG)
-Volcanic Carbonate Conglomerate (VCC)
-Red Algal Packstone / Grainstone (RAPG)
-Fine Grained Skeletal Peloidal Wackestone / Packstone (FGSPWP)
BASIN FACIES
-Volcaniclastic Skeletal Packstone-Grainstone
-Skeletal Foraminiferal Wacke-Packstone
-Foraminiferal Wacke-Packstone
-Volcaniclastic Foraminiferal Wacke-Packstone
-Red Fossiliferous Wackestone
-Carbonate Breccia (fine- to very coarse-grained matrices)
-Skeletal Grainstone
-Graded Fine- to Very Coarse-Grained Skeletal Packstone
-Agua Amarga Breccia
AGUA AMARGA
Agua Amarga Basin
Cala Del Plomo
Steep basin margin
Rellana Platform
Cala Montoya
N
Measured Sections
This study
Dvoretsky, 2009
1 km

Figure 3 (continued): Exposure of the Rellana platform and toe-of-slope basin deposits in Agua Amarga. A) Photomosaic of the east facing exposure of the Rellana Platform. Carbonate reef-rich deposits generally form resistant deposits on the top of the volcanic deposits. B) Cross section through the distal Rellana platform and Agua Amarga basin showing relative location of measured sections (LRS1-QS4 and AA 2, 5, 6, 8, 9 (Dvoretsky, 2009), Depositional Sequences (DS1-DS7), Basin unit designations (Dvoretsky, 2009) Sequence Boundaries (SB1-5) and lithofacies (color coded) (Table 1, 2). Due to abundant cover, SB1a and amalgamated sequence boundaries updip are picked at a significant break in slope. Vertical exaggeration of cross section is 4 X. Inset satellite image shows relative location of cross section (green line) and measured sections from this study (red dots, platform) and Dvoretsky (2009, basin, blue dots).

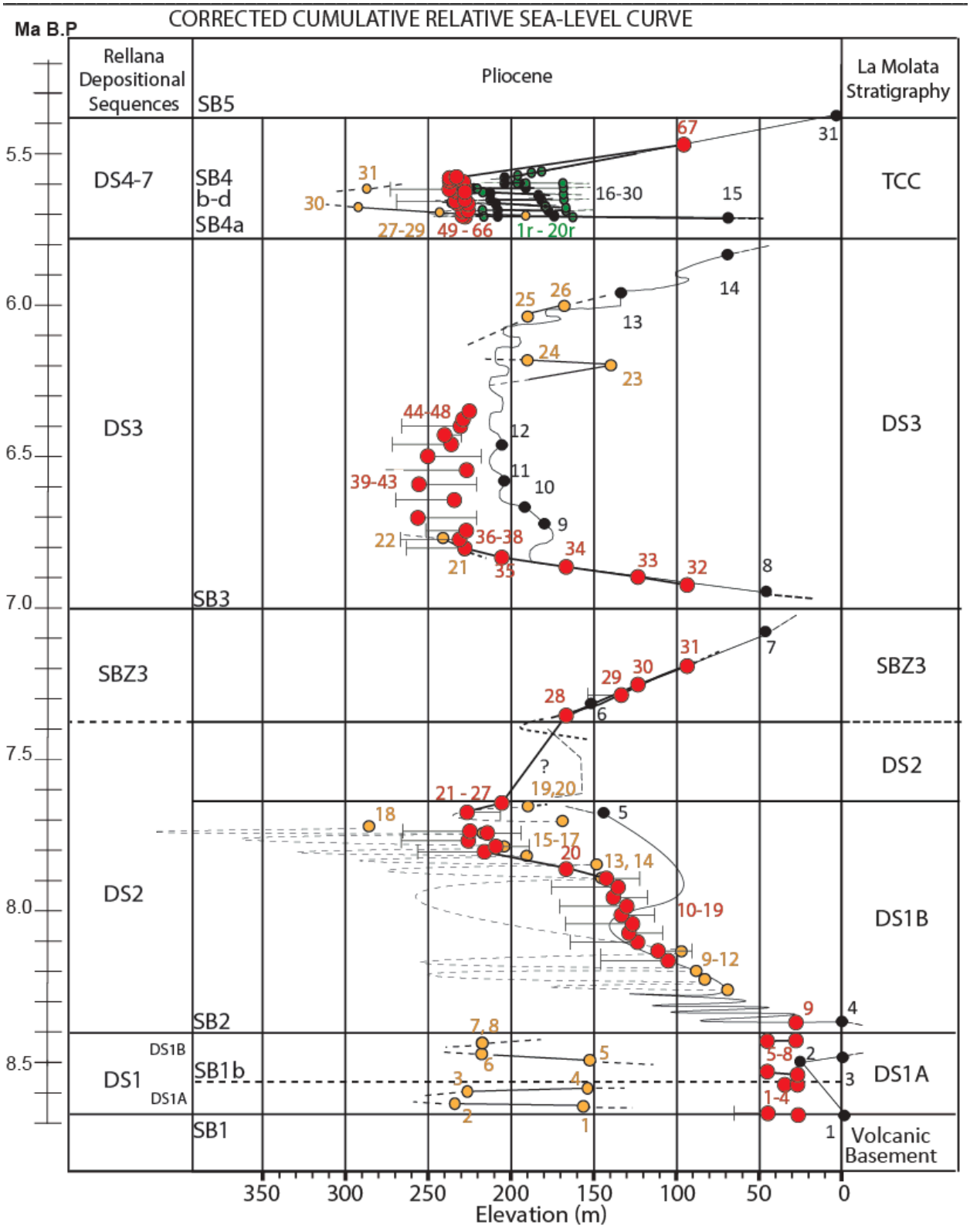
CORRECTED CUMULATIVE RELATIVE SEA-LEVEL CURVE
Ma B.P
Rellana Depositional Sequences
Pliocene
La Molata Stratigraphy
SB5
DS4-7
SB4 b-d SB4a
TCC
DS3
SB3
SBZ3
DS2
DS1B
DS1
DS1A
SB2
SB1b
SB1
Volcanic Basement
5.5
6.0
6.5
7.0
7.5
8.0
8.5
350
300
250
200
150
100
50
0
Elevation (m)
16-30
27-29
49 - 66
1r - 20r
44-48
39-43
36-38
21 - 27
19,20
15-17
13, 14
10-19
9-12
7, 8
5-8
1-4

Figure 4: Cumulative relative sea level curve combining uplift-adjusted data from Ricardillo Peak (orange dots; Toomey, 2003), Rellana Platform (red dots; this study), Ricardillo/Rellana TCC (green dots; Lipinski, 2010) and Las Negras (black dots; Franseen *et al.*, 1998). Age constraints are specific to Las Negras curve, other data points were placed on the curve based on correlation and comparison of depositional sequence interpretations made in this study and those studies related to the aforementioned field areas. Therefore, for all data points other than those identified by Franseen *et al.,* (1998) (black dots), age is approximate.

LITHOFACIES AND DEPOSITIONAL ENVIRONMENTS

The 13 facies observed on the Rellana platform are defined by grain composition, degree of abrasion, sorting and size. Facies for the Rellana platform area were defined using hand sample descriptions (Appendix 2) and refined through thin section analysis (Appendix 3), characteristics of the facies are summarized in Table 1. Components are listed in decreasing abundance as observed in hand samples and corroborated by thin section analysis. Grain size is described using the Wentworth size class, and no distinction is made between grains less than 0.0625 mm, all grains this size or below are collectively termed 'mud'. Sorting is defined through qualitative analysis of variability of allochem size and distribution. Porosity is determined through visual estimates of pore space in thin-section, emphasized through impregnation with blue epoxy.

The facies identified on the Rellana Platform are grouped into 7 depositional sequences (Figure 3). DS1a and DS1b deposits are restricted to the southern end of the Rellana platform; below 66 m. DS2 is present on both the northern and southern slopes, but features thicker deposits on the southern end of the platform, up to 78 m thick. DS3 deposits form the bulk of preserved carbonate sediments on the Rellana pattern and are found throughout the platform area, effectively reshaping paleotopography through reef development. DS4-7 are preserved at the top of the platform deposits and are laterally distributed throughout the platform area, ranging in thickness from 0 to 10 m. Depositional environment interpretations for the 13 lithofacies are discussed in detail in Chapter 2 and summarized in Table 1. Lithofacies of the Agua Amarga Basin are described in detail by Dvoretsky (2009); her Basin Unit (BU) definitions are used herein (Table 2).

Facies	Components	Grain size / sorting	Sedimentary Structures	Porosity	Depositional Environment
VC Volcanic Conglomerate	Volcanic clasts, bivalves (disarticulated and fragmented), bryozoan fragments, red algal fragments, peloids	Mud to boulder Average (avg.): Cobble Poorly sorted	Centimeter (cm)-scale trough cross bedding, 3 cm scale planar bedding, gradationally fining bedding, meter (m)-scale bedding,	< 5 - 5%- FR, WP	Poorly constrained; Shallow marine, near shore deposition to subaerially exposed
VCC Volcanic Conglomerate with Carbonate Matrix	Volcanic clasts, bivalves (disarticulated, fragmented), foraminifera (and fragments), red algal fragments, intraclasts (CGSPG, FGSWP, FWP, BFR), Coral fragments (P, T), peloids and unknown skeletal components	Mud to boulder Avg.: Cobble Poorly sorted	None visible	< 5% - 15% - MO, BP, BC, WP	Normal marine debris flows - minimum water depth range for deposition is > 10 - 30 m
FR Bivalve-rich Floatstone- – Rudstone	Bivalves (whole, disarticulated), peloids, gastropods, foraminifera, ostracods, red algae, echinoderm fragments, serpulid worms, coral fragments	Mud to Cobble Avg.: coarse sand Poor to moderate (mod.) sorting	Large bivalve clasts preferentially oriented roughly horizontally, concave orientation variable.	10% - 25%, MO, VUG, FE, WP, BP SH	Isognomon-dominated BFR-Shallow water (<~30m) or deeper Pectin-dominated BFR-20-60 m
FGSWP Fine-Grained Skeletal Wackestone -– Packstone	Peloids, bivalves (disarticulated and fragmented), bryozoans, gastropods, red algal fragments, serpulid fragments, foraminifera, ostracods, echinoderm fragments	Mud to very (v.) coarse sand Avg.: Medium sand Poor to mod. sorting	Massive beds (12 cm - 1.5 m), local thin bedding and laminations (.5 - 3 cm), local thin cross bedding (3 - 5 cm)	5% - 50%, average 10% - MO, BP, WP, FR, FE (rare)	High energy (e) occurrences - 10 -30 m water depth Low e occurrences - 20 - 50 m minimum depth
CGSPG Coarse-Grained Skeletal Packstone- – Grainstone	Bivalves (whole, disarticulated, fragmented), gastropods, serpulid worms, peloids, foraminifera, ostracods, echinoderm fragments, red algal fragments, coral fragments, intraclasts, Bryozoan fragments, coated grains, volcanic clasts	Mud to Pebble Avg.: v. coarse sand Mod. to well sorted	Massive beds (up to 5 m), Planar beds (3 - 5 cm) Laminated to thick (up to 3 m) low angle (<20˚) cross bedding, thin (1 -3 cm) trough cross bedding	10% - 40% average 20 - 25% - MO, BP, WP, VUG, FR, SH	High e occurrences - > 10 - 15 m estimated water depth range. Low e occurrences - forereef slope, 10 - 75+ m interpreted water depth
FWP Foraminiferal Wackestone -– Packstone	Peloids, foraminifera, serpulid worm fragments, bivalves, red algal fragments, gastropods and ostracods	Mud to v. coarse sand Avg.: lower medium/upper fine sand Mod. sorting	Thick (up to 2 m) and dm scale massive beds, thin (1 - 3 cm) planar bedding	< 5% - 40% average 5% - 10% MO, WP, BP, rare VUG	Hemipelagic - pelagic deposition - Deep marine environment, specific depth ranges unknown
RAPG Red Algal Packstone- – Grainstone	Red algae, bivalves, peloids, bryozoan fragments, foraminifera, echinoderm fragments, rare coral fragments, volcanic clasts, gastropods, ostracods	Mud to Cobble Avg.: Coarse to v. coarse sand mod. to poor sorting	Dm scale fining up beds, thick (1 - 4 m) gradationally fining beds, low angle (~10˚ - 20˚) cross beds (.25 - 1.5 m) and thick (1 - 4 m) massive beds.	10% - 40%, average ~20% - MO, BP, SH, FR, rare VUG	Normal marine sedimentation, potential depth range of 30-140 m

Table 1: Descriptive characteristics of the 13 lithofacies identified in this study. Abbreviations used for porosity types are; fracture (FR), intraparticle (WP), moldic (MO), Interparticle (BP), intercrystal (BC), vuggy (VUG), fenestral (FE), shelter (SH) after Choquette and Pray (1970).

Facies	Components	Grain size / sorting	Sedimentary Structures	Porosity	Depositional Environment
CAG Coralgal Grainstone	Coral fragments, serpulid worm fragments, gastropods, bivalves, ostracods, echinoderm fragments, coralline algae, intraclasts, bryozoan fragments, coated grains, volcanic clasts, peloids, foraminifera, unidentifiable skeletal grains	Mud to pebble Avg.: v. coarse sand - gravel Very well to poor sorting	Thick (10 cm to 2 m) massive beds, thin (2 - 5 cm) and thick (5 - 10 cm) trough cross beds.	5% - 50% - MO, BP, BC, WC	High e depositional environment – deposition in <~10 m water depth likely though not definitive
TF *Tarbellastraea* Framestone	Coral (*Tarbellastraea*) molds, bivalves, serpulid worm fragments, peloids, foraminifera, gastropods, ostracods, echinoderm fragments, coralline algal fragments, intraclasts bryozoan fragments, coated grains, volcanic clasts	Mud to cobble/boulder Poor sorting	Massive, topographic relief generating structures	~15%, MO/CH, MO, WP, BP, rare VUG	*In-situ* growth implies water depths between 10 m (head growth forms) - 30 m (branching / stick growth forms)
PF *Porites* Framestone	Coral (*Porites*), bivalves, serpulid worm fragments, peloids, foraminifera, gastropods, ostracods, echinoderm fragments, coralline algal fragments, intraclasts, bryozoan fragments, coated grains, volcanic clasts	Mud to cobble/boulder Poor sorting	Massive, topographic relief generating structures	~15%, MO/CH, MO, WP, BP, rare VUG	*In-situ* implies water depths between 5 - 40 m (branching / stick growth forms) and < 10 m (massive / encrusting growth forms)
ASBS Stromatolitic Boundstone	Peloids, foraminifera, gastropods, ooids (and other coated grains)	Mud to pebble, Clasts avg.: coarse sand, Sample avg.: Mud to v. fine sand Poor sorting	Algal laminations, Laterally linked hemispheroids, stacked hemispheroids	5% - MO, BP, FE, VUG	Normal marine to slightly restricted - low e < 10 m
TBS Thrombolitic Boundstone	Peloids, foraminifera, red algal fragments, gastropods, serpulid worms, coated grains, coral fragments	Mud to Pebble Avg. mud to medium sand Poor to well sorted	Topographic relief building (up to 3 m)	5 - 10% - MO, BP, MO, VUG	High-energy, shallow, near shore deposition likely > 10 - 10 m
OG Oolitic Grainstone	Ooids, coral fragments, bivalves, gastropods, bryozoans, foraminifera, volcanic clasts	Fine sand to pebble Avg.: Upper coarse sand Well - v. well sorted	Thick (5-10 cm) planar cross beds, dm scale trough cross-beds	10% - 40% - average ~20%, MO, BP, WP, FR	High e, shallow marine (< 10 m)

Table 1 continued: Descriptive characteristics of the 13 lithofacies identified in this study. Abbreviations used for porosity types are; fracture (FR), intraparticle (WP), moldic (MO), Interparticle (BP), intercrystal (BC), vuggy (VUG), fenestral (FE), shelter (SH) after Choquette and Pray (1970).

Facies	Components	Grain size	Sedimentary Structures	Carbonate Mud (relative abundance)	Depositional Environment
Volcaniclastic skeletal packstone-grainstone (Basin Unit 1)	Bryozoans; echinoids; red algae; mollusks; solitary corals; benthic forams; planktonic forams; volcanic grains	5-10 mm	Trough cross beds; low-angle planar beds; *Skolithos* burros	Very Low	Shallow-subtidal sedimentation
Red fossiliferous wackestone (pre-basin Unit 2 interval)	Solitary corals; octacorals; hydrozoans; gastropods; mollusks; bryozoans; echinoids; red algae; serpulid worms; small & large benthic forams; planktonic forams; volcanic pebbles to boulders	Whole: 2 – 4 cm Fragments: 0.5 – 2 mm	Massive beds; fissure-fill	High	Deeper water sedimentation
Skeletal grainstone (Basin Unit 2)	Bryozoans; red algae; echinoids' mollusks; benthic forams; solitary corals; planktonic forams	5 – 10 mm	Trough cross beds, low-angle planar beds	n/a	Shallow-subtidal sedimentation
Foraminiferal wacke-packstone	Planktonic forams; diatoms; sponge spicules; echinoid spines; whole pectin & echinoid shells; fish-scales & vertebrae	0.2 – 0.5 mm	Massive beds with *Zoophycus* burrows, fissile laminated bed	High	Pelagic-hemipelagic sedimentation
Volcaniclastic foraminiferal wacke-packstone	Planktonic forams; sponge spicules; echinoid spines; volcanic grains	0.2 – 1 mm	Massive beds; normally graded beds (subtle)	High	Pelagic-hemipelagic sedimentation or low-density turbidity currents
Skeletal foraminiferal wacke-packstone	Planktonic forams; echinoid spines & plates; mollusks	0.5 – 2 mm	Normally graded beds (subtle); basal scouring (minor)	Medium	Low-density turbidity currents
Graded fine- to very coarse-grained skeletal packstone	Mollusks; red algae; bryozoans; echinoids; benthic forams; serpulid worms; gastropods; planktonic forams; *Porites* (rare); *Tarbellastraea* (rare)	Fn-med: 1 – 3 mm Coarse (crs): 3 – 5 mm v. crs: >5 mm	Normally graded beds; basal scouring; mm- to cm scale foraminifera rich WS/PS (rare)	Low	High-density turbidity currents
Carbonate breccia (fine- to very coarse grained matrices)	Mollusks; red algae; rhodoliths; gastropods; serpulid worms; echinoids; benthic forams; planktonic forams; *Halemida*; *Porites*; *Tarbellastraea*	Fn: 2 – 4 mm Med: 4 – 6 mm Crs-v.crs:> 6 mm	Massive & chaotic beds; internal & basal scouring; flame & fold structures; m-scale clasts	Low – Medium	Debris flows

Table 2: Classification of Agua Amarga Basin lithofacies, from Dvoretsky, 2009. Units described above correlate to Basin Units (BU 1-7) in this study.

PLATFORM PROCESSES AND BASIN EQUIVALENTS

The following section summarizes data on location of the reefal margin in relation to the paleotopography (Fig. 3), data on sea level (Fig. 4) and proposes correlations to the basinal equivalents. Each time interval (T#) is documented diagrammatically with a corresponding image in Figure 5, reflecting the position of the reefal platform and interpreted time-equivalent process in the basin. Due to unknown total displacement (5 m minimum) of earliest deposits preserved on the platform and in the basin (DS1, BU1, pre-BU2), no paleotopographic or relative sea-level history reconstruction is applied to compare platform versus basin development for this time.

The results show that the interplay between relative sea level and paleotopography plays a crucial role in the (re)distribution of sediment from platform to basin. The distance between the steep (~25°) basin margin and the reefal margin is hypothesized to influence the type and abundance of sediment that is deposited in the basin. This distance is controlled by migration of the reefal margin as sea level changes or as the platform progrades during stillstand. A comparison between the position of the reefal margin and lateral extent of time-equivalent debrites is compiled in Table 3.

T-1

Initial basinal deposits (BU2, Dvoretsky, 2009) are interpreted to reflect shallow water deposition (Fig. 5) and are found at an elevation of 20 m. This elevation restricted marine deposition to topographic lows in the Agua Amarga area and corresponds to subaerial exposure of the volcanic basement of the platform area.

T-2

Subsequent relative sea-level rise up to 203m on the Rellana platform, (Rellana Platform pinning point 26, ReP26) and 218 m on Ricardillo Peak (Ricardillo Peak pinning point 18, RiP18) results in inundation of the platform and deposition of DS2 up to 1.3 km from the basin margin (Fig. 5, T2). The fining-upward cycles identified in DS2 consist of RAPG deposits that onlap volcanic basement and grade up into well-sorted FGSWP, indicating shoaling-upward (Table 1, Toomey, 2003). North of the platform drainage divide, DS2 deposits are preserved overlying the shallow dipping slope. At the basin margin and below, there are no RAPG DS2 deposits preserved. Equivalent basinal deposits consist of pelagic/hemipelagic sediments, low-density turbidites and less common high-density turbidites. No inferences are made regarding the location of the DS2 depocenter relative to the basin margin due to the broad water depth range exhibited by heterozoan dominated carbonate deposits in this and other study areas.

T-3, 4

A subsequent relative fall in sea level results in the formation of a subaerial exposure surface on the Rellana platform. During this fall a laterally discontinuous package of detrital coral (TF and PF), CAG and CGSPG is deposited, and is subsequently overlain by a subaerial exposure surface traceable down to an elevation of 93 m (ReP31) on the southern slope of the Rellana Platform. In the basin, this relative fall in sea level is expressed as an erosion surface in proximal locations (Sequence Boundary 3; as described by Dvoretsky, 2009). The coralgal detrital deposits preserved on the southern slope of the Rellana platform are the first evidence of reef development on the platform. Contemporaneous detrital material is interpreted to have been trapped on the shallow-dipping slope of the northern platform. The 1.3 km of separation between the drainage divide (likely the best candidate for reef development as an energy focal

point) and the basin margin provides a likely catchment for this material, though it is not readily apparent, and may be intermixed with volcanic material (basal VCC) and largely covered. The lack of preserved clasts of TF and PF on the northern slope may be due to material being washed over the drainage divide due to the dominant swell direction coming from the NE, similar to the modern (Lionello and Sanna, 2005; Lipinski, 2009) Some sediment bypass to the north is reflected by high-density turbidites in BU3 (Dvoretsky, 2009), however no definitive correlation could be made between these turbidite units and coralgal-rich deposits on the platform.

T-5-9

A relative rise in sea level eventually results in inundation of the platform and reef margin development at the drainage divide (1.5 km from basin margin) (ReP35). This transgression correlates to the lowest of the DS3 equivalent deposits (BU4-7) in the basin. BU4 consists of carbonate breccia units, which are interpreted to be debrites (Dvoretsky, 2009; Goldstein *et al.*, 2012). These debrites are interpreted to be the remnants of reefs that developed on the steep slope of the basin margin during transgression (T-5, 7), and then transported as debrites (T-6, 8) that reached into the basin 3 km and 1.7 km respectively. Once relative sea level rose past the basin margin (~150 m) coarse material (CGSPG, CAG, reef core and fore-reef slope deposits) was stored on the shallow-dipping platform slope (T-9), and the basin was dominated by hemipelagic and low-density turbidite deposition.

T-9-14

Following reef aggradational development (T-9, RiP36), the reefal margin prograded to the north as it filled accommodation on the shallow-dipping slope (T-10-14), thereby reducing the distance between the reef margin and the basin margin. This progradation is reflected by

increasing occurrences of coral-rich, high-density turbidites followed by carbonate debrites in the basin (BU5, 6). Intermittent shedding events are expressed on the platform as surfaces that truncate reef-core and clinoforms (T-12, 13, 14), which are interpreted to correspond with low- and high-density turbidites and overlying debrites of BU5, and 6 in the basin. The increasing coarse grain content and progressive basin-ward stepping nature of the sediment-gravity flows reflects decreasing relative distance between the prograding reef margin and the basin margin.

T-15-18

Once the reefal margin reached the basin margin, there was a significant increase of coarse sediment in the basin (carbonate breccias and graded skeletal packstones of BU6). The distal extents of carbonate breccia subunits of BU6 identified by Dvoretsky (2009) progressively stepped basinward, reflecting downstepping of the reef. Though only one downstepping event is preserved on the Rellana platform (ReP48), up to three have been identified in neighboring basins (e.g. Franseen *et al.*, 1993) and multiple events are suggested by the presence of the debrite subunits within BU6 and BU7.

T-19, 20

Subsequent fall in sea level led to subaerial exposure of the platform and basin (T18). A relative sea-level rise resulted in deposition of the Terminal Carbonate Complex (TCC) (T19). The TCC on the Rellana platform consists of four sequences composed of microbial, coralgal, and oolitic facies. Distinct basinal equivalents are lacking, but presumed to consist of pelagic/hemipelagic facies (for more information see Chapter 2).

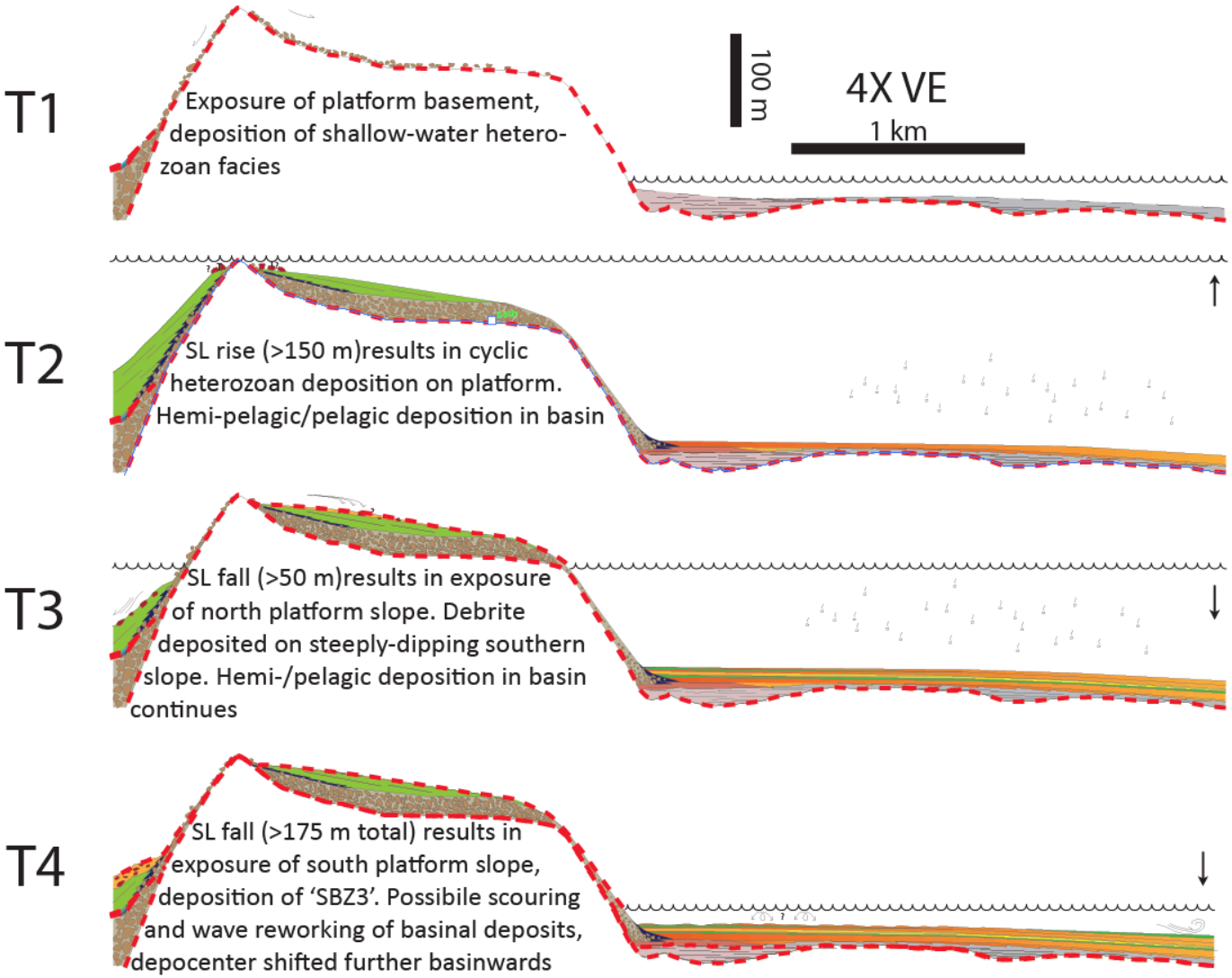
T1
Exposure of platform basement, deposition of shallow-water hetero-zoan facies
100 m
4X VE
1 km
T2
SL rise (>150 m)results in cyclic heterozoan deposition on platform. Hemi-pelagic/pelagic deposition in basin
T3
SL fall (>50 m)results in exposure of north platform slope. Debrite deposited on steeply-dipping southern slope. Hemi-/pelagic deposition in basin continues
T4
SL fall (>175 m total) results in exposure of south platform slope, deposition of 'SBZ3'. Possibile scouring and wave reworking of basinal deposits, depocenter shifted further basinwards

Figure 5: Simplified schematic cartoon showing development of Rellana platform and related basinal processes. T-1 through T-4 reflect deposition of the heterozoan-dominated carbonates and subsequent subaerial exposure of the platform. Scale is consistent throughout figure 5. SL = relative sea level, facies color scheme consistent with Fig. 3, 4x vertical exaggeration. The intermediate paleotopographic high was excluded from this schematic for clarity.

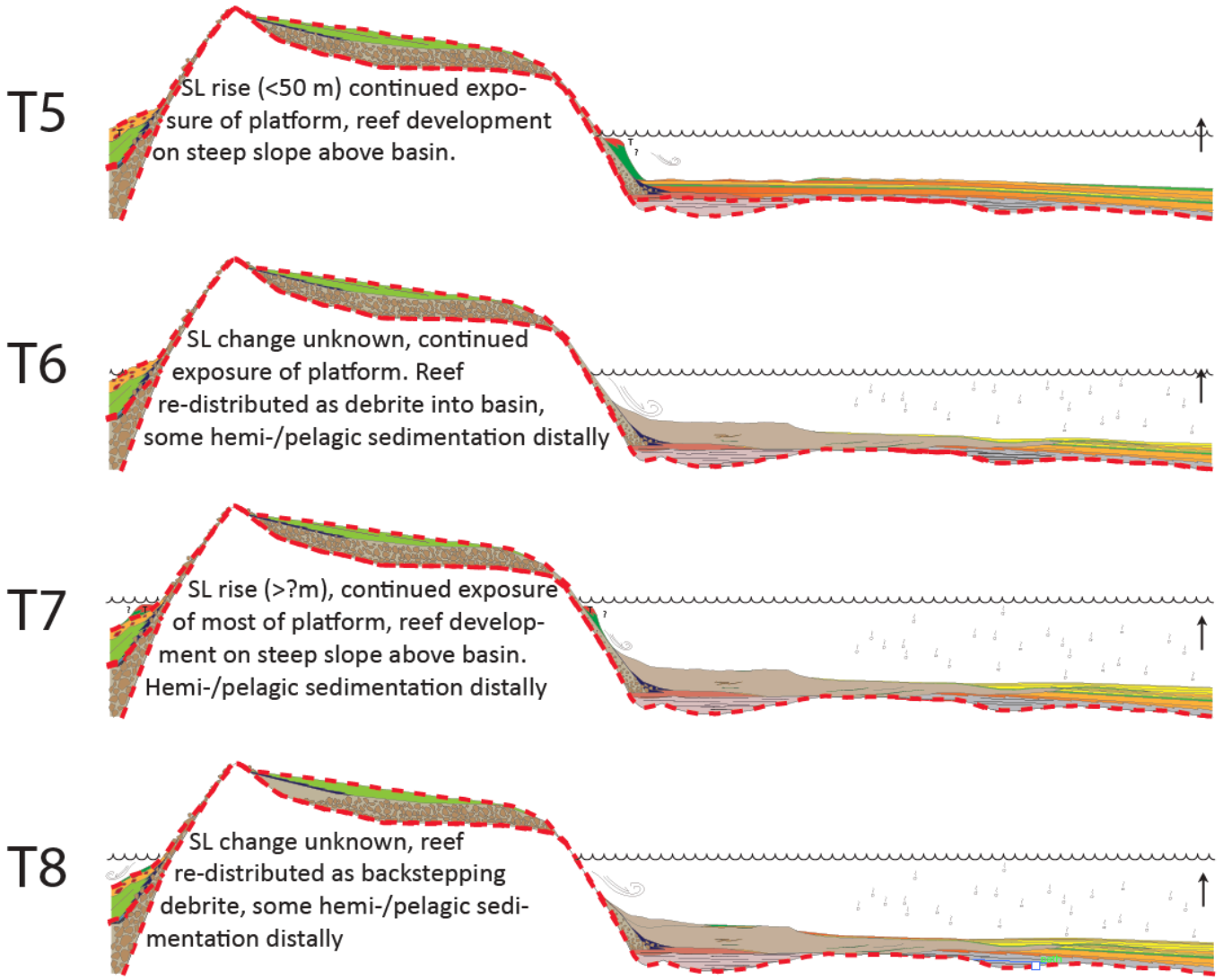
T5
SL rise (<50 m) continued exposure of platform, reef development on steep slope above basin.
T6
SL change unknown, continued exposure of platform. Reef re-distributed as debrite into basin, some hemi-/pelagic sedimentation distally
T7
SL rise (>?m), continued exposure of most of platform, reef development on steep slope above basin. Hemi-/pelagic sedimentation distally
T8
SL change unknown, reef re-distributed as backstepping debrite, some hemi-/pelagic sedimentation distally

Figure 5 (continued): Simplified schematic cartoon showing development of Rellana platform and related basinal deposits. T-5 through T-8 correspond to initial photozoan reef development, followed by backstepping of the reefal margin up the platform. and subsequent redistribution of reefal margins that grew on the steep substrate. Coarse material redistributed into the basin becomes less prevalent when the reef margin reaches the drainage divide (1.3 km from the basin margin).

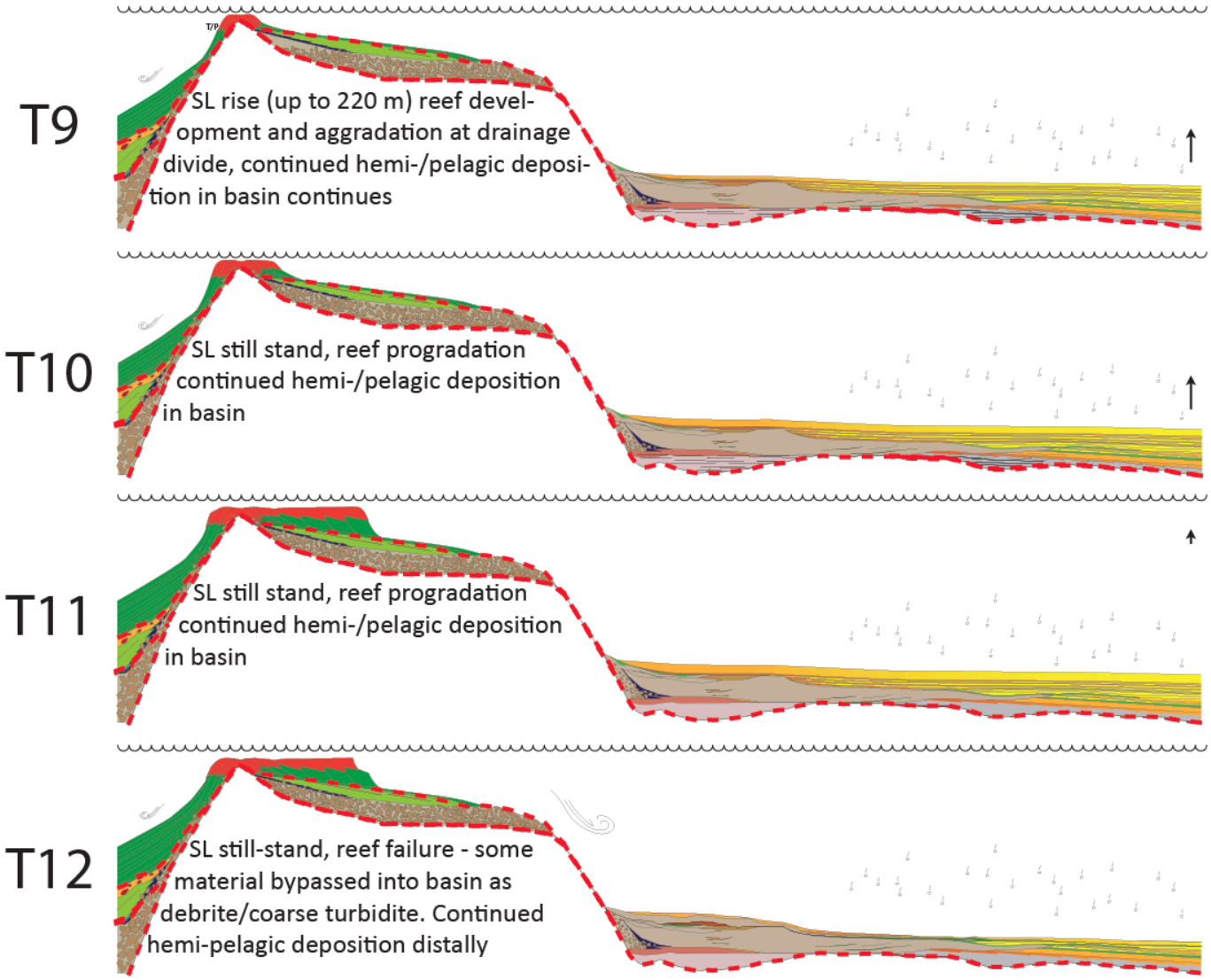
T9
SL rise (up to 220 m) reef development and aggradation at drainage divide, continued hemi-/pelagic deposition in basin continues
T10
SL still stand, reef progradation continued hemi-/pelagic deposition in basin
T11
SL still stand, reef progradation continued hemi-/pelagic deposition in basin
T12
SL still-stand, reef failure - some material bypassed into basin as debrite/coarse turbidite. Continued hemi-pelagic deposition distally

Figure 5 (continued): Simplified schematic cartoon showing development of Rellana platform and related basinal deposits. T-9 through T-12 shows inundation, reef aggradation and progradation across the shallow dipping north slope. This progradation is punctuated by several shedding events that are reflected in the basin as basinward-stacking coarse turbidites and debris flows, the first of which is seen in T12.

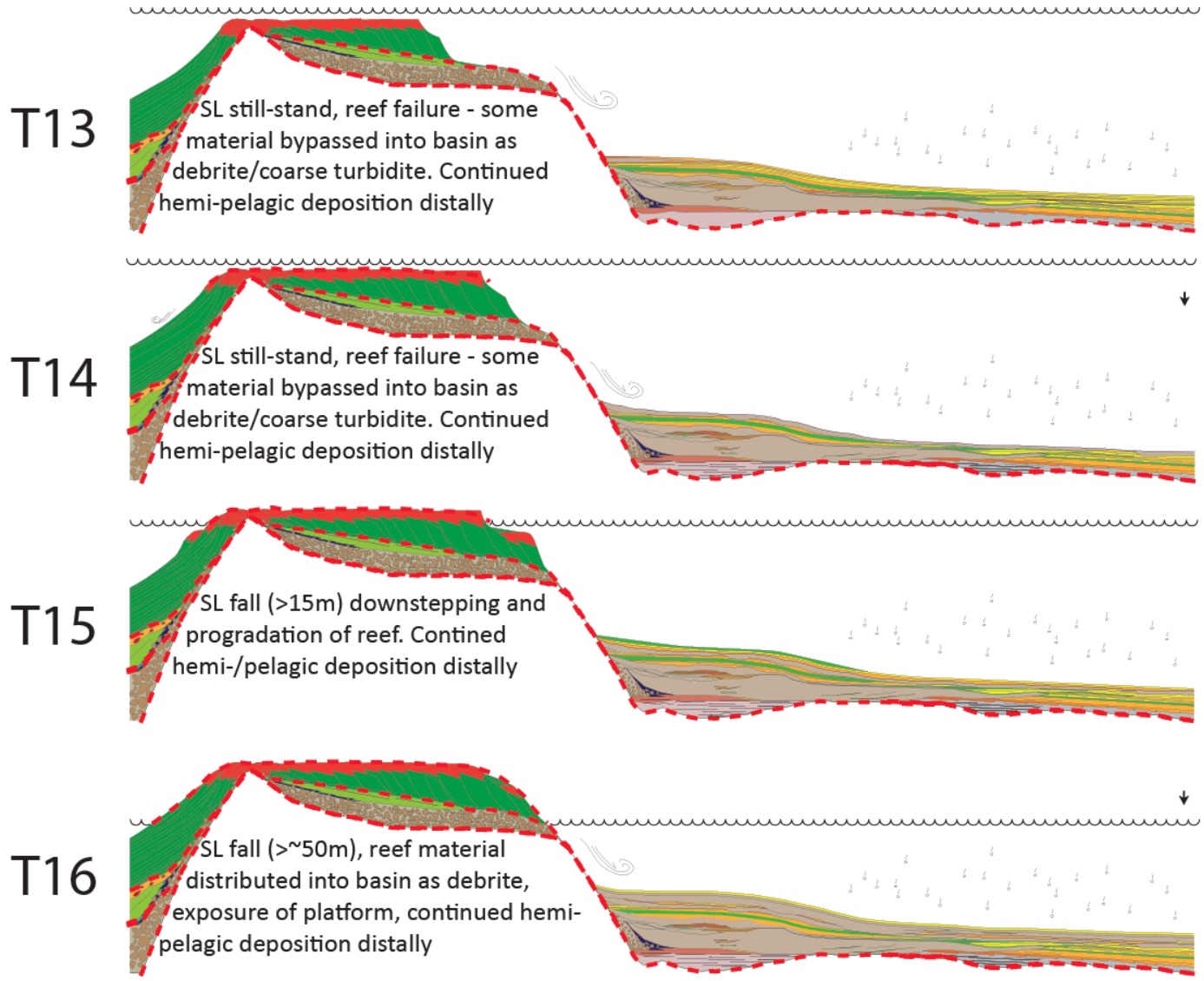
T13
SL still-stand, reef failure - some material bypassed into basin as debrite/coarse turbidite. Continued hemi-pelagic deposition distally
T14
SL still-stand, reef failure - some material bypassed into basin as debrite/coarse turbidite. Continued hemi-pelagic deposition distally
T15
SL fall (>15m) downstepping and progradation of reef. Contined hemi-/pelagic deposition distally
T16
SL fall (>~50m), reef material distributed into basin as debrite, exposure of platform, continued hemi-pelagic deposition distally

Figure 5 (continued): Simplified schematic cartoon showing development of Rellana platform and related basinal deposits. T-13 through T-26 shows progradation of the reefal platform punctuated by several shedding events that are reflected in the basin as basinward-stacking coarse turbidites and debris flows. Culminating in downstepping and subsequent subaerial exposure of the platform. These basinal deposits contain a higher concentration of coarse material as the reefal margin progrades closer to the basin margin.

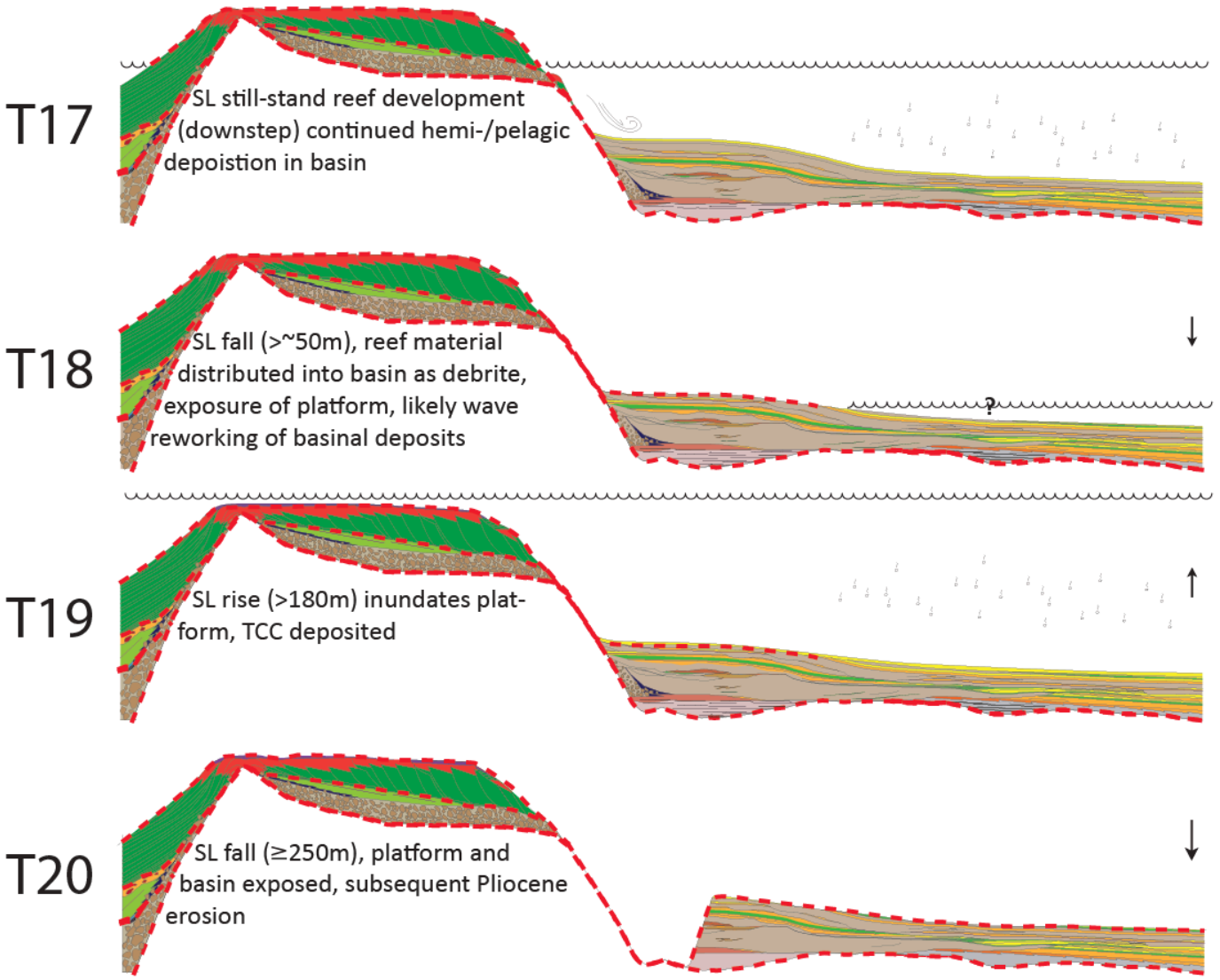
T17
SL still-stand reef development (downstep) continued hemi-/pelagic depoistion in basin
T18
SL fall (>~50m), reef material distributed into basin as debrite, exposure of platform, likely wave reworking of basinal deposits
?
T19
SL rise (>180m) inundates platform, TCC deposited
T20
SL fall (≥250m), platform and basin exposed, subsequent Pliocene erosion

Figure 5 (continued): Simplified schematic cartoon showing development of Rellana platform and related basinal deposits. T-17 through T-20 reflect a transition from high-stand progradation to episodic downstepping and progradation of the reefal platform. The proximity of the reefal and basin margin results in high volumes of coarse material reaching the basin. TCC deposition on the platform indicates a large rise in relative sea level and following drop resulting in modern subaerial exposure.

T-step	Reef to bypass	Slope height	Crest to Toe	Extent to Basin
T6	0	117	3085	3085
T6'	0	117	2060	2060
T8	0	132	1765	1767
T8'	1300	220	3065	1767
T12	860	245	3065	2205
T13	550	232	2891	2340
T14	325	242	3340	3016
T16	175	230	4520	4350
T18	80	195	4420	4350

Table 3: Measurement data of debrite unit extent into basin and interpreted correlative reef crest location. See figure 6 for location of reef crest and toe-of-debrite associated with each T step. T6' and T8' represent potential reef development on the intermediate paleotopographic high rather than the steep basin margin associated with the Rellana platform. All measurements in meters. Reef to bypass distance reflects proximity of reef margin development to the paleotopographically controlled break in slope separating the shallow north slope of the Rellana platform from the steeply dipping southern margin of the Agua Amarga Basin (bypass surface reference point in Fig. 6). Slope height measured from modern sea level and corrected for post-depositional uplift *sensu* Hess (2011). Crest to Toe distance reflects interpreted distance between the reefal margin and the most distal debrite that is considered to be time-equivalent. Extent to Basin reflects the distance between the steep southern margin of the Agua Amarga Basin and the most distal occurrence of debrite material interpreted for each time step.

DISCUSSION – CONTROLS ON PLATFORM SEDIMENT REDISTRIBUTION INTO THE BASIN

The development of a carbonate platform and basin system is intrinsically related to faunal variations, tendencies toward rim evolution in reef dominated systems, sediment type of the lithified margin and platform morphology (Playton *et al.,* 2011). It is proposed that deviations from traditional carbonate platform, slope and toe-of-slope models are a result of the antecedent topography of the Rellana platform; central to this topography is the shallow-dipping northern slope distally steepening into the basin margin.

Slope Angle Controls Sediment Bypass

Due to the high angle (~25°) of the basin margin, carbonate material generated in this area was redistributed into the basin. It is well documented that reefs can develop steeper profiles (up to 90°, e.g. Enos and Moore, 1983), and grain-supported facies with a mud matrix that lack a binding organism (e.g. RAPG or CGSPG) can accumulate on slopes of up to 30° in optimal conditions (Kenter, 1990). The friable nature of the volcanic substrate in this area likely facilitated failure along steep surfaces. In the neighboring Ricardillo area, bypass is interpreted on surfaces steeper than 17° for grain-dominated facies (Toomey, 2003). Bypass of sediment across steep surfaces was also described in the neighboring Las Negras area (Franseen and Goldstein, 1996; Franseen *et al.*, 1998). On the southern slope of the Rellana platform, DS2 and DS3 deposits show onlapping geometries on the ~20° paleoslope. Thus it is possible for grainy carbonate to accumulate on steep surfaces, especially with the additional support of coralgal binding. Accumulations on steep slopes are susceptible to subsequent transport downslope due

to any number of collapse triggers, including earthquakes, which are known to have occurred in the region (Nijar basin seismites, Fortuin and Dabrio, 2008).

Reef and Basin Margin Proximity Controls on Debrite Propagation

Submarine debrite and turbidite deposits are known to be highly variable and complex, as is described in a recent summary of calciclastic, point-sourced submarine fans by Payros and Pujalte (2008). Dvoretsky (2009) recognized that debrite packages in the Agua Amarga basin were similar to small-scale grainy carbonate submarine fans described in Payros and Pujalte (2008). Due to the complexity of these deposits and the inherent difficulty in correlating individual debrites to features in the platform, little quantitative analysis of debrite distribution vs. slope morphology exists for carbonate deposits. Existing data show a wide range of debrite package widths and lengths for a wide variety of slope profiles ranging from a few to hundreds of kilometers (Payros and Pujalte, 2007). Dvoretsky (2009) demonstrated that debrite deposits at the toe-of-slope of the Rellana platform in the Cala del Plomo area (Fig. 1, 3) demonstrate characteristics of point-sourced debris flows filling a paleovalley. With the additional information available due to the faunal shift from a diverse reef ecosystem to a *Porites* dominated reef system through the late Messinian (Esteban, 1996; Esteban *et al.,* 1996) it is possible to show that retrogradational reef equivalent debrites (Fig. 5, 6; T6, T8) are older than progradational/downstepping reef equivalent debrites (Fig. 5, 6; T12, T13, T14, T16, T18). A 2-dimensional cross section roughly perpendicular to the platform margin through the toe-of-slope deposits in the Agua Amarga basin (Figure 6a, Appendix 5) was used to attempt to quantify the distribution and relative timing of debrites in the basin and equivalent platform deposits. Measurements were made from the distal end of the carbonate breccia facies (debrites) as

identified by Dvoretsky (2009) back to the steep basin margin; from the steep basin margin to the reef margin location thought to be roughly time equivalent to the debrite; and also the elevation of the reef margin at that time (Figure 6b,c).

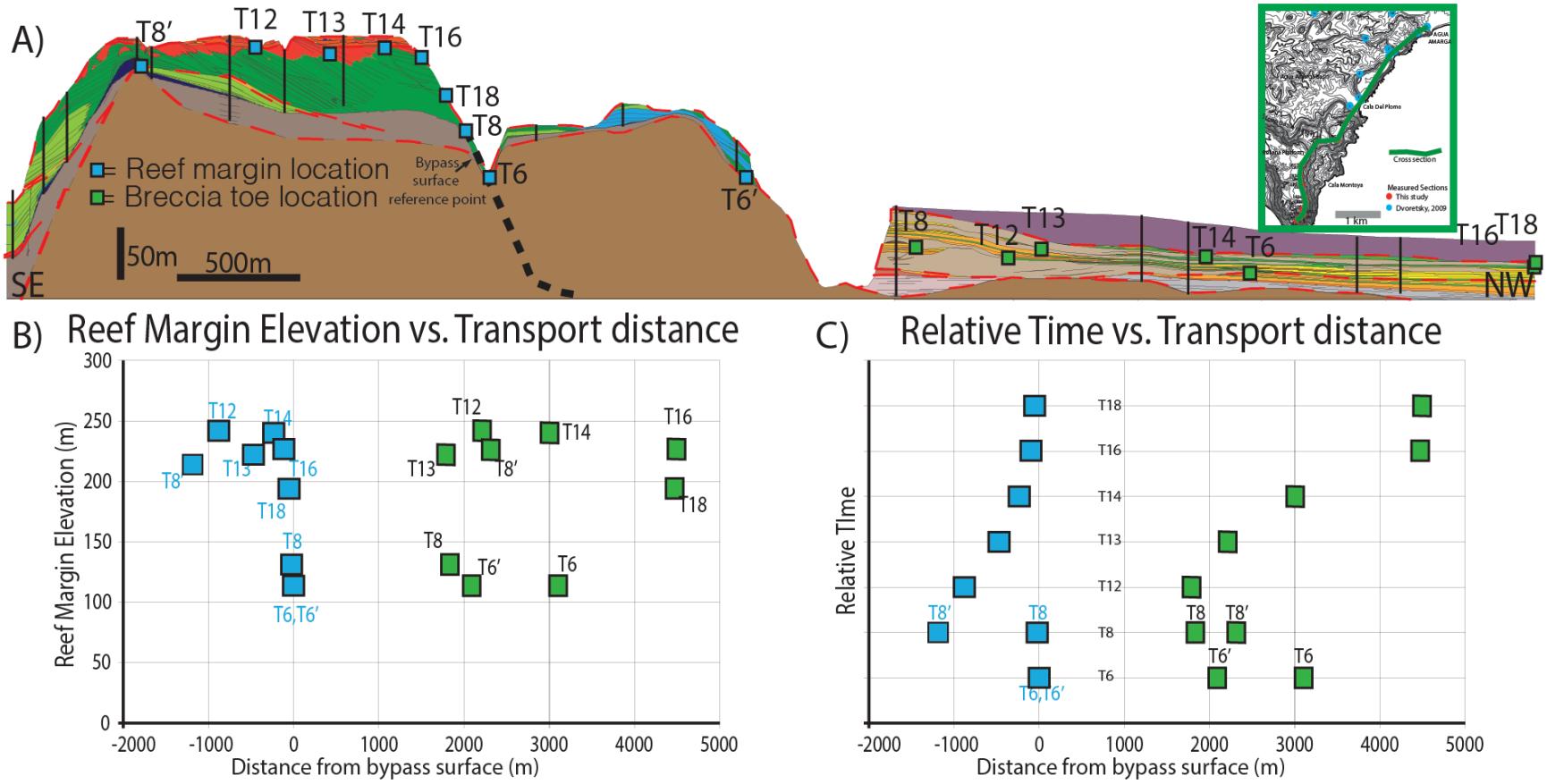
A)
T8′
T12
T13
T14
T16
T18
T8
T6
T6′
Reef margin location
Breccia toe location
Bypass surface reference point
50m
500m
SE
NW
T8
T12
T13
T14
T6
T16
T18
Cala Del Plomo
Cala Montoya
Cross section
Measured Sections
This study
Dvoretsky, 2009
1 km
B) Reef Margin Elevation vs. Transport distance
Reef Margin Elevation (m)
Distance from bypass surface (m)
T6,T6′
C) Relative Time vs. Transport distance
Relative TIme
Distance from bypass surface (m)
T6,T6′

Figure 6: Debrite propagation examination. A) Cross section along the coast from the Rellana platform to the Agua Amarga Basin (see inset map for location). The Agua Amarga Basin part of the cross section is modified from Dvoretsky (2009). Dashed line separating the Rellana platform from the intermediate volcanic high indicates location of basin margin inland of the intermediate high. Green data points represent the toe of the breccia component of debrites. Blue data points represent reef margin. The difference between blue and green data points of the same age is equivalent to the total interpreted transport distance between the reef margin and the toe of debrite breccia. The facies color scheme of cross section consistent with Figs. 3, 5. B) Plot of reef margin elevation versus transport distance. T6 has an alternate value (T6') associated with potential reef development on the slope of the intermediate volcanic high, rather than on the Rellana platform basin margin, as suggested by the elevation at which detrital TF is found on the southern end of the Rellana platform. The position of the reefal margin at T8 cannot be confidently placed, thus T8' is placed at 220m, the top of the volcanic basement during transgression associated with DS3, and 1.3 km of additional transport (the distance between the drainage divide and the basin margin) is inferred. Later debrites show a wide range of propagation distances despite variations in reef margin height C) Plot showing relative time vs. transport distance. The X-axis value of 0 corresponds to the steep basin margin. The location of the T6 toe of debrite breccia is shown as two points due to the potential for reef development on the intermediate volcanic high, which would affect basin transport distance. T8 has two data points reflecting reef margin location to demonstrate uncertainty with the reef margin location. This demonstrates that if the reef margin had been at the drainage divide, an additional 1.3 km of transport would have been required to deposit the interpreted correlative debrite. Later debrites show a trend of increasing propagation into the basin with increasing proximity of the reef to the basin margin. A dramatic increase in propagation distance occurs when the reef margin is within 400 m of the steep basin margin.

Reef margin elevation.--- Figure 6b displays reef margin elevation versus transport distance to test the hypothesis that increasing height of steep slope increases distance of debrite transport into the basin.

T6 and T8 are the earliest debrites measured and are interpreted to correspond to BU4. The abundance of *Tarbellastraea* detritus in BU4a, relative to other debrites in the basin, and stratal positioning. Measurements for T6 and T8 are speculative due to: 1) the lack of preserved reef margins, 2) truncation by later debrites, and 3) the presence of the intermediate paleotopographic high (Figure 6). T6 is shown as two data points (T6 and T6') to reflect the potential for reef development on the flank of the intermediate high (T6') rather than the Rellana platform (T6). T6 and T6' are placed at an elevation equivalent to the highest occurrence of detrital TF in SBZ on the southern slope of the platform. In Fig. 6B this uncertainty results in a transport distance span of 1.3 km, with no impact on interpreted reef margin elevation. T8 is assumed to have originated on the basin margin (T8), or above. T8` is placed at the point equivalent to reef margin development on the drainage divide. The variation between T8 and T8' shows an increase in transport distance as a result of increasing the assumed reef margin elevation (Fig 6B). The variation in the elevation of the reefal margin did not exert a strong control on the distance of propagation for debrites associated with T12 – T18.

Despite an increase in reef margin height between T6 and T8, there is a decrease in transport distance of the T8 debrite compared to T6, which indicates that reef margin height does not always correlate to transport distance. However, the debrites that extend the farthest into the basin (T16, T18) likely formed on the steep basin margin. Their extent into the basin could have been enhanced due to a high slope height, relative to the T6 and T8 debrites, which may have

had reef margins similarly located close to the steep basin margin, but with less reef margin elevation.

Margin separation – relative time vs. distance from bypass surface.--- Figure 6c shows relative time versus transport distance to highlight reef margin location change through time to test the hypothesis that increased proximity of reef margin to steep basin margin increases distance of transport into the basin. This plot facilitates comparison of scale of transport while limiting potential influence of misinterpretation of associated reef margin location. The X-axis value of 0 corresponds to the steep basin margin; negative x values represent distance towards the drainage divide, whereas positive distances increase basinward. Thus, the measured data are plotted independently of the interpreted reef location, preserving trends displayed by the measured data (green dots) and juxtaposing interpreted data associated with the downstepping surfaces (blue points) to attempt to identify controls. The trend of data in figure 6c indicates there may be a threshold proximity that must be reached before debrites can reach the basin.

T6 is considered as having originated on the basin margin, so a separation distance of 0 is used. As indicated in earlier text, due to the uncertainties associated with reef margin location, two points are used to demonstrate the potential variation due to reef development on the intermediate paleo-high and the Rellana platform. Similarly, for reasons discussed earlier, two T8 points are used (T8' and T8' blue). They show that if the reef margin developed on the drainage divide, the T8' debrite would have traveled 3 km, with 1.3 km of that travel occurring on the shallow dipping north slope. Interestingly, this fits the general trend shown by data

collected for later debrites, showing about 3 km of total propagation into the basin, where the reefal margin is separated by greater than 400 m from the basin margin.

T12 – T18 are interpreted to correspond to progradation and downstepping of the Rellana platform reef margin (fig. 6A). T16 and T18 basinal extent estimates are considered conservative because the data do not show the full basinal propagation of the coarse component of the debrite, as both of these debrites reach the end of the basinal cross section. Hypothetically this is the middle of the basin, so accurately determining provenance past this point would be difficult.

The data in figure 6C indicate a relationship between increasing proximity of the margins and increasing propagation of the debrite into the basin. The difference in propagation for T16 and T18 compared to T12-T14 indicates a significant increase in potential propagation occurs when the reef margin and basin margin are juxtaposed.

Discussion.--- Controls on debrite propagation are not well defined for carbonate systems (Payros *et al.,* 2007; Payros and Pujalte, 2008; Playton *et al.,* 2011). Although a limited data set, the results from this study (Figure 6) indicate that reef margin elevation had little influence in how far coarse debrite material propagated into the basin (Fig. 6b). Rather, coarse debrite material propagation into the basin is increased at times when the reef margin is interpreted to have been at or near the steep basin margin (Fig. 6c). The debrite associated with T-8 is an exception to this trend, possibly due to truncation by an overlying debrite. Further investigations on other distally steepened platforms are necessary to determine if the results of this study have broader application.

Timing for Coarse Sediment Redistribution

Traditional carbonate slope profile models applied to the Rellana platform suggest a high-energy open distally steepened ramp is applicable for the heterozoan dominated (DS2) deposits, and that the coralgal DS3 deposits represent an accretionary margin. The development of lowstand wedge and retrogradational reefs can lead to accumulation of material but is generally presented as less volumetrically significant than highstand shedding into basins (e.g. Read, 1985; Droxler and Schlager, 1985; Sarg, 1988; Coniglio and Dix, 1992; Playton and Kerans, 2002), or even considered unlikely (Schlager *et al.,* 1994). Additionally, the traditional highstand shedding model suggests platform contributions to the basin shut down when the platform top is exposed. The Rellana platform and Agua Amarga basin demonstrate a departure from the highstand shedding model. Due to storage on the shallow slope of the antecedent topography (e.g., Brooks and Holmes, 1989), the prevalence of lowstand and transgressive sediment generation on the slope, and the preservation of forced regression deposits, the sequence stratigraphic development is more closely related to a distally steepened ramp (*sensu* Read, 1985) than a flat-topped rimmed shelf, despite the abundant reef development.

Application of the traditional highstand shedding model (*sensu* Schlager *et al.,* 1994) would suggest the majority of the debris flows occurred during highstand. Backstepping geometries observed in BU 4 would then be attributed to variable volumes resulting from each debrite-inducing failure on the platform. Additionally, the basinward migrating debrites of BU 5-7 would be interpreted as aggradation and progressive expansion of the submarine system (*sensu* Galloway, 1998) (Figure 7, left column). Whereas this solution is theoretically feasible, it does not account for the observed stratal packaging or faunal variations.

Heterozoan facies similar to the rhodalgal-dominated facies in DS2 are widespread throughout much of the Mediterranean. They are essentially time equivalent deposits and indicate a temperate climate, possibly in conjunction with upwelling, for the Mediterranean (Franseen *et al*., 1997). An upward increase in coral clasts, including *Siderastraea, Tarbellastraea* and *Porites,* indicates a climatic shift toward more tropical climate (e.g. Rouchy, 1982; Carannante *et al.*, 1988; Saint Martin and Rouchy, 1990; Franseen and Mankiewicz, 1991; Franseen *et al.*, 1993; Esteban *et al.*, 1996, Brachert *et al.*, 1998). An upward increase in corals is seen in DS2 detrital deposits preserved on the southern slope of the Rellana platform and in BU4a in the basin, indicating that reefs developed at an elevation above these deposits. However, corals are not preserved in DS2 deposits on the north platform slope, which indicates reefs developed at lower elevations, or after DS2 facies were deposited on the north platform slope.

No evidence for subaerial exposure of the reef clasts from BU4a has been described, which is significant because it suggests that these deposits were redistributed into the basin prior to subaerial exposure of the platform (SB3), or that reefs grew and were eroded and bypassed during lowstand or initial transgression. If reef material was transported from the platform during highstand, one would expect to find in place reefs preserved, especially considering the large volume of coralgal material associated with the BU4a debrite and the low angle of the north slope. Given the lack of preserved *in situ* coral framestones or coral-rich debrites on the shallow-dipping platform slope, and the lack of evidence for subaerial exposure on the redistributed coral clasts, it seems probable that these reef deposits formed after the drop in relative sea-level that led to subaerial exposure of the platform, during lowstand or the subsequent transgression (Fig. 7, right column).

Additional evidence for lowstand or transgressive reef development comes from Miocene reef strata in other areas of southeast Spain. For example, backstepping, or retrogradational, reef sequences were identified in the Fortuna basin (~ 150 km north; Esteban *et al.*, 1996). Relative age dating indicates that the Fortuna basin reefs are roughly time equivalent to early reef development on the Rellana platform (Tortonian/Messinian; Esteban *et al.*, 1996; Franseen and Goldstein, 1996).

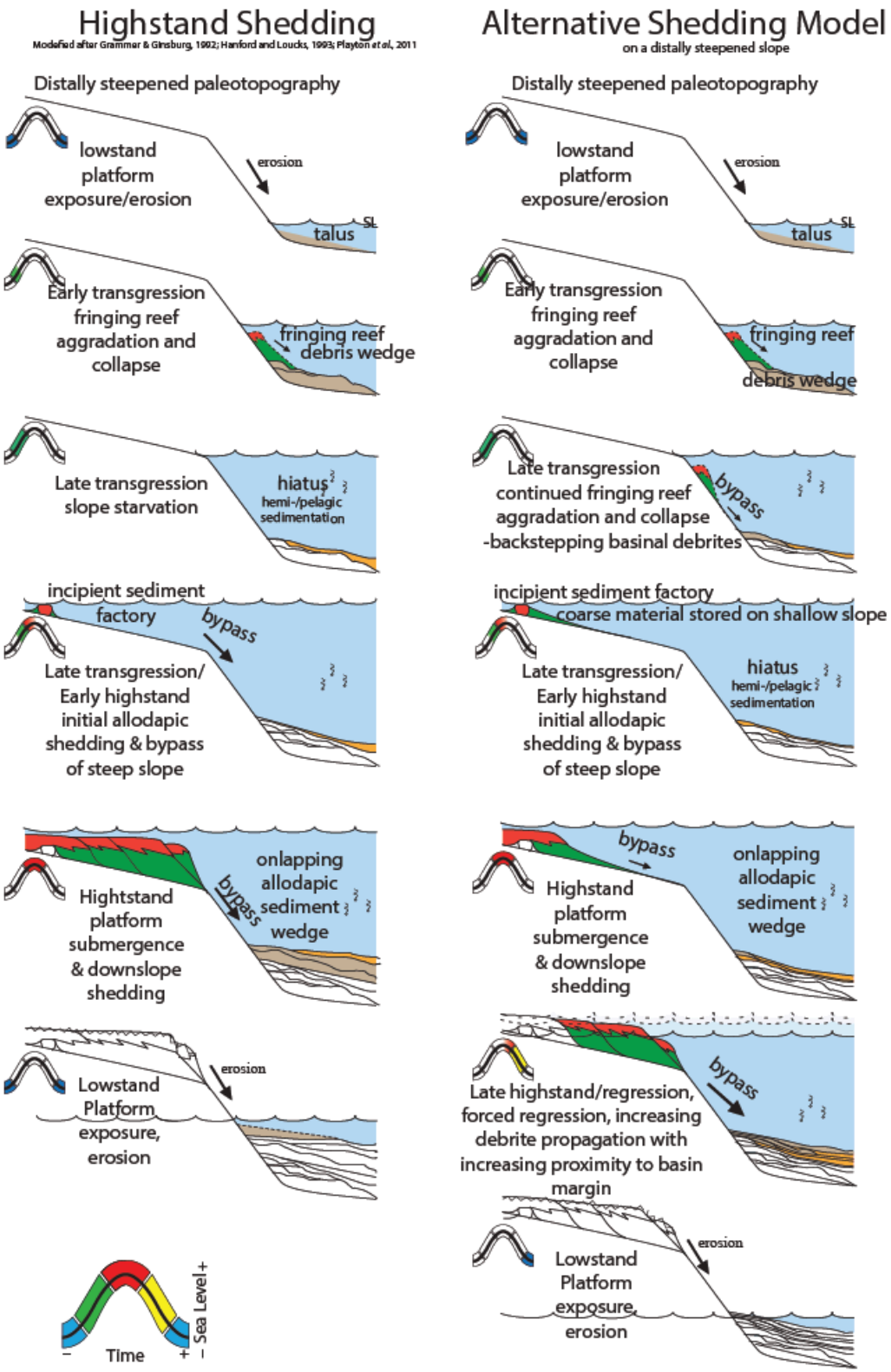
Highstand Shedding
Modified after Grammer & Ginsburg, 1992; Hanford and Loucks, 1993; Playton et al., 2011
Distally steepened paleotopography
lowstand platform exposure/erosion
erosion
talus
SL
Early transgression fringing reef aggradation and collapse
fringing reef
debris wedge
Late transgression slope starvation
hiatus
hemi-/pelagic sedimentation
incipient sediment factory
bypass
Late transgression/ Early highstand initial allodapic shedding & bypass of steep slope
Hightstand platform submergence & downslope shedding
onlapping allodapic sediment wedge
bypass
Lowstand Platform exposure, erosion
erosion
Sea Level
+
–
Time
Alternative Shedding Model
on a distally steepened slope
Distally steepened paleotopography
lowstand platform exposure/erosion
erosion
talus
SL
Early transgression fringing reef aggradation and collapse
fringing reef
debris wedge
Late transgression continued fringing reef aggradation and collapse -backstepping basinal debrites
bypass
incipient sediment factory
coarse material stored on shallow slope
Late transgression/ Early highstand initial allodapic shedding & bypass of steep slope
hiatus
hemi-/pelagic sedimentation
bypass
Highstand platform submergence & downslope shedding
onlapping allodapic sediment wedge
Late highstand/regression, forced regression, increasing debrite propagation with increasing proximity to basin margin
bypass
Lowstand Platform exposure, erosion
erosion

Figure 7: Schematic diagram showing (Left) anticipated platform development following traditional highstand shedding model (*sensu* Grammer and Ginsburg, 1992; Handford and Loucks, 1993; and Playton *et al.,* 2011). This model captures the potential for LST/TST reef development in early DS3, however it lacks the backstepping debrites associated with these early episodes of reef development. Additionally, the traditional highstand shedding model does not reflect forced regression reef development and associated basinward stepping debrites in the Agua Amarga basin. (Right) an alternative model for coarse material distribution into the basin in which multiple events of transgressive reef development are displayed to account for backstepping breccias in the basin. Additionally, downstepping of the reefal platform is recognized as a forced regression and the associated basinward stepping debrites are added to the model. Relative time steps are coordinated using color bar in lower left. Red = highstand, yellow = falling stage, blue = lowstand, and green = transgression. Figures are not to scale.

CONCLUSIONS

- Coarse-grained allodapic sediment was redistributed to the toe-of-slope during lowstand/transgression, during late highstand, and during forced regression. This is in contrast to the highstand shedding model, but may be a more plausible predictive model for deep-water sedimentation below distally steepened ramps and platforms with complex topography.
- Sediment-gravity flow interactions with paleotopography show that increased slope height does not necessarily increase the distance that coarse sediment gravity flow deposits extend into the basin.
- Areas of low-angle slope above a steep basin margin store sediment gravity flow deposits. Those deposits do not propagate into the basin until the reefal margin reaches critical proximity to the steep basin margin (400 m in this study).
- These observations can facilitate prediction of coarse reservoir facies in deep-water settings, where the paleotopography and sequence stratigraphy of the adjacent platform is known.
- Controls on platform carbonate deposition influence the nature and distribution of associated basinal deposits. Detailed reconstruction of sequence stratigraphic development of one component could be used to model other. Accuracy of these predictions is directly related to understanding of the paleotopography and relative sea-level history. Complicating factors introduce uncertainty to these predictions. For this study, predictions were complicated by relative timing of progradation and sea-level

fluctuations. The uncertainty inherent in these complications makes quantitative predictions difficult, but general trends are identifiable.

REFERENCES

Betzler, C., Brachert, T. C., Braga, J. C., and Martin, J. M., 1997, Nearshore, temperate, carbonate depositional systems (lower Tortonian, Agua Amarga Basin, southern Spain): implications for carbonate sequence stratigraphy: Sedimentary Geology, v. 113, pp. 27-53.

Betzler, C., Martin, J. M., Braga, J. C., 2000, Non-tropical carbonates related to rocky submarine cliffs (Miocene, Almeria, southern Spain): Sedimentary Geology, v. 131, pp. 51-65.

Brachert, T. C., Betzler, C., Braga, J. C., and Martin, J. M., 1998, Microtaphofacies of a Warm-Temperate Carbonate Ramp (Uppermost Tortonian/Lowermost Messinian, Southern Spain): Palaios, v. 13, pp. 459-475.

Braga, J. C., and Martin, J. M., 1988, Neogene coralline-algal growth-forms and their paleoenvironments in the Almanzora river valley (Almeria, S.E. Spain): Palaeogeography, Palaeoclimatology, and Palaeoecology, v. 67, pp. 285-303.

Brooks, G. R., and Holmes, C. W., 1989, Recent slope sediments and sedimentary processes bordering a non-rimmed platform: southwest Florida continental margin, *in* Crevello, P. D., Wilson, J. L., Sarg, J. F., and Read, J. F., *eds.*, Controls on Carbonate Platform and Basin Development: SEPM, Special Publication 44, pp. 259-272.

Carannante, G., Esteban, M., Milliman, J. D., and Simone, L., 1988, Carbonate Lithofacies as paleolatitude indicators: problems and limitations: Sedimentary Geology, v. 60, pp. 333-346.

Cook, H. E., McDaniel, P. N., Mountjoy, E. W., and Pray, L. C., 1972, Allochthonous carbonate debris flows at Devonian bank ("reef") margins, Alberta, Canada: Bulletin of Canadian Petroleum Geology, v. 20, pp. 493-497.

Cook, H. E., and Mullins, H. T., 1983, Ch. 11: Basin Margin Environments, *in* Scholle, P. A., Bebout, D. G., and Moore, C. H., *eds.* Carbonate Depositional Environments: AAPG Memoir 33, pp. 540- 617.

Cook, H. E., and Enos, P., *eds*., 1977, Deep-Water Carbonate Environments: SEPM, Special Publication 25, 336 p.

Choquette, P. W., and Pray, L. C., 1970, Geologic nomenclature and classification of porosity in sedimentary carbonates: AAPG Bulletin, v. 54, pp. 207-250.

Coniglio, M., and Dix, G. R., 1992, Carbonate Slopes, *in* Walker, R. G., and James N. P., *eds*., Facies Models: Response to Sea-Level Changes: Geological Association of Canada, pp. 349-374.

Dabrio, C. J., Esteban, M., and Martin, J. M., 1981, The Coral Reef of Nijar, Messinian (Uppermost Miocene), Almeria Province, SE Spain: Journal of Sedimentary Petrology, v. 51, pp. 521-439.

Dillett, P. M., 2004, Paleotopographic and sea-level controls on the sequence stratigraphic character of a heterozoan carbonate succession: Pliocene, Carboneras basin, southeast Spain: [Unpublished M.S. Thesis], University of Kansas, Lawrence, KS, 116 p.

Droxler, A. W., and Schlager, W., 1985, Glacial versus interglacial sedimentation rates and turbidite frequency in the Bahamas: Geology, v. 13, pp. 799-802.

Dvoretsky, R. A., 2009, Stratigraphy and reservoir-analog modeling of upper Miocene shallow-water and deep-water carbonate deposits: Agua Amarga basin, Southeast Spain: [Unpublished M.S. Thesis], University of Kansas, Lawrence, KS, 148 p.

Dvoretsky, R. A., Franseen, E. K., Goldstein, R. H., and Byrnes, A. P., 2008, 3-D Reservoir-Analog Characterization of Focused-Flow, Deepwater Carbonate Deposits, Upper Miocene Agua Amarga Basin, SE Spain: AAPG 2008 Annual Convention and Exhibition Abstracts Volume, p. 51.

Dvoretsky, R. A., Franseen, E. K., Goldstein, R. H., and Byrnes, A. P., 2009, Reservoir Characterization and 3-D Static Modeling of In Situ Shallow-Water and Resedimented Deepwater Carbonate Deposits, Agua Amarga Basin, SE Spain: AAPG Annual Convention & Exhibition; June 7-10, 2009; Denver, Colorado.

Dvoretsky, R. A., Goldstein, R. H., Franseen, E. K., and Byrnes, A. P., 2014, Reservoir-Analog Modeling of Focused-flow and Dispersed-flow Deepwater Carbonates: Miocene Agua Amarga Basin, Southeast Spain *in*, Harris, P. M., Playton, T. E., and Verwer, K. *eds*., Deposits, Architecture and Controls of Carbonate Margin, Slope, and Basin Systems: SEPM Special Publication 105, pp. 334- 358.

Enos, P., and Moore, C. H., 1983, Fore-reef slope environment *in* Scholle, P. A., Bebout, D. G., and Moore, C. H., *eds*., Carbonate Depositional Environments: AAPG Memoir 33, p. 507-537.

Esteban, M., 1979, Significance of the upper Miocene coral reefs of the western Mediterranean: Palaeogeography, Palaeoclimatology, Palaeoecology, v. 29, pp. 169-188.

Esteban, M., and Giner, J., 1980, Messinian coral reefs and erosion surfaces in Cabo de Gata (Almeria, southeastern Spain): Acta Geologica Hispanica, v. 15, pp. 97-104.

Esteban, M., 1996, An Overview of Miocene Reefs from Mediterranean Areas: General Trends and Facies Models, *in* Franseen, E. K., Esteban, M., Ward, W. C., and Rouchy, J. M., *eds*., Models for Carbonate Stratigraphy from Miocene Reef Complexes of the Mediterranean Regions. SEPM Concepts in Sedimentology and Paleontology, Series No. 5, pp. 3-54.

Esteban, M., Braga, J. C., Martin, J., and Santisteban, C., 1996, Western Mediterranean Reef Complexes, *in* Franseen, E. K., Esteban, M., Ward, W. C., and Rouchy, J. M., eds., Models for Carbonates Stratigraphy from Miocene Reef Complexes of Mediterranean Regions. SEPM Concept in Sedimentology and Paleontology, pp. 55-72.

Fernandez-Soler, J. M., 2001, Volcanics of the Almeria Province, *in* Mather, A. E., Martin, J. M., Harvey, A. M., and Braga, J. C., *eds*., A Field Guide to the Geology and Geomorphology of the Neogene Sedimentary Basins of the Almeria Province, SE Spain: Oxford, Blackwell, pp. 58-88.

Fortuin, A. R., and Dabrio, C. J., 2008, Evidence for Late Messinian seismites, Nijar Basin, south-east Spain: Sedimentology, v. 55(6), pp. 1595-1622.

Franseen, E.K., 1989, Depositional sequences and correlation of middle to upper Miocene carbonate complexes, Las Negras area, southeastern Spain [unpublished Ph.D. thesis]: University of Wisconsin–Madison, 374 p.

Franseen, E. K., and Mankiewicz, C., 1991, Depositional sequences and correlation of middle (?) to late Miocene carbonate complexes, Las Negras and Nijar areas, southeastern Spain: Sedimentology, v. 38, pp. 871-898.

Franseen, E. K., Goldstein, R. H., and Whitesell, T. E., 1993, Sequence stratigraphy of Miocene carbonate complexes, Las Negras area, southeastern Spain: Implications for quantification of changes in relative sea level, *in* Loucks, R.G. and Sarg, J. F., *eds*., Carbonate Sequence Stratigraphy: Recent Developments and Applications: AAPG Memoir 57, pp. 409-434.

Franseen, E. K., and Goldstein, R. H., 1996, Paleoslope, Sea-level and Climate Controls on Upper Miocene Platform Evolution, Las Negras Area, Southeastern Spain, *in* Franseen, E. K., Esteban, M., Ward, W. C., and Rouchy, J. M., *eds*., Models for Carbonates Stratigraphy from Miocene Reef Complexes of Mediterranean Regions: SEPM Concepts in Sedimentology and Paleontology, pp. 159-176.

Franseen, E. K., Goldstein, R. H., and Esteban, M., 1997a, Controls on Porosity Types and Distribution in Carbonate Reservoirs: A Guidebook for Miocene Carbonate Complexes of the Cabo de Gata Area, SE Spain: American Association of Petroleum Geologists Education Program, pp. 1-150.

Franseen, E. K., Goldstein, R. H., and Farr, M. R., 1997b, Substrate-Slope and Temperature controls on Carbonate Ramps: Revelations from Upper Miocene Outcrops, SE Spain, *in* James, N. P., and Clarke, A. D., *eds*., Cool-Water Carbonates: SEPM Special Publication, pp. 271-290.

Franseen, E. K., Goldstein, R. H., and Farr, M. R., 1998, Quantitative Controls on Location and Architecture of Carbonate Depositional Sequences: Upper Miocene, Cabo de Gata Region, SE Spain: Journal of Sedimentary Research, v. 68, pp. 283-298

Galloway, W. E., 1998, Clastic depositional systems and sequences: applications to reservoir prediction, delineation, and characterization: The Leading Edge, February, pp. 173-180.

Goldstein, R. H., and Franseen, E. K., 1995, Pinning points: a method providing quantitative constraints on relative sea-level history: Sedimentary Geology, v. 95, pp. 1-10.

Goldstein, R. H. and Franseen, E. K., 2002, Point sourced fill and fan sediment gravity flow deposits along a low relief basin margin, Miocene carbonates, Agua Amarga basin, southeast Spain: AAPG abstracts with programs, A65.

Goldstein, R. H., Franseen, E. K., Dvoretsky, R. A., and Sweeney, R. J., 2012, Controls on focused-flow and dispersed-flow deepwater carbonates: Miocene Agua Amarga Basin, Spain: Journal of Sedimentary Research v. 82, pp. 499–520.

Grammer, G. M., and Ginsburg, R. N., 1992, Highstand versus lowstand deposition on carbonate platform margins: Insight from Quaternary foreslope in the Bahamas: Marine Geology, v. 103, pp. 125-136.

Handford, C. R., and Loucks, R. G., 1993, Carbonate depositional sequences and systems tracts – responses of carbonate platforms to relative sea-level changes *in* Loucks, R. G., and Sarg, J. F., *eds*., Carbonate Sequence Stratigraphy: AAPG Memoirs, v. 57, pp. 3-42.

Hess, A. V., 2011, Heterozoan Carbonate Lithofacies and Sequence Stratigraphy: A Study of Pliocene Strata of the Agua Amarga Basin, Southeastern Spain: [Unpublished M.S. thesis], University of Kansas, Lawrence, KS, 256 p.

Johnson, C. L., Franseen, E. K., and Goldstein, R. H., 2005, The effects of sea level and paleotopography on lithofacies distribution and geometries in heterozoan carbonates, southeastern Spain: Sedimentology, v. 52, pp. 513-536.

Kenter, J. A. M., 1990, Carbonate Platform flanks: Slope angle and sediment fabric: Sedimentology, v. 37, pp. 777-794.

Lionello, P., and Sanna, A., 2005, Mediterranean wave climate variability and its links with NAO and Indian Monsoon: Climate Dynamics, v. 25, pp. 611-623.

Lipinski, C. J., 2010, Stratigraphy of upper Miocene oolite-microbialite-coralgal reef sequences

of the terminal carbonate complex: southeast Spain: [Unpublished M.S. thesis], University of Kansas, Lawrence, KS, 116 p.
Lopez-Ruiz, and Rodriguez-Badiola, E., 1980, La Region Volcanica Neogena del Sureste de España: Estudios Geológicos, v. 36, pp. 5-63.
Mapa Geológico de España, 1981, (1:50,000): Instituto Geológico y Minero de España.
Mankiewicz, C., 1996, The Middle to Upper Miocene carbonate complex of Nijar, Almeria Province, southeastern Spain, *in* Franseen, E.K., Esteban, M., Ward, W.C., and Rouchy, J. M., *eds*., Models for Carbonates Stratigraphy from Miocene Reef Complexes of Mediterranean Regions: SEPM Concept in Sedimentology and Paleontology, pp. 141-157.
Martin, J. M., Braga, J. C., Betzler, C., and Brachert, T., 1996, Sedimentary model and high frequency cyclicity in a Mediterranean, shallow-shelf, temperate-carbonate environment (uppermost Miocene, Agua Amarga Basin, Southern Spain): Sedimentology, v. 43, pp. 263-277.
Martin, J. M., Braga, J. C., and Betzler, C., 2003, Late Neogene - Recent uplift of the Cabo de Gata volcanic province, Almeria, SE Spain: Geomorphology, v. 50, pp. 27-42.
Montenat, C., Ott D'Estevou, P., and Mase, P., 1987, Tectonic-sedimentary characters of the Betic Neogene basins evolving in a crustal transcurrent shear zone (SE Spain): Bulletin Centres Rech. Explor.-Prod., Elf-Aquitaine, v. 11, pp. 1-22.
Montenat, C., and Ott D'Estevou, P., 1990, Le basin de Nijar-Carboneras et le couloir de Bas-Andarax, *in* Montenant, C., ed., Les Bassins Neogenes Du Domaine Betique Oriental (Espagne): Institut Geologique Albert-de-Lapparent, Paris, Documents et Travaux Institut Geologique Albert-de-Lapparent, pp. 129-164.
Montenat, C., and Ott D'Estevou, P**.**, 1996, Late Neogene basins evolving in the Eastern Betic transcurrent fault zone: an illustrated review, *in* Friend, P. F., and Dabrio, C. J., *eds.*, Tertiary basins of Spain: the stratigraphic record of crustal kinematics: Cambridge University Press, Cambridge, pp. 323-329.
Mullins, H. T., and Cook, H. E., 1986, Carbonate Apron Models: alternatives to the submarine fan model for paleoenvironmental analysis and hydrocarbon exploration: Sedimentary Geology, v. 48, pp. 37-79.
Payros, A., Pujalte, V., and Orue-Extebarria, X., 2007, A point-sourced calciclastic submarine fan complex (Eocene Anotz Formation, western Pyrenees): facies architecture, evolution and controlling factors: Sedimentology, v. 54, pp. 137-168.
Payros, A., and Pujalte, V., 2008, Calciclastic submarine fans: an integrated overview: Earth-Science Reviews, v. 86, pp. 203-246.
Platt, J. P., and Vissers, R. L. M., 1989, Extensional collapse of thickened continental lithosphere: a working hypothesis for the Alboran sea and Gibraltar arc: Geology, v. 17, pp. 540-543.
Playton, T. E., and Kerans, C., 2002, Slope and toe-of-slope deposits shed from a late Wolfcampian tectonically active carbonate ramp margin: Gulf Coast Association of Geological Societies Transactions, v. 52, pp. 811-820.
Playton, T. E., Janson, X., and Kerans, C., 2011, Carbonate Slopes, Chapter 18, *in* James, N.P., and Dalrymple, R.W., *eds*., Facies Models 4, GEOtext6, Geological Association of Canada, St. Johns, Newfoundland, pp. 449-476.
Read, F., 1985, Carbonate Platform Facies Models: AAPG Bulletin, v. 69, pp. 1-21.

Rehault, J. P., Boillot, G. and Mauffret, A., 1985, The western Mediterranean basin, *in* Stanley, D. J. and Wezel, F. C., *eds*., Geologic Evolution of the Mediterranean Basin: Springer-Verlag, New York, pp. 101-130.

Rouchy, J. M., 1982, La crise èvaporitique Messininenne de Méditerranée: nouvelles propositions pour une interpretation genetique: Paris, Bulletin du Museum National d'Histoire Naturelle, v. 50, p. 267.

Saint Martin, J. P. and Rouchy, J. M., 1990, Les plates-formes carbonatées Messiniennes en Méditerranée occidentale: leur importance pour la reconstruction des variations du niveau marin au Miocène terminal: Bulletin Societé Géologie France, v. 8, pp. 83-94.

Sanz De Galdeano, C. and Vera, J. A., 1992, Stratigraphic record and palaeogeographical context of the Neogene basins in the Betic Cordilleran, Spain: Basins Research, v. 4, pp. 21-36.

Sarg, J. F., 1988, Carbonate Sequence Stratigraphy *in* Wilgus, C. K., Hastings, B. S., Kendall, C. G. St. C., Posamentier, H. W., Ross, C. A., and Van Wagoner, J. C., *eds*., Sea Level Changes: An Integrated Approach: SEPM Special Publication No. 42, pp. 155-181.

Schlager, W., and Chermack, A., 1979, Sediment facies of platform-basin transition, Tongue of the Ocean, Bahamas, *in* Doyle, L. J., and Pilkey, O. H., *eds*., Geology of Continental Slopes: SEPM Special Publication 27, pp. 193-208.

Schlager, W., Reijmer, J. J. G., and Droxler, A., 1994, Highstand Shedding of Carbonate Platforms: Journal of Sedimentary Research, v. B64, pp. 270-281.

Serrano, F., 1992, Biostratigraphic control of Neogene volcanism in Sierra De Gata (southeast Spain): Geologie en Mijnbouw, v. 71, pp. 3-14.

Toomey, N., 2003, Controls on sequence stratigraphy in upper Miocene carbonates of Cerro de Ricardillo, southeastern Spain: [Unpublished M.S. thesis], University of Kansas, Lawrence, KS, 114 p.

APPENDICES

Appendix 1: Stratigraphic sections

Eleven stratigraphic sections were measured, describing over 630m of section in the Rellana platform area. Locations for measured section were determined by accessibility, coverage of platform area and intersection of characteristic or interesting features and were noted using topographic maps and a hand-held GPS unit (Figure 1b). Section descriptions were made on .1 m scale (accessibility allowing) and include; weathering profile, allochem types and relative concentration, sedimentary structures, Dunham facies classification and sample stratigraphic elevations and number. Digital copies of original sections (.pdf) and high-resolution computer traced sections (.ai) are available electronically. Section location information is presented below.

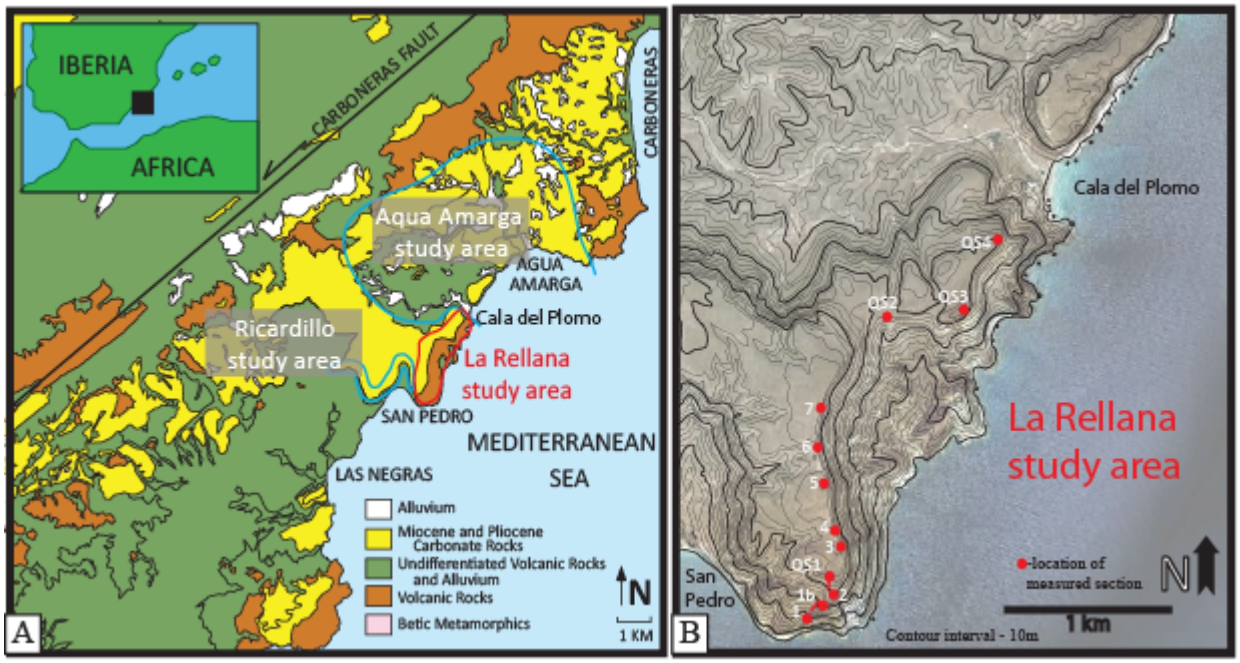

Location maps showing (A) location of the Cabo de Gata region of southeastern Spain (inset in A), the location of the Rellana platform study area relative to Neighboring Ricardillo and Aqua Amarga study areas and (B) locations of measured stratigraphic sections in the Rellana Platform region.

Appendix 2: Hand sample descriptions

Hand sample descriptions are available electronically in excel spreadsheet. Descriptions include Section of origin, stratigraphic elevation, associated facies, type and abundance of major

constituents, grain size, sorting trends, roundness and relative abrasion, and observed sedimentary structures.

Appendix 3: Thin section descriptions

Descriptions of 75 prepared thin-sections are available electronically (excel spreadsheet). Descriptions include Dunham classification, Type and abundance of constituents, grain size, sorting trends, roundness and relative abrasion, sedimentary structures, and porosity types and visually estimated percentage.

Appendix 4: Photomosaics/line drawings

Large scale photomosaics with overlain line drawings illustrating important surfaces including faults, facies contacts and distribution, sequence boundaries, major bedding trends, measured section locations and areas of covered section, these images are available electronically in their original format (.ai).

Appendix 5: Cross sections and fence diagrams

Measured stratigraphic sections were used in conjunction with photomosaics and field observations to generate cross sections through the Rellana platform are and into the updip and laterally equivalent Ricardillo peak area and downdip basinal equivalent Aqua Amarga basin. These cross sections and fence diagrams are available electronically in their original file formats (.ai).